National Park Service
U.S. Department of the Interior

Natural Resource Stewardship and Science

Alaskan National Park Glaciers - Status and Trends

Final Report

Natural Resource Technical Report NPS/AKRO/NRTR—2014/922

ON THE COVER

Recent rapid retreat of Muir Glacier from upper Muir Inlet, shown here, has revealed a new post-glacial landscape of changing sea levels, rocky moraines, and successional plants like *Dryas drummondii*. When USGS topographic maps were made in the mid-1950s, most of the area in this photo, including the vegetated foreground and all of the fjord itself out nearly to the gravelly creekbed in the far left side of the photo, were covered in glacier ice. The national parks of Alaska still have many, many glaciers. But as this report documents, the majority of them are shrinking, and newly deglaciated terrain is the fastest-growing landscape type in Alaskan parks. Glacier Bay National Park and Preserve, 9 July 2011. Photography by: JT Thomas

Alaskan National Park Glaciers - Status and Trends

Final Report

Natural Resource Technical Report NPS/AKRO/NRTR—2014/922

Michael Loso

Environmental Science Dept
Alaska Pacific University
4101 University Drive
Anchorage, AK 99508

Anthony Arendt, Chris Larsen, Justin Rich, Nate Murphy

Geophysical Institute
University of Alaska Fairbanks
903 Koyukuk Drive
Fairbanks, AK 99775

November 2014

U.S. Department of the Interior
National Park Service
Natural Resource Stewardship and Science
Fort Collins, Colorado

The National Park Service, Natural Resource Stewardship and Science office in Fort Collins, Colorado, publishes a range of reports that address natural resource topics. These reports are of interest and applicability to a broad audience in the National Park Service and others in natural resource management, including scientists, conservation and environmental constituencies, and the public.

The Natural Resource Technical Report Series is used to disseminate results of scientific studies in the physical, biological, and social sciences for both the advancement of science and the achievement of the National Park Service mission. The series provides contributors with a forum for displaying comprehensive data that are often deleted from journals because of page limitations.

All manuscripts in the series receive the appropriate level of peer review to ensure that the information is scientifically credible, technically accurate, appropriately written for the intended audience, and designed and published in a professional manner. This report received formal peer review by subject-matter experts who were not directly involved in the collection, analysis, or reporting of the data, and whose background and expertise put them on par technically and scientifically with the authors of the information.

This report is available from the Natural Resource Publications Management website (http://www.nature.nps.gov/publications/nrpm/). To receive this report in a format optimized for screen readers, please email irma@nps.gov.

Please cite this publication as:

Loso, M., A. Arendt, C. Larsen, J. Rich, and N. Murphy. 2014. Alaskan national park glaciers - status and trends: Final report. Natural Resource Technical Report NPS/AKRO/NRTR—2014/922. National Park Service, Fort Collins, Colorado.

NPS 953/127194, November 2014

Contents

Contents (continued)

Contents (continued)

Page

Figures

Figures (continued)

Page

Figures (continued)

Page

Figures (continued)

Page

Figures (continued)

Page

Figures (continued)

Page

Figures (continued)

Page

Tables

Page

Tables (continued)

Page

Executive Summary

This is the final technical report presenting results of a three-year project involving scientists from the National Park Service, the University of Alaska, and Alaska Pacific University. These results differ, in some cases, from preliminary results presented in four prior progress reports and take priority over them. Objectives of the project include mapping of all glaciers within Alaska's nine glaciated national parks at two time intervals, measurement of surface elevation changes on a subset of those glaciers, and an interdisciplinary summary of the nature and impacts of glacier change on 1-3 focus glaciers in each park. Objectives one and two are addressed here; the third focus glacier component will be presented in a companion interpretive report.

Mapping

- We digitized outlines for every glacier wholly or partly enclosed within nine glaciated national parks at two intervals. "Map date" outlines are derived directly, without editing, from USGS topographic maps dating to the mid-20th century. "Sat date" outlines are derived from imagery collected since 2000. These outlines, presented as an electronic database, document a half-century of changing glacier extents (Table 3).
- In modern satellite imagery, there are 7561 glaciers wholly or partly within the Alaskan national parks. These glaciers collectively cover 43,745 km^2 and, taken together, cover more land area than Maryland, the 42nd largest state in the U.S. (Table 6).
- Glacier cover has diminished since the 1950s at virtually all elevations, but most strongly below 2000 m. Overall, glacier cover has declined by 8%, converting formerly glaciated terrain to a mix of terrestrial and fjord ecosystems that total 3725 km^2—an area bigger than the state of Rhode Island (Table 6; Figure 5).
- Glacier cover diminished in every park over the last half-century. Per-park changes were -44% (ANIA), -8% (DENA), -44% (GAAR), -15% (GLBA), -14% (KATM), -11% (KEFJ), -74% (KLGO), -12% (LACL), and -5% (WRST).
- Our modern glacier inventory includes 968 more glaciers than were mapped by the USGS in the 1950s, but this does not reflect the creation of new glaciers where there were none before. Some "new" glaciers come from the breakup of large glaciers into numerous smaller, disconnected tributary glaciers. An even larger number come from our ability, using satellite imagery, to map small and/or debris-covered glaciers that were missed by the original cartographers (top panel Figure 6).
- Comparing the nine glaciated Alaskan parks, Wrangell-St. Elias has the most glaciers (3121) and the greatest ice cover (29,041 km^2) in modern imagery. At the other end of the spectrum, Klondike Gold Rush has only one small glacier (1.4 km^2). Lake Clark has the second largest number of glaciers (1740) but they are mostly small; Glacier Bay has fewer glaciers than Lake Clark, but the second greatest ice cover: 5323 km^2 (Figure 7).
- Considering glacier cover as a fraction of total park area, Kenai Fjords is the most intensively glaciated park (48.5% ice). Gates of the Arctic and Aniakchak are tied for last at 0.2% each (Table 7).

- Throughout the Alaskan parks, glaciers range from sea level to over 6000 m (Figure 8). They average 5.8 km^2, with a maximum size of 3388.2 km^2 (the main lobe of Malaspina Glacier, which is 4401 km^2 with all lobes combined, Table 6). Median glacier length, measured along the centerline, is around 1 km, with a maximum of ~200 km (Nabesna Glacier, Figure 12). Glacier slopes are typically between 10° and 40° with small high-elevation glaciers usually being the steepest (Figure 9). The vast majority of park glaciers have an overall aspect of NNE (Figure 11).

Elevation Change

- We present elevation change results, derived from airborne laser altimetry, for 59 distinct glaciers in five parks: DENA, GLBA, KEFJ, LACL, and WRST (Table 4). The earliest measurements began on some glaciers in 1994, and typically span a few years up to more than a decade. Elevation changes are summarized here, on a by-park basis, as glacier-wide averages in meters of water equivalent per year (m/yr w.e.).
- Eight glaciers in DENA, including both branches of Toklat 2 Glacier, generally thinned at modest rates between 0 and 1 m/yr w.e. (Figure 46). The only notable exception was a very slight net thickening of Muldrow Glacier between 2001 and 2008. Muldrow is a surge-type glacier in a quiescent phase, and its spatial pattern of elevation change is driven largely by recovery from the last documented surge in 1956/57.
- Sixteen glaciers in GLBA generally thinned between 1995 and 2011, mostly at rates between 0 and 1.5 m/yr w.e. Variability among glaciers was greatest between 2009 and 2011, with rates in that interval varying from -2.85 m/yr w.e. on Grand Plateau Glacier to 0.40 m/yr w.e. on Margerie Glacier (Figure 59).
- All twelve glaciers in KEFJ, most of which are outlet distributaries of the Harding Icefield, thinned overall between the mid-90s and 2007. In the early part of that interval, however, some of them thickened slightly, compensated by more dramatic thinning in the latter period (Figure 83). This result is at least partly an artifact of seasonally anomalous measurement dates and an unusually deep snowpack in 2001.
- Altimetry on six glaciers in LACL, including both branches of Double and Tlikakila Glaciers, revealed a pattern similar to that seen in KEFJ: thickening or modest thinning in an the mid-90s, followed by uniform thinning after 2001 (Figure 96). Measurement dates were seasonally consistent in LACL, but the deep snowpack of 2001 may have played a similar role to that suspected in KEFJ.
- Seventeen glaciers in WRST were the most variable, in terms of elevation change, of those in any park. Glaciers surveyed include at least two that surged during the measurement period (Bering and Logan), an advancing tidewater glacier (Yahtse), and several contiguous glaciers whose patterns of change are best understood as parts of larger ice masses (notably in the Bering/Bagley and Logan/Chitina systems). Excluding anomalous values from the surging Bering Glacier, observed mean annual elevation changes in the park tended, as in other parks but with wider variability including some thickening glaciers, towards modest thinning (0 to -1.5 m/yr w.e.; Figure 107).

Acknowledgments

We acknowledge the advice and contributions of our NPS collaborators Bruce Giffen, Guy Adema, Rob Burrows, Chuck Lindsay, Deb Kurtz, Dave Schirokauer, and Denny Capps. Thanks to Austin Johnson for altimetry work, Sam Herreid for digitizing a portion of the glacier outlines, Evan Burgess for sharing volume change results, and Christian Kienholz for developing and implementing the glacier delineation and centerline algorithms. We also thank all the many scientists whose work helped build the foundation for this project, including useful work in Kenai Fjords and Katmai by Giffen et al. (in press).

Introduction

Project Overview

Basic information on the extent of glaciers and how they are responding to climatic changes in Alaska NPS units is lacking. Because glaciers are a central component of the visitor experience for many Alaskan parks, because the complicated relationship between glaciers, humans, and the climate system constitutes a significant interpretive challenge for NPS staff, and because glacier changes affect hydrology, wildlife, vegetation, and hazards to persons and infrastructure, this project was initiated in October 2010 to document the status and recent trends in extent of glaciers throughout the nine glaciated park units in Alaska. The work will also be of substantial interest to scientists who recognize recent changes in Alaskan glaciers, including their collective contribution to sea level rise, as both globally significant and under studied.

Of Alaska's 15 national parks, preserves, and monuments, nine contain or adjoin glaciers: Aniakchak, Denali, Gates of the Arctic, Glacier Bay, Katmai, Kenai Fjords, Klondike Gold Rush, Lake Clark, and Wrangell-St. Elias. Under this project, status and trends of glaciers within these park units were assessed in three primary ways: changes in extent (area) for all glaciers, changes in glacier volume for all glaciers with available laser altimetry, and an interpretive-style description of glacier and landscape change for 1-3 "focus glaciers" per park unit. These three components are summarized in Table 1.

Table 1. Overall scope of project by component: Principal Investigator, glacier coverage, and types of analyses.

	Extent Mapping (this document)	**Volume Change (this document)**	**Focus Glaciers (interpretive report)**
Principal Investigator	Dr. Anthony Arendt	Dr. Chris Larsen	Dr. Michael Loso
Affiliation	Geophysical Institute, University of Alaska Fairbanks	Geophysical Institute, University of Alaska Fairbanks	Environmental Science Dept, Alaska Pacific University
Contact	arendta@gi.alaska.edu	chris.larsen@gi.alaska.edu	mloso@alaskapacific.edu
Analyses	Map modern and historic outlines of glaciers from topo maps and satellite imagery	Determine glacier surface elevation changes over time with repeat laser altimetry	Graphic/narrative summary of glacier response to climate and landscape-scale impacts
Glacier Coverage	All glaciers in all units, some park-adjacent glaciers	Existing coverage: ~1000 total flightlines in parks	1-3 per park unit

Scope

The work summarized in Table 1 is being presented in two written products: a technical report (this document) that contains details of the extent mapping and volume change components, and a separate interpretive report that presents the focus glacier component. Dr. Loso has primary responsibility for the writing of both publications.

This Natural Resource Technical Report is a comprehensive technical document prepared to thoroughly document the data sources, methodology, and results of the project, to analyze those results, and to discuss the implications of those analyses. It is accompanied by a permanent electronic archive of geographic and statistical data and is intended to serve a specialized audience interested in working directly with the project's datasets.

The accompanying interpretive report is a non-technical document suitable for glaciologists, park interpretation specialists. That document presents detailed, but accessible, summaries of the key data sources, methodologies, and findings of this technical report, and then utilizes the "focus glaciers" as a primary narrative tool to describe status and trends in NPS glaciers.

This project was initiated with a kickoff meeting held October 11, 2010. Interim project deliverables included four progress reports published separately in the Natural Resource Data Series. Results and conclusions in those progress reports—which are summarized in Table 2—were preliminary. This report should be considered and cited as the definitive result of our work on this project.

Table 2. Schedule and content of four previously published progress reports. This final report presents new data along with updates to the results presented in the progress reports.

Delivered Date	Report	Extent Mapping-Arendt	Volume Change-Larsen	Focus Glaciers-Loso
9/30/11	First Progress Report NPS/AKR/NRDS-2012/403	Glacier Bay, Denali	Glacier Bay	Glacier Bay
3/30/12	Second Progress Report NPS/AKR/NRDS-2012/404	Katmai, Lake Clark	Katmai, Lake Clark	
9/30/12	Third Progress Report NPS/AKRO/NRDS-2013/439	Gates of the Arctic, Klondike, Aniakchak	Denali	Katmai, Lake Clark, Denali
3/30/13	Fourth Progress Report NPS/AKRO/NRDS3-in press	Kenai Fjords, Wrangell-St. Elias	Kenai Fjords	

Study Areas

Alaska is the largest and most heavily glaciated of the fifty United States. The Randolph Glacier Inventory, an evolving database of glacier outlines supported in part by the work described here, counts 19,421 glaciers that are partly or wholly within state boundaries. These glaciers cover over 72,000 km^2, or about 5% of the state's total land area of 1.477 million km^2. Alaska's glaciers dwarf the collective glacier cover (<580 km^2, Fountain 2005) of the rest of the country.

Glaciers partly or wholly within the lands administered by the National Park Service comprise 43,745 km^2, or about 60%, of the state's total glacier coverage. Statewide, NPS administers 15 national parks, preserves, monuments, and national historical parks; glaciers occur in nine of those units. We list them by their full, formal names below, including the four-letter abbreviations which we will sometimes use, along with shortened names, in this report:

- Aniakchak National Monument and Preserve (ANIA)
- Denali National Park and Preserve (DENA)
- Gates of the Arctic National Park & Preserve (GAAR)
- Glacier Bay National Park and Preserve (GLBA)
- Katmai National Park and Preserve (KATM)
- Kenai Fjords National Park (KEFJ)
- Klondike Gold Rush National Historic Park (KLGO)
- Lake Clark National Park and Preserve (LACL)
- Wrangell-St. Elias National Park and Preserve (WRST)

This report addresses the status and trends of glaciers in all nine of those park units (Figure 1). We focus on glaciers that are partly or entirely within formal park boundaries, but in some cases include and discuss data from glaciers that are near, but technically outside of, the parks. Briefly, we describe each of these park units below, with a focus on glaciated geography and climate.

Aniakchak National Monument and Preserve

Aniakchak National Monument and Preserve (Figure 1) is the remotest and westernmost of the NPS units in this study, 1165 km southwest of Anchorage on the Alaska Peninsula. Visitation averages less than 200 persons per year, arriving mostly by air taxi from King Salmon to float the Aniakchak River, a National Wild and Scenic River, and to hunt moose and brown bear. The Monument is 2433 km^2 and centers on the 750 m deep Aniakchak Caldera, formed by a massive volcanic eruption 3500 years ago, and is located among other volcanoes between Bristol Bay and the Gulf of Alaska. Volcanic activity is ongoing in the region, and the Aniakchak Caldera most recently erupted in 1931. In Port Heiden, near the west edge of the Monument, average January low temperature is -9° C, average July high is 14° C, and the average total annual precipitation is 29 cm. Glaciers in the park ranges from 56° 51' to 57° 1' N and from 157° 24' to 158° 11' W.

The highest elevation in the park is ~1340 m, and glacier coverage is minimal—only about 5 km^2 of small glaciers exist, located primarily on shaded north-facing slopes and/or under insulating tephra-cover inside the caldera. A few very small glaciers are found in the headwaters of Main Creek on the eastern edge of the park. None of the park's glaciers reach tidewater, and the largest of them (in recent imagery) is about 3 km^2.

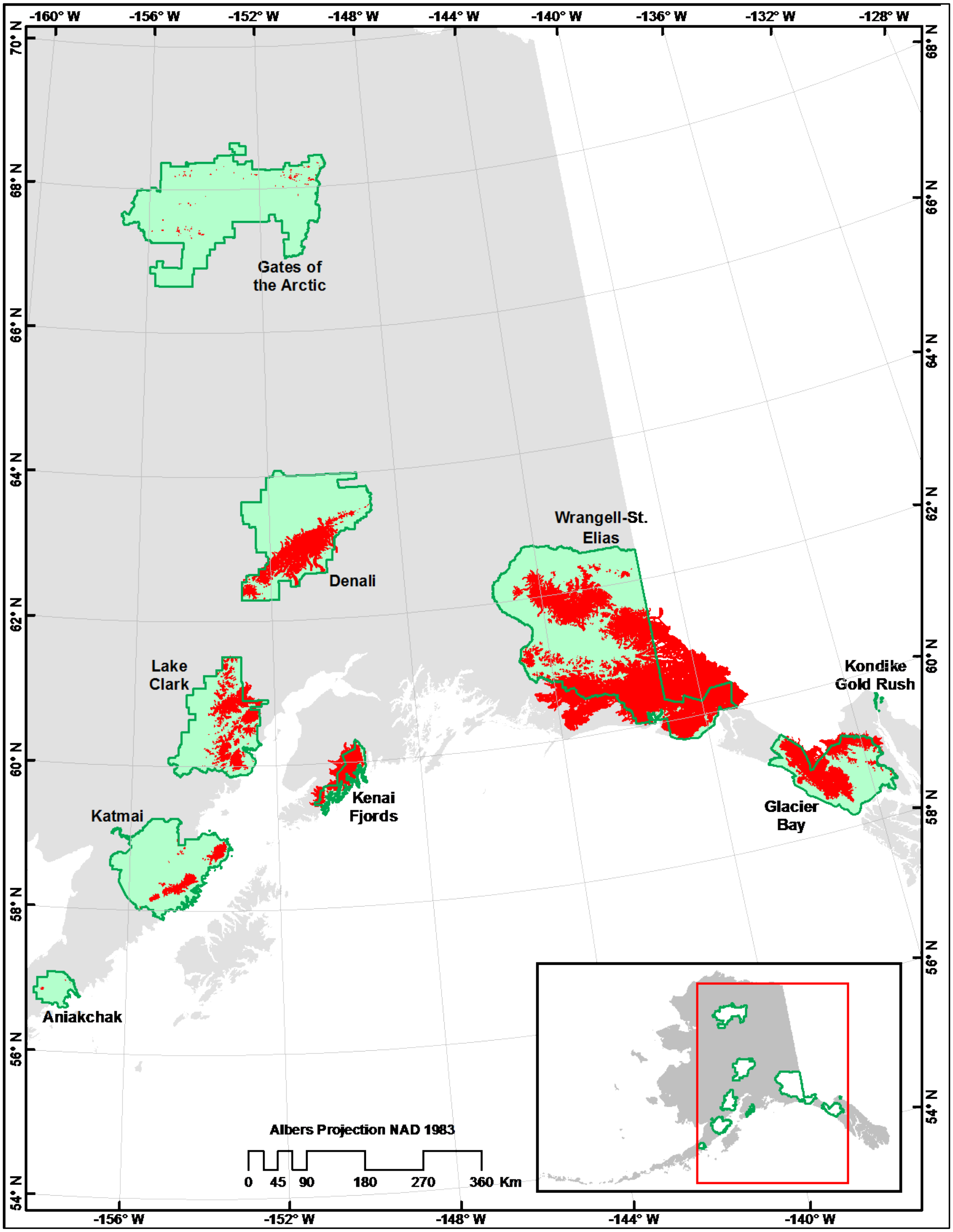

Figure 1. Locations of glaciated National Park units in Alaska. Green polygons are park units with modern glacier cover (including glaciers that are only partly within the park boundary) superimposed in red.

Denali National Park and Preserve

Denali National Park and Preserve (Figure 1) is located in interior Alaska, north of Anchorage and south of Fairbanks. The Park was first established in 1917 (as Mt. McKinley National Park) and expanded to its present size and designation in 1980. It contains 24,585 km^2 of land. In Denali NP&P, the Alaska Range attains its greatest height, containing the highest mountain in North America (Denali or Mt. McKinley, 6194 m) and numerous summits over 3000 m. The interior climate of Denali is cold in winter and warm in summer, with dry conditions and modest snowfall at low elevations but higher levels of precipitation in the mountains, especially on the south side of the range. Near park headquarters, average January low temperature is -22° C and average July high is 21 C. Annual total precipitation is 37 cm.

Glaciers wholly or partly inside the Denali park boundary cover 3735 km^2 and mainly flow northwest and southeast off the roughly SW-NE trending ridge of the Alaska Range. None of the glaciers reach tidewater, but many are large and extend many kilometers down low elevation valleys at their termini. Glaciers range from 62° 17' to 63° 32' N and from 148° 51' to 152° 53' W. The largest glacier is the 503 km^2 Kahiltna Glacier, well known to many mountaineers as home of the most common climbing routes on Mt. McKinley.

Gates of the Arctic National Park and Preserve

Gates of the Arctic National Park and Preserve (Figure 1) was first established by Congress in 1978 as the Arctic National Monument, and later upgraded to a National Park and Preserve in 1980 for its wild and undeveloped character and its opportunities for solitude and wilderness travel. In total, the Park encompasses 34,287 km^2 of terrain, including portions of six National Wild and Scenic Rivers, the headwaters of an international Biosphere Reserve (the Noatak River drainage), and peaks up to 2594 m (Mt. Igikpak). The Park is almost entirely mountainous, encompassing portions of the central Brooks Range, and the ancillary Schwatka and Endicott Mountains. In Anaktuvuk Pass, the average January low temperature is -30° C and the average July high is 16° C, with an average total annual precipitation of 58 cm.

In the most recent imagery, the park contains over 172 glaciers scattered throughout the Park, all of which are small, relative to other Alaskan parks (average 0.3 km^2, maximum 2.3 km^2) and land-terminating. Glaciers range from 67° 19' to 68° 20' N and from 149° 34' to 155° 54' W. Glaciers in Gates of the Arctic are unique in this study for being entirely north of the Arctic Circle, and glaciers on the north side of the Brooks Range experience a true Arctic climate with extremely cold temperatures and very light snowfall. All of the glaciers are remote, even by Alaskan standards, and even the most visited glaciers (in the Arrigetch Peaks) have probably <100 visitors per year.

Glacier Bay National Park and Preserve

Glacier Bay National Park and Preserve (Figure 1) is located directly adjacent to the Gulf of Alaska. The park was first established in 1925 (as a national monument) and expanded to its present size and designation in 1980. It contains 13,281 km^2 of land. Mount Fairweather, which is only 25 km from the Pacific Ocean, is the highpoint of the Fairweather Range at 4,671 m and is the source of the Margerie, Grand Plateau, and Fairweather glaciers. The maritime climate created by the Pacific Ocean, combined with the large vertical relief of the mountains, results in copious amounts of precipitation that feed the accumulation areas of the region. Near park headquarters, average January low temperature is -5° C and average July high is 18° C. Annual precipitation is 177 cm.

Glacier Bay NP&P (including glaciers wholly or partly inside of the park boundary) has an ice-covered area of around 5114 km^2 as of this writing. Glaciers range from 58°19’ N to 59° 24’ N and from 135° 18’ W to 138° 20’ W. There are two distinct areas of ice coverage: the glaciers located in the Fairweather Range, which includes Grand Pacific and Brady Glaciers, and those located northeast of the West Arm of Glacier Bay in the Alsek and Chilkat Ranges, which includes Carroll and Muir Glaciers. These two areas were previously part of the much more extensive Glacier Bay Icefield that has experienced a massive glacial retreat since the end of the Little Ice Age (LIA). This retreat has been substantially influenced by the fact that many of Glacier Bay’s glaciers terminated in tidewater and still do.

Katmai National Park and Preserve

Katmai National Park and Preserve (Figure 1) was established in 1918 (as Katmai National Monument) to preserve the spectacular and dynamic landscape associated with the 1912 eruption of Novarupta Volcano—the world’s largest volcanic eruption of the 20th century. The Valley of Ten Thousand Smokes was and is a central attraction of the Park, but Katmai is now equally famous for its populations of brown bears and fish. The Park encompasses ~16,564 km^2 of land. Located on the Alaska Peninsula between Cook Inlet and Bristol Bay, the park’s mountains are relatively low and reach their greatest heights on the eastern edge of the Park where the Aleutian Range crests at 2318 m on Mount Denison. Near park headquarters in King Salmon, average January low temperature is -13° C and average July high is 17° C. Annual precipitation is 48 cm.

Katmai NP&P (including glaciers wholly or partly inside of the Park boundary) has an ice-covered area of around 915 km^2 based on satellite imagery mostly since 2009. Glaciers are clustered in 3 groups: on the Kejulik Mountains to the south, on Fourpeaked Volcano in the east, and scattered in the Walatka Mountains in the north. Collectively, the glaciers range from 58° 06’ N to 58° 59’ N and from 153° 27’ W to 155° 27’ W. Glaciers in the Park are mostly modestly-sized (average size 3.3 km^2) and land-terminating, and stand out in a regional sense mostly for their response to extensive deposition of volcanic ash, especially after the massive 1912 Novarupta eruption.

Kenai Fjords National Park

Kenai Fjords National Park (Figure 1) was established in 1980 by the Alaska National Interest Lands Conservation Act to preserve icefield, fjord, and rainforest ecosystems, the Harding Icefield, and marine and terrestrial wildlife. The Park includes 2711 km^2 of terrain along the southeastern Kenai Peninsula, and is dominated in map view by the Harding Icefield, its distributary glaciers, and convoluted fjord systems on the Park’s southern marine margin. The topography of the park is almost completely mountainous, with elevations ranging from sea level to 1996 m on the Harding Icefield. Though largely undeveloped backcountry, the Exit Glacier area is accessible by road from the city of Seward, about 150 km south of Anchorage. The climate of Kenai Fjords is cool and wet. At sea level on the coastal side of the park in Seward, the average January low temperature is -6° C and the average July high is 17° C, with an average total annual precipitation of 168 cm. There is a strong climatic gradient across the mountains of the park, with warmer and wetter conditions in the southeastern coastal areas compared with the inland portions of the Harding Icefield.

Kenai Fjords (including glaciers wholly or partly inside of the park boundary) has an ice-covered area of 2080 km^2, based on recent imagery. In the most recent imagery, there are 275 glaciers in and adjacent to the Park, ranging from small glaciers less than 1 km^2 to the Tustumena Glacier at 393 km^2. Average glacier area is 7.5 km^2. The popular park access road terminates at Exit Glacier—an outlet of the above-mentioned Harding Icefield (~750 km^2) and one of the most visited glaciers in Alaska. Within the Park boundary, glaciers range from 59° 25' to 60° 16' N and from 149° 32' to 150° 59' W.

Klondike Gold Rush National Historic Park

Klondike Gold Rush National Historic Park (Figure 1) is the smallest NPS unit in this study at only 53 km^2. Congress established it in 1976 to preserve historic structures and trails associated with the Klondike Gold Rush of 1898, and the Park's lands are concentrated around the historic townsites of Skagway and Dyea and in narrow corridors along the Chilkoot Trail and White Pass & Yukon Route Railroad. All these areas lie between tidewater on the Pacific Ocean's Taiya Inlet and ridges of the St. Elias Mountains at elevations over 1800 m. The average January low temperature in Skagway (park headquarters, near sea level) is -8° C and the average July high is 20° C. Total annual precipitation in Skagway is 67 cm, with as much as 500 cm (and lower temps) in the mountainous reaches of the park.

Glacier coverage in the park is minimal, including only a portion (<1 km^2) of a glacier that straddles the international boundary with Canada in the northernmost edge of the Chilkoot Trail corridor at 59° 41' N and 135° 14' W. The status and trends of glaciers outside the park boundary are important, however, because many are visible and relatively accessible to recreational users of the park trails, and also because lakes associated with some of those glaciers have caused damage in the past and continue to threaten historic park resources. In our subsequent analyses, we give special attention to these glaciers near the park (most of which drain meltwater into the park boundary).

Lake Clark National Park and Preserve

Lake Clark National Park & Preserve (Figure 1) is located in western Alaska, southwest of—and across Cook Inlet from—Anchorage. The Park was first established in 1980 to protect scenic beauty (including volcanoes, glaciers, wild rivers, and waterfalls), populations of fish and wildlife, watersheds essential for red salmon, and the traditional lifestyle of local residents. It contains 16,309 km^2 of land. Along with its signature feature, 66 km long Lake Clark, the Park features two active volcanoes (Redoubt and Iliamna) and the intersection of two major mountain ranges: the Aleutian and Alaska Ranges. Climate is quite variable; elevations range from sea level on the Cook Inlet coast to over 3100 m on Redoubt Volcano. Near park headquarters in Port Alsworth, average January low temperature is -15° C and average July high is 20° C. Annual total precipitation is 36 cm.

Lake Clark's glaciers (including glaciers wholly or partly inside of the Park boundary) covered around 2604 km^2 in recent satellite imagery. Glaciers are scattered throughout the central and eastern portion of the park, originating on two volcanoes (Iliamna and Redoubt) and three mountain ranges (the Chigmit and Neacola Mountains and the southernmost extension of the Alaska Range). In the northeastern part of the park, glaciers of the Neacola Mountains are contiguous with ice outside the park boundary that adds a substantial amount to the glacier areas measured in this park. Indeed, the two largest glaciers in this inventory, Tanaina Glacier and

Blockade Glacier, originate outside the park boundary. The largest glacier contained mostly within the Park boundary is Double Glacier, with a main ice mass area over 137 km^2. Within the Park proper, glaciers range from 59° 52’ N to 61° 31’ N and from 152° 12’ W to 154° 04’ W. None of the Park’s glaciers reach tidewater.

Wrangell-St. Elias National Park and Preserve

Wrangell-St. Elias National Park and Preserve (Figure 1) is the largest NPS unit in Alaska and the nation, with 53,321 km^2 of land. It was first designated a national monument in 1978, but ANILCA expanded the boundaries when creating the Park and Preserve in 1980. The Park and Preserve contains 35,208 km^2 of designated wilderness, and along with Canada’s adjacent Kluane National Park comprises the largest protected wilderness in the world, outside Antarctica. The Park has low visitation, due largely to its location far from urban centers and its wilderness character, but it does have relatively good road access from adjacent highways and from two gravel roads that penetrate the interior of the Park. The Park spans several mountain ranges, including essentially all of the Wrangell Mountains and portions of the Chugach and St. Elias Mountains. Nine of the 16 highest peaks in North America lie within the Park boundary; the highest is Mt. St. Elias at 5489 m. Given the Park’s size, it is difficult to adequately summarize either the geography or the climate. Coastal regions are cool and wet, while the northern portion of the Park has a very continental climate. Coastal Yakutat has an average January low of -7° C, a July high of 15° C, and an annual average total precipitation of 384 cm. In comparison, Slana at the northcentral edge of the Park has a January low of -26° C, a July high of 21° C, and total precipitation of only 37 cm.

Glacier coverage within the Park/Preserve boundaries ranges from 59° 43’ to 62° 23’ N and from 139° 4’ to 144° 52’ W, but many of the individual glaciers and icefields in the park extend well outside the park boundary. Recent imagery indicates that there are a staggering 3102 glaciers; the largest is over Glacier at 4601 km^2. These glaciers cover 29,206 km^2. The massive glaciers of the Park and Preserve were specifically cited by Congress in the ANILCA legislation, and indeed these glaciers, along with adjacent glaciers to the west and east, constitute the largest contiguous nonpolar icefields on the planet.

Methods-Mapping

The objectives of our mapping project are to provide the following products for every glacier in the 9 glaciated park units:

- Mapped glacier outline
- Hypsometry (glacier surface area as a function of elevation)
- Summary statistics (areas, centerline length, average slopes and aspects)

These products are presented for two time intervals ranging from the mid-20th century ("map date") to the early part of the 21st century ("satellite date"). As implied by the names, data sources for these two intervals are historic topographic maps and contemporary satellite imagery, respectively.

This project is part of a broader effort to map and digitize all glacier outlines for the entire state of Alaska. The leaders of this component of our work (Arendt and Rich) are working, with other collaborators and other funding sources, to complete that effort. The funding for this project benefits that broader statewide effort, and the statewide effort provides two immediate benefits to the funders of this particular project. First, the electronic database of glacier outlines provided as an accompaniment to this report includes outlines of all Alaskan glaciers—not just the Park glaciers. In this report, we focus our presentation and interpretation on park glaciers (defined here as those that are partially or entirely within NPS park unit administrative boundaries), but the larger database will provide opportunities for NPS staff to examine non-park glaciers and broader statewide trends. The larger database also comprises one of 19 global glacier regions being inventoried as part of a broader global effort known as the "Randolph Glacier Inventory" or RGI. One advantage of this coordinated approach is that the data for Alaska follow a data model that is consistent with the global inventory, which has been well documented in a new publication (Pfeffer et al. 2014).

The second benefit of embedding this project in a larger statewide effort is the access this will provide to continued updates. As new data becomes available—particularly higher resolution satellite imagery—the statewide database continues to be refined. Also, it is likely that the RGI will continue to expand its list of attributes as new algorithms become available, and as more people work to improve the metadata. For example, the inventory does not presently contain information on glacier surges, but we are aware of international collaborators presently working on this. This report reflects the best available information at the time of writing, but enhancements to the database are ongoing and will update aspects of the results presented here. The public database of glacier outlines being developed by Arendt and others is directly compatible with the one we are submitting, however, and will permit NPS staff to access new and improved information without charge.

Data

As described above, we mapped all glaciers in the Alaskan National Park units in two time intervals ranging from mid-20th century ("map date") to the early part of the 21st century ("satellite date"). For each glacier, the first time interval was determined by the date of the published USGS topographic map (or more specifically, the date of the aerial photography upon which each map was based), and the second time interval was determined by the date of the most recent satellite imagery available to us. These dates vary throughout the project region (Table 3), but median map dates at all parks cluster between 1951 and 1960 and median satellite dates cluster between 2004 and 2011. With the one exception of Gates of the Arctic NP&P, where topographic maps were made later (in the 1970s), our mapping effort therefore documents concurrent glacier evolution over approximately five decades at the end of the 20th century.

Table 3. Years of maps (for 'map date') and satellite images (for 'satellite date') used to map glacier extents in this project.

	Map date		Satellite date	
Park	**Range**	**Median**	**Range**	**Median**
ANIA	1960-1962	1960	2004-2005	2004
DENA	1949-1957	1953	2004-2010	2010
GAAR	1970-1979	1970	2006-2009	2007
GLBA	1948-1987	1951	2010-2010	2010
KATM	1951-1951	1951	2008-2010	2009
KEFJ	1950-1951	1950	2005-2007	2005
KLGO	1948-1948	1948	2011-2011	2011
LACL	1954-1957	1957	2006-2010	2008
WRST	1948-2006	1957	2004-2010	2010

The specific maps and satellite images used for this effort are detailed in an accompanying electronic database, but we summarize them here. We based the map date outlines on 393 topographic maps (typically electronic versions available as "DRG's"—digital raster graphics). Of these, all but 79 were 1:63,360 (100 ft contours) topographic maps published by the US Geological Survey. The others were 1:50,000 topographic maps (40 m contours) published by the Canada Department of Energy, Mines, and Resources and used to draw boundaries of glaciers just outside the margins of three park units: WRST, GLBA, and KLGO. Because our explicit goal for the map date outlines was to create a precise digital record of the published glacier boundaries, we did not supplement these maps with any other data sources. For consistency, our outlines are based strictly upon the published boundaries, even in rare cases where we were aware of potential errors in the original maps. We note here the potential ambiguity introduced into these map dates by the presence of partial published revisions for some sheets. Our policy has been to always rely on the original map source, but it is possible that some of our map date outlines depict subsequently published glacier boundaries.

Satellite date outlines were based on a wider range of image sources, and reflect the best available imagery at the time of our work. We list 753 primary satellite images in our database, of which all but 24 were from the IKONOS satellite (our preferred source, due to its greater spatial resolution of 3.2 m multispectral, 0.82 m panchromatic). IKONOS was the primary data sources for ANIA, GAAR, KATM, KEFJ, KLGO, and WRST. We also used IKONOS for LACL, but the specific data source was an image mosaic provided by NPS for which we have no metadata. Where IKONOS was unavailable, we mostly relied on Landsat7 ETM+ (enhanced thematic mapper plus; 30 m multispectral and 15 m panchromatic). The Landsat scenes have a larger footprint (mean 35,869 km^2 in this study) than IKONOS (mean 404 km^2), so ETM+ was the primary image source for a significant portion of our study area, including most of DENA and GLBA and the central (Wrangell Mountains) portion of WRST.

Unlike the map date outlines, which were based strictly on the interpretations of the original cartographers, the satellite date outlines reflect digitizer judgment. As a consequence, we in many cases supplemented the satellite imagery described above with other data sources, when available. These “other” sources include other satellite images like SPOT-4 and 5, available aerial photographs, and especially online Google Earth images. In all cases, our goal was to faithfully map the glacier boundaries in our primary base image, but where shadows, clouds, seasonal snow, or other phenomena made delineation of such boundaries difficult, these other data sources provided an opportunity to refine our judgment.

Glacier outlines are two-dimensional features, but we required topographic information to delineate individual glacier basins and calculate hypsometry. For map date outlines, we used the National Elevation Dataset (NED). The NED is a compilation of best-available raster-format elevation data, and in Alaska it is still based primarily upon the original topographic maps (those used for our map date outlines) with elevations interpolated between contours at 2-arc-second (~60 m) spacing. Elevation data for modern outlines came from a continuous 60 m DEM constructed by Kienholz et al. (2013b) from a combination of Shuttle Radar Topography Mission (SRTM, from 2000) data in areas south of 60° N and airborne Interferometric Synthetic Aperture Radar (IFSAR, from 2010 and 2012) data elsewhere. In some small areas, the IFSAR data was supplemented by SPOT (from 2007 to 2009) and ASTER (from 2000-2011) imagery. This composite DEM contains spatially variable errors that we do no quantify in this report.

Digitizing

PI Anthony Arendt and research technician Justin Rich developed a standardized workflow for the generation and distribution of shapefiles and associated geostatistics (Figure 2). As discussed above, map date outlines were digitized directly from digital raster graphics. Manual editing, in that case, consisted solely of examining the digitized shapefiles to check for gross errors. For modern glacier outlines, the process was more involved.

Outlines for modern glaciers began either with existing datasets, where such exist, or with automatic delineation where they did not. Most existing outlines were in DENA, KATM, KEFJ, and LACL. We automated the digitizing procedure whenever possible to maximize consistency and efficiency, and to provide for future outline generation after this project is complete. Justin Rich developed algorithms that automatically delineate glacier boundaries from multispectral satellite imagery, and also produced an algorithm to improve the usability of post-2003 Landsat imagery that is corrupted by scan line correction (SLC) errors. Whether preliminary outlines came from existing datasets or from automatic delineation, they were in all cases then manually edited.

Manual editing was generally conducted at 1:20,000-25,000 scale for Landsat and 1:2000-8000 scale for IKONOS imagery. As mentioned previously, other data sources were often consulted at other scales to resolve ambiguities. Though debris-covered glacier ice is sometimes challenging to delineate with remote sensing, it was our goal to include all debris-covered ice within our mapped outlines, with the exception of clearly detached debris-covered ice left stranded by

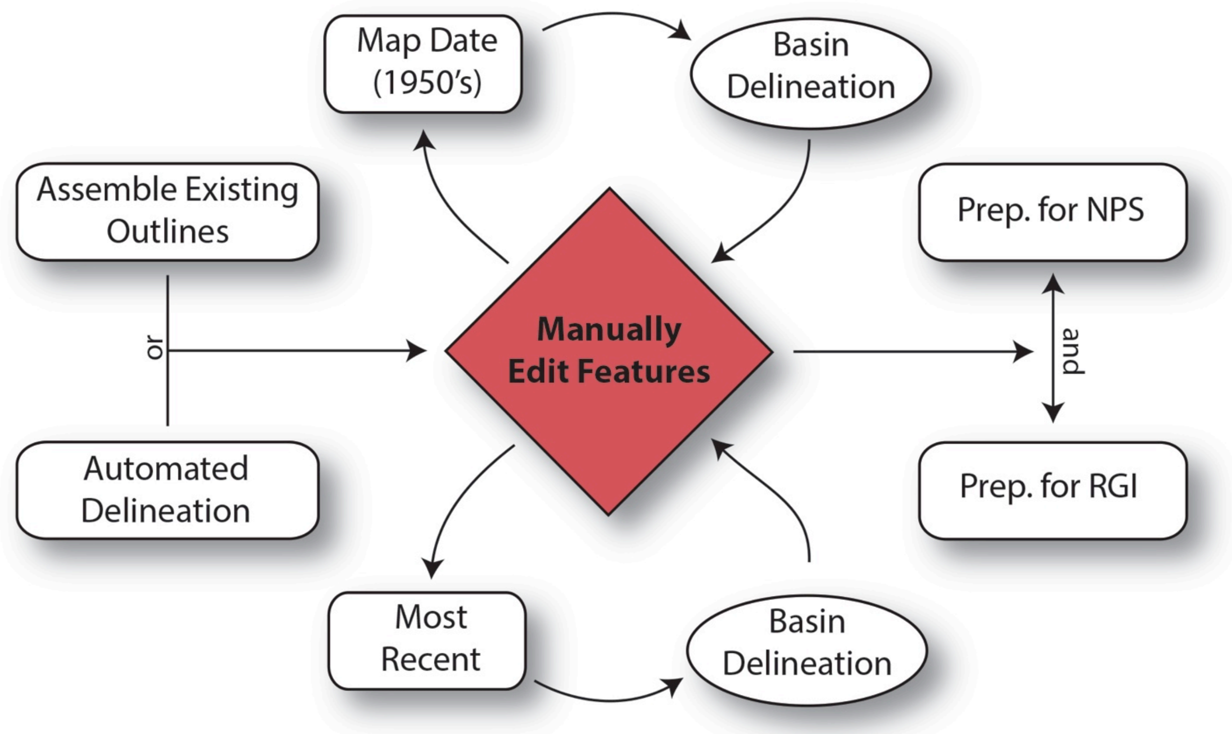

Figure 2. Workflow for the generation of glacier inventory data for NPS glaciers.

glacier retreat. Original USGS cartographers were less consistent in their treatment of debris-covered ice, leading in some cases to substantial differences between map date and satellite date outlines where debris-covered ice was omitted from original maps.

All glacier outlines in our database are presented as ArcGIS shapefiles. We checked the geometry of all shapefiles to ensure all polygons had correct closure and ordering of points. Sliver polygons, which can occur when glacier divides have not been edited correctly, were identified using ArcGIS topology tools, and were manually corrected. Scripts to run many of our topology checks are available at https://github.com/AGIScripts/script_glaciers. In our inventory of modern glaciers, we followed the recommendations of the World Glacier Inventory and removed glaciers with areas less than 0.01 km^2. For the mapdate inventory, remaining true to our goal of digitizing exactly the original mapped glaciers included by original cartographers, we left in smaller glaciers. 91 mapdate glaciers (1.3% of the total number) were smaller than 0.01 km^2.

Analysis

Digitized glacier outlines permitted straightforward analysis of glacier numbers and areas at both time intervals and consequent changes over time. The database associated with this report includes a broader collection of all Alaskan glaciers, including ice in adjacent icefields of British Columbia and the Yukon. Throughout this report, however, we limit our analyses to glaciers within the parks, defining such "park glaciers" as those with at least some portion of their area within park boundaries. We adopt this approach to avoid splitting individual glaciers into units smaller than their hydrological basin, which is problematic, for example when calculating glacier contributions to runoff. In most parks the additional ice extending beyond the boundary is relatively small, with the exception of the case of the Bering Glacier, a distributary of WRST's

Bagley Icefield that is itself largely outside of the park boundary. Because this exaggerates the glacier cover within strict park boundaries, we separately present a calculation of glaciated area in each park, clipping the modern glacier outlines at the precise park boundary.

We used elevation data to calculate glacier divides, basin hypsometry, glacier centerlines, and associated metrics. Glacier divides were calculated using an automated algorithm (Kienholz et al. 2013a) applied to surface elevations of the NED, and were manually edited as necessary. The use of NED elevations preserved divides from one time step to the next (over which time very small actual changes in centerline location were possible) for the purposes of comparison. We note that in some regions, for example the Harding Icefield, the divides have likely changed over time, however at the time of this report we lacked sufficiently accurate elevation datasets to map this well. Future updates will incorporate surface velocity data to more accurately map glacier divides on relatively flat and featureless icefields.

Hypsometry was calculated on a per glacier basis in 50 m bins using the distinct map date and modern DEMs described above. Glacier centerlines, which were necessary for calculations of glacier length and centerline slope, were determined (only for glaciers with a surface area greater than 0.1 km^2) using an algorithm developed by UAF's Christian Kienholz and summarized in Kienholz et al. (2013b). Glacier-wide aspects and slopes were calculated as average values of all pixels within the glacier outlines. Average aspects were obtained mathematically by summing the aspect sines and cosines of each cell within a glacier, followed by taking the inverse tangent of the quotient of the two sums.

Volumes of glacier ice cannot be directly calculated from glacier outlines, but can be estimated using area-volume scaling (Bahr et al. 1997). This approach is suitable for regional estimates, but confidence in granular estimates of individual glacier volumes is low. We applied Bahr's technique using the equation $V = cA^{\gamma}$ where V is the volume of a single glacier (in m^3) and A is area (in m^2) of that glacier, c is 0.2055 $m^{3-2\gamma}$ and γ is 1.375 (parameters from Radić and Hock, 2010). Volumes are presented for glacier populations grouped by park, but we refrain from calculating volume changes (from map date to satellite date) using this method due to large and poorly-quantified uncertainties.

Data Presentation

Results of this project component are presented in two forms: narrative and electronic. Narrative results are presented in this technical report, and include figures, tables, and maps that summarize glacier numbers, areas, and changes over time. The maps are shown at relatively coarse scales, but can be reprinted by NPS staff from provided electronic databases. These and related analyses, presented and discussed later in this report, are otherwise self-evident and require no further discussion here. Here, we focus on describing the structure and contents of an electronic database that accompanies this report.

The database presented in conjunction with this document is, in particular, a geodatabase that includes both spatial and tabular information. The spatial information consists of map date and satellite date glacier outlines, and also includes glacier centerlines derived using the Kienholz algorithm. The spatial data are presented concurrently in two formats that vary only by map datum and projection. The first is provided at the request of NPS, and presents results in the Alaska Albers projection with the North American Datum of 1983 (NAD 1983). The other form is presented for convenience and consistency for the many users that work commonly in GCS_WGS_1984, which uses a latitude-longitude coordinate system and the World Geodetic System (WGS 1984) datum. In outline form, the geodatabase will be organized as follows:

- Glacier Basemaps (Feature Dataset)
    - Base Images (Feature Class)
    - Base Maps (Feature Class)
- Glaciers Albers (Feature Dataset)
    - Glaciers (Feature Class)
        - Map date
        - Sat date
    - Glacier Centerlines (Feature Class)
        - Map date
        - Sat date
    - Hypsometry (Feature Class)
        - Map date
        - Sat date
- Glaciers WGS84 (Feature Dataset)
    - All same fields as above, just re-projected in WGS84 as discussed above
- Hypsometry (Table)
    - Map date
    - Sat date

Tabular data embedded within the geodatabase are designed to be similar to, and consistent with, the Randolph Glacier Inventory (RGI; Pfeffer et al. 2014). RGI is a recently developed database of glacier outlines designed to be geographically comprehensive—a task that has eluded the more well-known Global Land Ice Measurements from Space (GLIMS) database in part because the GLIMS database requires a large amount of metadata for each glacier outline—something that does not exist for all glaciers at this time (Raup et al. 2013). The motivation for the RGI was the need for a more comprehensive inventory for the recent Fifth Assessment Report of the Intergovernmental Panel on Climate Change (IPCC 2013). Both GLIMS and RGI are hosted by the National Snow and Ice Data Center (NSIDC) and are meant to eventually be merged, as glaciers in the RGI are slowly made ready for the more labor-intensive migration into GLIMS. At present, however, most outlining work in Alaska is dedicated to completing and updating the RGI database. By remaining consistent with that effort, the NPS geodatabase will be easily updated as new or improved data are entered into the RGI—an ongoing process.

Every glacier is identified throughout the database by a standardized GLIMS ID, and the geodatabase structure described above collectively summarizes each glacier (both map date and sat date) with the following attributes. Fields in bold are part of the RGI database, which can be accessed online for periodic updates through the GLIMS website (http://www.glims.org/RGI/Randolph.html) along with technical documentation (Arendt et al. 2013). Fields in regular font below are added for this project:

- **RGIID**: Standard 14 character identifier in the format RGI*vv*-*rr*.*nnnnn* where *vv* is the version number, *rr* is the first-order region number and *nnnnn* is an arbitrary identifying code that is unique within the region. The *nnnnn* code is assigned sequentially within each version of RGI, and has neither intrinsic meaning nor necessarily any consistency from one version to the next.
- **GLIMSID**: Standard 14 character glacier identifier with format G*nnnnnn*E*mmmmm*[N/S] where 'G' indicates a GLIMS-ID, *n*'s are longitudes with three decimal point precision (eg, 149.54345° E is 149543), 'E' indicates that all longitudes are measured eastwards from Greenwich by default, *m*'s are latitudes with three decimal point precision, and [N/S] is either 'N' or 'S' depending on northern or southern hemisphere. The latitude and longitude refer to the centroid of the glacier polygon, and may or may not be within the glacier's boundaries.
- **RGIFLAG**: 'Glacier' for all ice in this inventory (as opposed to "ice cap" in Antarctica, etc.).
- **BGNDATE**: First date of imagery or map used for outline. If only one source was used, this would be the sole date for that source. Format is *yyyymmdd*.
- **ENDDATE**: If more than one image or map source was used, the date of the last source. "-9999999" if only one source.
- **CENLON**: Longitude of glacier centroid. WGS 1984.
- **CENLAT**: Latitude of glacier centroid. WGS 1984.
- **01REGION**: First order global region (01 for Alaska).
- **02REGION**: Second-order Alaskan region, where 01 is N Alaska, 02 is Alaska Range, 03 is Alaska Peninsula and Aleutians, 04 is Western Chugach Mountains and Talkeetna Mountains, 05 is St. Elias Mountains, and 06 is N Coast Ranges.
- **AREA**: Glacier area in km^2.
- **GLACTYPE**: A code describing glacier type from Table 1 of Paul et al. (2009). 4 digits are possible (Figure 3), but in most cases only 2 or 3 digits are populated. At present this field only contains information on terminus characteristics (i.e. tidewater, land or lake terminating). It will be updated as other users provide metadata on surge and other glacier characteristics.
- **NAME**: Glacier name based on USGS formally registered geographic names. Blank is no name available. No informal names are included.
- PARK: 4-letter code designating the Alaskan park unit in which the glacier is wholly or partly enclosed, or 'NONE' if the glacier is completely outside park boundaries.
- MIN: Minimum elevation of the glacier terminus, in m.
- AVG: Area-weighted mean elevation of the glacier surface, in m.
- MAX: Maximum elevation of the glacier head, in m.

- LENGTH_CL: length, in km, of the glacier centerline, measured along the longest major branch of the glacier from glacier head to terminus.
- SLOPE: average glacier surface slope, in degrees, averaging maximum slopes of each cell within the glacier outline.
- SLOPE_CL: average glacier surface centerline slope, in degrees, averaging longitudinal slope angle along the glacier centerline.
- ASPECT: average glacier surface aspect, in degrees from true north.

Code	1: Snow	2: Calving	3: Surging	4: Divides
0	normal	normal	normal	normal
1	hides 5–50% of perim.	tidewater	reported	uncertain
2	hides >50% of perim.	freshwater	signs	compound
3	perennial snowfield	dry	signs & reported	ice cap
4	seasonal snowfield	regenerated	–	–
8	spec. rem.	spec. rem.	spec. rem.	spec. rem.
9	not spec.	not spec.	not spec.	not spec.

Figure 3. Field codes for GLACTYPE in our database. Reproduction of Table 1 in Paul et al. (2009).

Errors

Errors in our mapped glacier outlines can be treated differently for the two time periods. For map date glaciers, in which our outlines are direct digital reproductions of already mapped glacier outlines, our digitizing errors are insignificant in comparison with the errors made by the original cartographers. We therefore focus our error analysis of map date outlines on a generalized assessment of those historical outlines. For modern, satellite date glaciers, the errors are entirely our own, and the error analysis considers all potential sources of error.

Errors in the original USGS topographic maps were considered by Arendt et al.(2006) and their conclusions are summarized here. They cite problems with improperly drawn contours, poorly defined map dates, and poor geodetic controls in concluding that these maps were a primary source of error in their work. Glacier outlines can be in error due to map registration errors and human digitizing mistakes, recognizing that in some case “mistakes” were really just judgment calls that differ from our own. An example of this phenomenon is the clear evidence, in some areas, that cartographers purposely excluded areas of debris-covered ice from their glacier outlines, in contrast with our decision to include such areas. In other cases, mistakes were likely a result of base imagery that was either poor in quality or seasonally unfavorable for drawing distinctions between glacier ice and seasonal snow. Generalizations about the magnitude or distribution of such digitizing errors is difficult, though they are probably more important overall than the influence of map registration errors, and in agreement with Arendt et al. (2006) we do not quantify them. The impact of such errors on our results will be considered more in the discussion.

In terms of mapped elevations, which we relied upon to derive hypsometry, basin divides, and other associated geometric data, Arendt et al. (2006) accepted the nominal contour errors of 15 m in ablation zones of glaciers on the original USGS topographic maps. In accumulation zones, they cited Aðalgeirsdottir et al. (1998) in assuming a 45 m random contour error.

Errors in the digitizing of glacier outlines derived from modern satellite imagery have been more thoroughly investigated (including discussion of Landsat by Hall et al. 2003, and most recently by Paul et al. 2013), but like the map date outlines these errors are largely dictated by digitizer judgment, especially in difficult areas with shadows or debris cover. Automated outline delineation based on spectral algorithms can minimize this problem on clean, debris-free glaciers in high-resolution cloud-free imagery, but these conditions are not always met, especially in Alaska. Where they are, errors in outline position are usually on the order of 1 pixel and resolve to somewhere between 2 and 5% of the actual glacier area (Paul et al. 2013), trending to the higher values on smaller glaciers because errors scale with the length of the glacier perimeter.

Svoboda and Paul (2010) point out, though, that accuracy of glacier mapping projects generally are more strongly related to issues of glaciological interpretation than to the technical accuracy of the technique employed because of challenges presented in identifying ice divides, debris-covered ice, and seasonal snowfields. We manually corrected all automated outlines, focusing especially on these challenging areas, and acknowledge the greater errors likely in such a diverse dataset by adopting the error estimate assumed for RGI glaciers worldwide,

$$e(s)=ke_1s^p$$

where $e(s)$ is the error in glacier area s (km^2), p is 0.70, and e_1 is 0.039 is the estimated fractional error in a measured glacier with area of 1 km^2, and the correction factor k is conservatively estimated to be 3. Values of these parameters were fit to published estimates of uncertainty in areas of glaciers and glacier complexes (Pfeffer et al. 2014), and yield standard errors in glacier area ranging from nearly 24% on glaciers of 1 km^2 to 5% on glaciers of 16 km^2. This estimate of course ignores the spatial variability in quality and resolution of our source imagery, the distribution of debris-covered (as opposed to clean) ice, and the use in some cases of outlines derived from other technicians. In best cases, our errors are probably therefore much smaller than this estimate.

Methods-Elevation Change

The objective of the elevation change component of this project is to characterize changes in surface elevations (within glaciated Alaska parks) that have existing laser point data from two or more time intervals since the mid 1990s. These data permit direct measurement of elevation change that can be used to estimate volume changes over time, and can be used to estimate mass balance (the change in mass of a glacier over a particular period of time—typically one full year; Cogley et al. 2011) on individual glaciers.

Like the mapping component of this project, the elevation change work is part of a broader, ongoing effort. Since Keith Echelmeyer commenced this work in 1993 (Echelmeyer et al. 1996), the University of Alaska Fairbanks (UAF) has profiled over 200 glaciers. Portions of that work have been published in the peer-reviewed literature (e.g. Arendt et al. 2002, Johnson et al. 2013) but this project funded the completion of analyses on all extant data from within the national parks. No new laser altimetry data were collected under the scope of this project.

Data

We present analyses of elevation changes for 59 distinct glaciers in five Alaskan parks (Table 4). These include 8 glaciers in DENA, 16 in GLBA, 12 in KEFJ, 7 in LACL, and 17 in WRST. Elevation change estimates are based upon laser point data acquired from aircraft at nearly 200 discrete times ranging from May 1994 to August 2012. In general, the technique uses simultaneous measurements of the aircraft's position (using GPS), the aircraft's orientation (using a gyro and compass or inertial navigation system), and the relative position of the ice surface below (using transmitted laser beams) to precisely calculate ice surface positions in georeferenced coordinate frame.

The laser point data have been acquired with three different systems since data collection began, including two different laser profilers through summer 2009 and a scanning laser system since then. The laser profilers used a fixed nadir laser to collect a single track of points under the aircraft trajectory. Technical specifications are available in Echelmeyer et al. (1996) and Arendt et al. (2002). The scanner produces data (familiar to some as LiDAR) using a laser beam that sweeps 30° off-nadir to produce a swath of points with a width determined by the aircraft altitude. Specifications of this system were summarized by Johnson et al. (2013). Both the profiler and the scanner systems yield laser points with a footprint of approximately 20 cm at an along-track point spacing of approximately 1 m. The scanner provides across-track spacing of ~1 m with a typical track width of 500 m.

Translating point data, which even with the scanner covers only a portion of the entire glacier surface, into an estimate of volume change requires knowledge of the overall glacier geometry. We used the satellite date glacier outlines described elsewhere in this report to characterize glacier boundaries. Glacier hypsometries were generally based on the National Elevation Dataset, but with many exceptions. For DENA we used the 2010 IFSAR DEM, and in Glacier Bay and on other park glaciers south of 60°, elevations were based on the DEM acquired by the Shuttle Radar Topography Mission in February 2000. Where glaciers spilled across park boundaries into Canada, we used the NGS DEM. Importantly, we do not use any of these elevation products to directly calculate surface elevation changes, but instead simply to extract the area altitude distribution for extrapolation of laser-derived elevation changes over the entirety of the glacier surface.

Table 4(a). Dates of laser altimetry flights for glaciers in Denali National Park & Preserve (DENA).

Kahiltna	Ruth	Toklat 1	Toklat 2	Toklat 3	Muldrow	Traleika	Tokositna
7/31/94	4/30/01	5/7/96	5/21/01	5/21/01	8/3/94	8/22/01	4/30/01
5/18/08	5/17/08	5/17/08	5/17/08	5/16/08	8/22/01	5/17/08	5/18/08
5/22/10			5/22/10		5/17/08		
					5/22/10		

Table 5(b). Dates of laser altimetry flights for 12 glaciers in Glacier Bay National Park & Preserve (GLBA).

Brady	Lamplugh	Reid	Grand Pacific	Muir	Margerie	Riggs	Casement	Fair-weather	Carroll	Tkope	Davidson
6/4/95	6/4/95	6/4/95	6/7/96	5/28/00	6/2/05	6/1/05	6/1/05	6/2/09	6/2/09	6/2/09	6/1/05
5/25/00	5/25/00	5/25/00	6/6/01	6/1/05	6/2/09	6/2/09	6/2/09	5/30/11	5/30/11	5/30/11	6/2/09
6/1/05	6/1/05	6/1/05	6/2/09	6/2/09	5/30/11	5/30/11	5/30/11				5/30/11
6/2/09	6/2/09	6/2/09	5/29/11	5/30/11							
5/30/11	5/30/11	5/30/11									

Table 6(c). Dates of laser altimetry flights for the four remaining glaciers in Glacier Bay National Park & Preserve (GLBA).

Grand Plateau	Melbern	Little Jarvis	Konamoxt
6/2/05	6/2/09	5/31/95	6/7/96
6/2/09	5/29/11	5/28/00	5/30/11
5/30/11			

Table 7(d). Dates of laser altimetry flights 13 glaciers in Kenai Fjords National Park (KEFJ).

Aialik	Bear	Chernof	North-western	Harris	McCarty	Exit	Kachemak	Dinglestadt	Tustumena	Skilak	Holgate
5/29/94	5/28/94	5/20/96	5/19/96	5/29/96	5/20/96	5/28/94	5/19/96	5/20/96	5/29/94	5/29/94	5/29/94
5/18/01	5/19/01	5/18/01	5/17/01	5/17/01	5/18/01	5/14/99	5/18/01	5/18/01	5/19/01	5/19/01	5/18/01
6/14/07	6/14/07	6/14/07	6/14/07	6/14/07	6/14/07	5/18/01	6/14/07	6/14/07	6/14/07	6/14/07	6/14/07
						6/14/07					

Table 8(e). Dates of laser altimetry flights for thirteen glaciers in Lake Clark National Park & Preserve (LACL).

Double	Shamrock	Tanaina	Tlikakila	Tuxedni	Turquoise
5/14/96	5/14/96	5/14/96	5/13/01	5/13/96	5/16/96
5/13/01	5/13/01	5/13/01	5/21/08	5/13/01	5/13/01
5/26/08	5/21/08	5/21/08		5/26/08	5/26/08

Table 9(f). Dates of laser altimetry flights for 12 glaciers in Wrangell - St Elias National Park & Preserve (WRST).

Guyot	Hubbard	Kennicott	Nabesna	Barnard	Miles	Klutlan	Malaspina	Yahtse	Steller	Bagley W	Bagley E
8/26/07	5/3/00	6/17/00	6/21/00	8/19/03	9/2/04	8/19/03	6/5/95	8/29/06	8/22/03	8/22/03	8/22/03
8/23/10	6/10/07	6/3/07	6/3/07	8/18/07	8/19/09	8/19/07	6/24/00	8/26/07	8/28/07	8/28/07	8/27/00
8/22/12	5/25/12			8/16/12	8/30/12	8/16/12	8/27/00	8/23/10	8/21/10	8/21/10	8/22/03
							8/25/03	8/22/12	8/18/12	8/18/12	8/24/07
							8/26/07				8/21/10
							8/23/10				8/18/12
							8/22/12				

Table 10(f). Dates of laser altimetry flights for the remaining five glaciers in Wrangell - St Elias National Park & Preserve (WRST).

Jefferies	Bering	Walsh	Logan	Ogilvie
6/10/95	6/22/00	8/19/03	8/19/03	8/24/03
8/19/07	8/22/03	8/19/07	8/19/07	8/19/07
8/23/10	8/24/07	8/16/12	8/16/12	8/16/12
8/18/12	8/21/10			
	8/16/11			
	8/18/12			

Analysis

Our first step in calculation of elevation change and mass balance is processing of the point data. Data acquired during early profiler missions have been reprocessed with the same methods as post-2009 scanner data, and surface elevations are derived by integrating the GPS-based position of the aircraft, its orientation, and laser point positions relative to the airplane. The combination of these data determines the position in 3-dimensional space of the laser point where it was reflected from the glacier surface. The points are referenced in ITRF00 and coordinates are projected to WGS84 with elevation data recorded as height above ellipsoid.

The glacier surface elevation profiles from different years are differenced to find the surface elevation change (Δh), and dividing by the time elapsed between profiles gives the rate of thickness change ($\Delta h/\Delta t$). This is determined with slightly different methods depending on whether data from the profiler (1995 – early summer 2009) or scanner (late summer 2009 – 2011) are being used.

For profiler to profiler differencing, points that were located within 10 m of each other in the x-y plane were selected as common points between the different years. If more than one contemporaneous point is located within a 10 m grid cell, then the mode of the elevation was used to represent that point. Use of the mode diminished the importance of anomalous returns (from crevasses, for example). These common points were then used in the determination of $\Delta h/\Delta t$. Since data points were recorded only along the flight track with the laser profiler it was critical that these earlier flight paths were repeated as accurately as possible to obtain a large number of common points. Sometimes the flights were not repeated closely enough and provided minimal elevation change measurements.

For scanner to profiler differencing, a 10 x 10 m grid was made of the laser scanner swath. Elevation values in this grid were based upon the mode of all points within each cell. Then, for each point in the older profile that overlaps with the scanner swath, an elevation was derived from the identical coordinate on the scanner grid using bilinear interpolation. Differences between the two elevations were used to calculate $\Delta h/\Delta t$. A similar approach was used for scanner to scanner comparisons, but we simply differenced the modal values of each overlapping grid cell from both intervals. Elevation changes calculated from data using scanners for one or both intervals typically use many more data points than profiler-profiler comparisons, regardless of flight path fidelity.

The complete series of Δh/Δt measurements along the glacier flight line was then plotted, as a function of elevation, and summarized by plotting the median value within a 12-point smoothing window from the bottom to the top of the glacier. The choice of 12 points for the moving window was somewhat arbitrary, and was altered in some cases for glaciers with very sparse data (4 or 8 point window) or with many points (≥20 point window). Confidence intervals were defined as the lower and upper quartiles of this moving window. Because thickness changes cannot be greater than zero where ice approaches zero thickness at the glacier margin, Δh/Δt was assumed to be zero at both the lower and upper elevations of each glacier. We note that this assumption is problematic in the cases of glaciers whose upper elevations are joined at an ice divide to other glaciers and where thinning or thickening can consequently occur, especially where the equilibrium-line altitude (ELA) is higher than the glacier's uppermost elevations.

To calculate mass loss and mass balance of the glaciers, we first integrated the Δh/Δt-elevation curve over the area-altitude distribution (AAD) of the glacier to calculate a glacier-wide volume change. We assumed that all measured elevation changes represent loss or gain of ice with a constant density of 900 kg/m^3. To facilitate comparison among glaciers of different sizes, the calculated mass change rate (gigatons per year, typically "mass change" in our figures) was expressed as a specific mass-balance rate (glacier-wide mean change in mass, expressed by convention in units of meters water equivalent per year, typically "mass balance" in our figures) by converting the mass change to volume, using the density of water, and dividing by glacier area.

Data Presentation

The fundamental unit of analysis for this component of the project is a summary of the elevation changes as a function of elevation for some given time interval, and we present these summaries as individual figures ("DZ plots") in the results section. As described above, these figures plot individual laser-based difference measurements along with smoothed lines summarizing the median and lower/upper quartiles for each profile. Lower/upper quartile lines are dashed where there is insufficient data to calculate the quartiles. Mass change and mass balance are included for each interval, along with a single plot of the AAD used for the glacier in question.

For glaciers with more than two laser-measurement dates, analyses of multiple intervals are possible. We typically present all possible combinations of intervals, including long periods that encompass or overlap other, shorter intervals. In a few cases, we have omitted analyses of one or more intervals where we judge sparse data and/or noisy results to justify such omission. These details are pertinent when plotting the data for multiple glaciers and time intervals simultaneously, which we do to facilitate investigation of trends by park. In our tabular presentation of results, we also note for each glacier whether it is a land (L), lake (LK), or tidewater (T) terminating glacier, and whether it has a history of surging (S).

We also present the data in an electronic format suitable for visualization. The smoothed elevation changes (in m/yr) are summarized, as a function of elevation, in raster images (geo-tiffs) for each glacier and time interval for which we present corresponding data in this report. Only a subset of those images are presented here in this report. All rasters are presented in WGS 1984.

In this report, we do not directly estimate volume changes of NPS glaciers that were not measured my laser altimetry, but we do present preliminary results of such an effort by our colleague Evan Burgess. His work, currently in preparation, uses methods similar to those applied by Johnson et al. (2013), and is based directly on the same altimetry data presented in this report. His results are presented in the discussion section of this document.

Errors

Errors in our estimates of elevation change and inferred mass balance/mass change result from uncertainties in measurements, from uncertainties in the degree to which our point measurements represent the entire glacier, from uncertainties in the true shape of the glacier, from varying seasonality of our measurements, and from the assumption of a constant density profile. These uncertainties, which were recently assessed for these same data in greater detail in Johnson et al. (2013), are summarized here. The total reported uncertainties in mass balance and mass change were calculated by combining, in quadrature, all the uncertainties described below.

Measurement uncertainty arises from errors in the simultaneous collection of aircraft position and orientation data and also laser range and pointing angle. Of these errors, the largest is error in aircraft position and orientation, which interact with the laser rangefinder systems to generate laser coordinate error. Based on repeated surveys of fixed objects with both systems, the generalized error in point measurements from both systems have been empirically determined to average ±0.2 m (Johnson et al. 2013).

As described above, we used closely overlapping points to estimate surface elevation change at discrete locations, but then were required to interpolate changes between those points along the flight path and subsequently to extrapolate those changes laterally to glacier regions at comparable elevations. We calculated error in the along-path interpolation as the upper and lower quartiles of measurements in the typically 12-point moving window. These commonly generate uneven upper and lower confidence intervals. Above (towards the glacier head) and below (towards the terminus) the along-path range of our measurements, we used the full range (instead of upper/lower quartile) of our measurements to estimate the errors. When then applying these calculated $\Delta h/\Delta t$ values to the full AAD of the glacier, we are implicitly assuming that ice thickness changes are perfect functions of elevation. Berthier et al. (2010) have pointed out the potential errors associated with this assumption, and Johnson et al. (2013) quantified this error in GLBA by comparing profile-generated estimates of mass balance with DEM-based estimates on glaciers where both data were available. They found discrepancies of <1%.

Extrapolation of measured thickness changes to the full glacier also depend upon accurate models of glacier shape, represented by a glacier outline and an area-altitude distribution (AAD). More important than outright errors in those data products is the typical constraint of having only one outline and AAD available for each glacier, despite the fact that the glacier shape in fact changes continually over the period of our measurements. This can generate large errors over long time intervals, but in the <20 year interval spanned by our measurements the introduced error is dominated by changes in AAD (rather than outline), and is typically smaller than the error bounds modeled by our upper and lower quartiles.

Finally, our results depend on the related assumptions that two measurements which bracket an interval were made on the same day of year (and hence represent annual changes with no effect of seasonal accumulation or melt) and that any differences between the two represent gain or loss of ice with a constant density of 900 kg/m^3. The former assumption is violated in most cases, but typically by only a few days to weeks, well within the interannual variability of the snowpack's seasonal progression. Where the discrepancy is greater, we discuss this on a case by case basis and consider the implications. As to the latter assumption, known commonly as Sorge's law (Bader, 1954), we know it to be true over very long periods and increasingly problematic over shorter intervals. Huss (2013) found that our assumption tends to systematically overestimate mass change by 2-15% over periods of "some years to several decades," and can both over and underestimate mass change by larger amounts in intervals of 1-3 years. This agrees with the conclusion of Johnson et al. (2013) that invoking Sorge's law over the intervals typical of this study (median difference between day of year on successive measurements = 5 days) introduces an error in mass balance of up to 10%.

Methods-Focus Glaciers

The focus glacier component of this project provides additional information about a small subset of glaciers in each glaciated Alaskan park to demonstrate the unique ways in which A) glaciers change in response to climate and other forcings, and B) landscapes respond to glacier change. The focus glacier results are not part of this report, but are instead included in an accompanying interpretive report. Those results include narrative descriptions of each glacier along with collections of photos, maps, figures, and other graphical information. In comparison with other components of this project, which are directed clearly towards generating and analyzing new or existing data, the focus glacier component is focused on interpretation and synthesis. Here, for completeness, we address briefly how the focus glacier component of the project was conducted.

Focus Glacier Selection

The final list of focus glaciers is included below (Table 5) and mapped in Figure 4. The focus glaciers are not intended to be statistically representative of Alaskan glaciers as a whole, but rather were selected to collectively represent the diversity of glacier types and climatic responses evident statewide. Additional supporting criteria for inclusion in the list were a rich history of visitation / documentation and relative public accessibility. Since October 2010, the list evolved some under the advice and guidance of NPS staff, particularly including NPS unit resource staff and regional I&M staff.

Table 11. Focus glaciers for each of Alaska's 9 glaciated park units. "Snapshot" briefly denotes unique aspects of each glacier. PI Loso has personal knowledge of "visited" glaciers.

Park	Glacier(s)	Snapshot	Visited
ANIA	Caldera icefields	Only permanent ice in Aniakchak. Virtually unstudied. Tiny.	no
DENA	Kahiltna Glacier	Popular climbing and flightsee route. Non-surging valley glacier.	yes
	Muldrow Glacier	Backcountry accessible surge-type valley glacier.	yes
	Toklat Glacier	Small backcountry accessible glacier with history of NPS study.	no
GAAR	Arrigetch glaciers	High visitation for a remote park. Small, arctic cirque glaciers.	yes
GLBA	Brady Glacier	Remote tidewater glacier with very low-elev accumulation zone.	yes
	Margerie Glacier	Cruise-ship visible, tidewater. High-elev accumulation zone.	yes
	Muir Glacier	Formerly tidewater glacier with spectacular retreat history.	yes
KATM	Knife Creek Glaciers	Unusual tephra-covered glacier with long historic record.	yes
KEFJ	Aialik Glacier	Tidewater glacier with historically stable terminus position.	no
	Exit Glacier	Tourist-popular, on coastal side of Harding Icefield.	yes
KLGO	Nourse Glacier	Outside park; moraine-dammed threatens infrastructure.	no
LACL	Tanaina Glacier	On flightseeing route at Lake Clark Pass. Changing hydrology.	yes
	Tuxedni Glacier	Valley glacier on an active volcano. Remote.	yes
WRST	Bagley Icefield	Huge icefield with multiple distributaries. Remote.	yes
	Kennicott Glacier	Highly visited, tourist-friendly valley glacier. Jokulhlaup history.	yes
	Yahtse Glacier	Tidewater glacier that is currently advancing.	yes

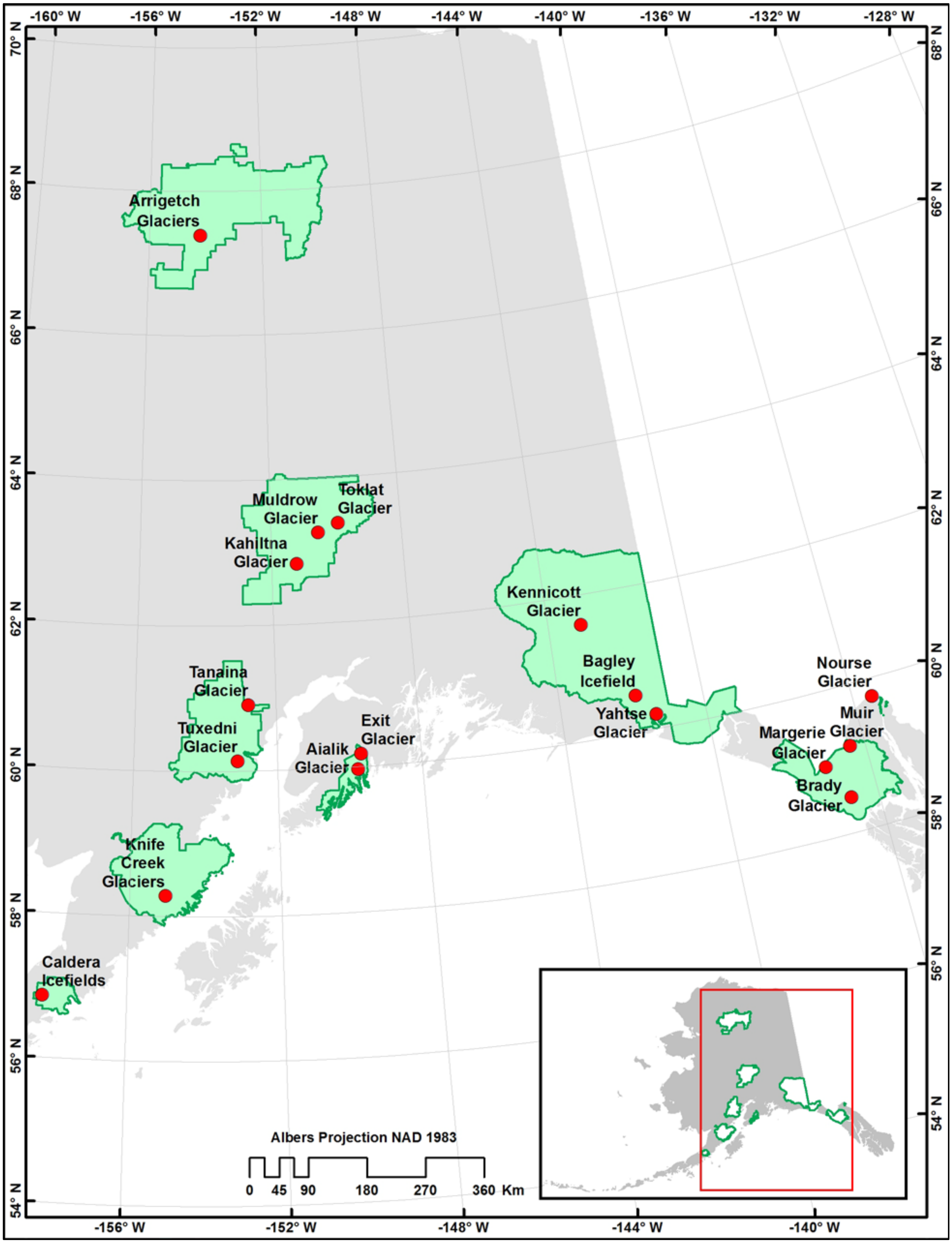

Figure 4. Overview of focus glacier locations. Green polygons are NPS unit outlines.

Fieldwork, Resource Collection, and Development of Vignettes

In summer 2011, PI Loso visited several NPS units to collect existing resource materials and develop first-hand familiarity with some of the focus glaciers. The objectives were to understand the field site geography, collect photographs (including, in some cases, repeat photographs of historic imagery), interview researchers and NPS staff working on or near each glacier, and qualitatively document evidence of landscape change.

The diverse historic and contemporary reference materials necessary for development of the focus glacier vignettes cannot be found solely through traditional library and internet resources; many resources are available only from NPS/NPS-affiliated personnel at the Alaska Regional Office and at the individual parks. Examples of collected materials include:

- Published, peer-reviewed journal articles
- Internal NPS (and occasionally other agency) reports
- Internal NPS unpublished data, when available
- Historic maps
- Satellite and aerial imagery
- Interviews with knowledgeable persons
- Original and historic photography

Results-Mapping

Results of our mapping effort consist of map date and satellite date outlines and associated metadata, as described in the methods section. Below, we first summarize the major statewide trends among all Alaskan park glaciers, then summarize trends in glacier geometry, and finally present results for each park unit individually.

For consistency, we present the same metrics for each park. We begin with a table that simply summarizes glacier numbers, total glacier area, mean and maximum glaciers sizes, and inferred glacier volume for map date and modern outlines. We show changes over time in map view, with a note that the scale and orientation of each map varies from park to park. In all cases, we present the maps at no less than 1:1,000,000 scale. More detailed maps can be generated from the electronic database that accompanies this document. We then summarize the total cumulative glacier cover by elevation, as a frequency distribution, and finally present histograms of glacier numbers grouped by glacier size and glacier mean elevation.

Finally, we note that many of the measures of parkwide glacier numbers and areas differ in this report from the results presented previously in progress reports one to four. This partly reflects updates, refinements, and the availability of additional imagery. The most important source of differences, however, is the fact that our progress reports sometimes included glaciers outside the park boundaries, whereas here we focus solely on glaciers wholly or partly within the parks. In all cases, results from those progress reports should be considered preliminary, and the results presented here take precedence.

Statewide Summary

Statewide, the National Park Service is a steward for 7561 glaciers, by our best count of existing satellite imagery (Table 6). These glaciers collectively cover 43,745 km^2, with glacier sizes averaging 5.8 km^2 but rising to a maximum of 3388 km^2 (the Malaspina Glacier, which we have treated, in the modern mapping, as three separate basins and would therefore count as even larger [4401 km^2] if the three were added together). As is typical of the parks individually, the statewide satellite date inventory shows the seemingly contradictory trend of more glaciers, but less total glacier area, when compared with the map date inventory. When taken at face value, these trends reveal creation of 968 new glaciers (an increase of 15%) and the simultaneous loss of 3725 km^2 glacier area (-8%). As discussed more thoroughly later in this report, this increase in glacier abundance is partly caused by breakup of larger glaciers into multiple, smaller tributaries. We attribute much of this change, however, to high-quality satellite imagery that permitted the mapping of smaller glaciers than were generally visible to the original USGS cartographers.

Table 12. Changes in glacier numbers, total glaciated area, mean/maximum glacier area, and volume for all Alaskan national parks.

Time Period	Number of glaciers	Total glacier area (km^2)	Mean glacier size (km^2)	Max glacier size (km^2)	Total glacier volume (km^3)
Map date	6593	47,469.7	7.2	4700.6	21,034.6
Satellite date	7561	43,745.0	5.8	3388.2	16,880.1
Absolute change	*968*	*-3,724.7*	*-1.4*	*-1,312.4*	*-4,154.5*
Percent change	*15%*	*-8%*	*-20%*	*-28%*	*-20%*

Alaskan park glaciers range in elevation from sea level to nearly 6000 m, but the glacier cover is most abundant between 1000 and 2000 m (Figure 5). The bimodal distribution of glacier elevations, with a secondary peak below 500 m, is a result primarily of the presence of two major glacier lobes near the coast: Malaspina Glacier and Bering Glacier. Glacier cover diminished over time at essentially all elevations, a result primarily of glacier shrinkage but also partly reflecting the changes, for thinning but still extant glaciers, of their surfaces to lower elevations. This loss was most pronounced at and below the modal elevation. Most glaciers lose the most area in their lowest elevations (near their termini), but because this plot reflects the cumulative loss of area from all Park glaciers, including a majority whose termini are much higher than sea level, we see the greatest loss of glacier ice between 500 and 1500 m. When looking at the statewide gain in total number of glaciers, some insight can be gleaned from the distribution of this gain by glacier size and elevation. The added glaciers were overwhelmingly concentrated in the smallest size classes (<0.5 km^2) but appear to be scattered somewhat sporadically through a wide range of elevations (Figure 6).

Comparing the various parks, the most conspicuous result is the clear dominance of Wrangell-St. Elias (Figure 7). WRST has twice as many glaciers as the closest competitor, Lake Clark, and dwarfs by nearly a factor of six the glacier coverage of its nearest competitor for glacier area—Glacier Bay. This result is expected; WRST is the largest park, and averaged over the entire park area it has the lowest mean annual temperature of all parks and the third highest precipitation (it would have the highest precipitation if ignoring the substantial interior portions of the park). Klondike Gold Rush, Aniakchak, and Gates of the Arctic barely show up at the scale of these charts, except for the modest but visible number (but not cover) of glaciers in GAAR, which has many very small glaciers. Katmai and Kenai Fjords occupy a middle range between these barely-glaciated parks and the glacier heavyweights of WRST, LACL, GLBA, and DENA.

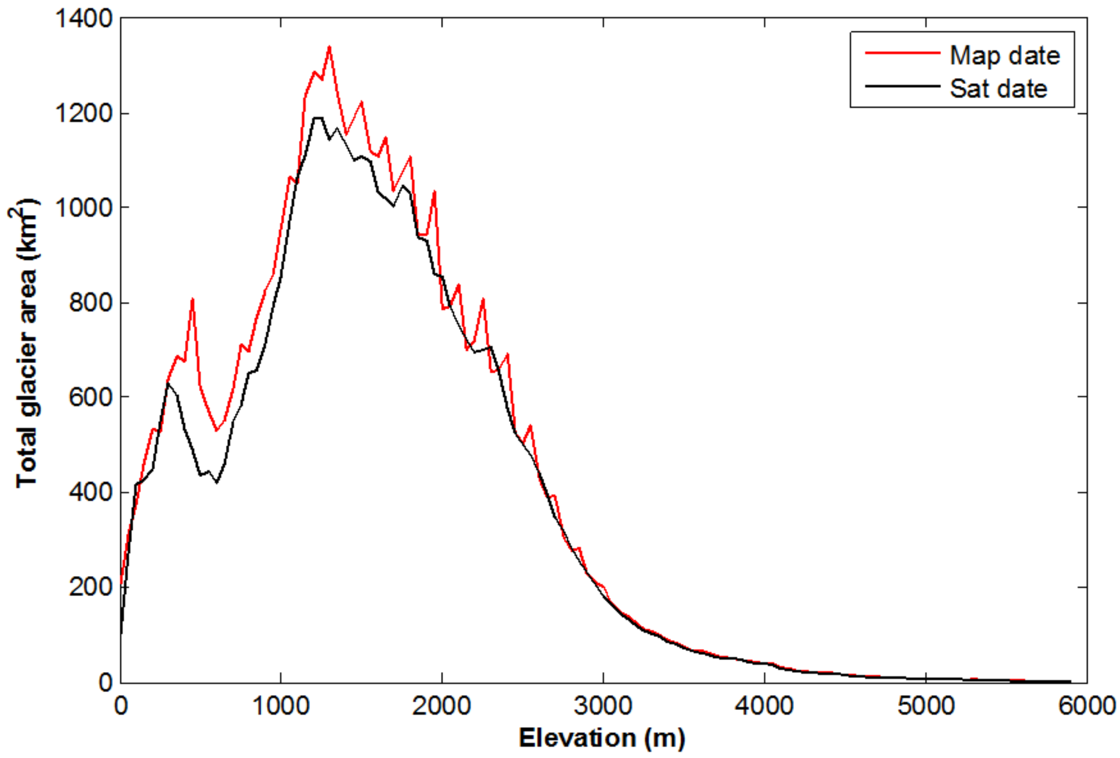

Figure 5. Total glacier-ice coverage by elevation in all Alaskan park units over two time periods.

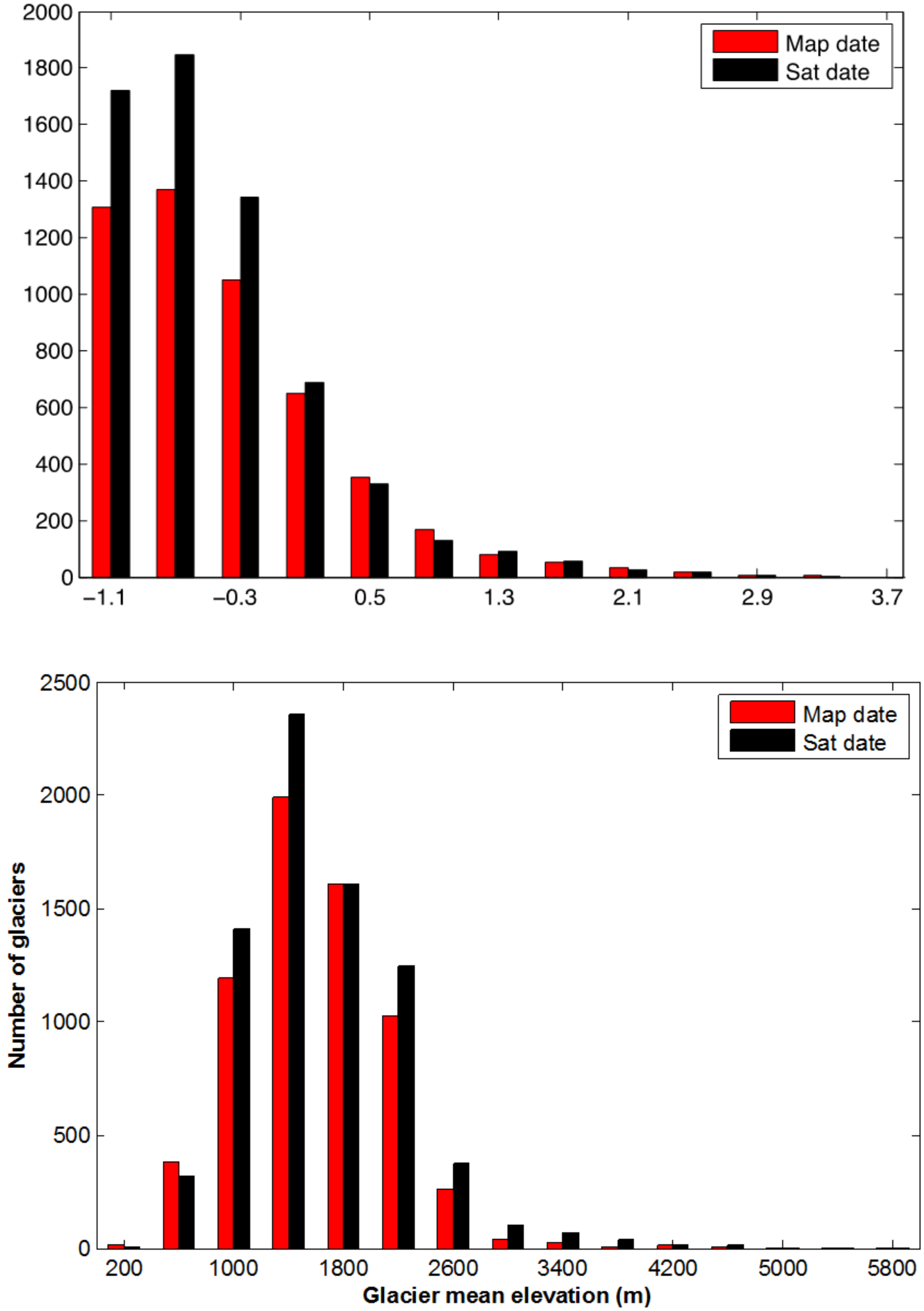

Figure 6. Changes in the numbers of glaciers in all Alaskan National Park units by glacier size (upper panel) and glacier mean elevation (lower panel). Note that the x-axis of the upper panel is logarithmic.

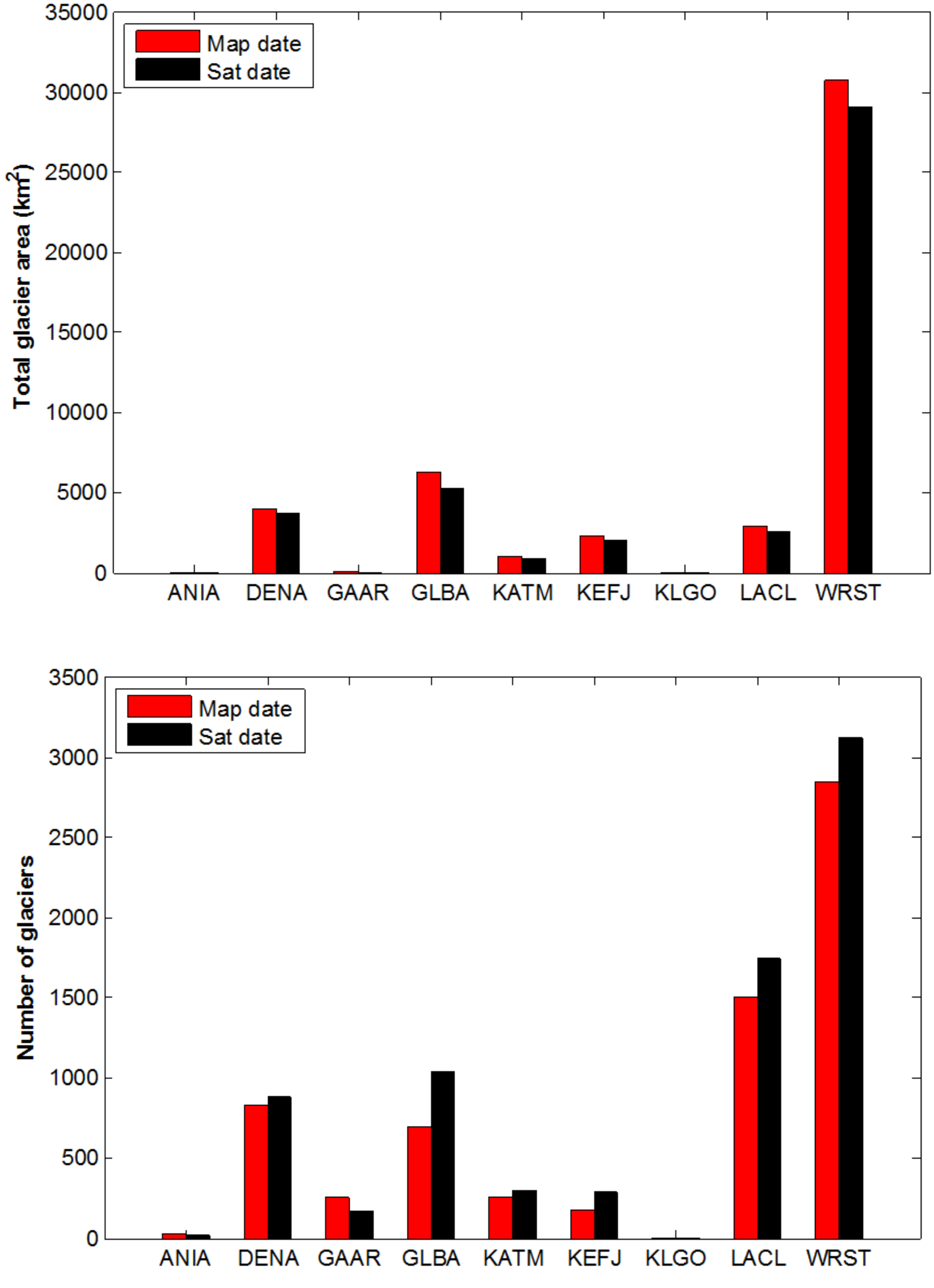

Figure 7. Park by park comparison of glacier area (upper panel) and glacier number (lower panel) over two time periods.

The data presented above, and throughout this report, account for all “park glaciers”, already defined as those with at least some portion of their area within park boundaries. At the request of NPS staff interested in glacier cover solely on NPS land, Table 7 shows glacier coverage clipped to park boundaries. As expected, glacier coverage is smaller, for most parks, than that shown in Table 6.

Table 13. Satellite date glacier cover in nine Alaskan national parks. Glacier areas reported here, unlike the remainder of this report, were clipped at the glacier boundary and therefore include partial glaciers.

Park	Total park area (km^2)	Total glacier area (km^2)	Percent glaciated
ANIA	2,433	5	0.2%
DENA	24,585	3,682	15.0%
GAAR	34,287	54	0.2%
GLBA	13,281	4,068	30.6%
KATM	16,564	913	5.5%
KEFJ	2,711	1,315	48.5%
KLGO	53	1	1.6%
LACL	16,309	2,339	14.3%
WRST	53,321	18,534	34.8%
ALL	163,544	30,910	18.9%

Glacier geometry

Here, we summarize trends in glacier geometry for the park glaciers outlined in our modern dataset. None of the following reflect map date glaciers. We first discuss glacier elevations, then glacier slopes and aspects, and finally glacier centerline lengths.

Distributions of maximum, area-weighted mean, and minimum glacier elevations are depicted by park in Figure 8. The highest maximum glacier elevations are >6000 m (in DENA), followed closely by WRST. Median area-weighted mean elevations range from ~800 m in ANIA to ~2000 m in WRST. The lowest minimum elevations are tidewater glaciers in GLBA, KEFJ, and WRST. Statistically, such glaciers in GLBA and WRST are outliers, but in KEFJ they are included within the interquartile range, reflecting the relative importance of such glaciers in that park.

Area-averaged glacier slopes are shown in Figure 9 as functions of glacier area and glacier mean elevation. The smallest (<1 km^2) glaciers tend to be the steepest, with average slopes greater than about 25°. Most glaciers larger than 1 km^2 have average slopes between 10 and 25°, and the largest glaciers (>100 km^2) range from 5 to 15°. Glaciers with mean elevations of up to about 2500 m show no strong trend in average slope, but the highest elevation glaciers (>2500 m) do tend to be the steepest, with typical slopes of 40° up to a maximum of nearly 60°. The two panels in Figure 9, taken together, show clearly that the steepest glaciers tend to be both small and high.

Note that the metric for glacier slope shown in Figure 9 is area-averaged glacier-wide slope. An alternative measure is glacier centerline slope, where the slope is defined simply as the quotient of glacier elevation range (maximum elevation minus minimum elevation) and glacier centerline length (for the longest branch). The two measures of slope are closely correlated, as would be expected, but area-averaged slope is typically slightly greater than glacier centerline slope

(Figure 10). We interpret this as reflecting the contribution of relatively steep glacier margins, particularly in upper elevations of many mountain glaciers.

The distribution of average glacier aspects in all parks (Figure 11) is strongly dominated by north facing slopes, as would be expected in a northerly state where most solar radiation is concentrated on south facing slopes. We emphasize that the distributions shown here reflect glacier-wide averages, where each glacier—regardless of size— is represented by a single aspect that reflects the average slope direction of every pixel in the glacier's DEM. The most common single aspect bin is NNE, but the mean of all average glacier aspects (red line in Figure 11) is NNW, reflecting the small but relatively larger group of west facing glaciers compared with east facing glaciers. We do not show the distributions by individual park because they closely mimic the parkwide trend. The only exception is Gates of the Arctic. Glaciers in GAAR represent an extreme version of the parkwide trend: north facing glaciers not only dominate, but are almost exclusively present. South facing glaciers are essentially absent from GAAR, and >50% of the glaciers are in the single NNE facing bin.

Glacier centerline lengths are fairly consistent among parks (Figure 12), at least in terms of the central tendency of each park's distribution. Very long outliers are most notable in in DENA, GLBA, and WRST (with the longest glacier at ~200 km), but for all parks the median glacier length is around 1 km. Perhaps surprisingly, the park with longest median centerline length is KATM (excluding KLGO, whose distribution reflects only a single glacier). GAAR has the shortest.

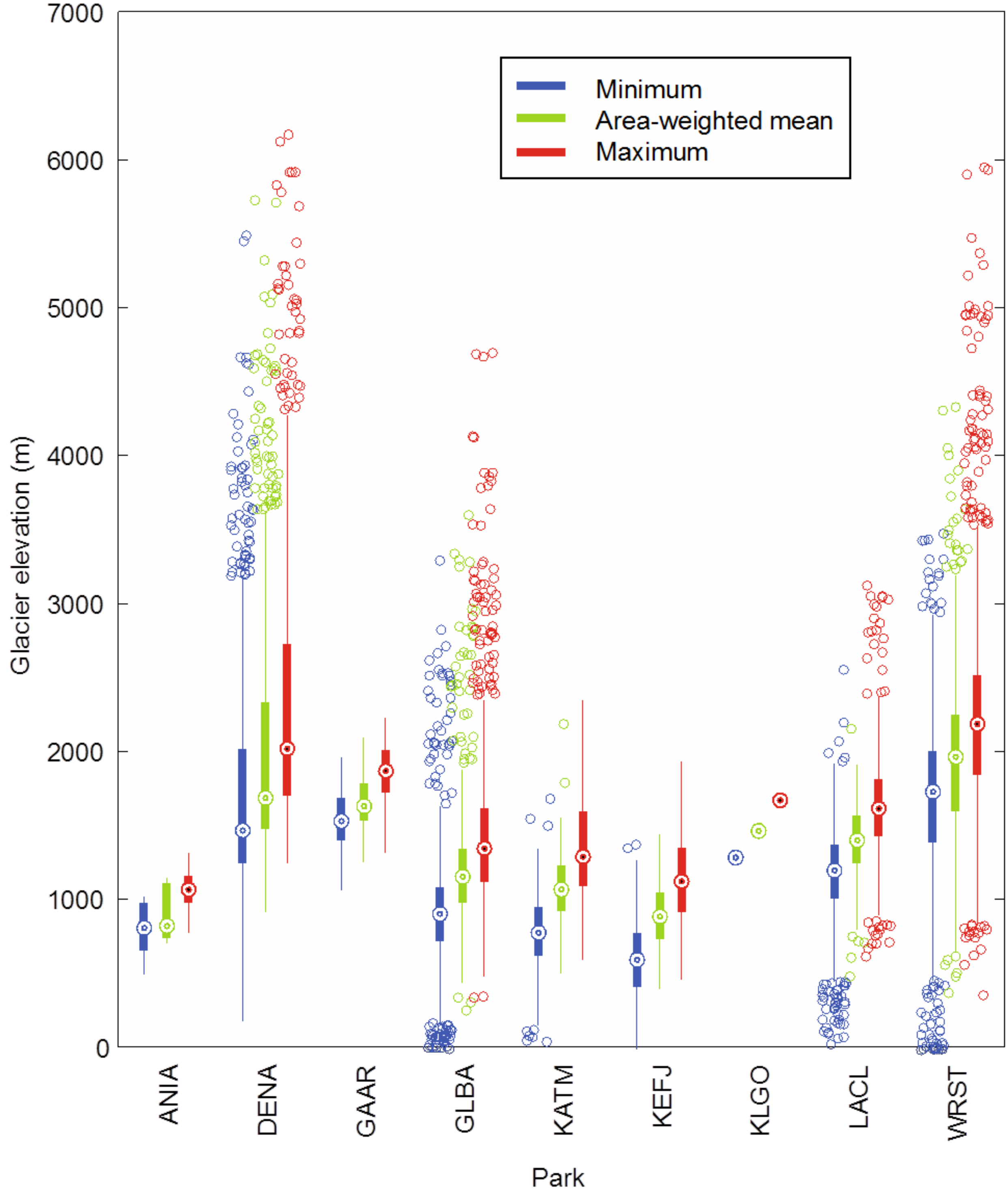

Figure 8. Boxplots showing distributions of glaciers in each Alaskan national park on basis of glacier minimum elevation (blue), area-weighted mean elevation (green), and maximum elevation (red). Filled bars include all data between the 25th and 75th percentile and show the median as a white dot; whiskers include all data within +/- 2.7σ.

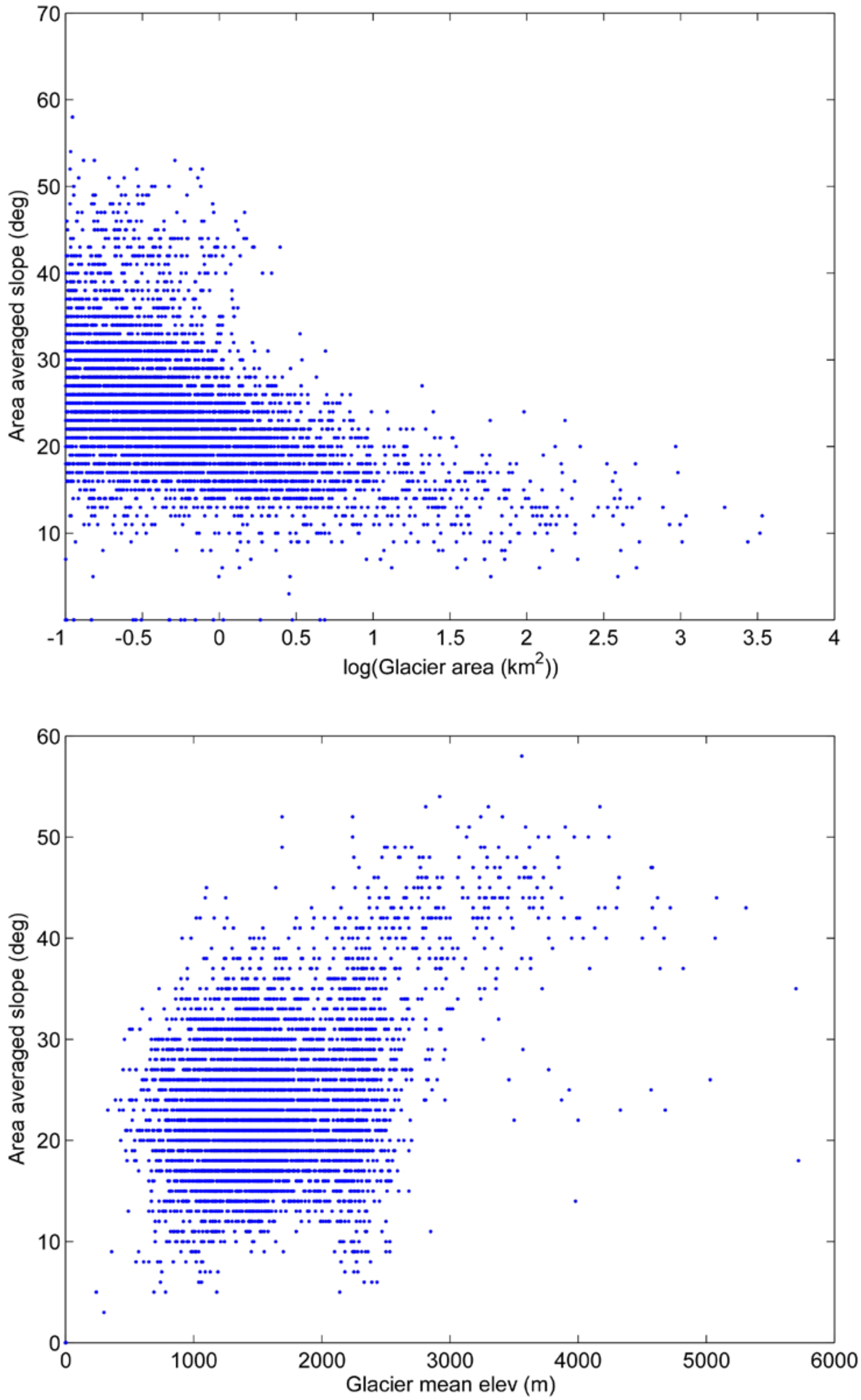

Figure 9. Scatterplots of area-averaged glacier surface slope, where each dot represents the mean for a single glacier, as functions of glacier area (upper panel) and glacier mean elevation (lower panel). Plots include data for all glaciers in the Alaskan parks. Note the x-axis of the upper panel is logarithmic.

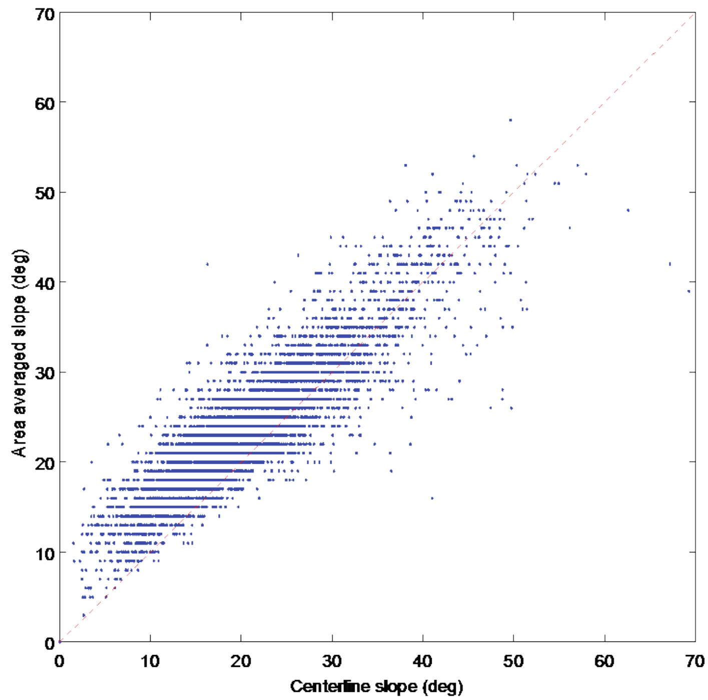

Figure 10. Scatterplot of area-averaged glacier surface slope, where each dot represents the mean for a single glacier, as a function of glacier centerline slope. Red dashed line depicts a one-to-one correspondence between the two measures of slope. The preponderance of points above the line indicates that area-averaged glacier-wide slopes are typically greater than a simple measure of average slope along the glacier centerline.

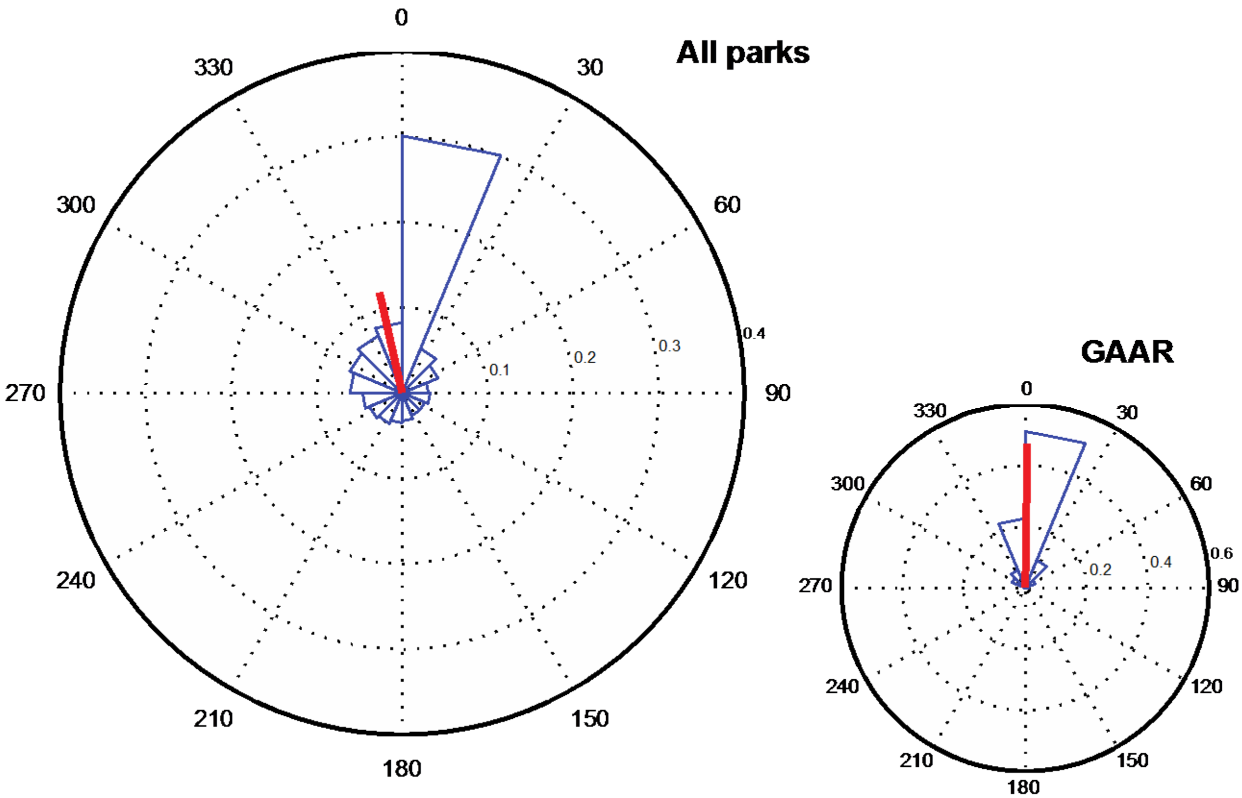

Figure 11. Aspect histograms for all glaciers in all parks (large plot at left) and Gates of the Arctic (right). Most parks individually closely resemble the overall pattern shown here, where the mean glacier aspect (red line) is to the NNW and the most common single aspect in NNE. Gates of the Arctic is the slightly unique among other park units in having virtually no south facing glaciers at all. In both plots, small font figures along ENE axis scale the dotted circular lines with proportions of the population's glaciers in a given bin.

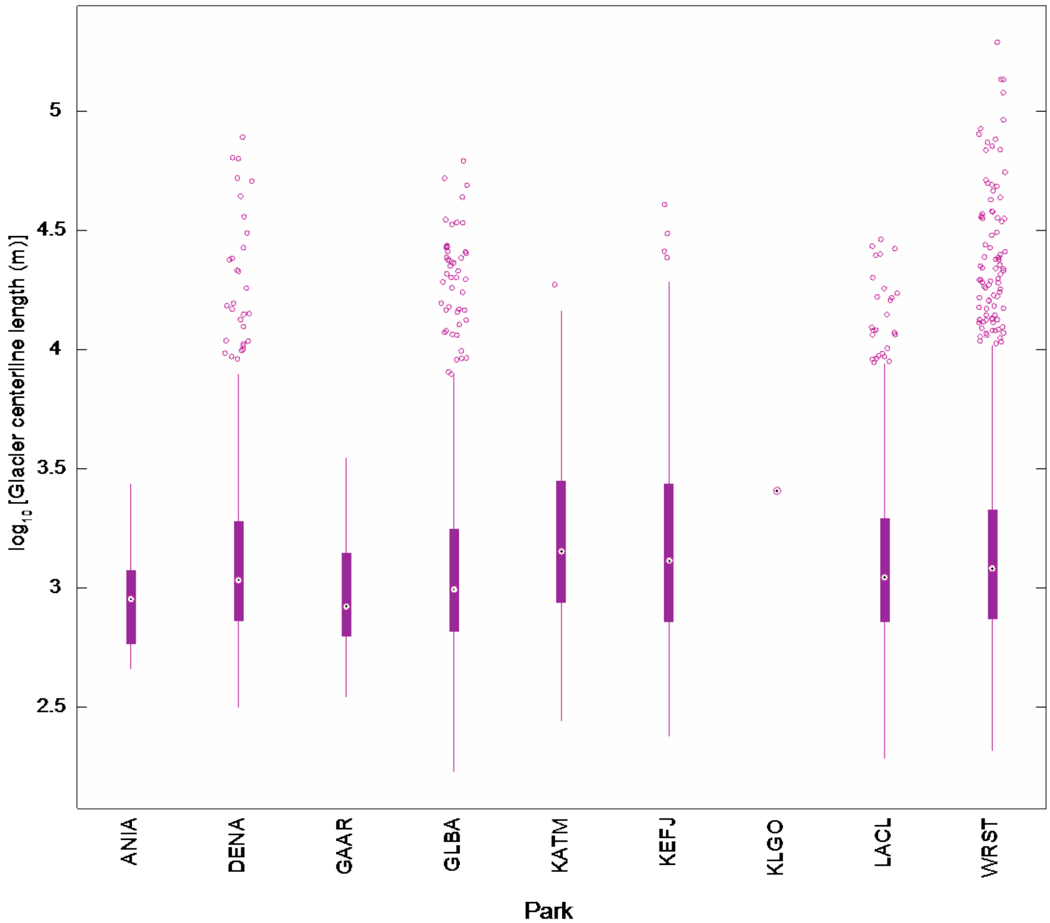

Figure 12. Boxplots of glacier centerline lengths for the longest branch of each glacier in the nine national parks. Filled bars include all data between the 25th and 75th percentile and show the median as a white dot; whiskers include all data within +/- 2.7σ. Note that the y-axis is logarithmic.

Aniakchak National Monument and Preserve

Mapped outlines for ANIA are shown in Figure 14 and summarized in Table 8. Aniakchak has few glaciers overall—16 in satellite imagery—but that number has diminished over time, from 29 in the map era. Total glacier area, on the other hand, increased slightly from 4.1 to 4.6 km^2. Interestingly, the changes in glacier number and coverage differ strongly across the park: small glaciers in the low peaks of the Aleutian Range on the eastern boundary of the park primarily shrank or disappeared, while larger glaciers in the caldera proper either grew or were mapped for the first time in satellite imagery.

These observations, and those that follow from plots of glacier coverage by elevation (Figure 16) and histograms of glacier numbers by glacier size and elevation (Figure 15) should be interpreted with more caution than those of other parks in this report. On the one hand, the map date glaciers in the eastern portion of the park were mapped by the original cartographers from a very early season aerial photograph with substantial lingering snow cover that we believe led to the mapping of glacier ice where there may have been none (only five of 29 original glaciers are visible there in modern imagery). On the other, the larger ice masses mapped in the caldera proper are substantially debris-covered and visible only in very high-resolution, late season imagery that permits imaging of distinct crevasses and other features indicative of buried glacier ice Figure 13. We are certain that these glaciers were present at the time of the original mapping.

We therefore have much greater confidence in the satellite date outlines than in the map date outlines, and advise that the implied changes over time should, in this park, be disregarded. What can be said with confidence is that today the glacial ice in Aniakchak is confined to 16 individual glaciers that collectively cover barely 4 square km in and along the margins of the caldera at elevations ranging from ~500-1500 m.

Table 14. Changes in glacier numbers, total glaciated area, mean/maximum glacier area, and volume for Aniakchak.

Time Period	Number of glaciers	Total glacier area (km^2)	Mean glacier size (km^2)	Max glacier size (km^2)	Total glacier volume (km^3)
Map date	29	4.1	0.1	0.8	0.1
Satellite date	16	4.6	0.3	2.6	0.2
Absolute change	*-13*	*0.6*	*0.2*	*1.8*	*0.1*
Percent change	*-45%*	*14%*	*115%*	*221%*	*93%*

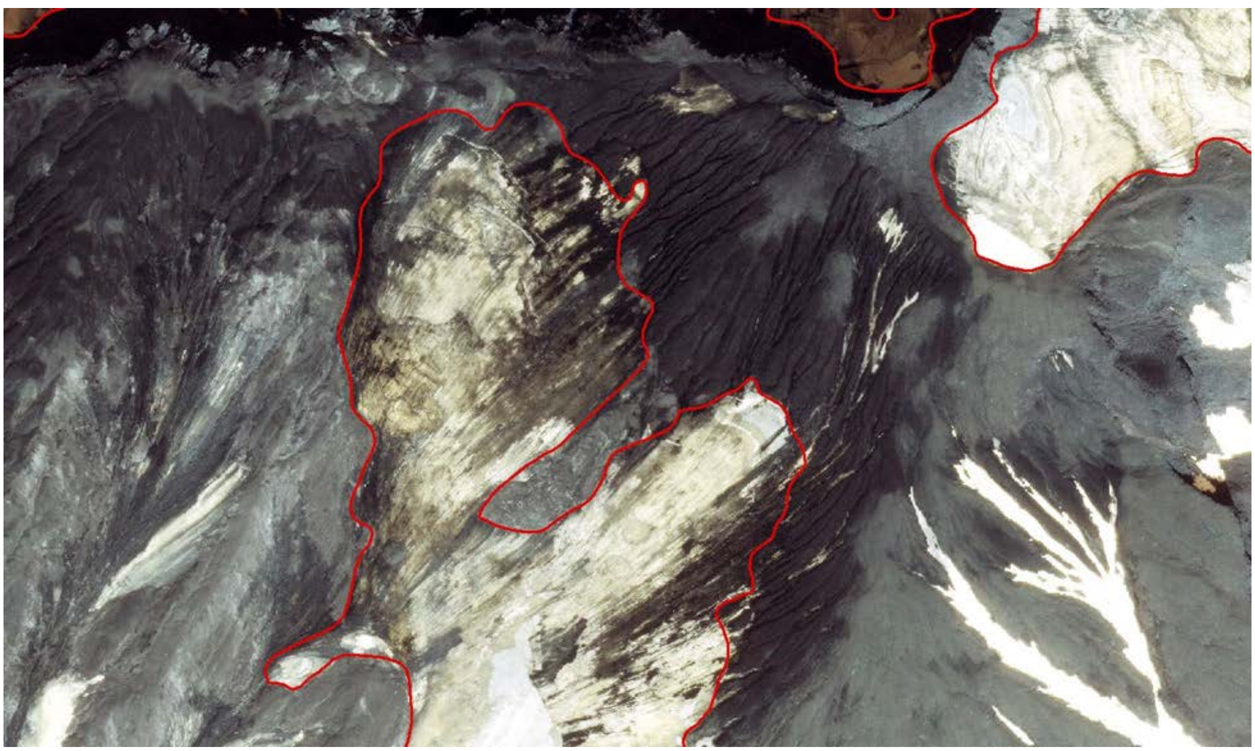

Figure 13. Screen capture from high-resolution satellite imagery clearly showing crevasses in the obscure, dirty surface of a glacier in the Aniakchak caldera.

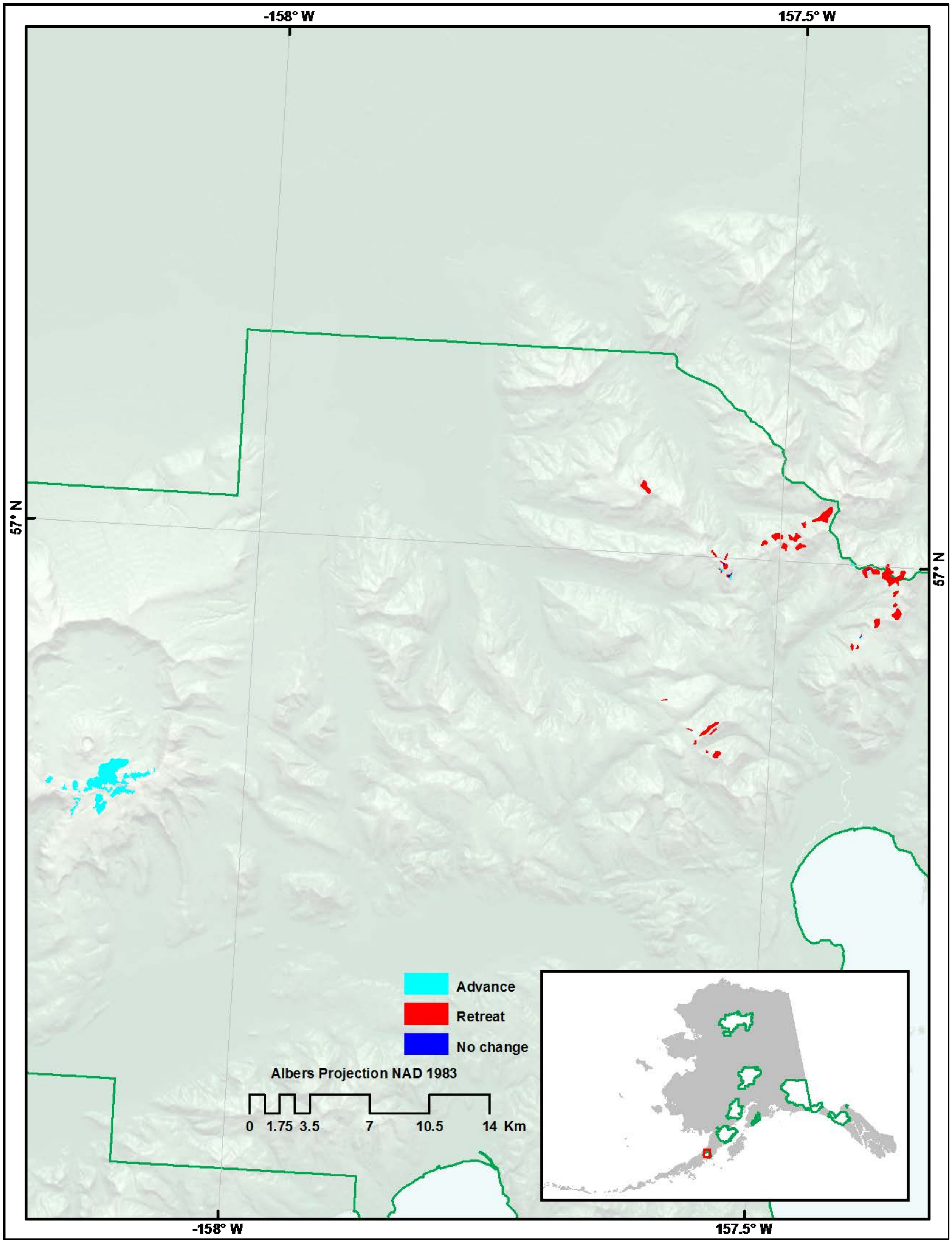

Figure 14. Changes in mapped glacier extent from map date to satellite date in Aniakchak.

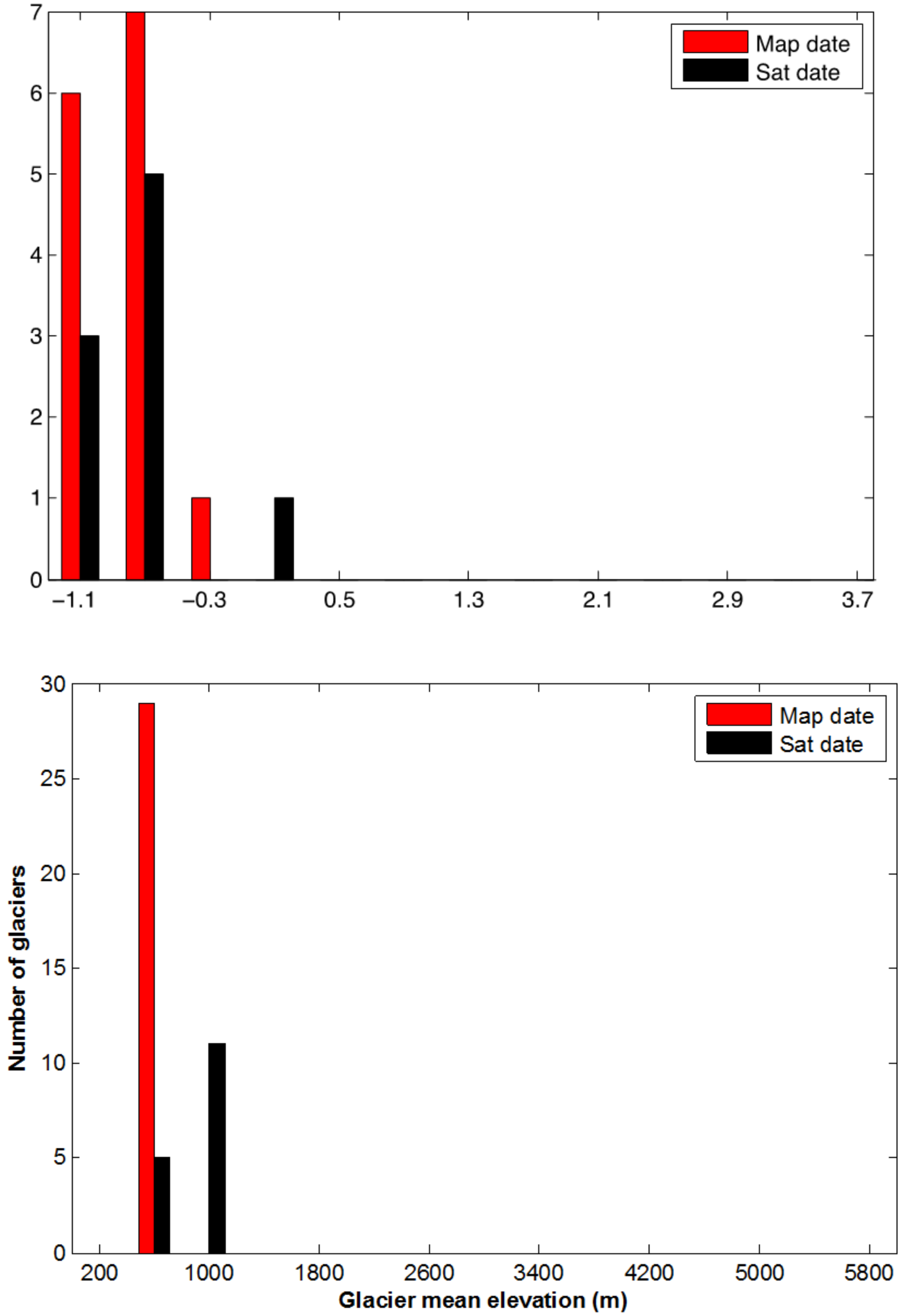

Figure 15. Changes in the numbers of glaciers in Aniakchak NM&P by glacier size (upper panel) and glacier mean elevation (lower panel). Note that the x-axis of the upper panel is logarithmic.

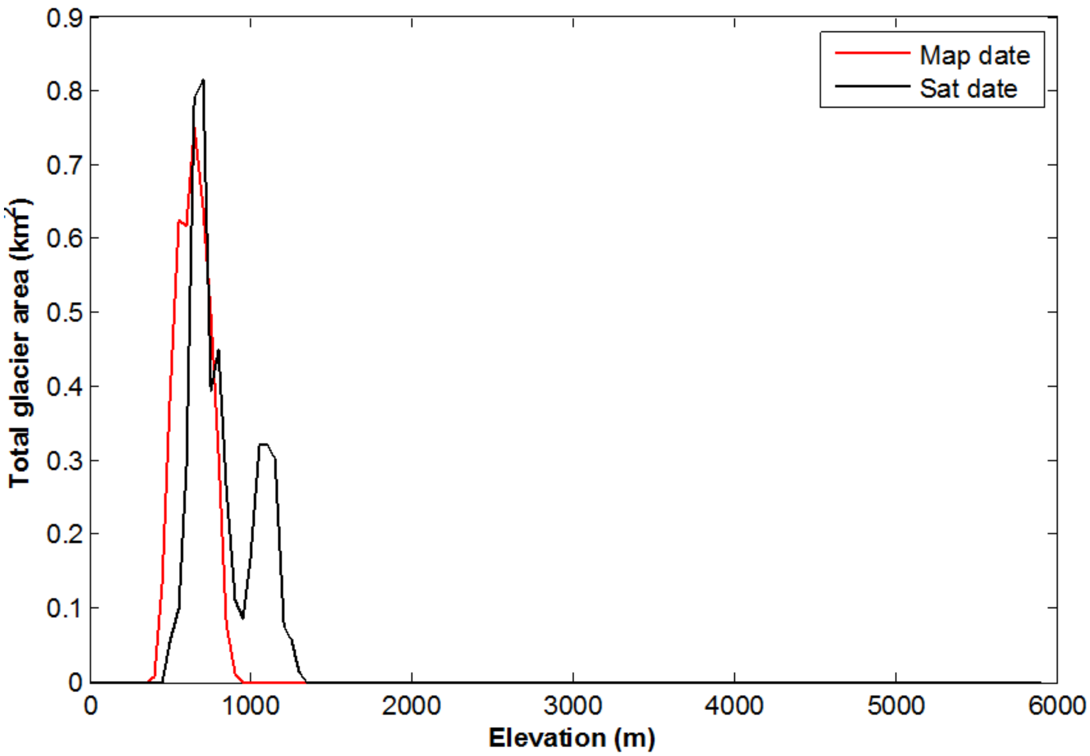

Figure 16. Total glacier-ice coverage by elevation in Aniakchak NM&P over two time periods.

Denali National Park and Preserve

Mapped outlines for DENA are shown in Figure 19 and summarized in Table 9. In total, Denali had 835 map date glaciers and just slightly more—881—in satellite date imagery. Total ice-covered area decreased over that time interval by 8%, from a high of 4038 km^2, at which time we estimate a glacier volume of approximately 1,046 km^3. Terminus retreat was the type of change seen in most individual glaciers, but the Muldrow and Peters Glaciers exhibit evidence of substantial terminus expansion. Because many of the glaciers in Denali, particularly on the north side of the Alaska Range, are surge-type glaciers that periodically transport large amounts of accumulated mass from an upper reservoir area to the lower terminus area, it is tempting to view these terminus expansions as evidence of surges. But it appears likely that the expansions we mapped are primarily due to the decision, by early USGS cartographers, to exclude substantial amounts of debris-covered ice from their mapped glaciers (Muldrow Glacier provides a well-documented example; Figure 17).

These overall changes in area are summarized on a per-glacier basis in Figure 20. Ranking glaciers by size (top panel), small to medium-sized glaciers increased in abundance while abundance of large glaciers was mostly unchanged. Ranking them by area-weighted mean elevation (bottom panel), low-elevation glaciers diminished in abundance, mid-elevation (~1500 m) glaciers did not change much, and higher-elevation glaciers increased in numbers. Cumulative changes in total area of glaciers, by elevation, are shown in Figure 18 and are probably the best indicator of overall change in glaciers in the park. Total ice cover is most abundant around 1500 m and extends to the highest glacier cover in Alaska, on Mt. McKinley's

Table 15. Changes in glacier numbers, total glaciated area, mean/maximum glacier area, and volume for Denali.

Time Period	Number of glaciers	Total glacier area (km^2)	Mean glacier size (km^2)	Max glacier size (km^2)	Total glacier volume (km^3)
Map date	835	4,038.2	4.8	531.6	1,046.3
Satellite date	881	3,734.5	4.2	483.8	920.1
Absolute change	*46*	*-303.7*	*-0.6*	*-47.8*	*-126.2*
Percent change	*6%*	*-8%*	*-12%*	*-9%*	*-12%*

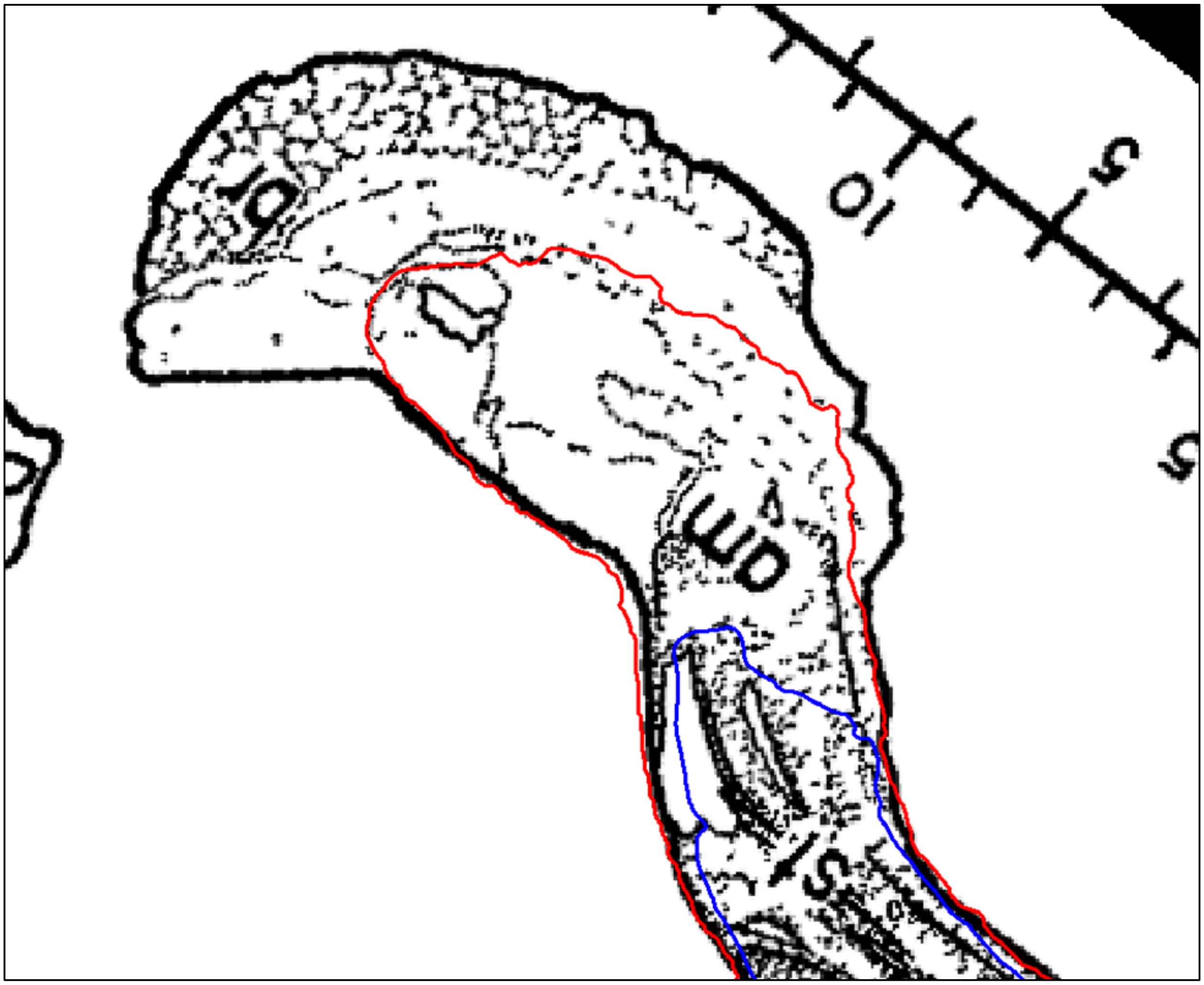

Figure 17. Crudely georeferenced map of the terminus of Muldrow Glacier, circa 1952, from Figure 1 of Post (1960). Overlaid outlines are map date (blue) and satellite date (red). Post's abbreviations are stagnant ice ('st'), ablation moraine ('am'), and brush ('br'). The map date outline was based on 1952 photography that was likely identical to that used by Post, but the USGS cartographers clearly omitted stagnant, debris-covered, and brush-covered ice from their glacier outline. North is up in this image. Muldrow Glacier. Above 3300 m, absolute changes in glacier area overall are almost indistinguishable, and between 1800 and 3000 m glaciers lost a small area. The largest absolute loss of glacier area was between 1400 and 1800 m, and the pattern of change is mixed in sign and magnitude in the lowest elevations.

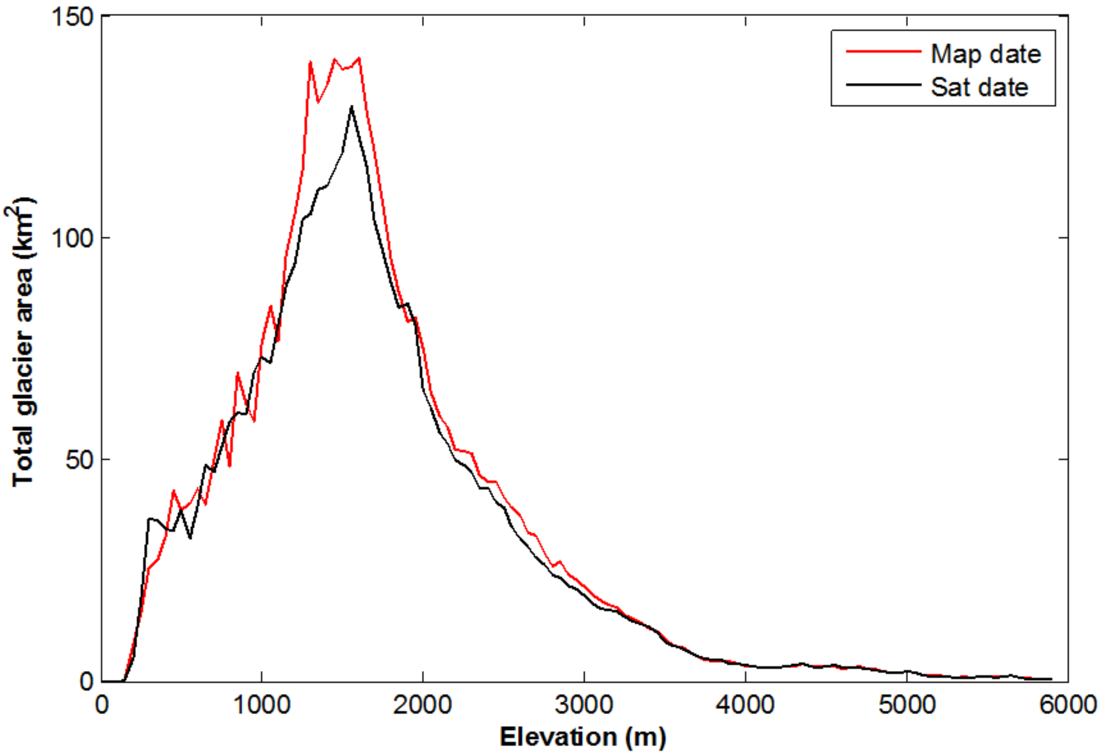

Figure 18. Total glacier-ice coverage by elevation in Denali NP&P over two time periods.

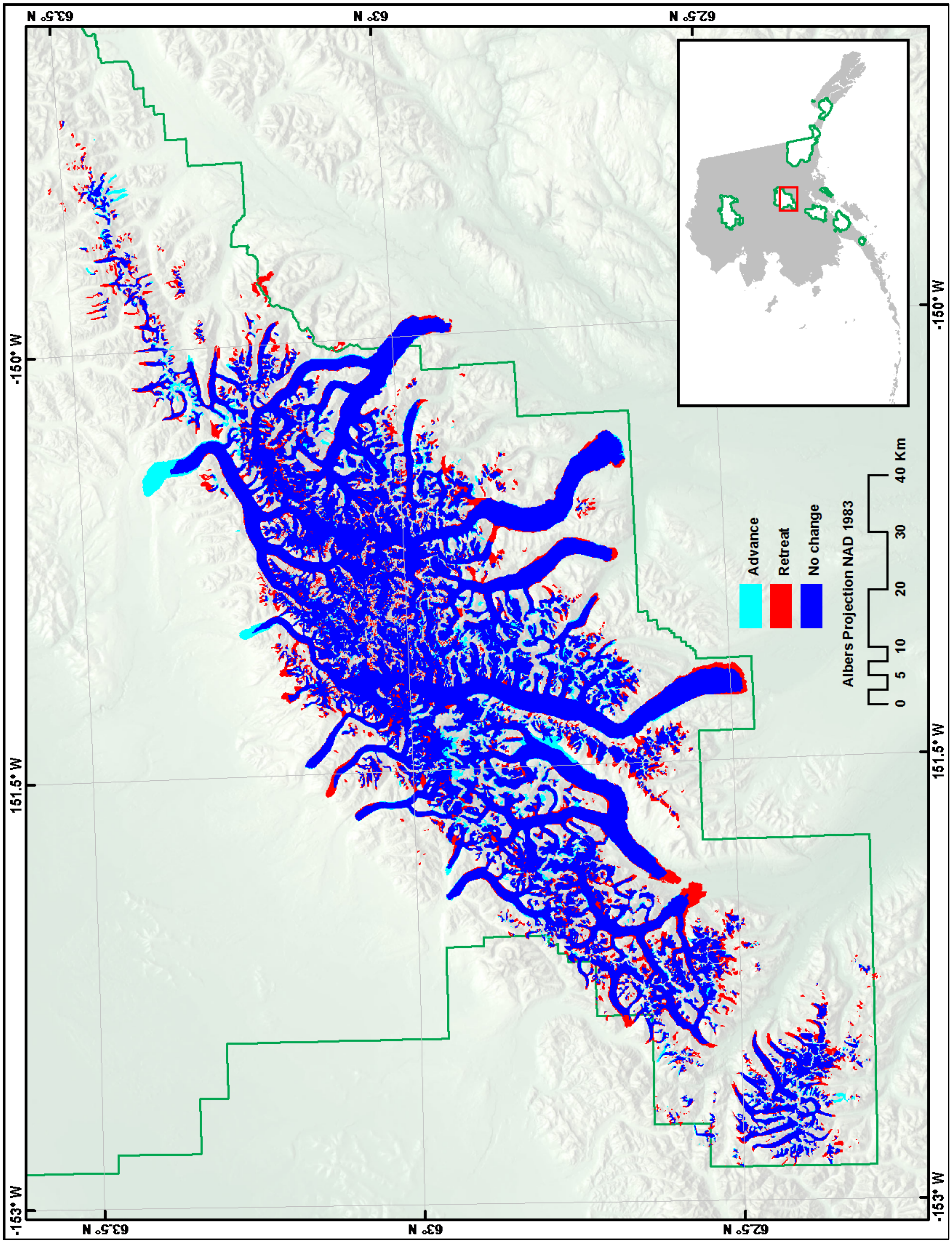

Figure 19. Changes in mapped glacier extent from map date to satellite date in Denali. Note map rotation.

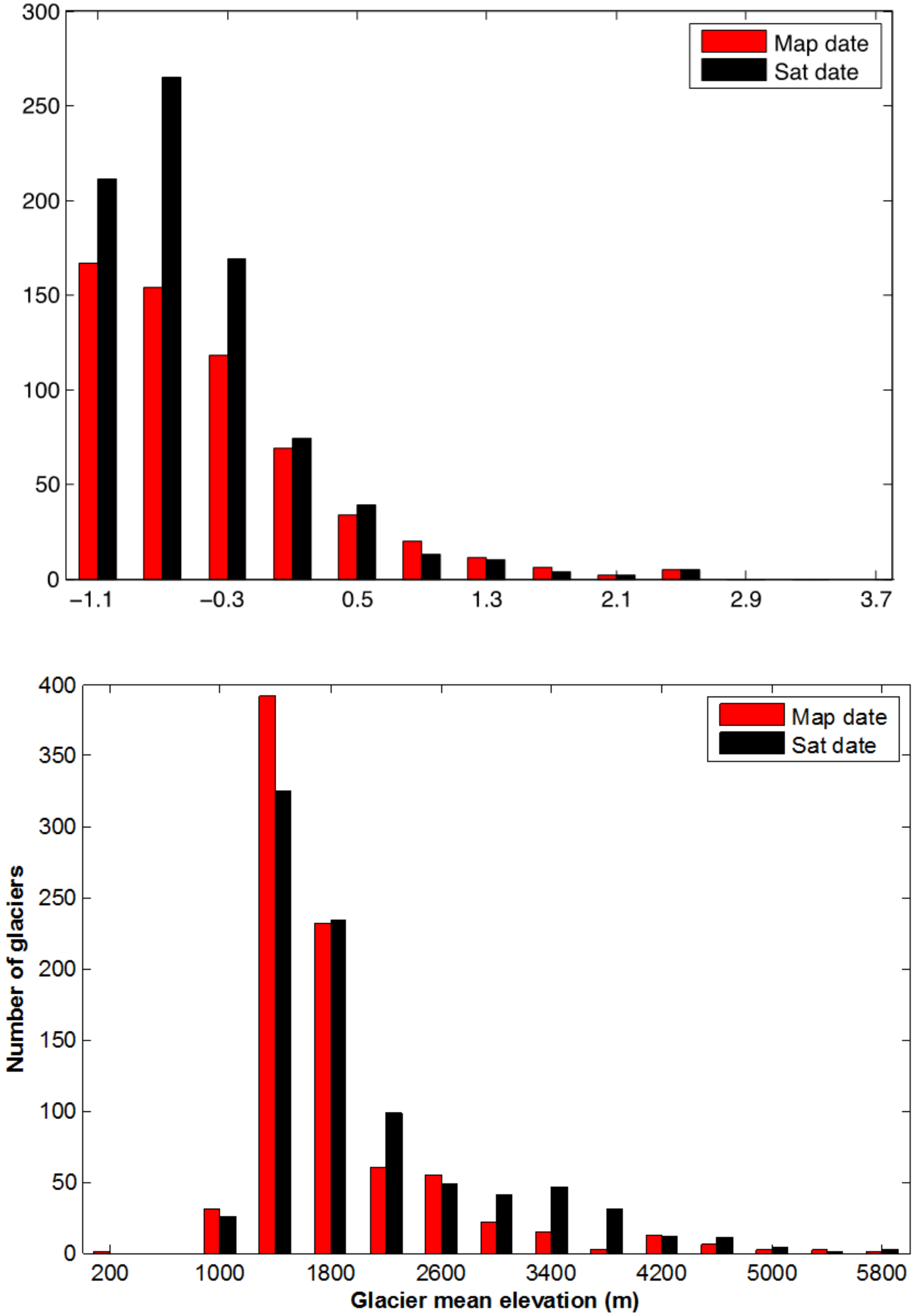

Figure 20. Changes in the numbers of glaciers in Denali NP&P by glacier size (upper panel) and glacier mean elevation (lower panel). Note that the x-axis of the upper panel is logarithmic.

Gates of the Arctic National Park and Preserve

Mapped outlines for Gates of the Arctic NP&P are shown in Figure 21 and Figure 22 and summarized in Table 10. Note that map date photography dates range 1970-1990 for GAAR (Table 3), meaning the described changes are from a shorter time period than in some of the other park units in this study. At both intervals, glaciers are small (average size 0.3 km^2) and scattered throughout the park, barely showing up at the scale of a whole-park map. In total, Gates had 253 map date glaciers and 32% fewer in modern satellite imagery. In that same time, total glacier area decreased 44% from 96 km^2 to 54 km^2. Terminus retreat is an important cause of this glacier area loss, but compared with other Alaskan parks, the diminished glacier cover also prominently reflects the complete disappearance of many glaciers, especially in the northern portion of the park.

These overall changes are summarized on a per-glacier basis in Figure 23. Glaciers of all sizes diminished in abundance, but ranking glaciers by mean elevation we see that the lowest and highest elevation glaciers were the least changed in abundance, while glaciers with a moderate mean elevation diminished most strongly (bottom panel). It is likely that low elevation glaciers in heavily shaded north-facing cirques are less sensitive to increases in air temperature because the lack of solar radiative heating on the surrounding terrain reduces the frequency of above freezing temperatures for these glaciers. Similarly, the highest elevation glaciers may rarely experience above freezing temperatures. These patterns are also reflected by Figure 24, which shows change in total glacier coverage (rather than individual glaciers) as a function of elevation. Ice at and above the modal elevation (1500-1600 m at map date, 1600-1700 m at satellite date) diminished most noticeably, with the least proportional change at the lowest elevations.

Table 16. Changes in glacier numbers, total glaciated area, mean/maximum glacier area, and volume for Gates of the Arctic.

Time Period	Number of glaciers	Total glacier area (km^2)	Mean glacier size (km^2)	Max glacier size (km^2)	Total glacier volume (km^3)
Map date	253	95.6	0.4	2.1	3.0
Satellite date	172	53.9	0.3	2.3	1.6
Absolute change	*-81*	*-41.6*	*-0.1*	*0.3*	*-1.4*
Percent change	*-32%*	*-44%*	*-17%*	*13%*	*-47%*

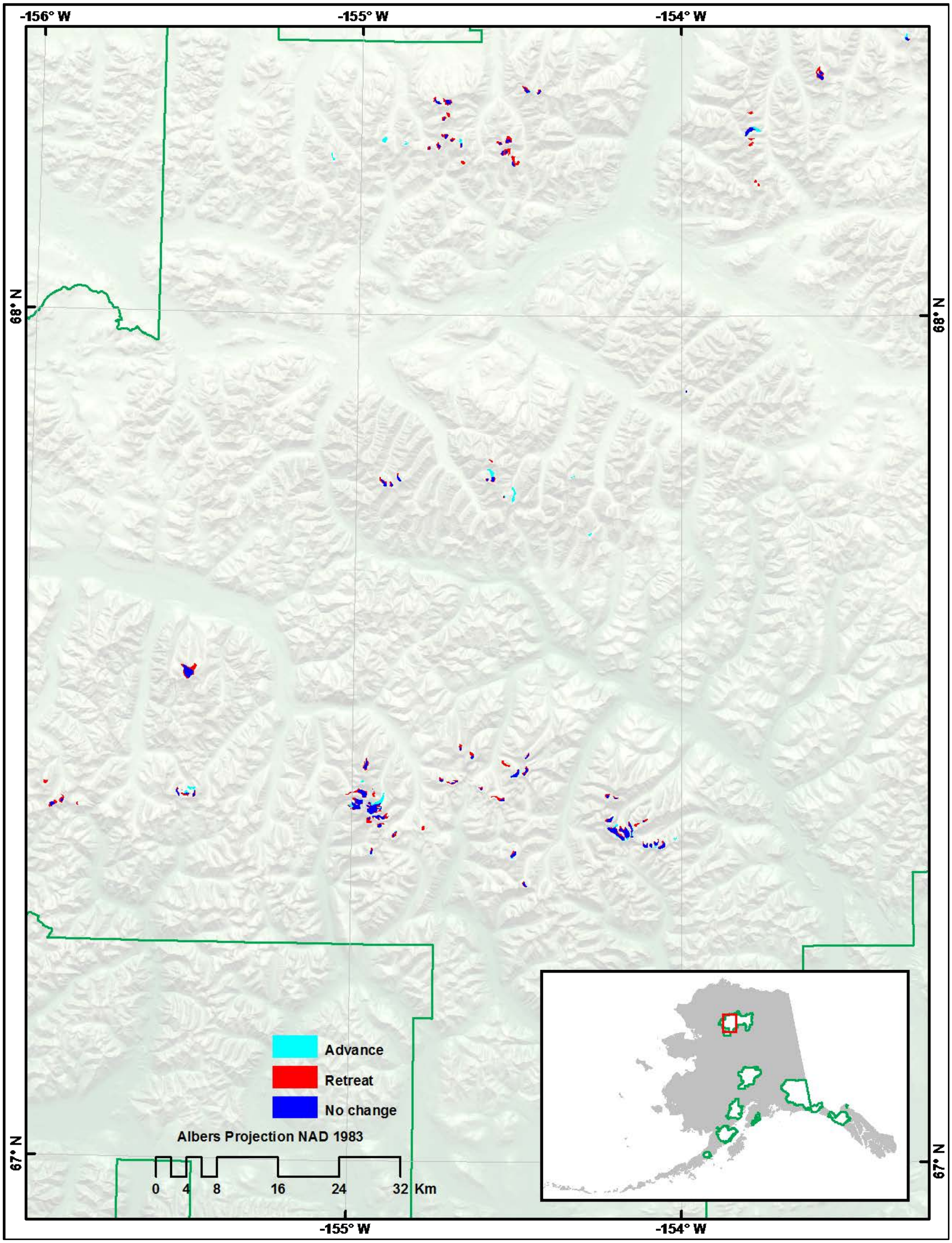

Figure 21. Changes in mapped glacier extent from map date to satellite date in western Gates of the Arctic.

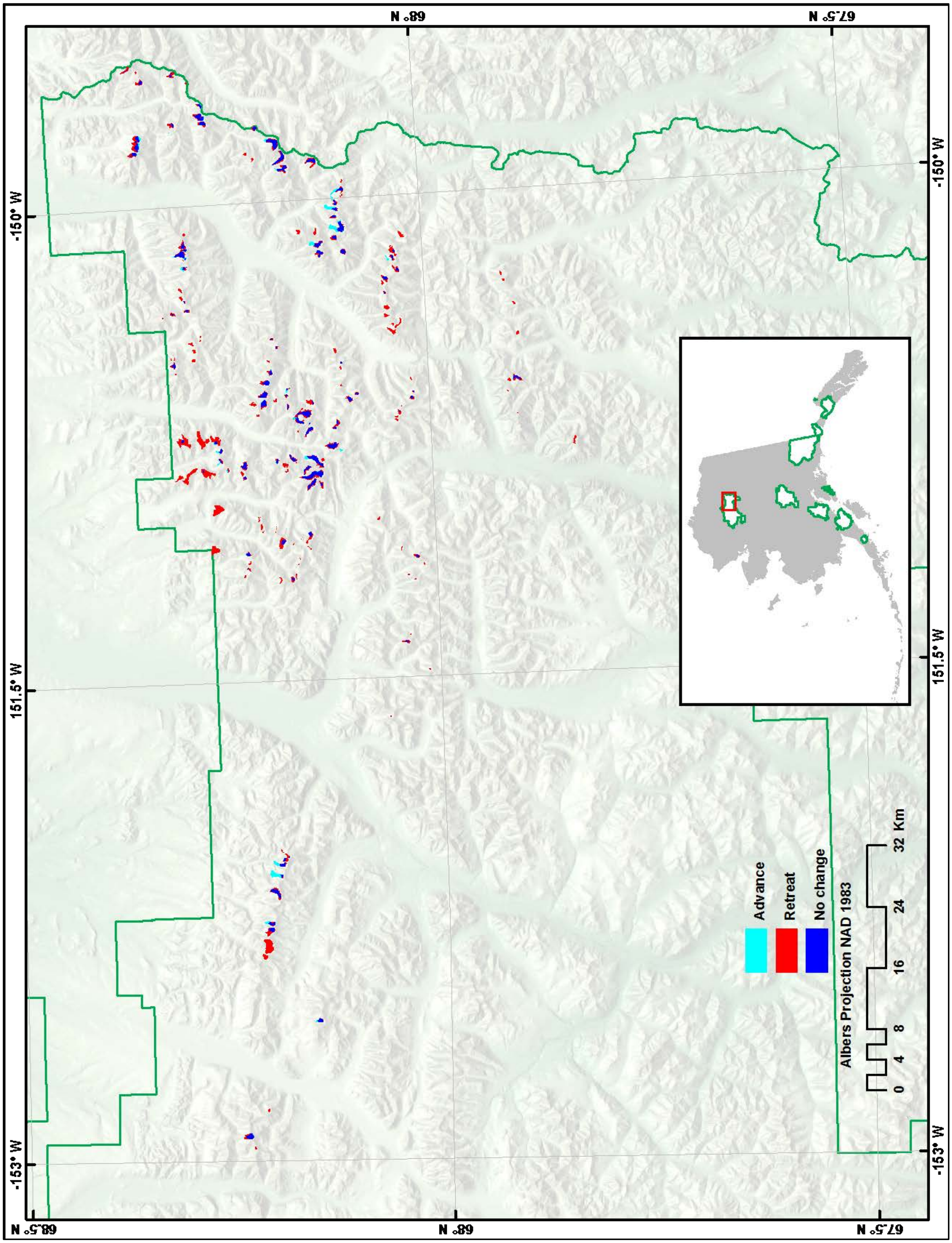

Figure 22. Changes in eastern Gates of the Arctic. Note map rotation.

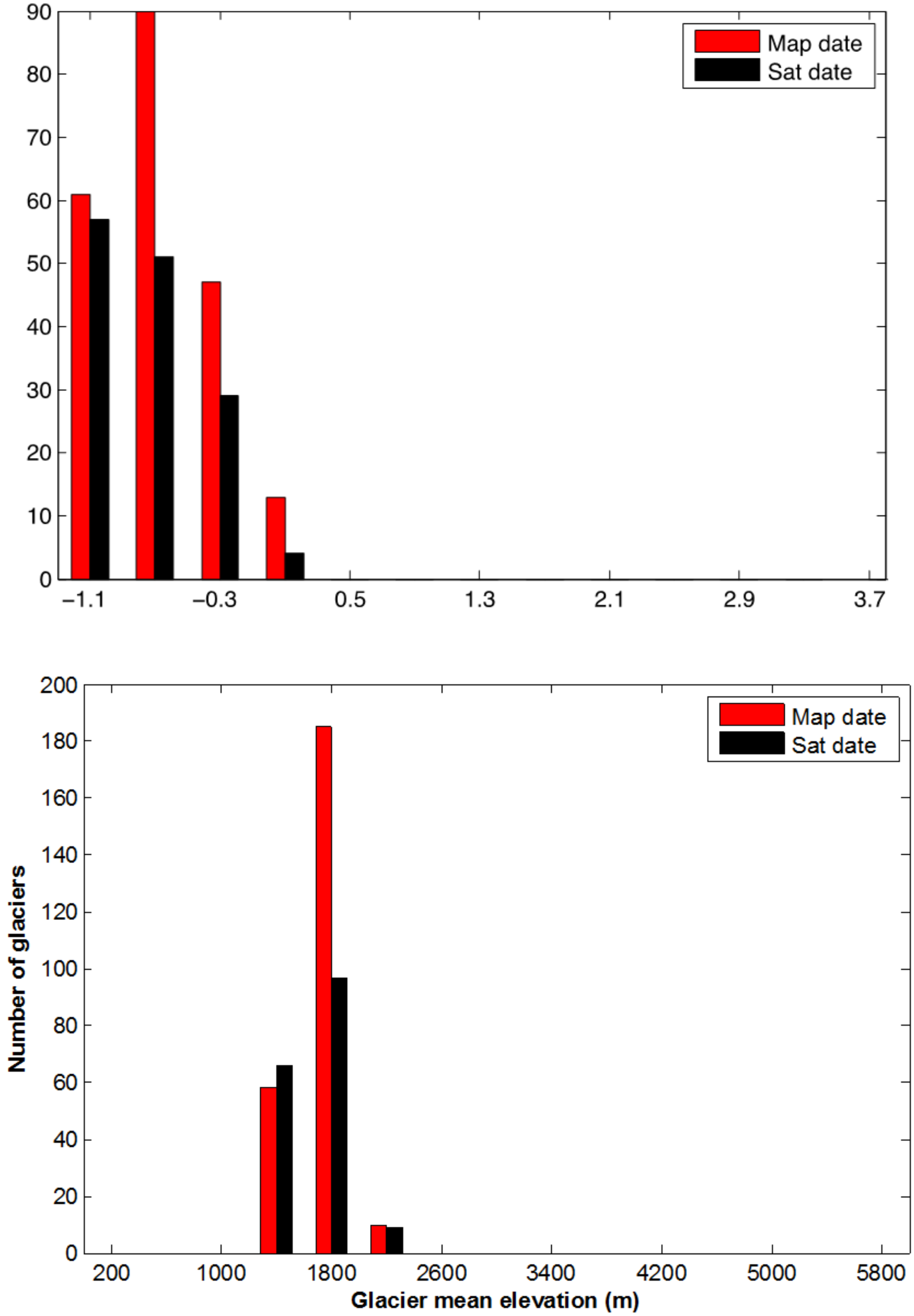

Figure 23. Changes in the numbers of glaciers in Gates of the Arctic NP&P by glacier size (upper panel) and glacier mean elevation (lower panel). Note that the x-axis of the upper panel is logarithmic.

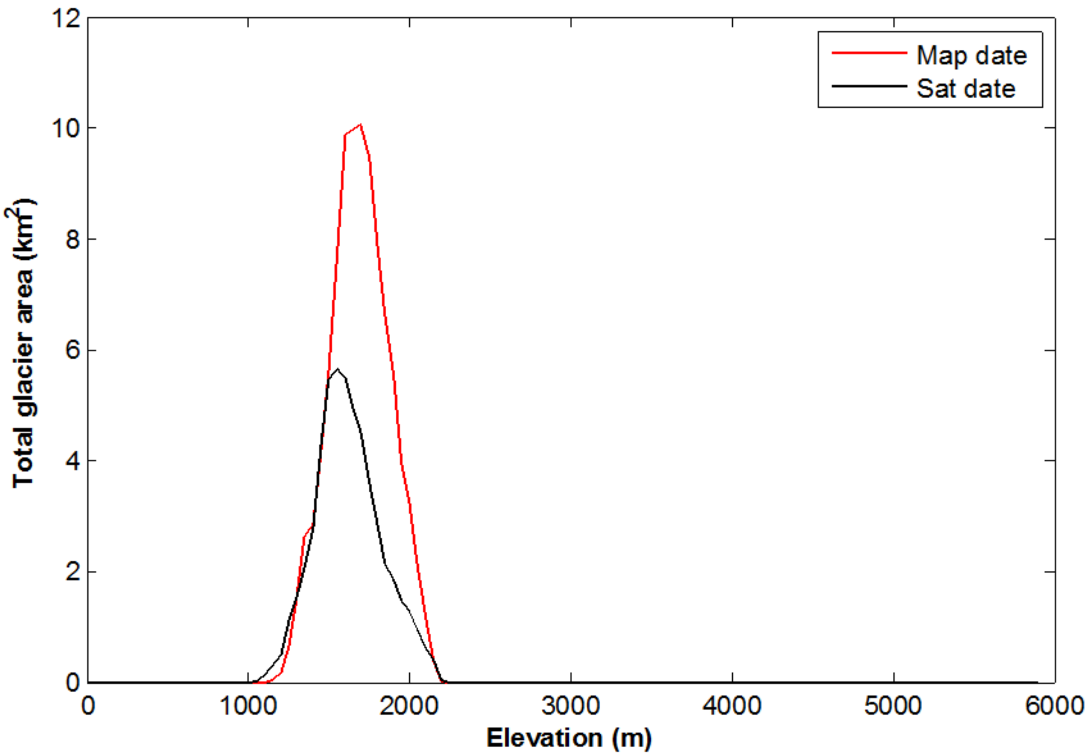

Figure 24. Total glacier-ice coverage by elevation in Gates of the Arctic NP&P over two time periods.

Glacier Bay National Park and Preserve

Mapped outlines for Glacier Bay NP&P are shown in Figure 26 and summarized in Table 11. In total, Glacier Bay had 698 glaciers in original topographic maps (including, as reported elsewhere in this report, all glaciers wholly or partly within the park) and 50% more in recent satellite imagery. However total ice-covered area decreased over that time interval by 15%, from a high of 6285 km^2. As implied by the overall loss of ice-covered area and decrease in mean glacier size, numerous glaciers shrank, primarily through terminus retreat, including notable retreats by Grand Plateau, Desolation, Geikie, Casement, McBride, Burroughs, Plateau, and Muir Glaciers (Figure 26). A few glaciers advanced, too, including significant expansions by Grand Pacific, Johns Hopkins, Lamplugh, Rendu, and North Crillon Glaciers.

Table 17. Changes in glacier numbers, total glaciated area, mean/maximum glacier area, and volume for Glacier Bay.

Time Period	Number of glaciers	Total glacier area (km^2)	Mean glacier size (km^2)	Max glacier size (km^2)	Total glacier volume (km^3)
Map date	698	6,284.5	9.0	641.1	1,689.0
Satellite date	1045	5,323.2	5.1	539.0	1,250.4
Absolute change	*347*	*-961.3*	*-3.9*	*-102.1*	*-438.5*
Percent change	*50%*	*-15%*	*-43%*	*-16%*	*-26%*

These overall changes in area are summarized on a per-glacier basis in Figure 27. Ranking glaciers by size (top panel), small to medium-sized glaciers (up to about 1 km^2) glaciers increased substantially in abundance over time while abundance of large glaciers was mostly unchanged. Ranking them by area-weighted mean elevation (bottom panel), low-elevation glaciers diminished slightly in abundance while mid to high-elevation glaciers became more common. This increase in abundance of small, high-elevation glaciers is partly caused by breakup of larger glaciers into multiple, smaller tributaries. We attribute much of this change, however, to our use of high-quality satellite imagery that permitted the mapping of smaller glaciers than were generally visible to the original USGS cartographers.

The patterns shown in Figure 27 highlight again the difficulty of using glacier numbers (as opposed to cumulative changes in total area) as a reliable metric of overall glacier change. Cumulative changes in total area of glaciers, by elevation, are shown in Figure 25 and probably best reflect the overall change in glaciers in the park. Above 1600 m, absolute changes in glacier area are small, while at lower elevations ice loss dominates. Particularly between 400 and 800 meters, the loss of ice-covered area in the park is substantial.

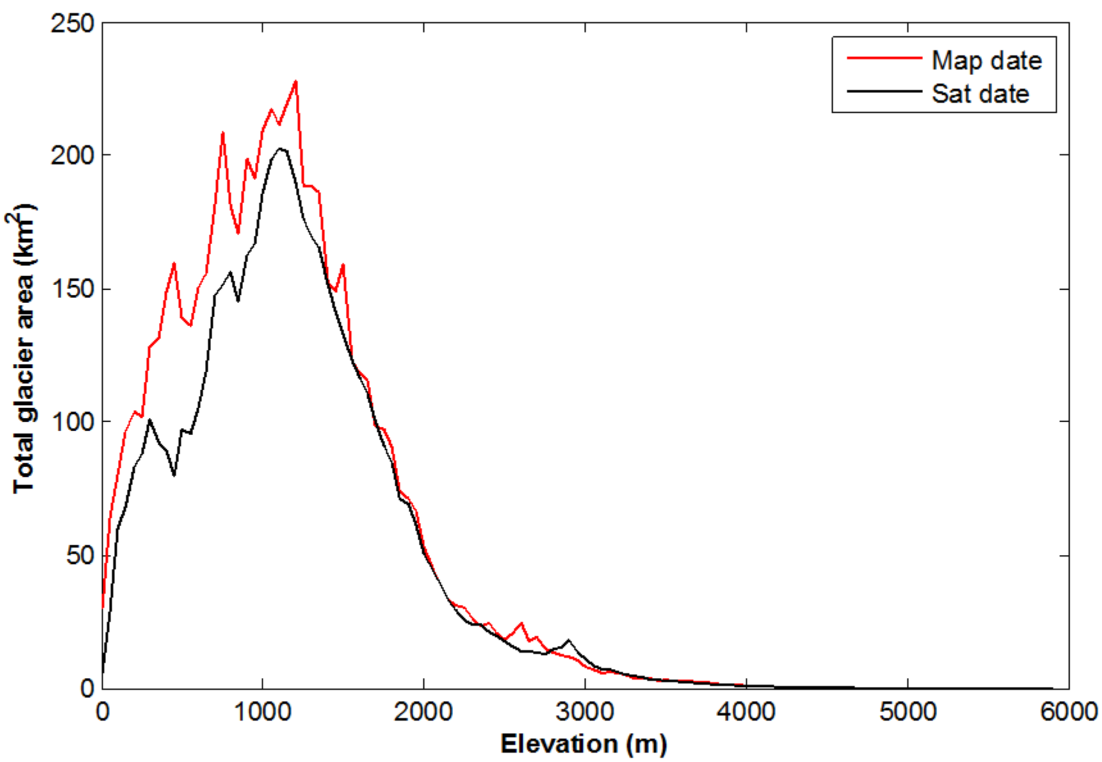

Figure 25. Total glacier-ice coverage by elevation in Glacier Bay NP&P over two time periods.

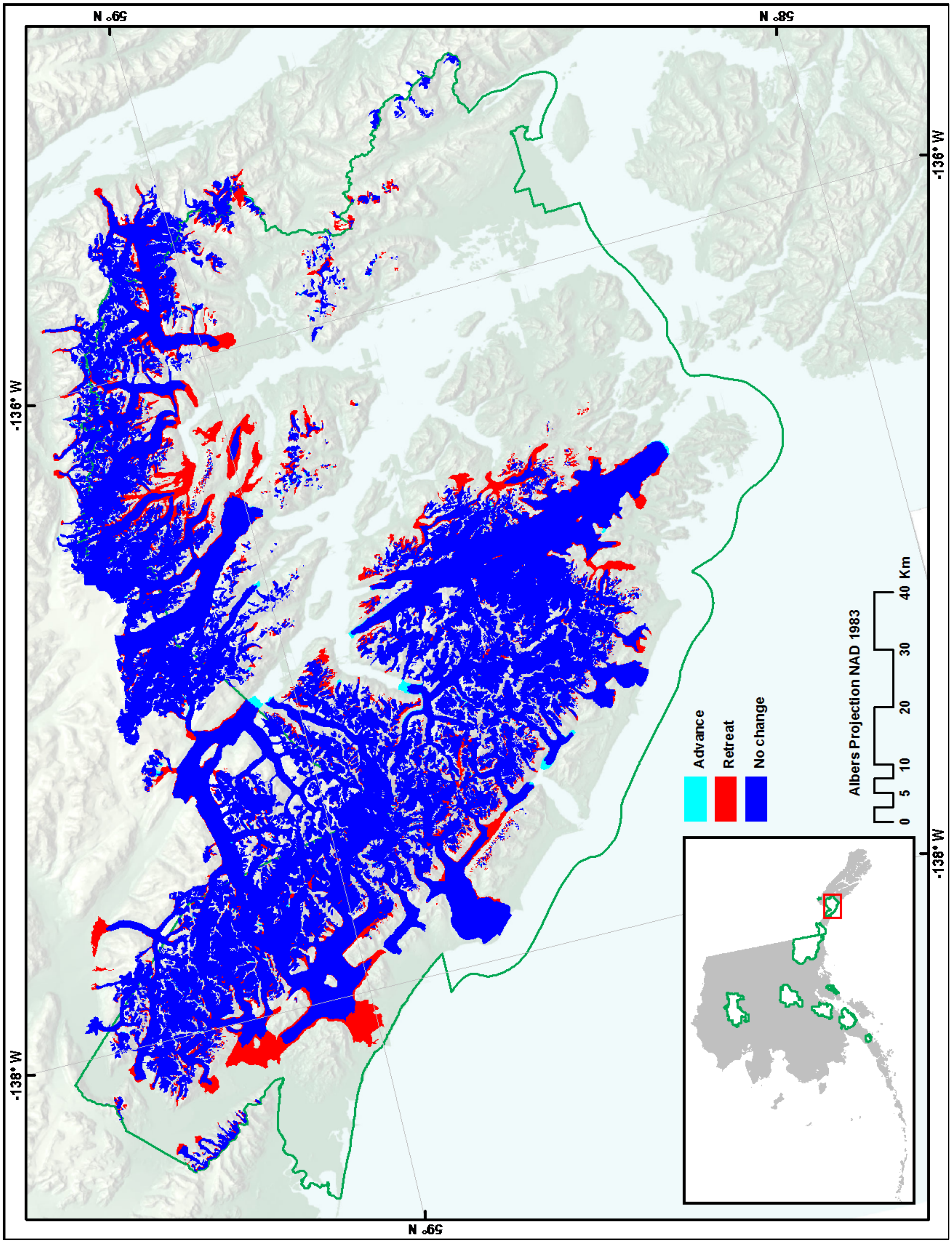

Figure 26. Changes in mapped glacier extent from map date to satellite date in Glacier Bay. Note map rotation.

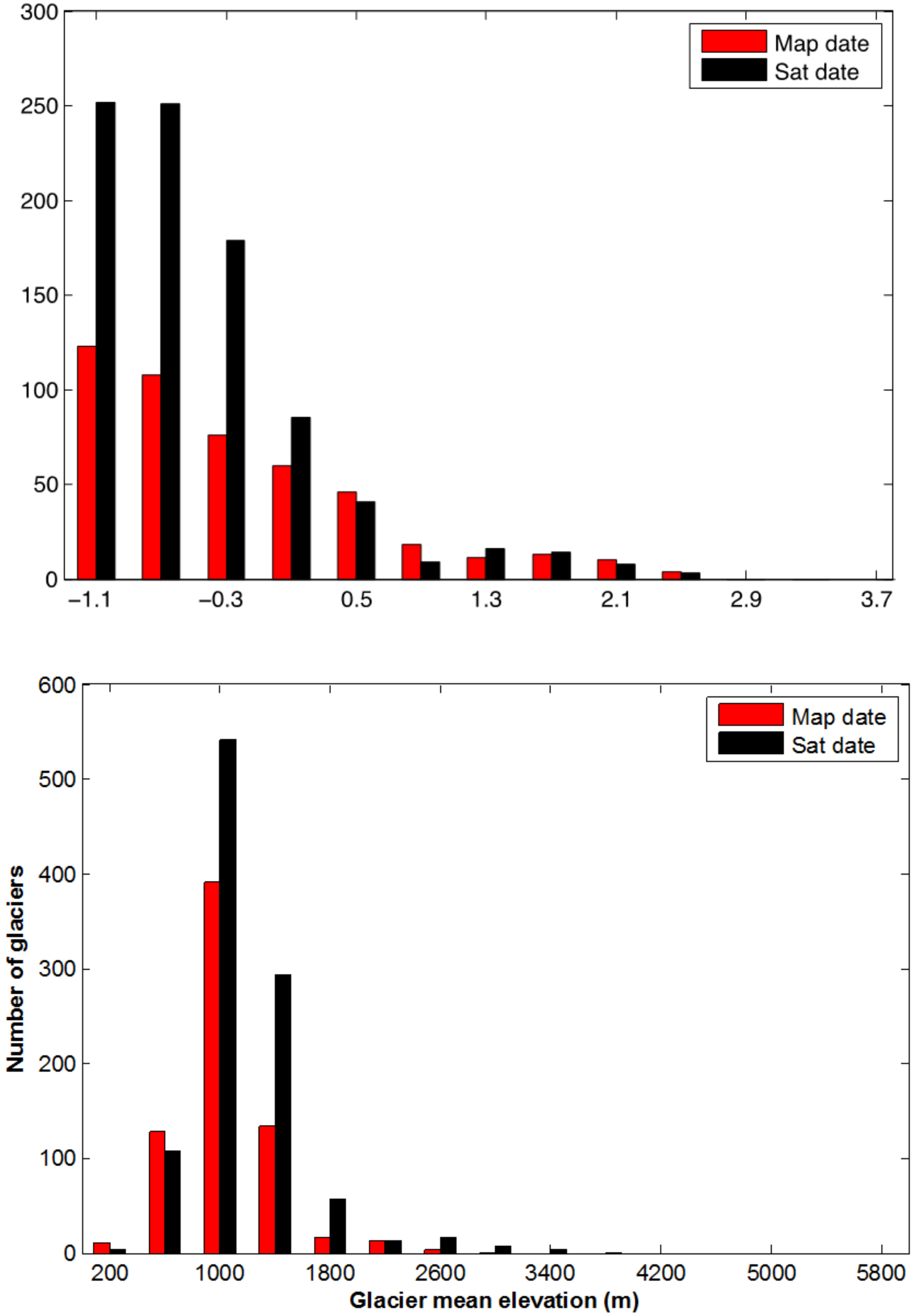

Figure 27. Changes in the numbers of glaciers in Glacier Bay NP&P by glacier size (upper panel) and glacier mean elevation (lower panel). Note that the x-axis of the upper panel is logarithmic.

Katmai National Park and Preserve

Mapped outlines for KATM are shown in Figure 28 and summarized in Table 12. In total, Katmai had 255 map date glaciers and 17% more in satellite imagery. Total ice-covered area decreased over that time interval by 14%, from a high of 1064 km^2. Estimated total ice volume decreased too, by 20%, as would be expected because volumes are here calculated simply by scaling known area changes of individual glaciers. As implied by the overall area changes without an accompanying reduction in glacier numbers, terminus retreat was the response seen in most individual glaciers, including notable retreats by glaciers on Fourpeaked and Douglas Mountains in the northeast section of the park, and Hallo Glacier and others on the Kukak Volcano edifice (Figure 28). Importantly, several glaciers advanced, too, primarily in the southwestern area impacted by ash fallout from the 1912 Novarupta eruption.

These overall changes in area are summarized on a per-glacier basis in Figure 29. Consistent with our findings in other parks, small to medium-sized glaciers increased in abundance over time while abundance of large glaciers diminished slightly. The balance point was around 1 km^2. Ranking them by area-weighted mean elevation (bottom panel), low-elevation glaciers diminished slightly in abundance while mid to high- elevation glaciers (1000 to 1500 m, in this case) became more common. Cumulative changes in total area of glaciers, by elevation bin, are shown in Figure 30 and probably best reflect the overall change in glaciers in the park. Above 1300 m, absolute changes in glacier area overall are small, while below 1300 m reductions dominate and are substantial. This latter finding primarily reflects the retreat of low-elevation glacier termini.

Table 18. Changes in glacier numbers, total glaciated area, mean/maximum glacier area, and volume for Katmai.

Time Period	Number of glaciers	Total glacier area (km^2)	Mean glacier size (km^2)	Max glacier size (km^2)	Total glacier volume (km^3)
Map date	255	1,063.6	4.2	98.9	126.9
Satellite date	298	914.2	3.1	79.5	101.9
Absolute change	*43*	*-149.4*	*-1.1*	*-19.4*	*-25.0*
Percent change	*17%*	*-14%*	*-26%*	*-20%*	*-20%*

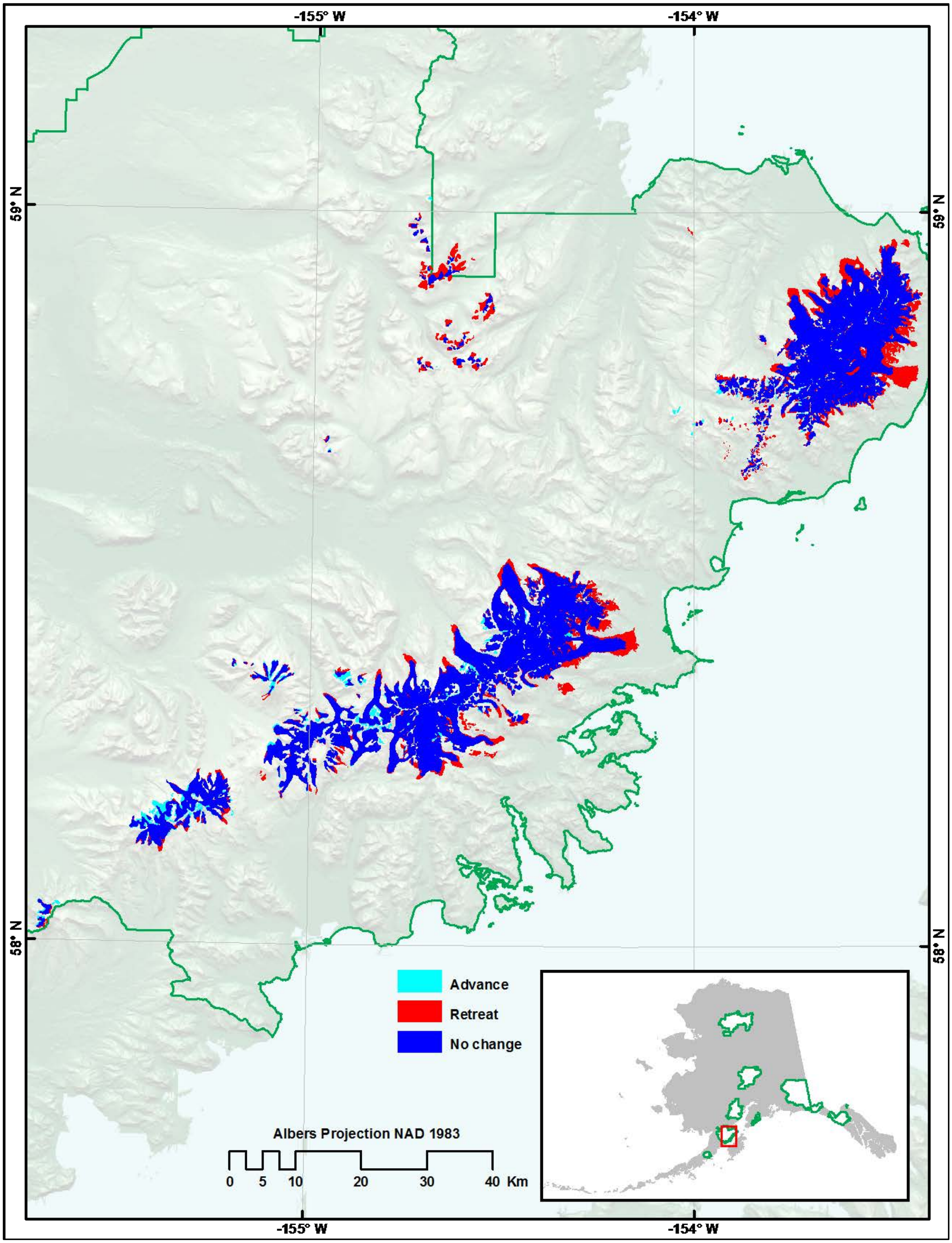

Figure 28. Changes in mapped glacier extent from map date to satellite date in Katmai.

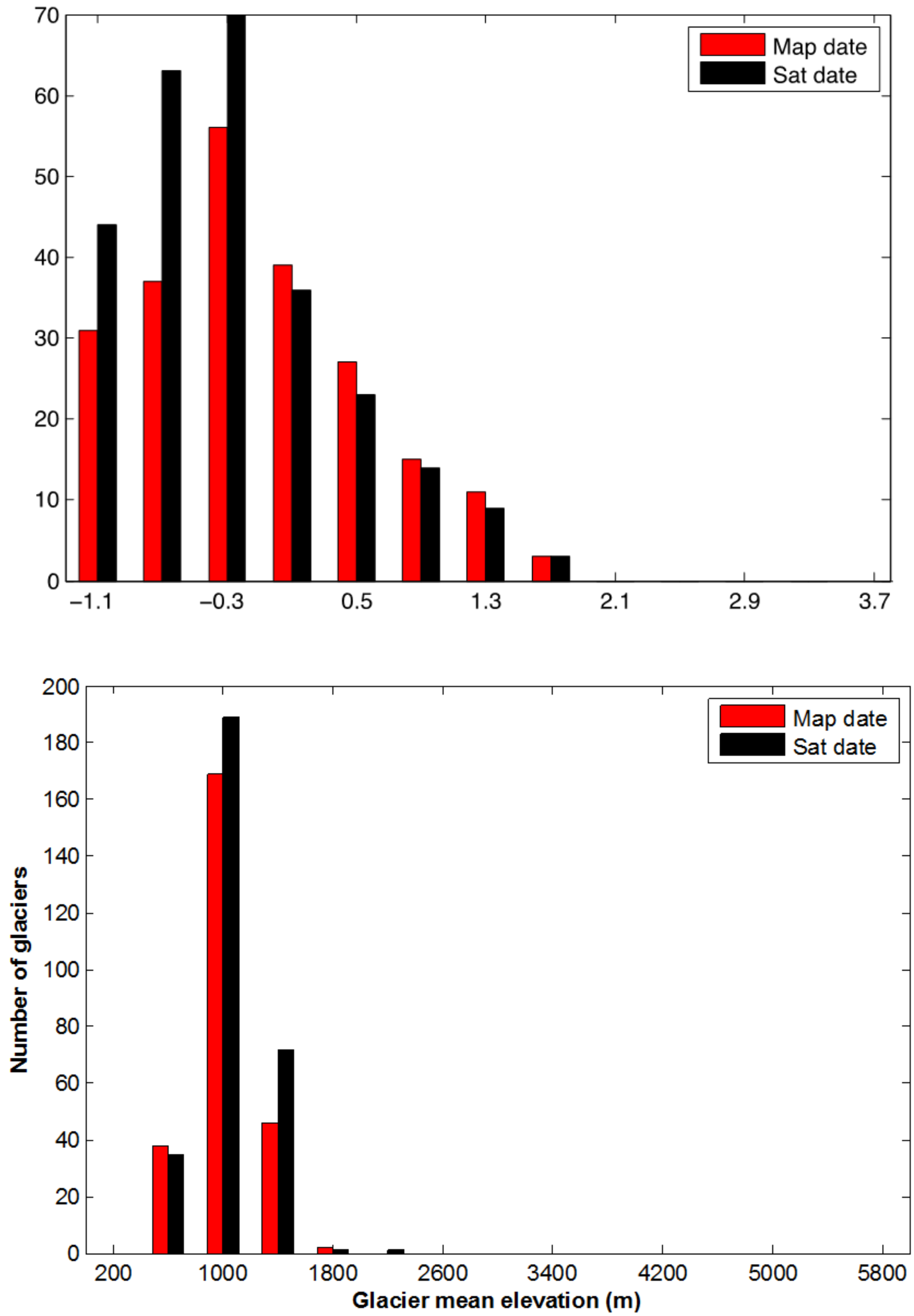

Figure 29. Changes in the numbers of glaciers in Katmai NP&P by glacier size (upper panel) and glacier mean elevation (lower panel). Note that the x-axis of the upper panel is logarithmic.

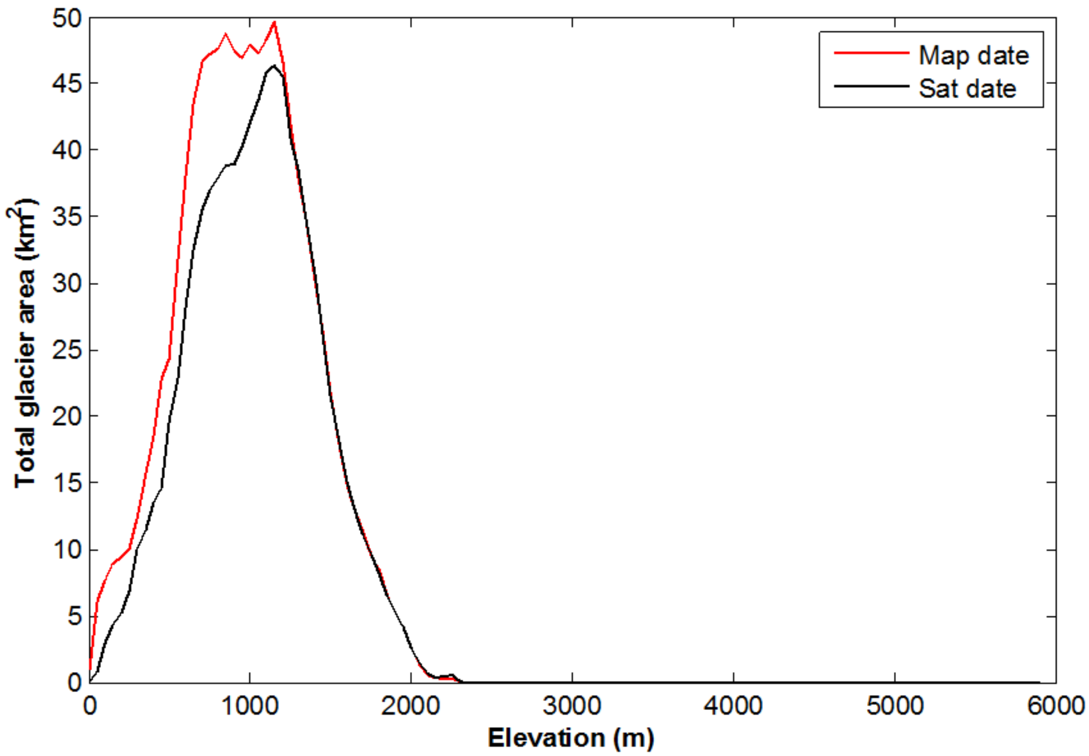

Figure 30. Total glacier-ice coverage by elevation in Katmai NP&P over two time periods.

Kenai Fjords National Park

Mapped outlines for glaciers in and around KEFJ are shown in Figure 32 and summarized in Table 13. In total, KEFJ and surrounding areas had 177 glaciers mapped on the topographic maps and 62% more in modern satellite imagery. In that same time, total glacier area decreased 11% from 2326 km^2 to 2074 km^2. The loss of glacier cover was dominated, as in other parks, by terminus retreat, which is distributed fairly evenly throughout all large glaciers in the park (Figure 32). This conclusion is supported by a plot of glacier cover, by elevation, showing that glacier area decreased most in the lower elevations below 600 m and in the narrow modal elevation band around 1250 m (Figure 31). Glacier expansion was mapped only in ice margins other than termini, suggesting that these changes were mainly mapping artifacts. Virtually all glacier cover in the park is below 2000 m.

These overall changes are summarized on a per-glacier basis in Figure 33. Small and medium sized glaciers (<9 km^2) were more common in modern mapping, whereas larger glaciers showed little change in abundance (top panel). Ranking glaciers by mean elevation, all but the lowest elevation glaciers increased in abundance (bottom panel). Ice at the modal elevation (~1000 m) diminished most noticeably.

Table 19. Changes in glacier numbers, total glaciated area, mean/maximum glacier area, and volume for Kenai Fjords.

Time Period	Number of glaciers	Total glacier area (km^2)	Mean glacier size (km^2)	Max glacier size (km^2)	Total glacier volume (km^3)
Map date	177	2,326.4	13.1	412.4	494.7
Satellite date	287	2,074.1	7.2	391.0	420.2
Absolute change	*110*	*-252.3*	*-5.9*	*-21.4*	*-74.5*
Percent change	*62%*	*-11%*	*-45%*	*-5%*	*-15%*

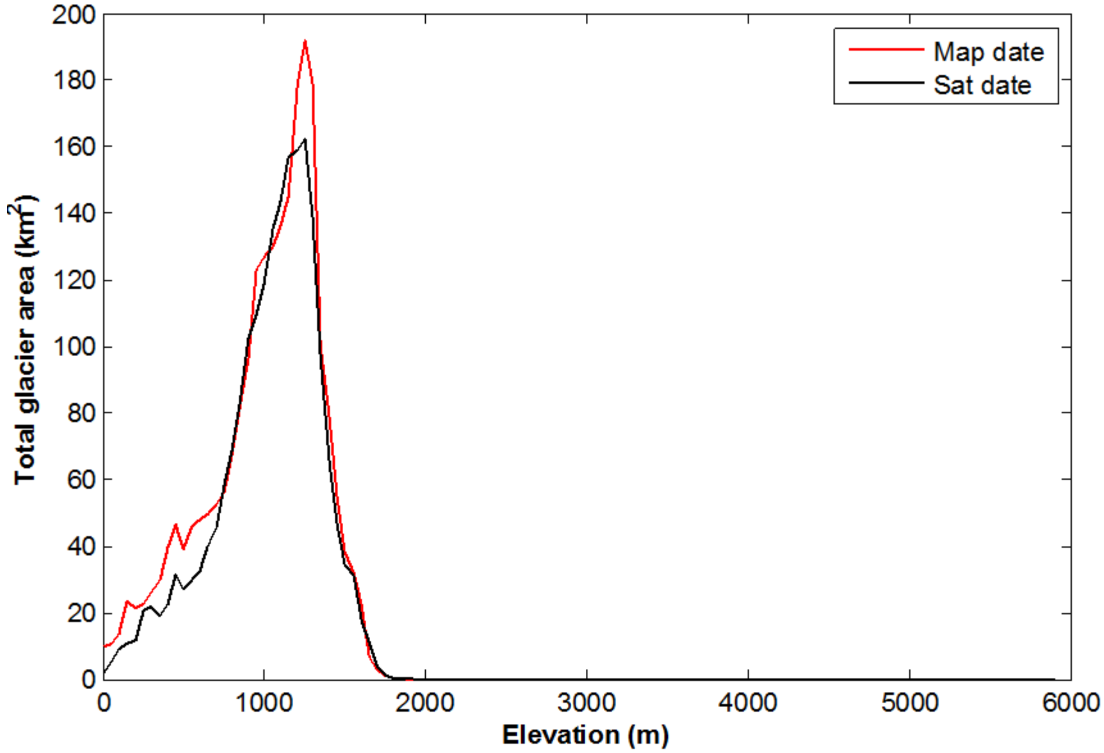

Figure 31. Total glacier-ice coverage by elevation in Kenai Fjords NP over two time periods.

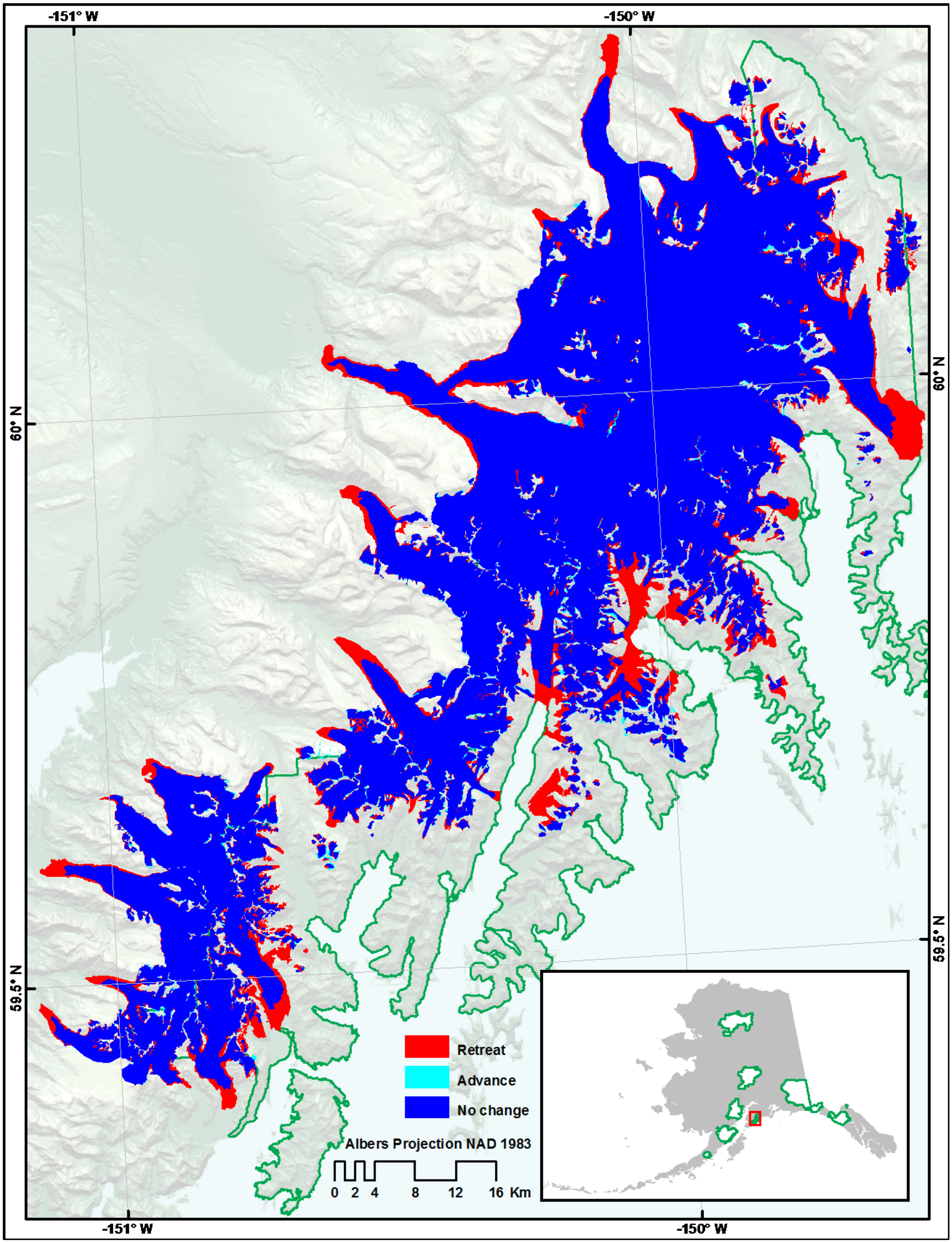

Figure 32. Changes in mapped glacier extent from map date to satellite date in Kenai Fjords.

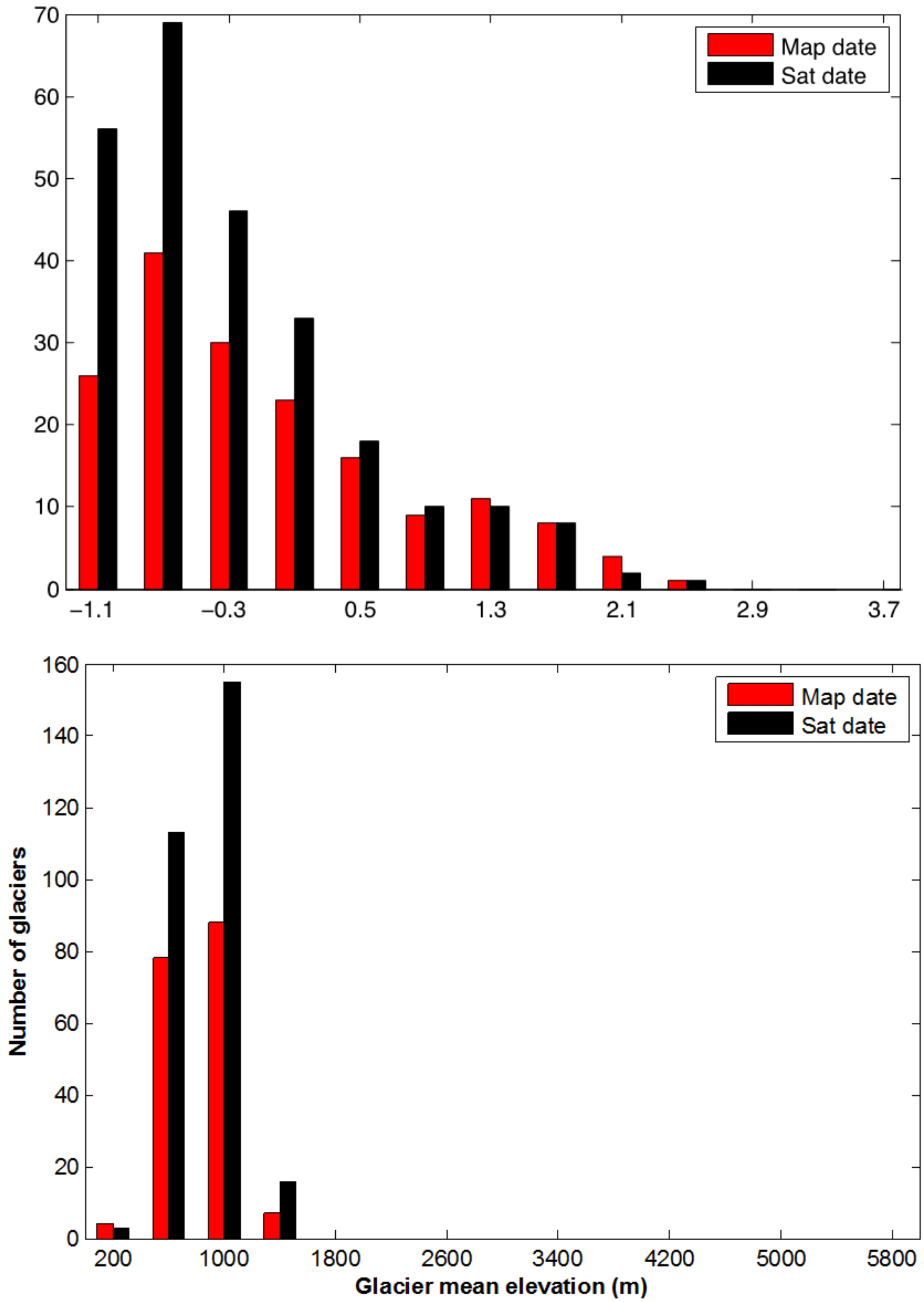

Figure 33. Changes in the numbers of glaciers in Kenai Fjords NP by glacier size (upper panel) and glacier mean elevation (lower panel). Note that the x-axis of the upper panel is logarithmic.

Klondike Gold Rush National Historic Park

Mapped outlines for KLGO are shown in Figure 34 and summarized in Table 14. As shown by the table, glacier cover technically within the park boundary is minimal: two glaciers overlapped the park boundary in original topographic maps, both in the upper Taiya River. Terminus retreat eliminated one in the modern satellite imagery, reducing KLGO's glacier contribution to the statewide inventory to one glacier only: a glacier terminus just south of Chilkoot Pass. The reduction in glacier area (a 74% reduction, from 5.3 to 1.4 km^2) is mostly a reflection of the loss of that one glacier from the modern inventory. Associated plots are similarly a reflection, more than anything of else, of the change from two glaciers to one (Figure 35 and Figure 36).

We also show the changes of other glaciers within the park vicinity in Figure 34. The boundary for glaciers shown in this view was requested by NPS. Metrics for glacier change within this larger boundary are not presented here, but the glacier outlines shown are contained within the accompanying database and can be assessed there by interested NPS staff. In general, however, it is clear that terminus retreat dominates the response of glaciers in and near the park, including substantial retreat in the headwaters of the Nourse River. These changes are discussed more in the accompanying interpretive report, where the Nourse Glacier is featured as a focus glacier.

Table 20. Changes in glacier numbers, total glaciated area, mean/maximum glacier area, and volume for Klondike Gold Rush.

Time Period	Number of glaciers	Total glacier area (km^2)	Mean glacier size (km^2)	Max glacier size (km^2)	Total glacier volume (km^3)
Map date	2	5.3	2.6	3.9	0.3
Satellite date	1	1.4	1.4	1.4	0.1
Absolute change	*-1*	*-3.9*	*-1.3*	*-2.5*	*-0.2*
Percent change	*-50%*	*-74%*	*-48%*	*-65%*	*-81%*

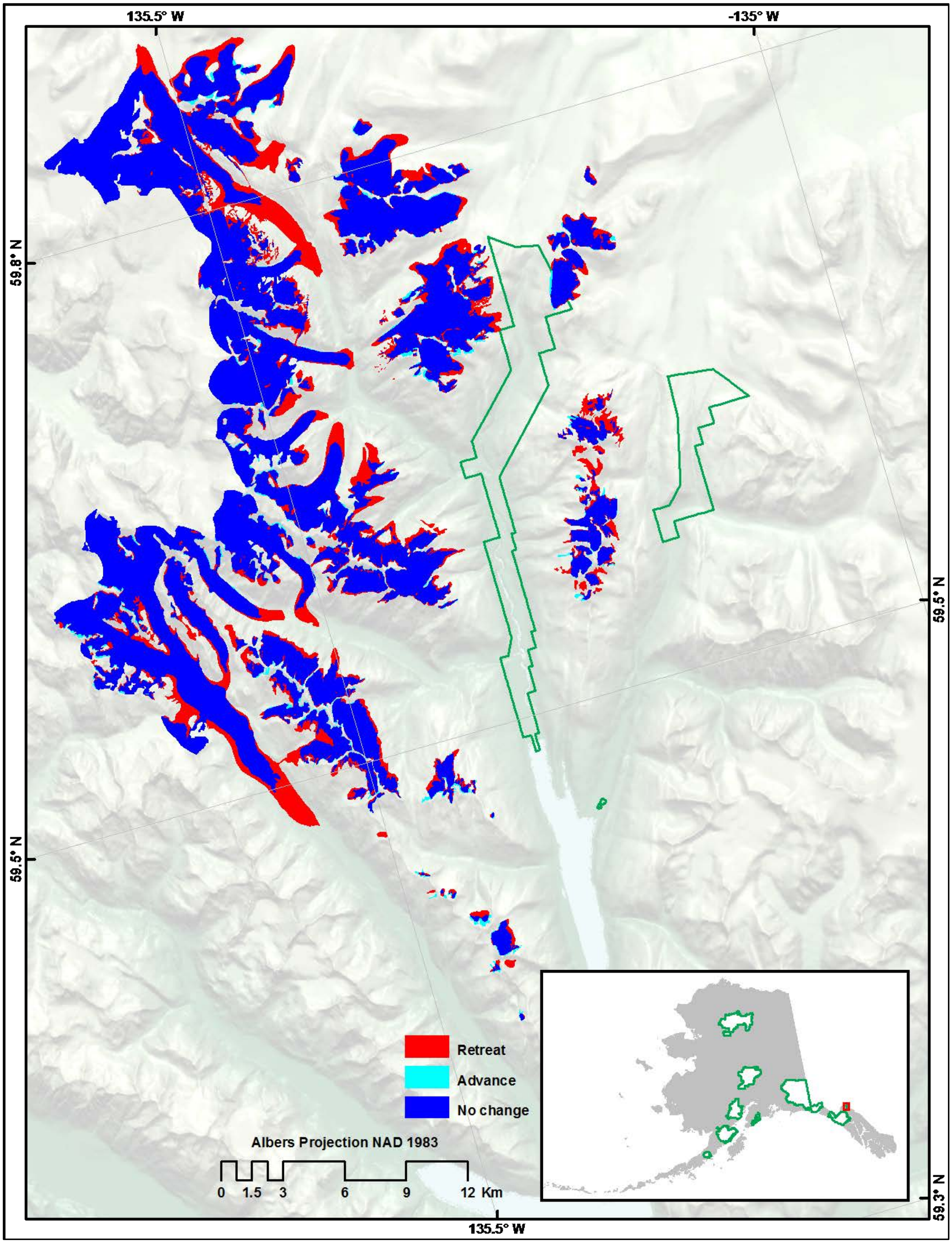

Figure 34. Changes in mapped glacier extent from map date to satellite date in Klondike Gold Rush.

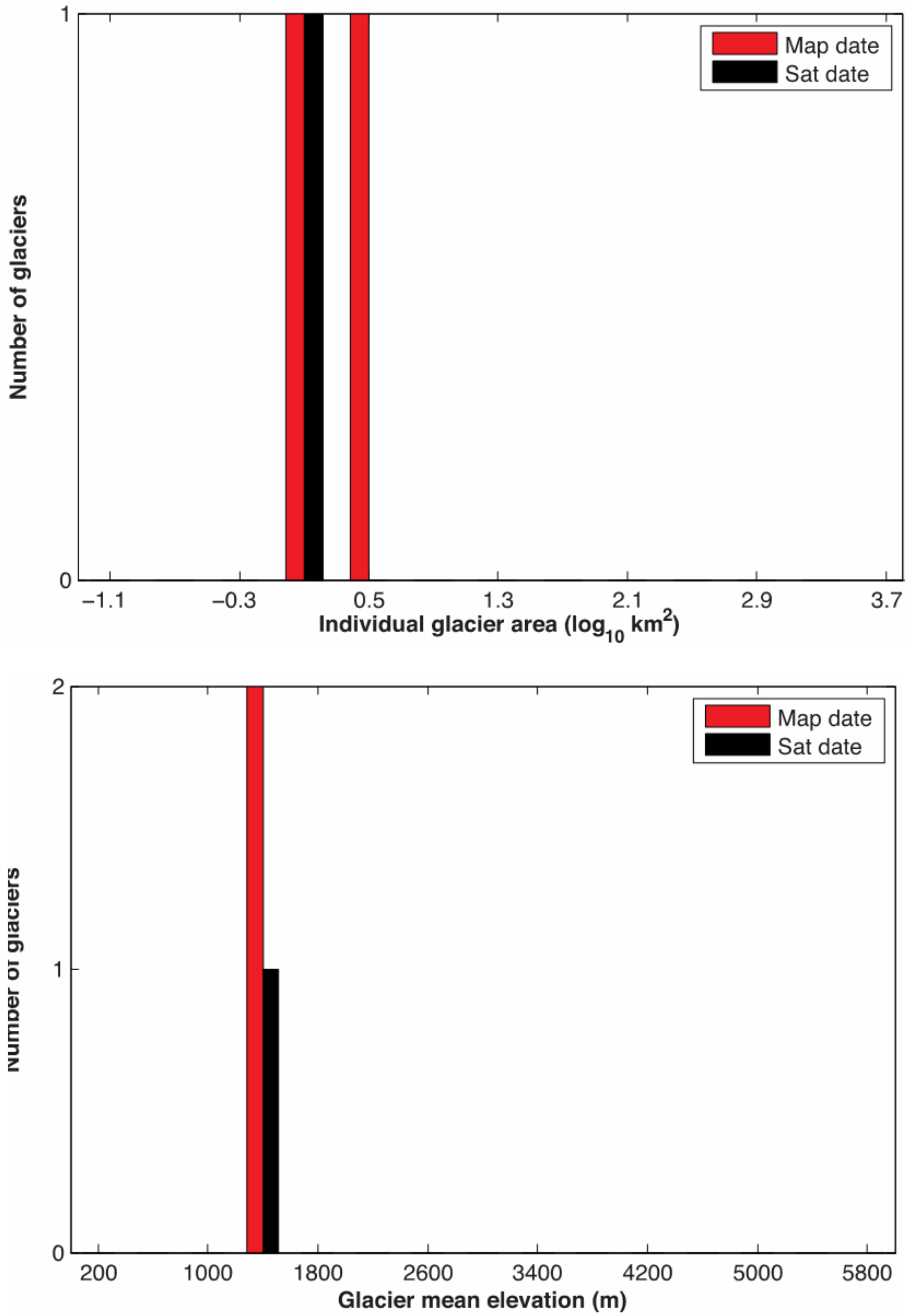

Figure 35. Changes in the numbers of glaciers in Klondike Gold Rush NHP by glacier size (upper panel) and glacier mean elevation (lower panel). Note that the x-axis of the upper panel is logarithmic.

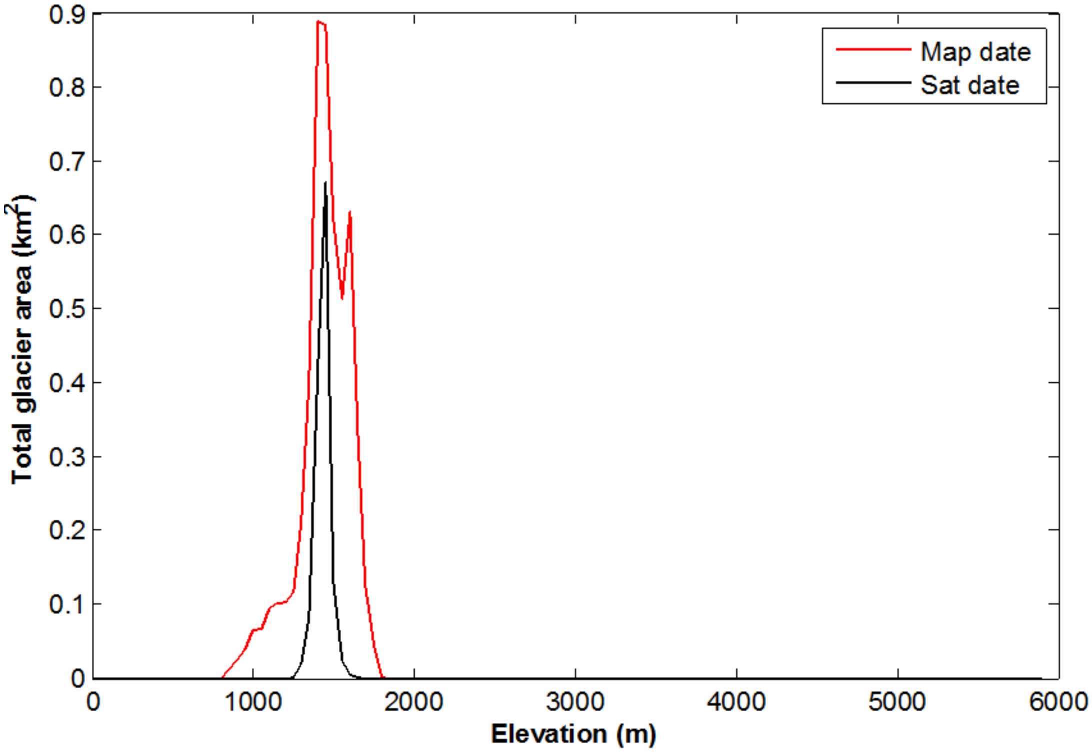

Figure 36. Total glacier-ice coverage by elevation in Klondike Gold Rush NHP over two time periods.

Lake Clark National Park and Preserve

Mapped outlines for LACL are shown in Figure 38 and summarized in Table 15. Glacier numbers in LACL increased 16% from 1501 to 1740 over approximately a half-century, but glacier cover diminished 12% from 2956 to 2598 km^2. As in other parks, we attribute much of the increase in glacier numbers to better mapping of small glaciers using modern satellite imagery, a phenomenon corroborated by the dominance of small glaciers in the increase in glacier numbers (Figure 39, top panel). Here, however, we draw attention to another occasional cause of increasing glacier numbers in a period of generally decreasing glacier cover: the breaking of shrinking "parent" glaciers into a number of smaller, disconnected tributary "children." A good example is the North Fork Tlikakila Glacier, in the central western portion of Figure 38, which while retreating into its tributary valleys changed from one to two glaciers. Like the Tlikakila, glaciers throughout the park shrank mostly by generalized terminus retreat. The most significant examples include Double Glacier, Tanaina Glacier, and Shamrock Glacier.

Glacier cover in LACL extends to just above 3000 m, and diminished at virtually all elevations (Figure 37). The most extensive loss of glacier cover was around the modal elevation around 1250 m. Ranking individual glaciers by mean elevation (Figure 39, bottom panel), low-elevation glaciers diminished slightly in abundance while mid to high-elevation (~>1300 m) glaciers became more common.

Table 21. Changes in glacier numbers, total glaciated area, mean/maximum glacier area, and volume for Lake Clark.

Time Period	Number of glaciers	Total glacier area (km²)	Mean glacier size (km²)	Max glacier size (km²)	Total glacier volume (km³)
Map date	1501	2,955.5	2.0	168.2	358.8
Satellite date	1740	2,598.2	1.5	158.2	297.6
Absolute change	*239*	*-357.3*	*-0.5*	*-10.0*	*-61.3*
Percent change	*16%*	*-12%*	*-24%*	*-6%*	*-17%*

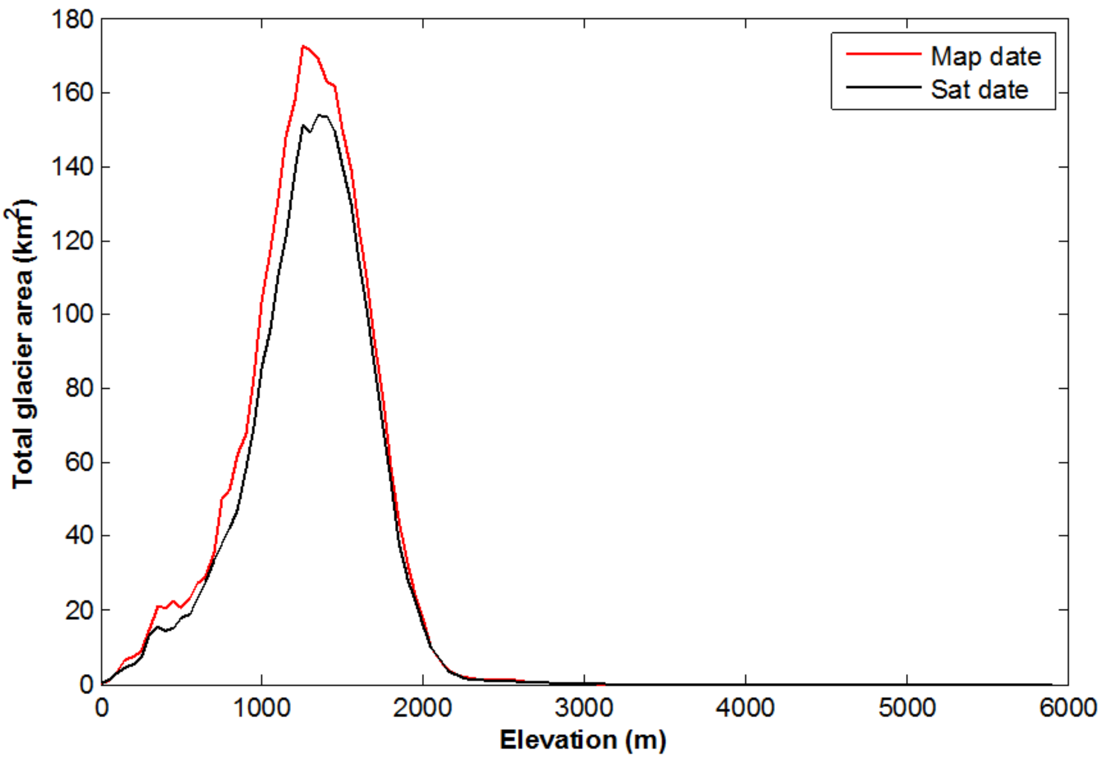

Figure 37. Total glacier-ice coverage by elevation in Lake Clark NP&P over two time periods.

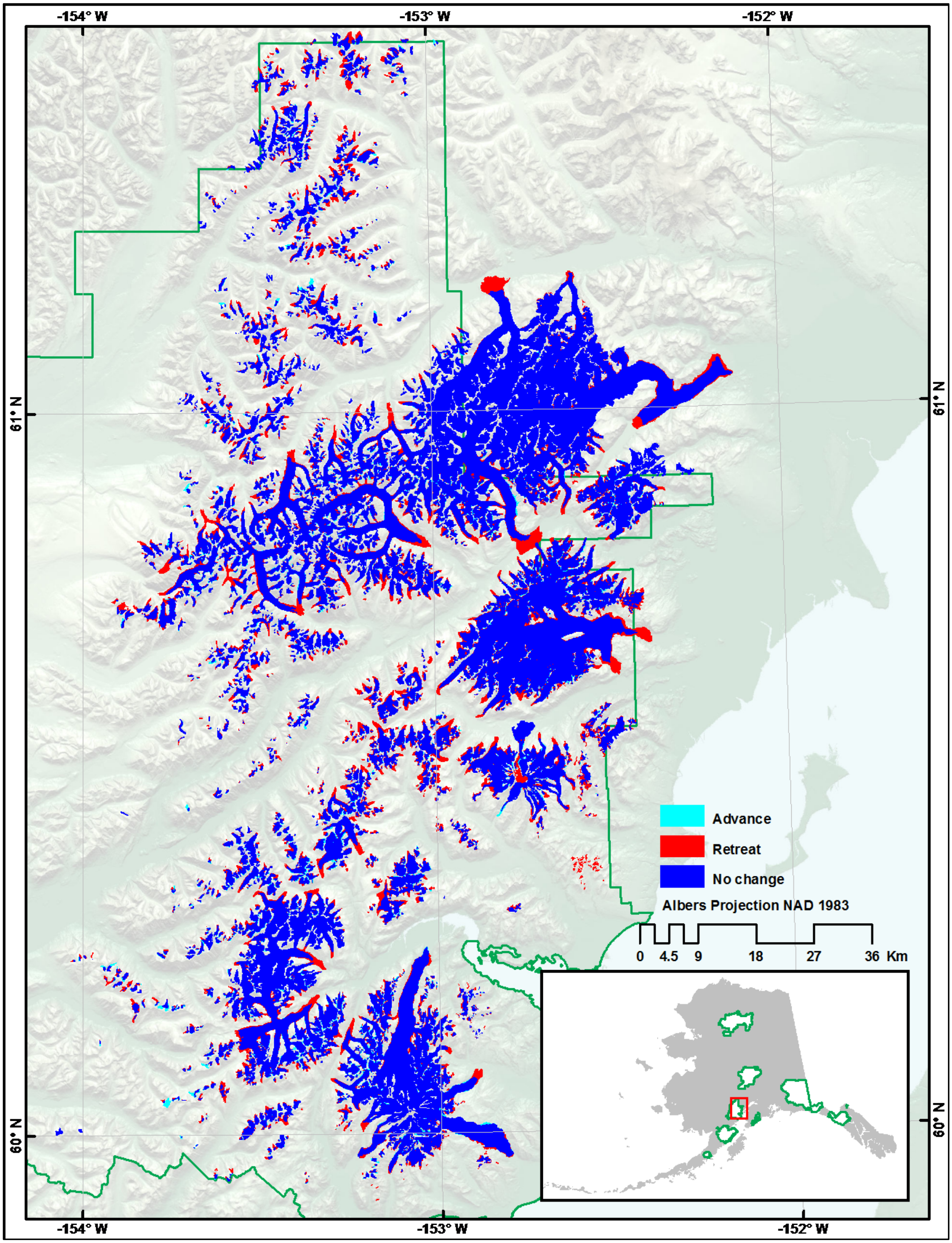

Figure 38. Changes in mapped glacier extent from map date to satellite date in Lake Clark.

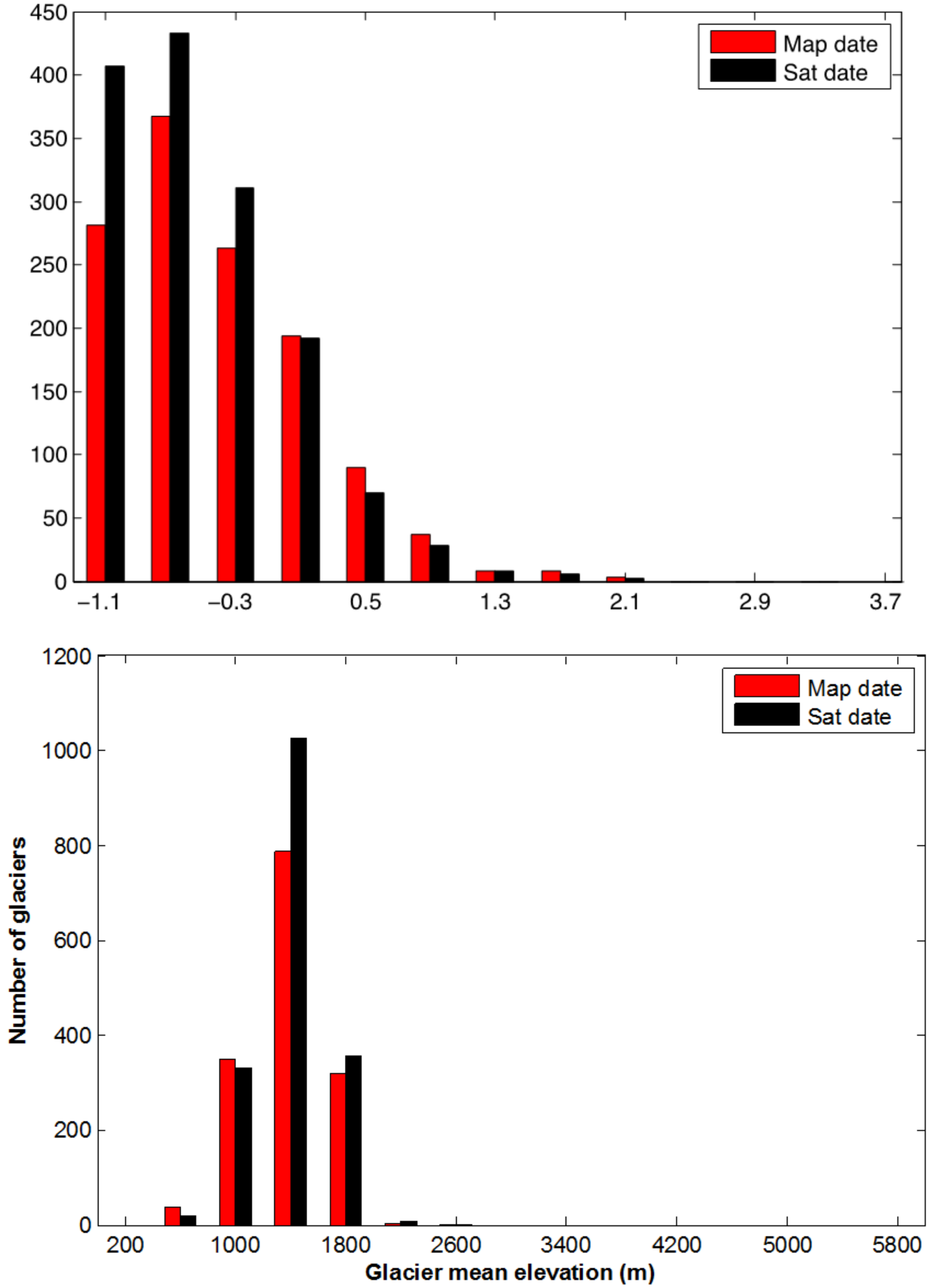

Figure 39. Changes in the numbers of glaciers in Lake Clark NP&P by glacier size (upper panel) and glacier mean elevation (lower panel). Note that the x-axis of the upper panel is logarithmic.

Wrangell-St. Elias National Park and Preserve

Mapped outlines for glaciers in WRST are shown in Figure 40 and Figure 41 and Figure 42 and summarized in Table 16. As mentioned earlier, WRST is the glacier leader in Alaskan parks, and the numbers bear this out. 2843 glaciers in the early topographic maps increased, by our mapping, to 3121 in satellite imagery. Glacier cover meanwhile diminished 5% from 30,697 to 29,041 km^2. Some notes are pertinent about these numbers. First, a substantial amount of ice included in these calculations is technically outside the park boundary. This is true for most other parks, too, but in WRST there are some very large glaciers that fit into this category, including some very long glaciers originating in Canada's Kluane National Park, and also Bering Glacier—a distributary of the Bagley Icefield (Figure 41). The scale of our map hides all but the largest glacier changes, but these nonetheless stand out clearly: major retreat of the Bering, Chitina, Barnard, Klutlan, and Russell Glaciers, and of several glaciers entering Icy Bay. At this scale only one glacier, the Hubbard, stands out for terminus advance (Figure 42).

Glacier numbers are summarized by size and elevation in Figure 43. In the top panel, the ubiquitous increases in small glaciers is shown, in this case including everything less than about 1 km^2. Looking at glacier mean elevation (bottom panel), we see that glaciers below about 1500 m diminished in abundance, while those above 2000 m largely increased in numbers. Grouping all glaciers and plotting their total cover by elevation, Figure 44 shows that ice cover between 500 and 2500 m generally diminished, with minor changes above and below those elevations masked somewhat by spikiness (due probably to low quality DEMs) in the map date curve.

Table 22. Changes in glacier numbers, total glaciated area, mean/maximum glacier area, and volume for Wrangell-St. Elias.

Time Period	Number of glaciers	Total glacier area (km^2)	Mean glacier size (km^2)	Max glacier size (km^2)	Total glacier volume (km^3)
Map date	2843	30,696.5	10.8	4700.6	17,315.5
Satellite date	3121	29,041.0	9.3	3388.2	13,888.2
Absolute change	*278*	*-1,655.5*	*-1.5*	*-1,312.4*	*-3,427.3*
Percent change	*10%*	*-5%*	*-14%*	*-28%*	*-20%*

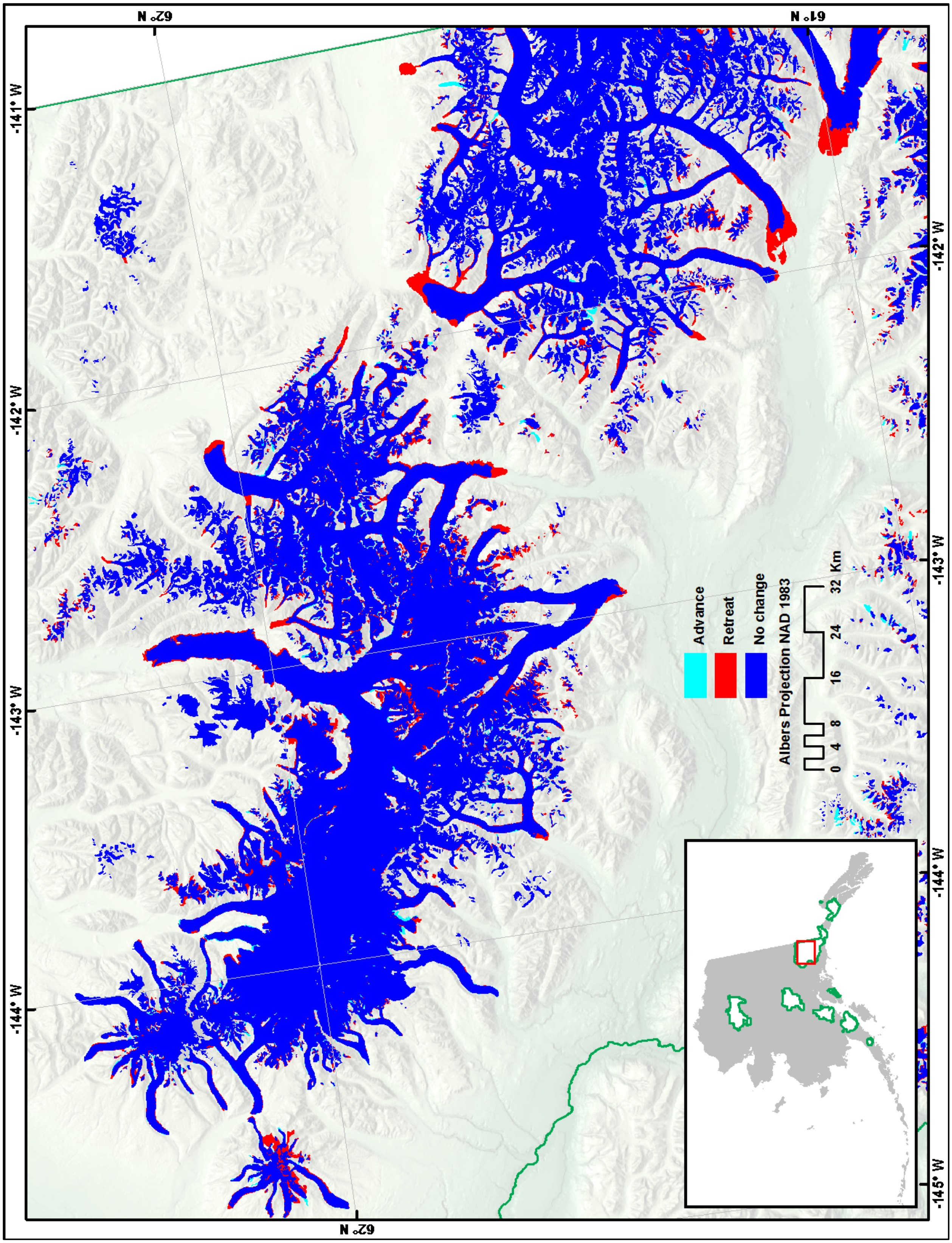

Figure 40. Changes in mapped glacier extent from map date to satellite date in northern Wrangell-St. Elias. Note map rotation.

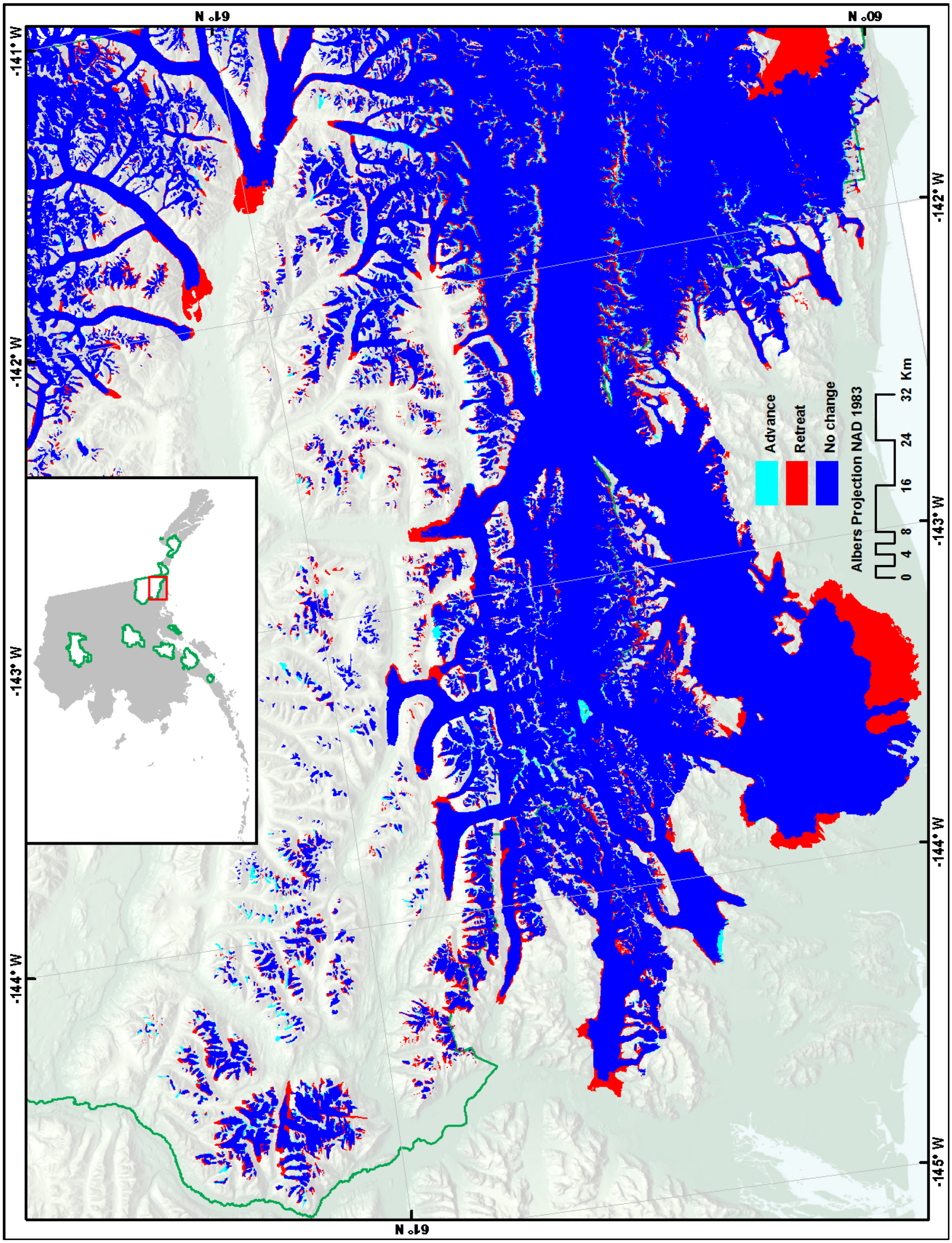

Figure 41. Changes in southwestern Wrangell-St. Elias. Note map rotation.

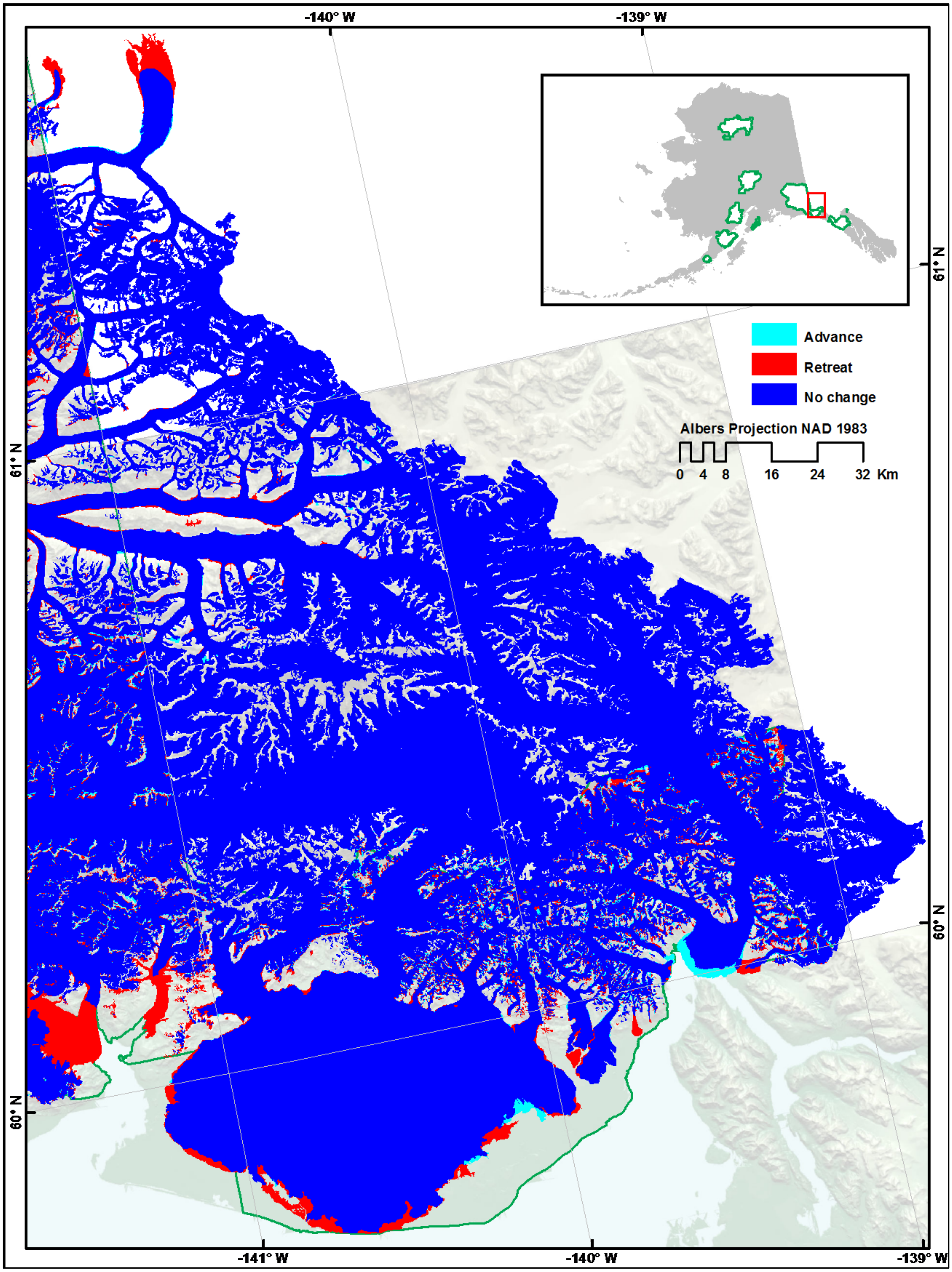

Figure 42. Changes in southeastern Wrangell-St. Elias.

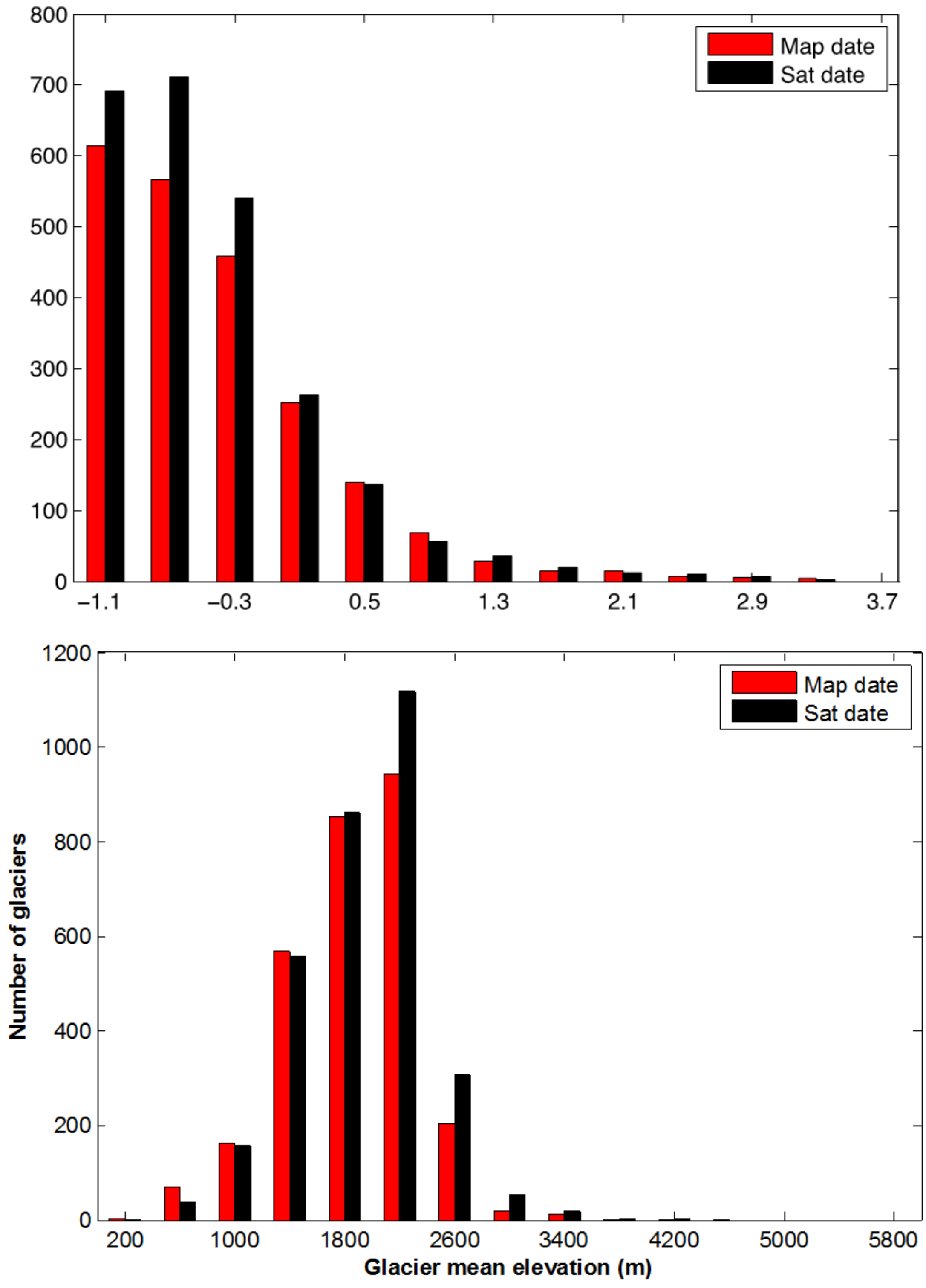

Figure 43. Changes in the numbers of glaciers in Wrangell-St. Elias NP&P by glacier size (upper panel) and glacier mean elevation (lower panel). Note that the x-axis of the upper panel is logarithmic.

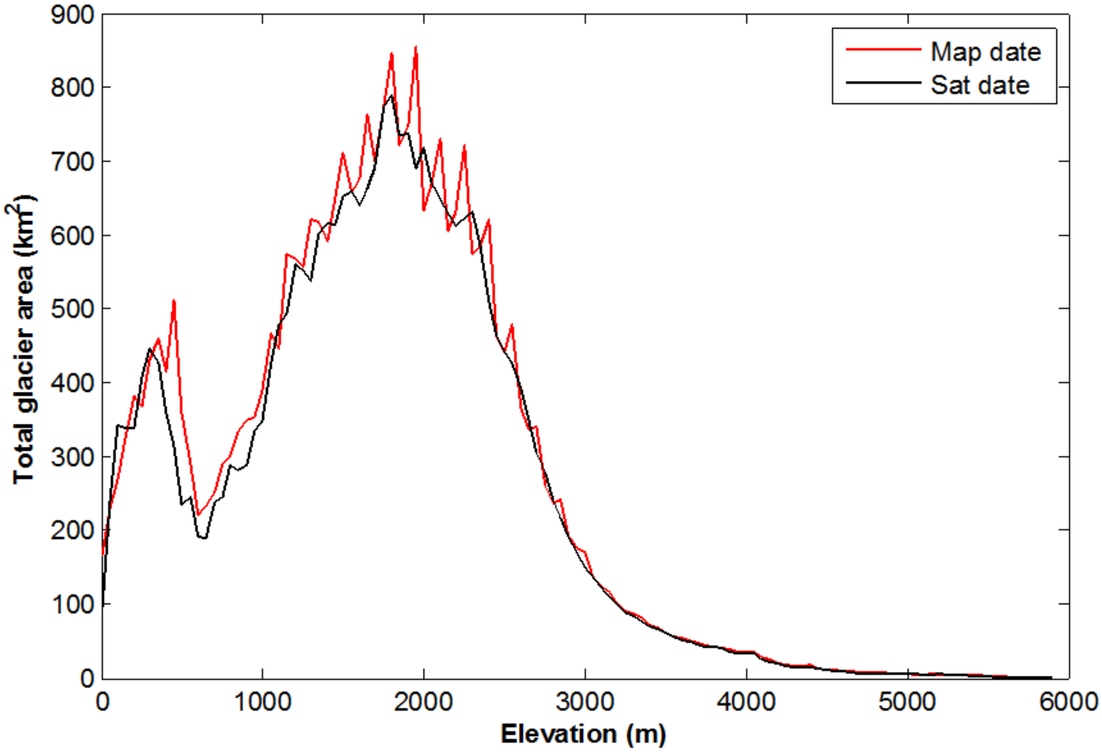

Figure 44. Total glacier-ice coverage by elevation in Wrangell-St. Elias NP&P over two time periods.

Results-Elevation Change

Results of our elevation change work consist of derived differences in elevation between successive surveys of glacier centerlines and/or swaths, plotted as functions of elevation and then used to infer total mass change and area-averaged mass balance (formally, the glacier-wide mass balance rate, which summarize mass loss as the spatially averaged gain or loss of a given thickness of water equivalent from the glacier surface). For each glacier, our primary data are presented as plots of derived elevation differences ('DZ plots') for each measured time interval. These figures plot individual laser-based difference measurements (gray diamonds) along with smoothed lines summarizing the median (red line) and lower/upper quartiles (blue lines) for each profile. Lower/upper quartile lines are dashed where there is insufficient data to calculate the quartiles. The DZ plots are accompanied by a plot of the glacier's area altitude distribution (AAD). We present these analyses on a park-by-park basis for all intervals of 59 distinct glaciers, including distinct branches of some glaciers, in five parks (Table 4).

The DZ plots, which are output from matlab scripts that analyze the raw data, include text that summarizes the mass change and mass balance. These results are also combined, for each park, in a single table. Some of these results should be interpreted with caution, however. In some cases, the measured "glacier" is only one branch of a larger glacier system, and the mass balance/mass change for that branch are only properly interpreted after combining with such results from all other branches. The massive Bagley Icefield system in WRST provides an important example, where mass balance on individual segments (Bagley East, Bagley West, Bering, Jefferies, or Tana Glaciers) must be combined to derive a meaningful mass change estimate for the whole system. In other cases, results are given for multiple overlapping intervals (2000-2005, 2005-2010, and 2000-2010, for example). Such results are therefore non-exclusive and can present seemingly contradictory rates of mass change for a given year.

For these reasons, we caution that mass balance and mass change results included on the DZ plots and in the associated table should not be taken out of context. The best comparative summary of meaningful mass balances is a time-series plot, presented for each park, of mass balances for all non-overlapping intervals of whole glacier systems (e.g. Figure 46). These time-series plots reflect the most complete, accurate, and up-to-date results at the time of this publication, and are suitable for interpretation and comparison of trends among glaciers and parks.

For some glaciers and intervals, we also summarize trends with raster maps that show changes graphically for the measured glaciers. These figures use a colorbar to summarize the annual rates of glacier surface elevation change as a function of elevation (the red line in the DZ plots) over the modern, satellite date outline of each glacier. As such, they present no unique information, but just combine existing results in a more intuitive format.

No repeat laser altimetry is available for ANIA, GAAR, KATM, or KLGO. Elevation changes of glaciers within these park units may make excellent targets for future research, but they are not discussed further in this portion of the report. Because of the heterogeneous geographic distribution of elevation change results, no statewide summary is included in this section.

Denali National Park and Preserve

We measured elevation change on 9 glaciers (including both branches of Toklat 2 Glacier and counting Traleika Glacier as a separate branch of Muldrow Glacier) in Denali NP&P and present results for 17 discrete intervals of glacier change (Table 17). Glacier names, locations, and flight tracks are shown in Figure 45.

In general, between 1994 and 2010, most measured glaciers in DENA lost mass (expressed here as glacier-wide mass balance rates, which summarize mass loss as the spatially averaged gain or loss of a given thickness of water equivalent from the glacier surface) at modest average rates of between 0 and 1 m/yr w.e. (Figure 46). The only notable exceptions are between 2001 and 2008, when Toklat 3 and Tokositna Glaciers lost mass slightly more rapidly, and when Muldrow Glacier exhibited a very slight gain in overall mass. We describe these trends, by glacier, and also present some important caveats below. Some of these results are shown in map view in Figure 56 and Figure 57.

Kahiltna Glacier was measured in 1994, 2008, and 2010 (Figure 47) and has generally excellent data coverage, including all but the highest elevations, which contribute little to the overall AAD. Interpretation of mass change on the Kahiltna, however, is complicated by the fact that the 1994 data were collected in latest July while the 2008 and 2010 data were collected in mid-May.

Table 23. Mass balance and mass change of glaciers in Denali NP&P inferred from laser altimetry at discrete time intervals. ‘MB+’, ‘MB-‘, ‘MC+’, and ‘MC-‘ give positive and negative 95% confidence intervals for mass balance and mass change, respectively.

Glacier	Type	Size (km^2)	Mean Elev (m)	Start date	End date	Mass Balance (m/yr)	MB+	MB-	Mass Change (gt/yr)	MC+	MC-
Kahiltna	(L)	496	1890	7/31/94	5/18/08	-0.75	0.29	0.33	-0.36	0.05	0.05
Kahiltna	(L)	496	1890	7/31/94	5/22/10	-0.76	0.23	0.24	-0.38	0.04	0.04
Kahiltna	(L)	496	1890	5/18/08	5/22/10	-1.07	0.54	0.44	-0.52	0.21	0.21
Muldrow all	(S)	352	2310	8/3/94	8/22/01	-0.50	1.20	1.30	-0.20	0.40	0.40
Muldrow all	(S)	352	2310	8/3/94	5/22/10	-0.40	0.50	0.50	-0.10	0.20	0.20
Muldrow all	(S)	352	2310	8/22/01	5/17/08	0.10	1.50	1.30	0.00	0.50	0.50
Muldrow all	(S)	352	2310	8/22/01	5/22/10	0.10	0.60	0.70	0.00	0.20	0.20
Muldrow all	(S)	352	2310	5/17/08	5/22/10	-0.70	1.70	1.30	-0.20	0.50	0.60
Ruth	(L)	338	1620	4/30/01	5/17/08	-0.80	0.90	0.50	-0.28	0.16	0.16
Toklat 1	(L)	6	1750	5/7/96	5/17/08	-0.70	0.80	0.40	0.00	0.00	0.00
Toklat 2E	(L)	4	1810	5/21/01	5/22/10	-1.51	0.03	0.04	-0.01	0.00	0.00
Toklat 2E	(L)	4	1810	5/17/08	5/22/10	-1.17	0.28	0.34	-0.01	0.00	0.00
Toklat 2W	(L)	4	1760	5/21/01	5/22/10	-1.29	0.18	0.19	0.00	0.00	0.00
Toklat 2W	(L)	4	1760	5/17/08	5/22/10	-1.74	0.71	0.63	-0.01	0.00	0.00
Toklat 3	(L)	9	1770	5/21/01	5/16/08	-1.33	0.84	0.43	-0.01	0.00	0.00
Tokositna	(S)	207	1530	4/30/01	5/18/08	-1.60	1.70	1.60	-0.30	0.30	0.30
Traleika	(L)	37	2070	5/17/08	5/22/10	1.41	0.26	0.25	0.05	0.01	0.01

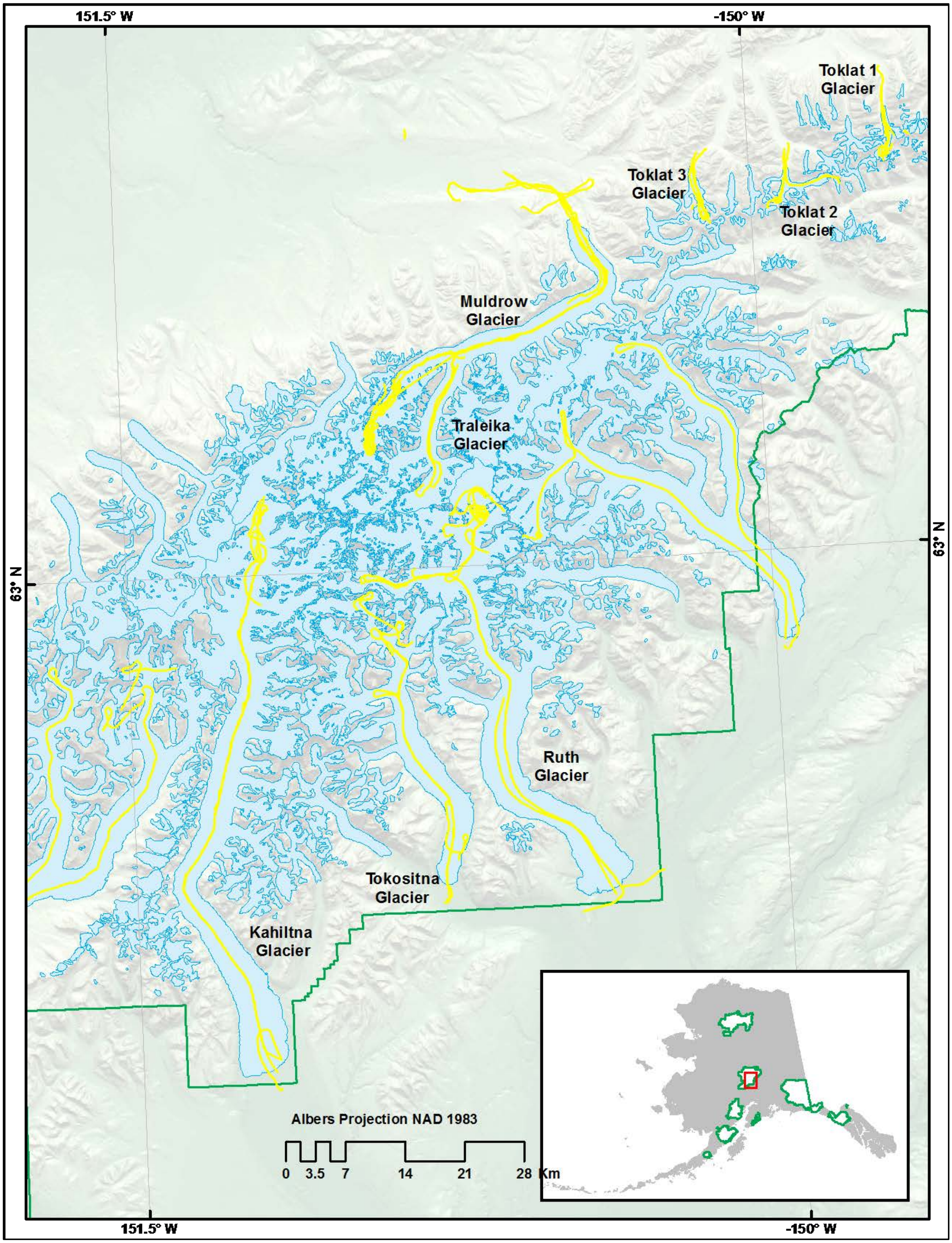

Figure 45. Locations of glaciers in Denali with elevation change results reported in this paper. Laser altimetry tracks are shown in yellow.

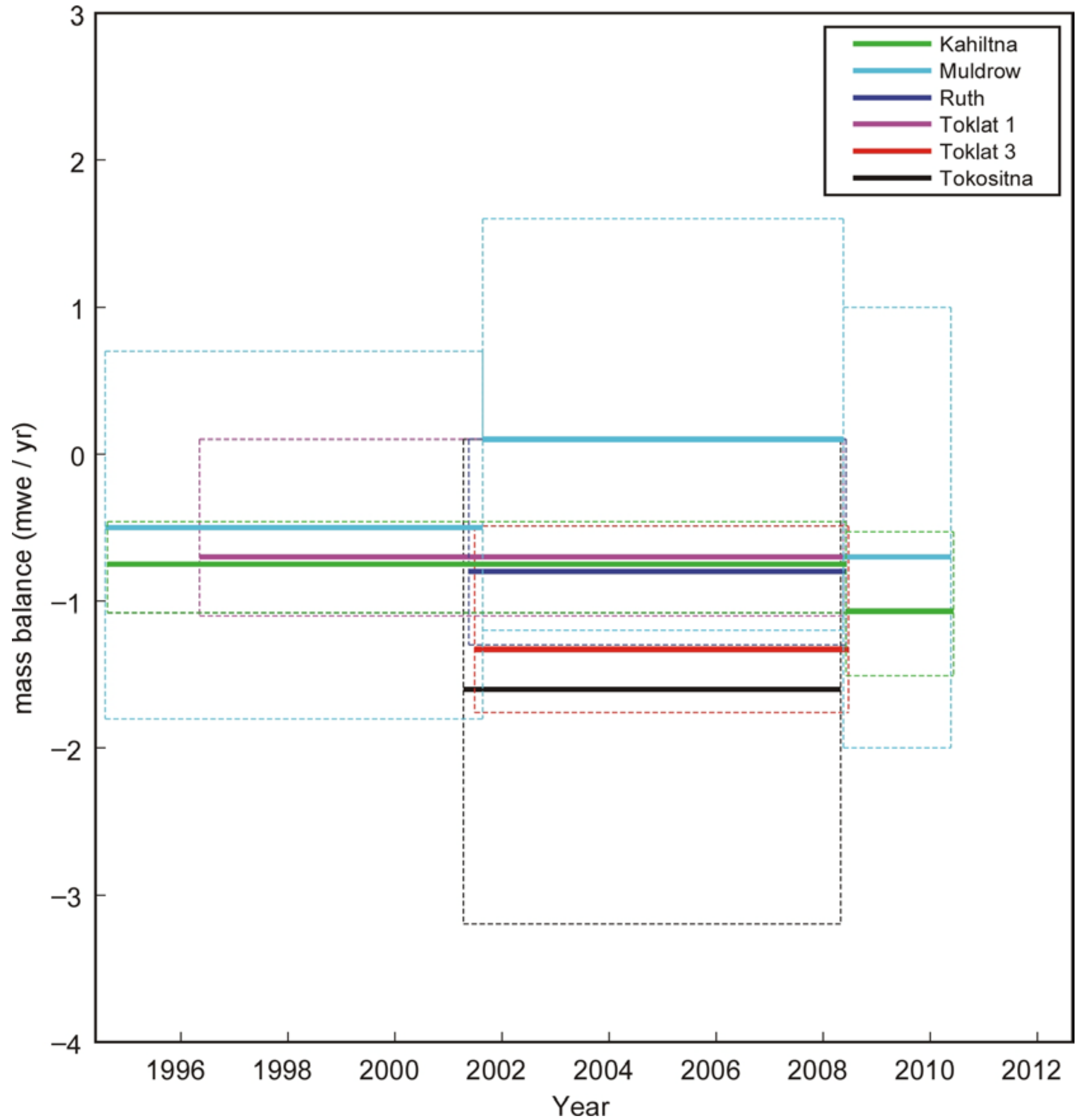

Figure 46. Mass balance of select glaciers in Denali National Park & Preserve. Thick solid lines are mass balances; upper and lower dashed lines reflect confidence intervals for each time period. For clarity, some lines have been shifted a few pixels left or right to minimize overlap.

We can crudely estimate the impact of that seasonally anomalous measurement by noting that average annual melt on the Kahiltna over summers 2010 and 2012, was about 5.9 m w.e. at the terminus and 1.2 m w.e. at the mean elevation of 1890 m (Young 2013). If we very conservatively assume that all that melt occurred by latest July, 1994, and that the melted material was entirely snow with a density of 500 kg/m^3, then the measured 1994 elevations (at least in the lower portion of the glacier considered here) would have 11.8 and 2.4 m higher at the terminus and mean elevation, respectively. This is almost certainly an overestimate, but we can use it to provide an outside boundary on the sensitivity of our 1994-2008 and 1994-2010 annual DZ profiles. Dividing by the elapsed time in those intervals (14 and 16 yr; we use 14 here to remain conservative), we see that annual thinning might be underestimated in the upper two panels of Figure 47 by a maximum of 0.4 m at the terminus and 0.1 m at 1890 m. Thus, the small

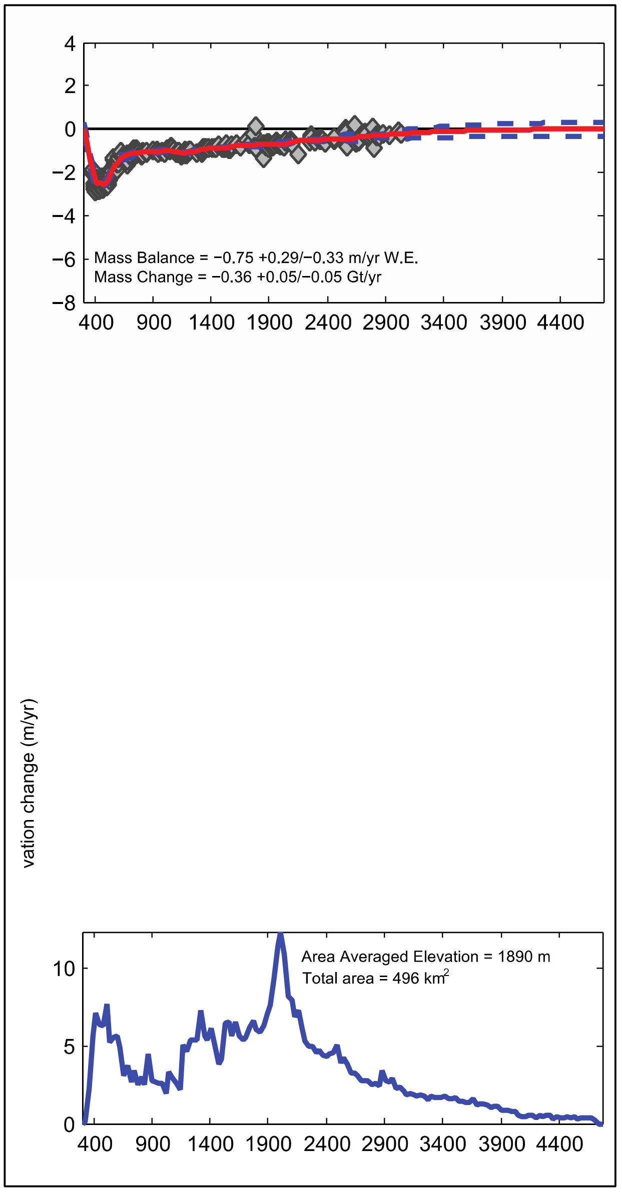

Figure 47. Elevation change and AAD for Kahiltna Glacier.

apparent increase in mass loss rate in the 2008-2010 (to -1.07 m/yr w.e.) interval may partly be an artifact of this problem.

It is interesting to note the more complicated spatial pattern of mass change during that interval, however, perhaps reflecting the passage of a kinematic wave.

Ruth Glacier was measured in 2001 and 2008 (Figure 48), and also has generally good data coverage. Mass balance in that interval was -0.8 m/yr w.e., comparable to other non-surging Denali Glaciers. The greatest mass loss was in the lower elevations, a pattern of change common in glaciers throughout this study.

Results from Muldrow and Traleika Glacier are shown in Figure 49 and Figure 51, but should be read with caution since Traleika Glacier is a tributary of Muldrow that is included within the AAD and mass balance results presented for Muldrow alone. We consider the Muldrow first; it was measured in 1994, 2001, 2008, and 2010. Muldrow is a long-period surging glacier and last surged in 1956/57 (Post 1960). The elevation changes documented during all intervals were thus consistent with our expectation of low elevation mass loss and upper elevation mass gain during the quiescent phase of a surging glacier. The upper Muldrow (above the Traleika confluence) gained mass during all periods measured, but this positive mass change was overwhelmed by the negative mass change in the lower Muldrow during all but the 2001-2008 period, which was overall very modestly positive (0.1 m/yr w.e.).

Measured elevation differences on the Muldrow over these intervals show great scatter, largely because of the complicated looped moraines of the Muldrow, which cause great spatial variability in melt rates. The Muldrow data are also complicated, like the Kahiltna data, by seasonally anomalous measurements. The first two measurements were in late August, while the last two were in mid-late May. We lack summer melt estimates for the Muldrow, so cannot make even a crude estimate of the quantitative impact of these anomalies on measured DZ profiles, but we note here simply that intervals which compare an initial August measurement with a subsequent May measurement will almost certainly bias the DZ plots towards more positive (or less negative) values, most substantially in the shortest (2001-2008) interval. It is interesting to note that this was the most positive balance rate recorded for the Muldrow.

Traleika Glacier was measured independently of Muldrow only in 2008 and 2010, and because it is a relatively high-elevation tributary, it mimics the pattern of mass gain above ~1800 m seen on the Muldrow as a whole. Note that the mass balance of Traleika is not comparable to those of other glaciers, since it does not include a complete ablation zone. We therefore omitted it from Figure 46.

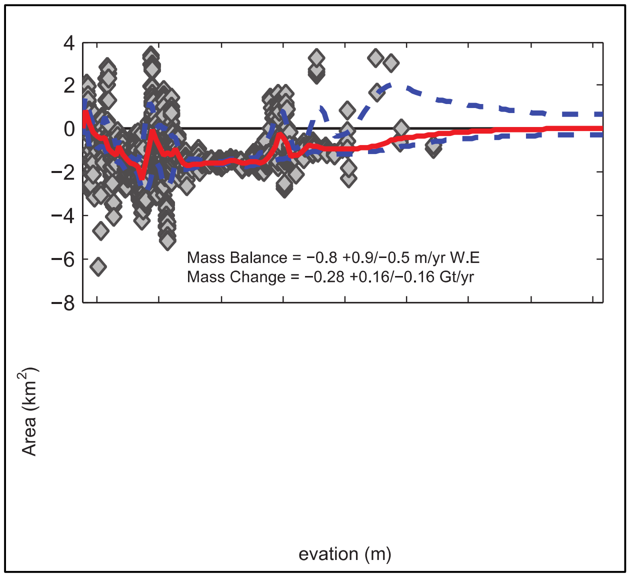

Figure 48. Elevation change and AAD for Ruth Glacier.

This calculation includes all tributaries.

Tokositna Glacier was measured in 2001 and 2008 (Figure 50). Elevation changes over that interval are difficult to interpret, with strongly negative values between about 400 and 700 m, small areas of apparently positive elevation changes just above and below that, and more negative values above 1000 m. These values may be real and reflective of some complicated dynamics, perhaps involving transport of debris-covered ice to lower elevations, or may simply reflect the relative sparsity of the data for Tokositna. In any case, the balance seems to be more negative than most other glaciers measured in DENA: -1.3 m/yr w.e.

Finally, we consider the glaciers of the Toklat group, shown graphically in Figure 57. Toklat 1 Glacier, the easternmost of the Toklat group, was measured in 1996 and 2008 (Figure 52). It has sparse data, but they depict a typical pattern of generalized mass loss with the greatest loss at low elevations, giving a mass balance of -0.7 m/yr w.e. Toklat 3 Glacier, the westernmost of the group, is shown in Figure 53 and was measured in 2001 and 2008. Results on Toklat 3 are remarkably similar to that of Toklat 1, with a slightly greater mass loss estimated at -1.33 m/yr w.e.

The West (Figure 54) and East (Figure 55) Branches of Toklat 2 Glacier were surveyed independently in 2001, 2008, and 2010. The overall 2001-2010 results are similar to the Toklat 1 and 3 results, but the data appear more complicated over the short 2008-2010 interval. This may be due to the high signal-to-noise ratio during that 2-year interval, but the mass gain of over 5 meters w.e./yr around 2000 m on the East Branch is intriguing. Regardless, mass balance is negative at all intervals for all the Toklat group. Note that the independent mass balance of the two branches of Toklat 2 are not strictly comparable to those of other glaciers, since neither reflects a complete glacier system. We therefore omitted these results from Figure 46.

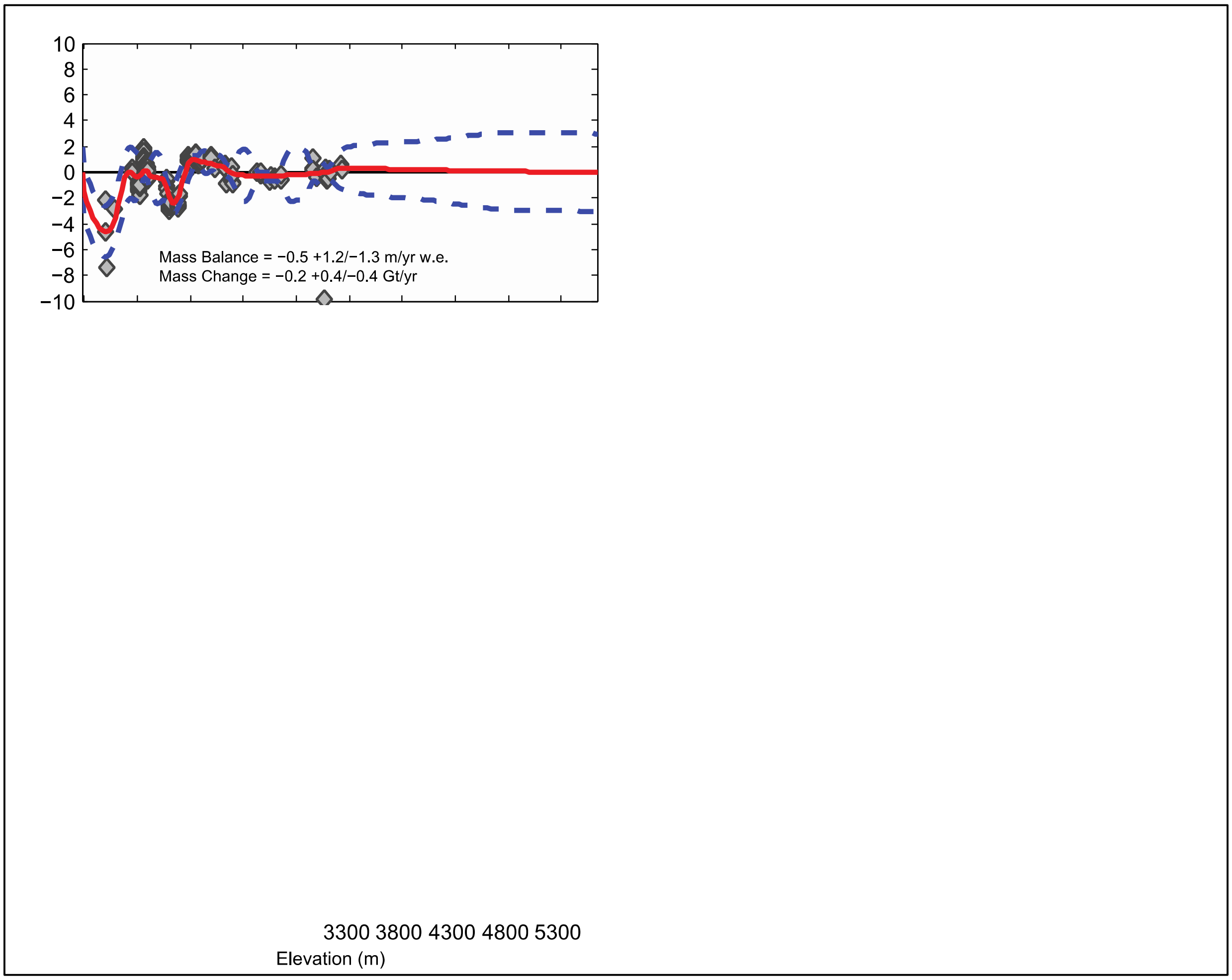

Figure 49. Elevation change and AAD for Muldrow Glacier.

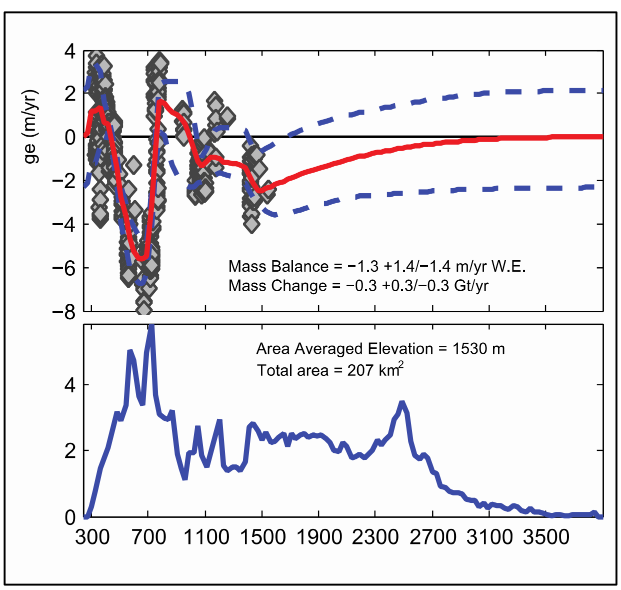

Figure 51. Elevation change and AAD for Tokositna Glacier.

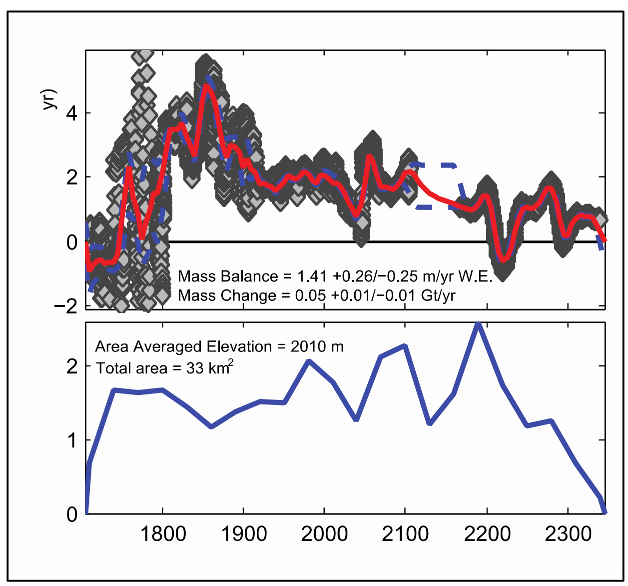

Figure 51. Elevation change and AAD for Traleika Glacier.

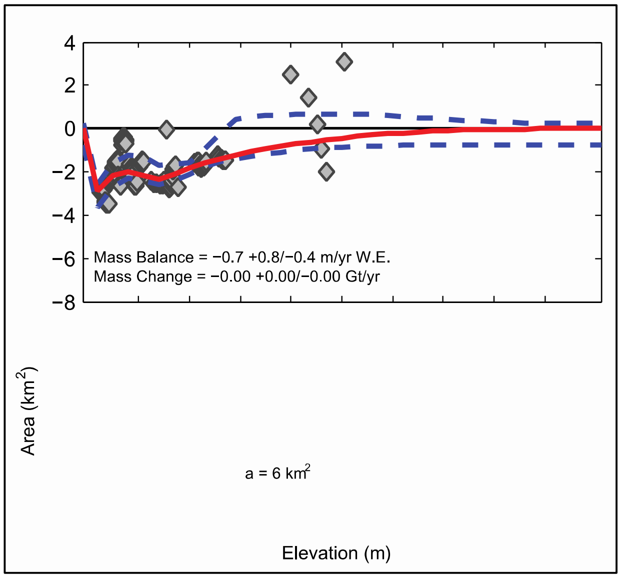

Figure 53. Elevation change and AAD for Toklat 1 Glacier.

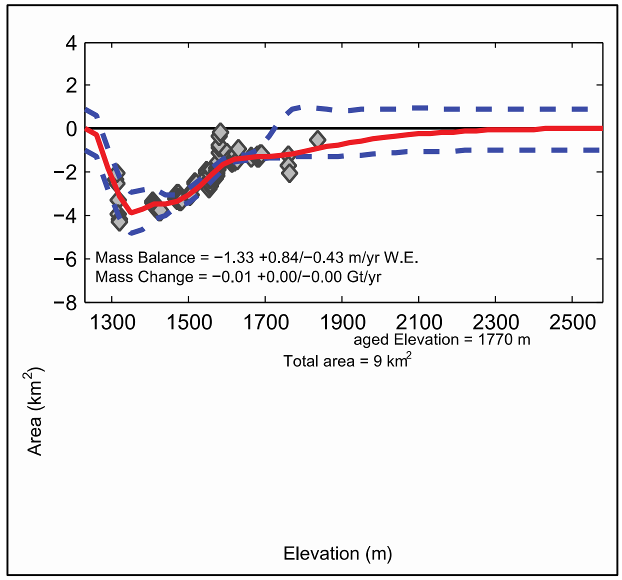

Figure 53. Elevation change and AAD for Toklat 3 Glacier.

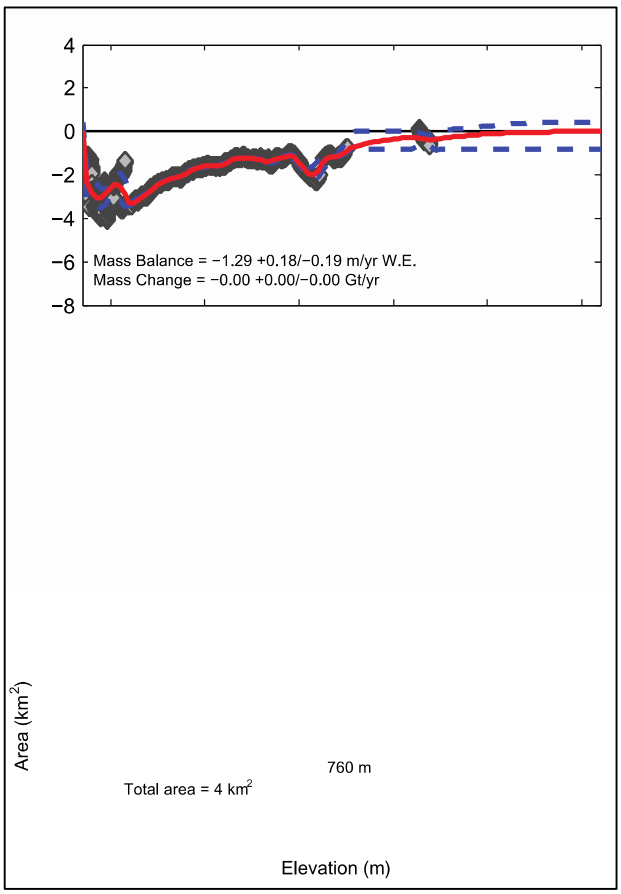

Figure 55. Elevation change and AAD for Toklat 2 West Branch Glacier.

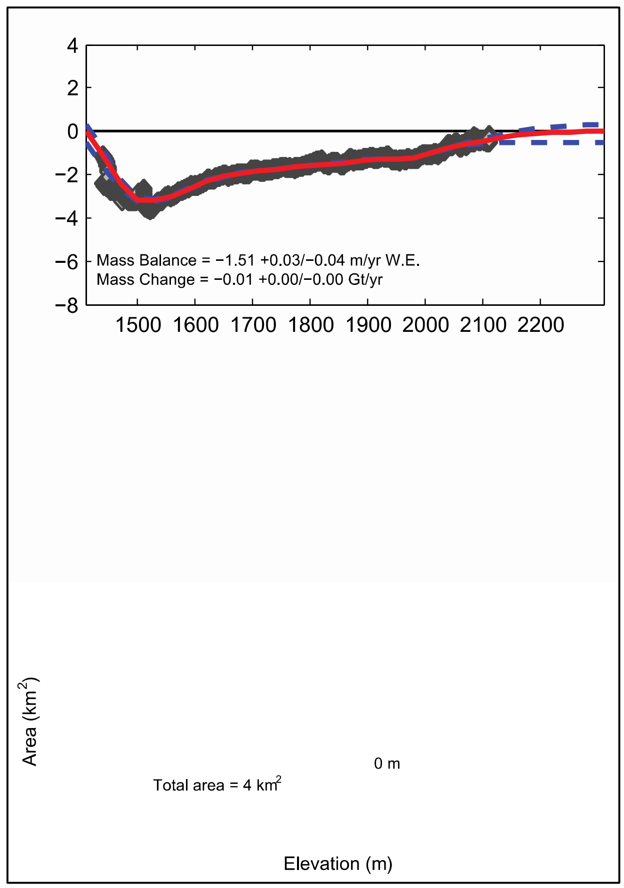

Figure 55. Elevation change and AAD for Toklat 2 East Branch Glacier.

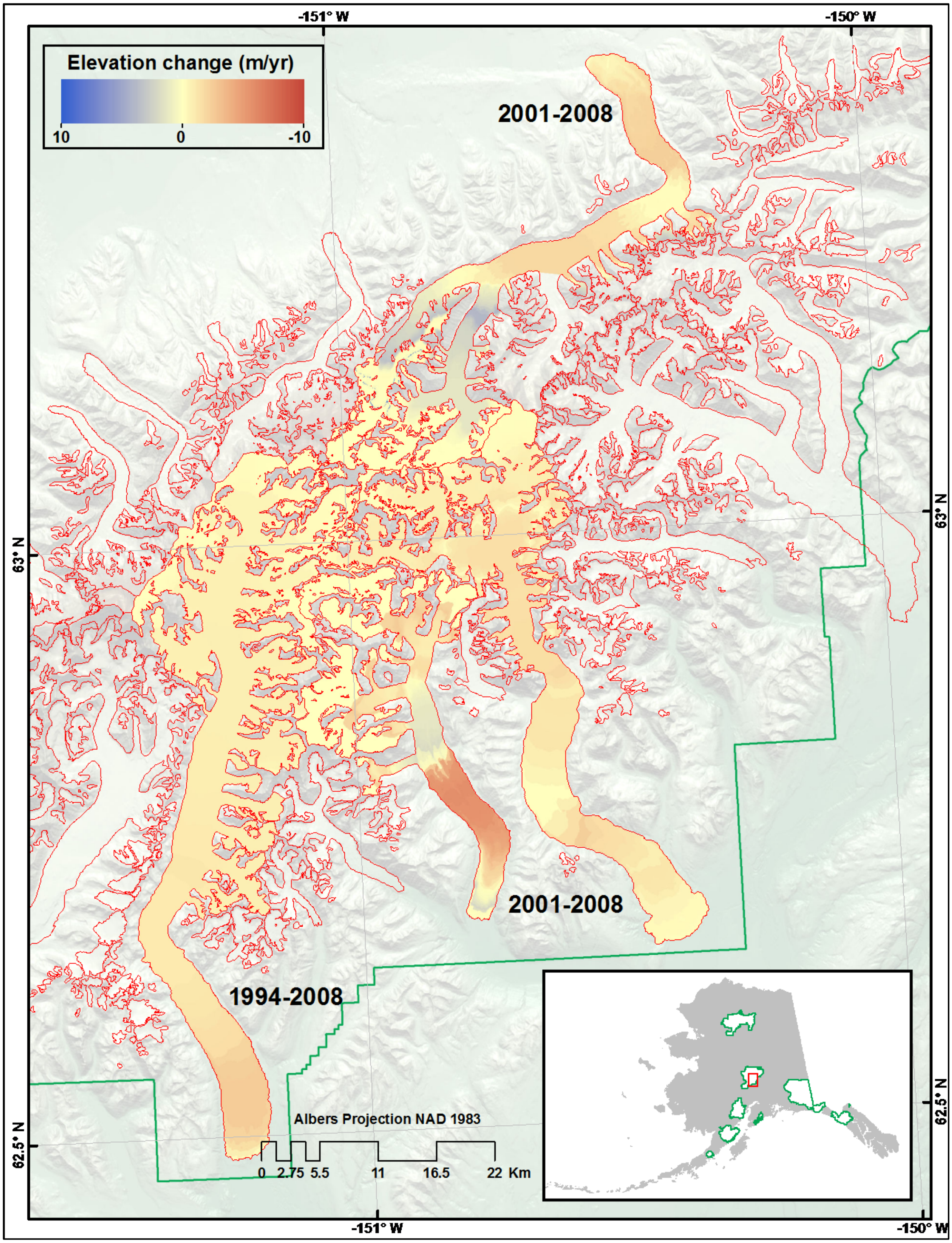

Figure 56. Annual rates of elevation change, by elevation, for glaciers in the glaciers in central Denali NP&P. Values are averages over the indicated time intervals.

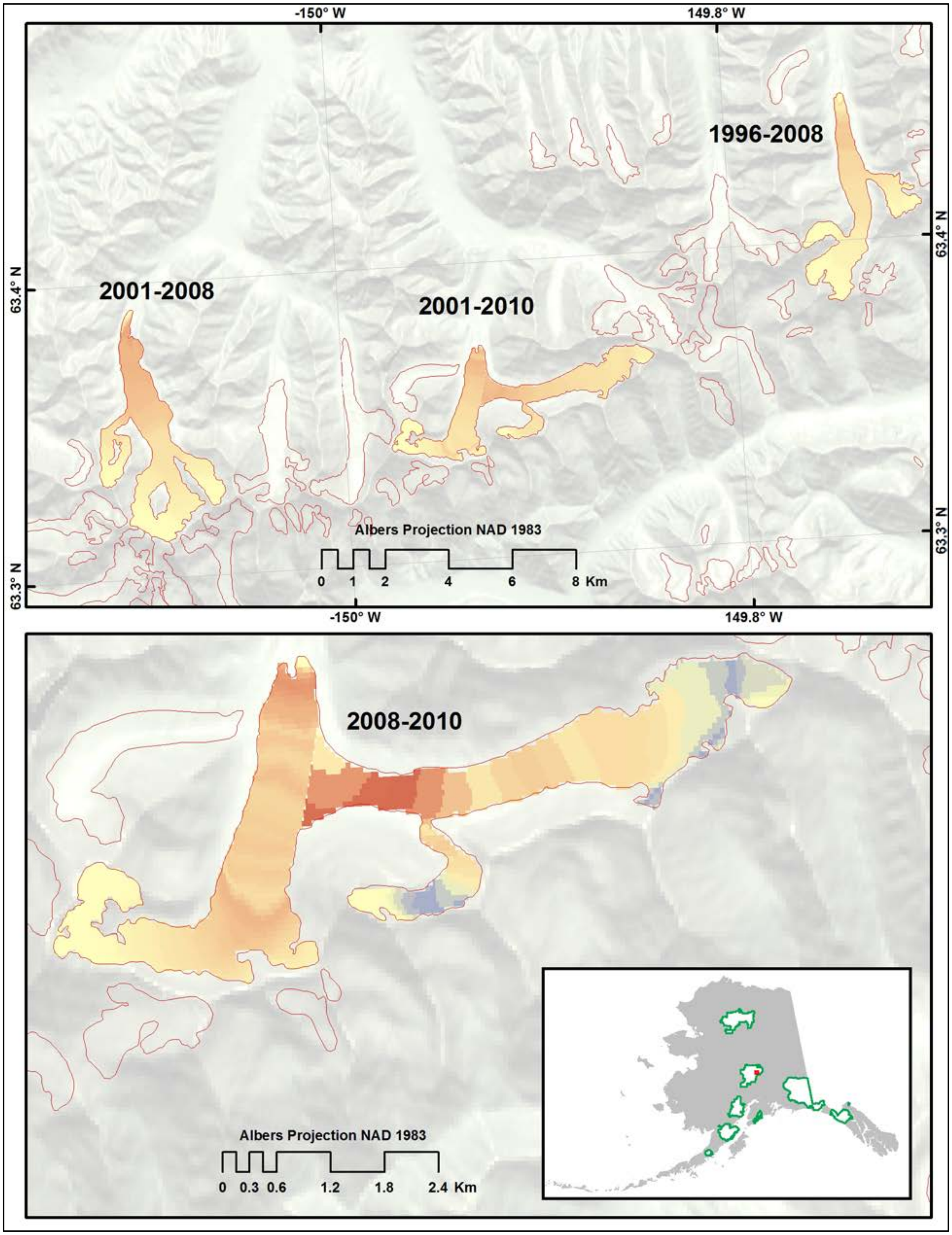

Figure 57. Annual rates of elevation change, by elevation, for Toklat Glaciers. Values are averages over the indicated time intervals.

Glacier Bay National Park and Preserve

We measured elevation change on 16 glaciers in Glacier Bay NP&P and present results for 33 discrete intervals of glacier change (Table 18). We note here that a full peer-reviewed analysis of the Glacier Bay elevation change results was recently published (Johnson et al. 2013). Glacier names, locations, and flight tracks are shown in Figure 58. Glacier-wide mass balance rates for all sampled glaciers are summarized in Figure 59, which shows that between 1995 and 2011 most glaciers lost mass at a rate of between 0 and 1.5 m/yr w.e. Mass balance variability appears to have increased in the most recent interval of measurement (2009-2011), with values ranging from -2.85 to 0.40 m/yr w.e. for Grand Plateau and Margerie Glaciers, respectively, but this is partly an artifact of a larger sample size in that time period. We describe these trends by individual glacier below, and show some results in map view in Figure 78-Figure 80.

We start with Brady Glacier (Figure 60), Lamplugh (Figure 61), and Reid Glaciers (Figure 62), which like many other glaciers in GLBA were flown in 1995, 2000, 2005, 2009, and 2011. These three glaciers share a flow divide around 750 m, where Brady flows south and the others flow north. Brady is the largest of the three and lost mass consistently over all four time periods with mass balance rates ranging -1.84 to -0.73 m/yr w.e. Brady has the best high elevation data coverage of the three glaciers, and the temporal pattern of mass loss at higher elevations was variable, including evidence for a slight mass gain around 1400 m between 2009 and 2011, but overall Brady Glacier lost the most mass, and most consistently, at lower elevations below the flow divide. Lamplugh and Reid Glaciers lost mass at all intervals, mostly at modest rates but fastest, like Brady, between 2000 and 2005. During that time, the mass balance of Lamplugh was -0.54 m/yr w.e. and of Reid was -0.93 m/yr w.e.

Riggs Glacier (Figure 63) showed some contrasts with nearby Muir Glacier (Figure 72). Both were flown in 2005, 2009, and 2011, and Muir alone was flown in 2000. Both glaciers lost mass modestly (between 0.0 and -1.0 m/yr w.e.) at all sampled intervals, with most mass loss occurring at the lowest elevations. But the upper elevations of these glaciers, which are nearly adjacent, behaved differently. Riggs lost mass consistently at the upper elevations, but Muir thickened above 1100 m after 2005. Interestingly, nearby Little Jarvis Glacier was flown in 1995 and 2000 (Figure 64), and during that interval it thickened slightly at elevations above about 1250 m, as well. Overall, Little Jarvis lost most at a rate of -0.43 m/yr w.e.

Casement Glacier and Davidson Glacier were both flown in 2005, 2009, and 2011 (Figure 65 and Figure 66). Both thinned substantially, including mass loss at their shared divide around 1200 m. Mass loss for both was highest between 2009 and 2011, with -1.46 and -1.18 m/yr w.e. for Casement and Davidson respectively. Land-terminating Casement Glacier has been thinning more rapidly than lake-calving Davidson near its terminus, with rates of -6 to -8 m/yr between 200 and 300 m surface elevation.

Carroll Glacier was flown in 2009 and 2011 (Figure 67). The pattern of mass loss with elevation suggests there may have been a surge there during this period, as the glacier lost ~3 m/yr between 1600 and 1800 m while gaining mass in a broad zone between 1200 and 1500 m. We have no direct observations to corroborate this, and note that in any case the terminus lost mass at a substantial rate of up to 8 m/yr, suggesting it was unaffected by any contemporary surging. The glacier-wide mass balance rate was -0.68 m/yr w.e. Across the divide from Carroll, Tkope Glacier (Figure 75) was flown over that same interval and exhibited a more straightforward pattern of increasing mass loss at lower elevations, with an overall mass balance rate of -0.2 m/yr w.e.

Table 24. Mass balance and mass change of glaciers in Glacier Bay NP&P inferred from laser altimetry at discrete time intervals. 'MB+', 'MB-', 'MC+', and 'MC-' give positive and negative 95% confidence intervals for mass balance and mass change, respectively.

Glacier	Type	Size (km^2)	Mean Elev (m)	Start date	End date	Mass Balance (m/yr)	MB+	MB-	Mass Change (gt/yr)	MC+	MC-
Brady	(L)	502	720	6/4/95	5/25/00	-1.04	0.19	0.19	-0.52	0.10	0.10
Brady	(L)	502	720	5/25/00	6/1/05	-1.84	0.26	0.24	-0.92	0.12	0.12
Brady	(L)	502	720	6/1/05	6/2/09	-0.73	0.37	0.31	-0.37	0.15	0.15
Brady	(L)	502	720	6/2/09	5/30/11	-1.35	0.23	0.24	-0.68	0.12	0.12
Carroll	(L/S)	401	1020	6/2/09	5/30/11	-0.68	0.37	0.28	-0.27	0.11	0.11
Casement	(L)	159	1160	6/1/05	6/2/09	-1.18	0.41	0.44	-0.19	0.07	0.07
Casement	(L)	159	1160	6/2/09	5/30/11	-1.46	0.42	0.51	-0.23	0.08	0.08
Davidson	(LK)	84	1170	6/1/05	6/2/09	-0.68	0.35	0.35	-0.06	0.03	0.03
Davidson	(LK)	84	1170	6/2/09	5/30/11	-1.18	0.28	0.26	-0.10	0.02	0.02
Fairweather	(L)	225	920	6/2/09	5/30/11	-1.35	0.70	0.93	-0.30	0.21	0.21
Grand Pacific	(T)	533	1350	6/7/96	6/6/01	-0.50	0.70	0.70	-0.20	0.40	0.40
Grand Pacific	(T)	533	1350	6/6/01	6/2/09	-1.15	0.62	0.62	-0.61	0.33	0.33
Grand Pacific	(T)	533	1350	6/2/09	5/29/11	-1.58	0.44	0.64	-0.84	0.34	0.34
Grand Plateau	(LK)	390	1300	6/2/05	6/2/09	-1.02	0.46	0.51	-0.40	0.20	0.20
Grand Plateau	(LK)	390	1300	6/2/09	5/30/11	-2.85	0.77	0.83	-1.11	0.32	0.32
Konamoxt	(LK)	72	1300	6/7/96	5/30/11	-1.28	0.62	0.65	-0.09	0.05	0.05
Lamplugh	(T)	139	950	6/4/95	5/25/00	-0.32	0.31	0.30	-0.04	0.04	0.04
Lamplugh	(T)	139	950	5/25/00	6/1/05	-0.54	0.44	0.42	-0.08	0.06	0.06
Lamplugh	(T)	139	950	6/1/05	6/2/09	-0.10	0.50	0.50	0.00	0.10	0.10
Lamplugh	(T)	139	950	6/2/09	5/30/11	-0.10	0.40	0.40	0.00	0.10	0.10
Little Jarvis	(L)	2	1220	5/31/95	5/28/00	-0.43	0.34	0.26	0.00	0.00	0.00
Margerie	(T/S)	173	1670	6/2/05	6/2/09	0.00	0.60	0.20	0.00	0.00	0.00
Margerie	(T/S)	173	1670	6/2/09	5/30/11	0.40	0.80	0.80	0.10	0.10	0.10
Melbern	(LK)	81	1140	6/2/09	5/29/11	-0.80	1.00	1.00	-0.10	0.10	0.10
Muir	(L)	119	1120	5/28/00	6/1/05	-0.50	0.50	0.60	-0.10	0.10	0.10
Muir	(L)	119	1120	6/1/05	6/2/09	0.00	0.40	0.40	0.00	0.00	0.00
Muir	(L)	119	1120	6/2/09	5/30/11	-0.10	0.30	0.40	0.00	0.10	0.10
Reid	(T)	69	800	6/4/95	5/25/00	-0.31	0.27	0.30	-0.02	0.02	0.02
Reid	(T)	69	800	5/25/00	6/1/05	-0.93	0.23	0.22	0.06	0.02	0.02
Reid	(T)	69	800	6/1/05	6/2/09	-0.10	0.30	0.30	0.00	0.00	0.00
Reid	(T)	69	800	6/2/09	5/30/11	-0.20	0.40	0.50	0.00	0.00	0.00
Riggs	(L)	114	1050	6/1/05	6/2/09	-0.41	0.29	0.29	-0.05	0.03	0.03
Riggs	(L)	114	1050	6/2/09	5/30/11	-0.93	0.32	0.31	-0.11	0.04	0.04
Tkope	(L)	116	1260	6/2/09	5/30/11	-0.10	0.40	0.40	0.00	0.10	0.10

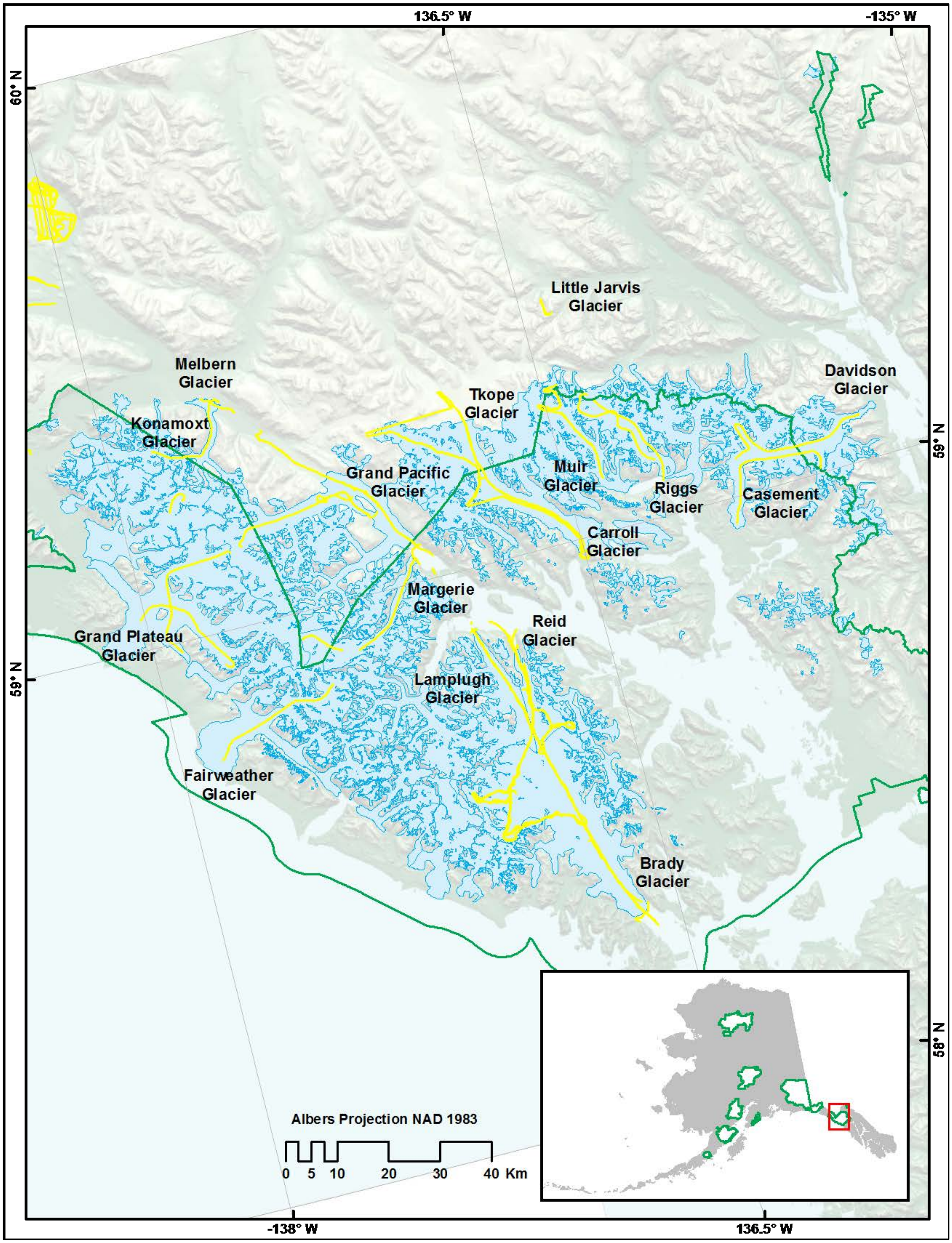

Figure 58. Locations of glaciers in Glacier Bay with elevation change results reported in this paper. Laser altimetry tracks are shown in yellow.

Fairweather Glacier was also flown in 2009 and 2011 (Figure 68), and its mass balance of -1.35 m/yr w.e. was among the lower in GLBA during that interval. Fairweather is a land-terminating glacier, and its near-sea level terminus thinned by up to 3 m/yr.

Grand Pacific Glacier had increasingly negative mass balances over the intervals of flights in 1996, 2001, 2009, and 2011 (Figure 71). This recent decrease in mass contrasts with the terminus advance that we documented over a longer (half-century) time-frame. Near its terminus, thinning was about 4 m/yr in the earlier intervals and up to 8 m/yr between 2009 and 2011, while upper elevations underwent a sometimes more complicated pattern of more moderate thinning. The 2009-2011 mass balance rate of -1.58 m/yr w.e. was the second most negative value in GLBA over our period of record.

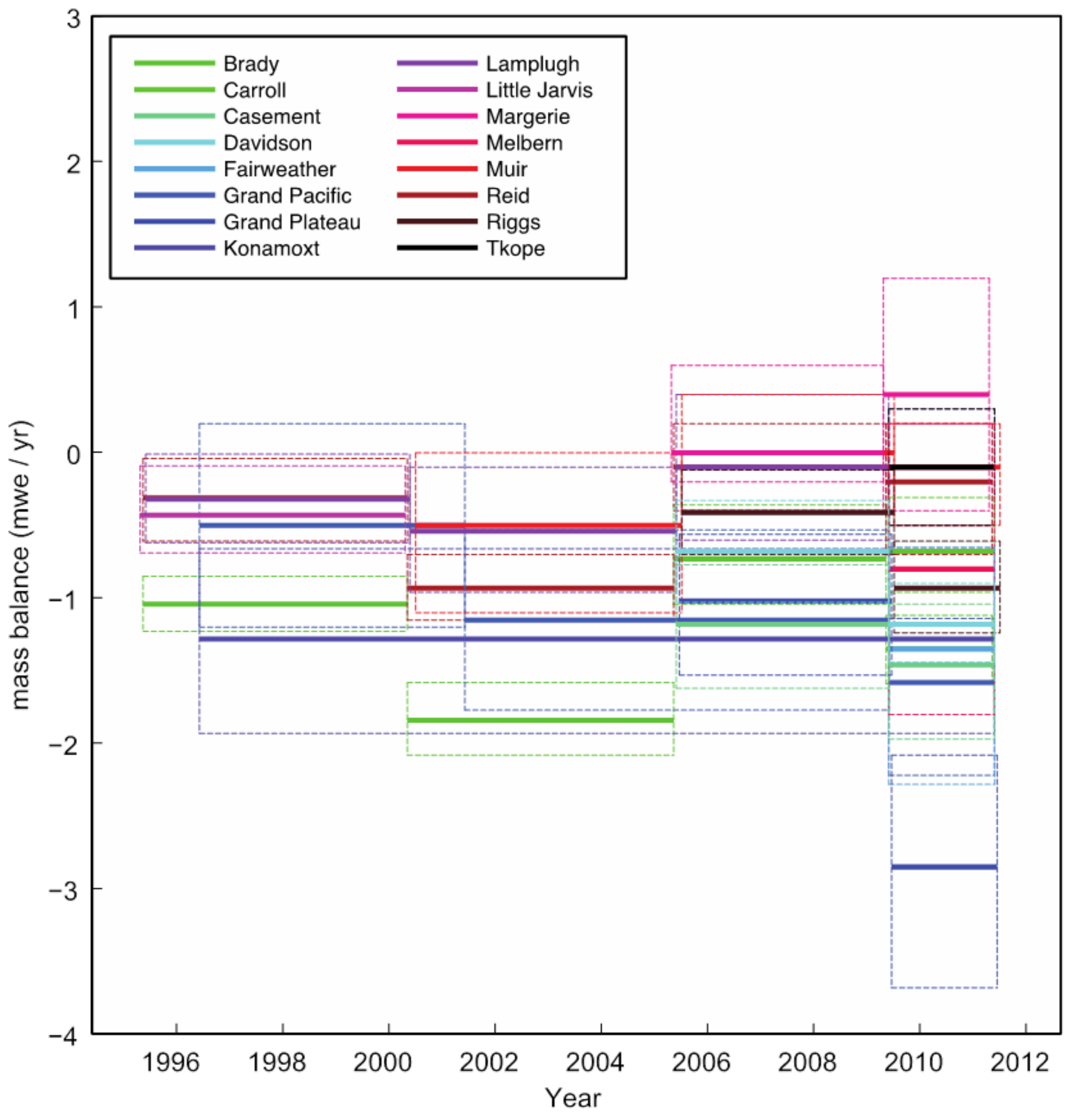

Figure 59. Mass balance of select glaciers in Glacier Bay National Park & Preserve. Thick solid lines are mass balances; upper and lower dashed lines reflect confidence intervals for each time period. For clarity, some lines have been shifted a few pixels left or right to minimize overlap.

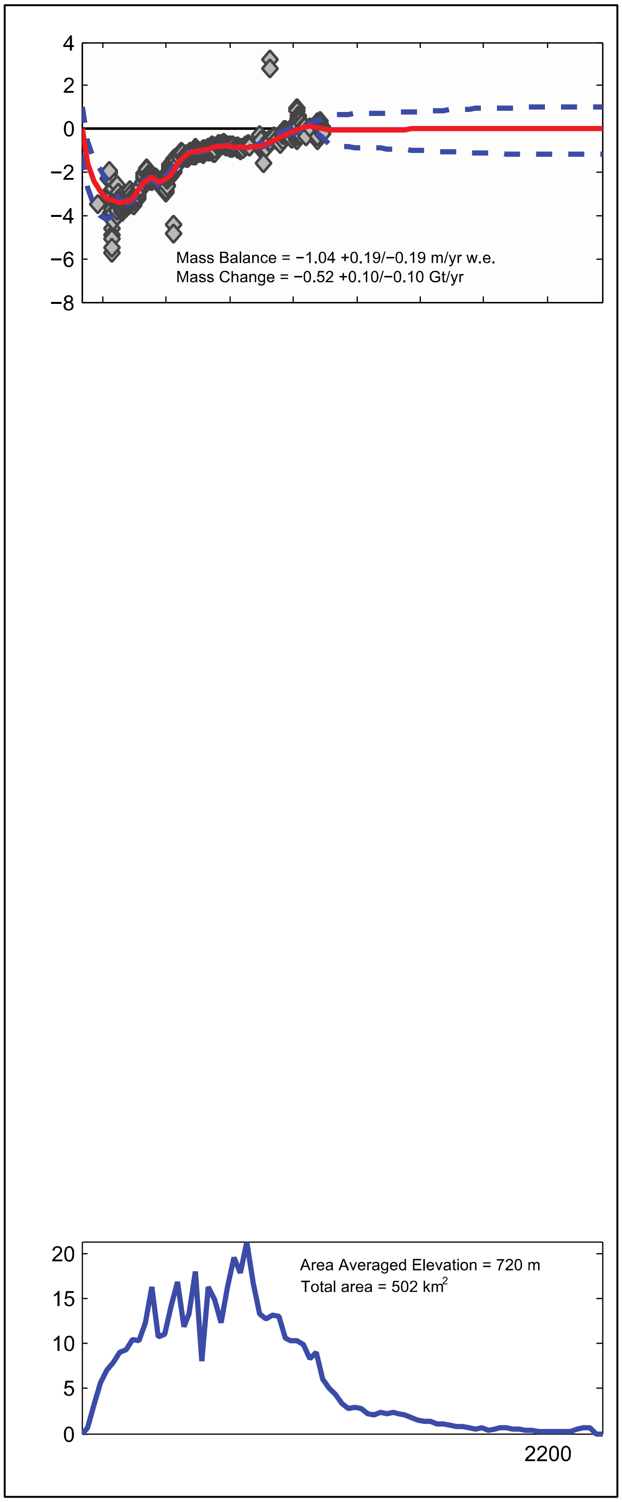

Figure 61. Elevation change and AAD for Brady Glacier.

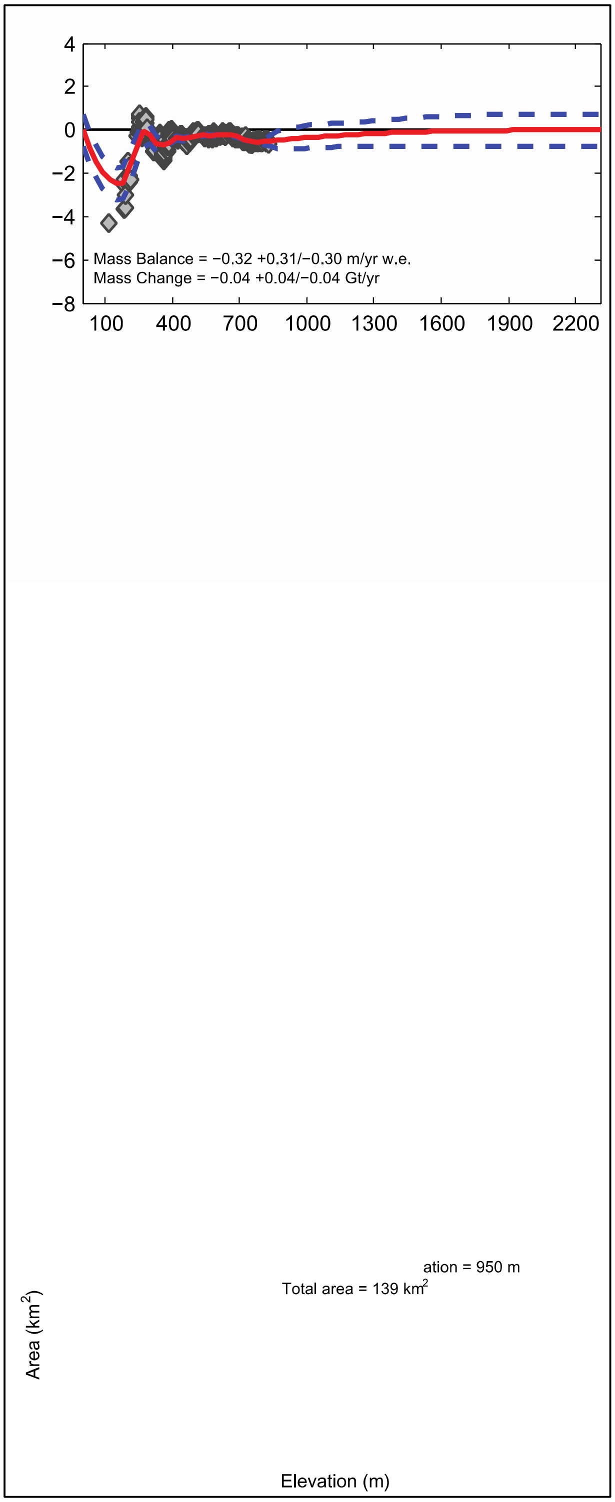

Figure 61. Elevation change and AAD for Lamplugh Glacier.

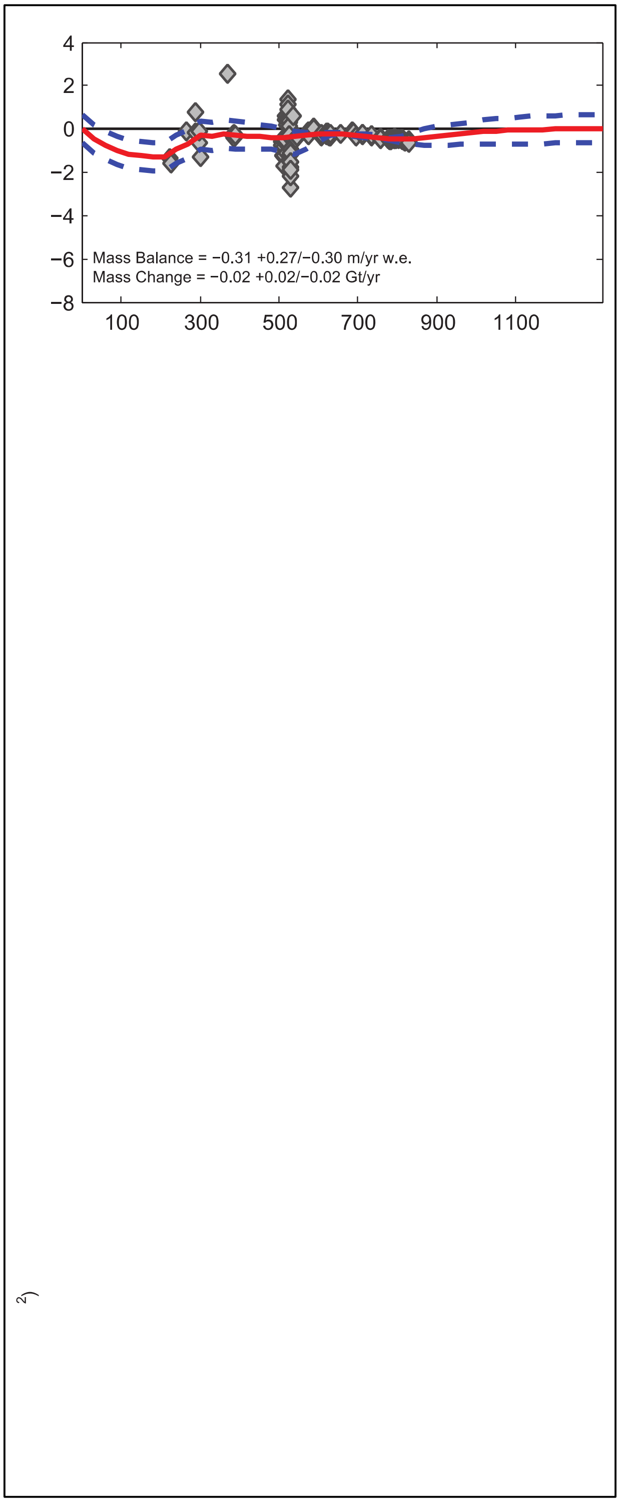

Figure 64. Elevation change and AAD for Reid Glacier.

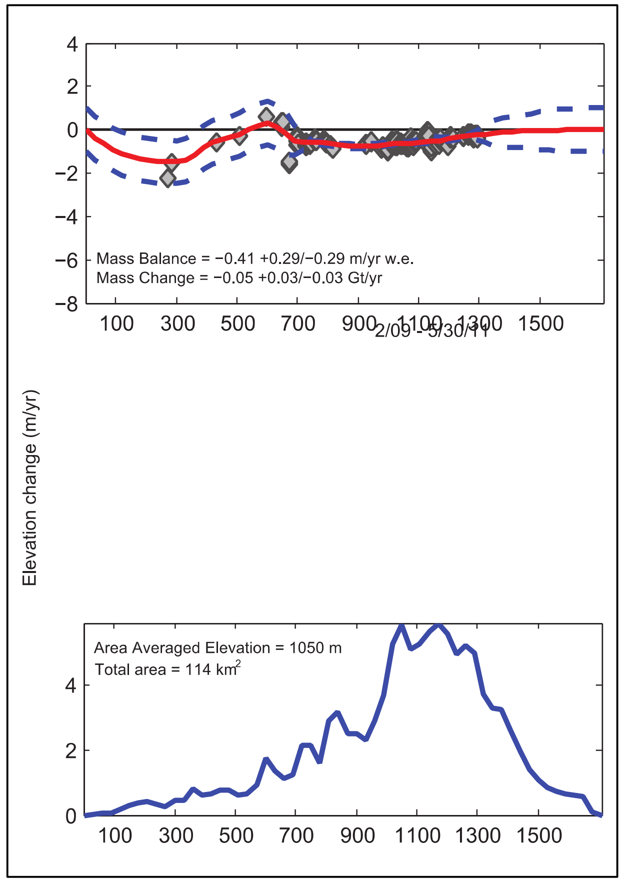

Figure 64. Elevation change and AAD for Riggs Glacier.

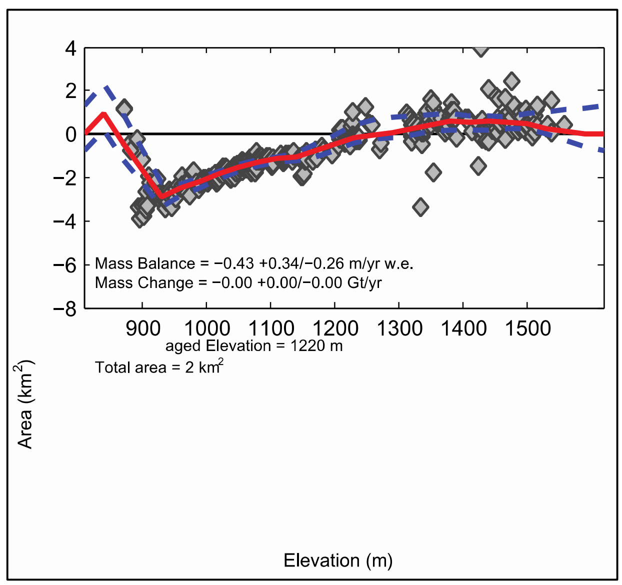

Figure 64. Elevation change and AAD for Little Jarvis Glacier.

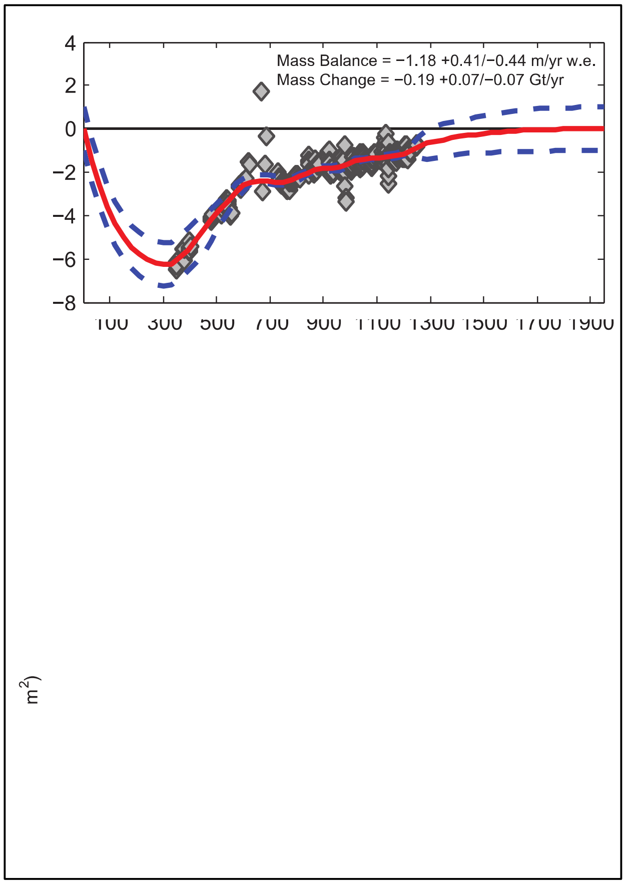

Figure 66. Elevation change and AAD for Casement Glacier.

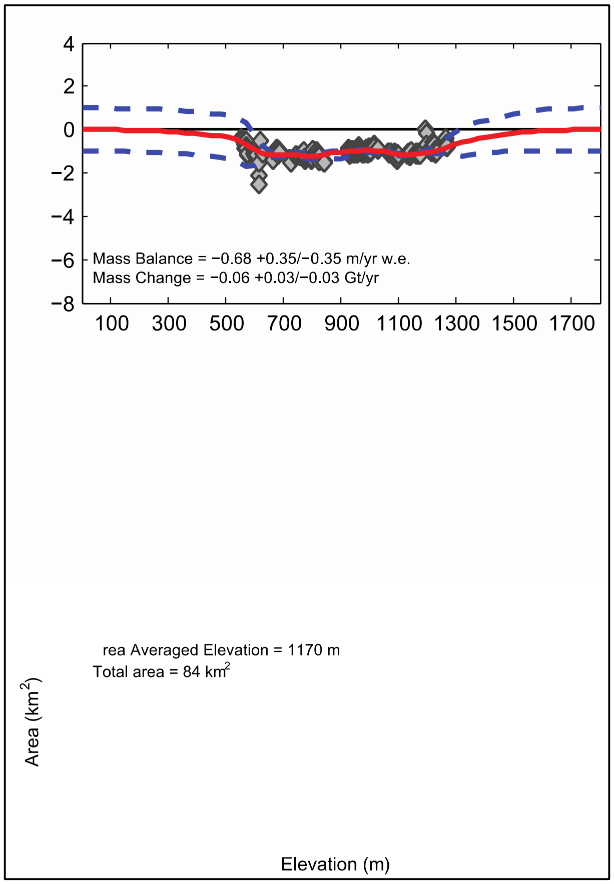

Figure 66. Elevation change and AAD for Davidson Glacier.

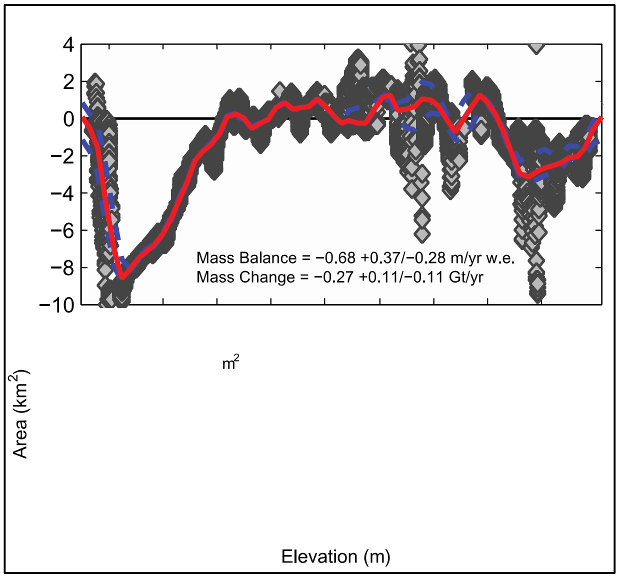

Figure 67. Elevation change and AAD for Carroll Glacier.

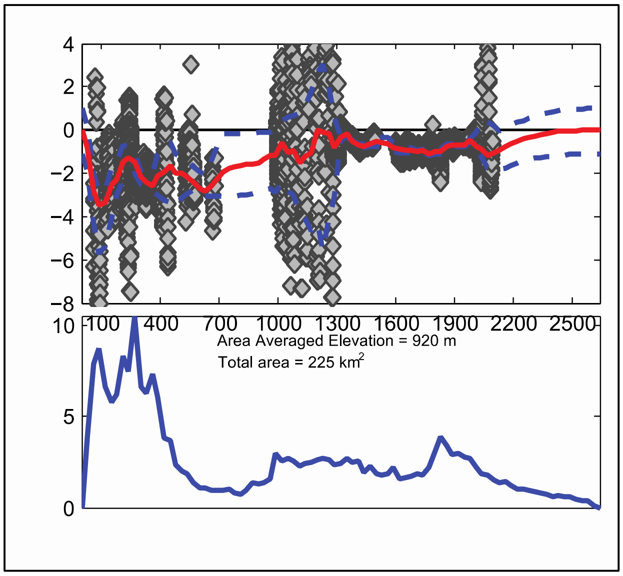

Figure 68. Elevation change and AAD for Fairweather Glacier.

Grand Plateau Glacier, a lake-calving glacier across the divide from Grand Pacific, was flown in 2005, 2009, and 2011 (Figure 71). Like Grand Pacific, its terminus area had thinning rates of nearly 8 meters between 2009 and 2011, but it also had substantial thinning of up to 2 m/yr in its uppermost elevations, and the mass balance during that period was very negative—in fact, the lowest in GLBA over our period of record: -2.85 m/yr w.e. This value is large compared with other glaciers but also compared with the previous interval on Grand Plateau itself, when the value was -1.02 m/yr w.e.

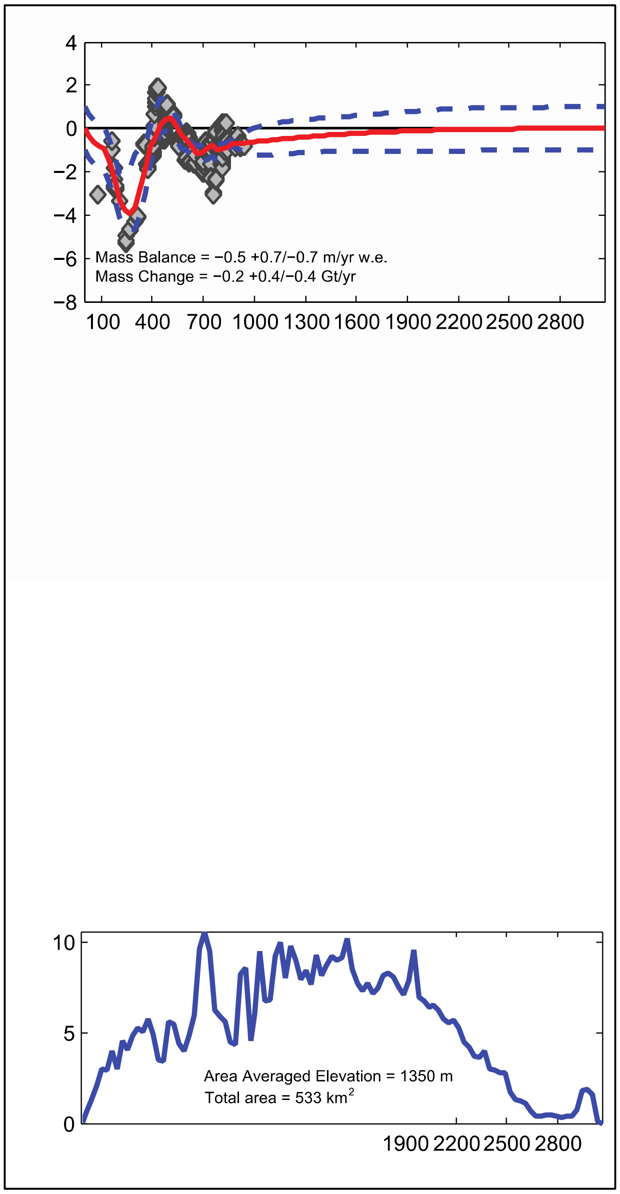

Figure 69. Elevation change and AAD for Grand Pacific Glacier.

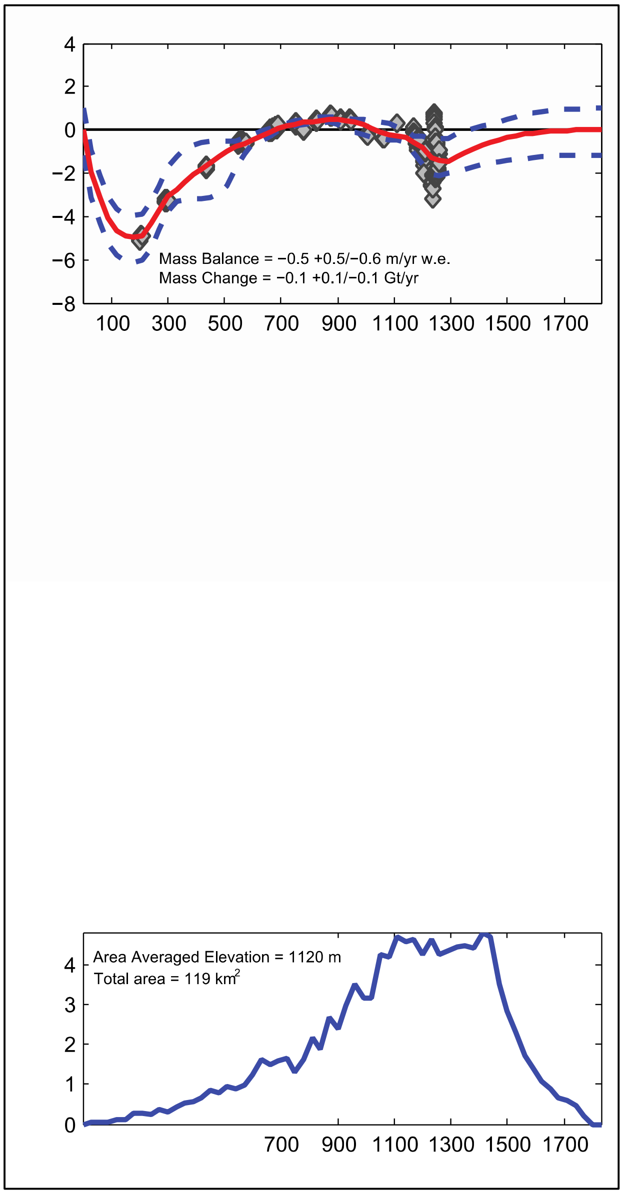

Figure 70. Elevation change and AAD for Muir Glacier.

Margerie Glacier was flown in 2005, 2009 and 2011 (Figure 72), and the pattern of change on this surge-type tidewater glacier is not typical of others in our study. The main (southern) branch of Margerie Glacier last surged between late 1980 and 1986 (Molnia, 2008), and since 2005 its terminus has been thickening by 1-5 m/yr. Combined with variable but modest rates of elevation change at upper elevations, including some evidence for thickening above 2100 m, we infer mass balance rates of approximately 0.0 m/yr w.e. (no change) between 2005 and 2009 and 0.4 m/yr w.e. from 2009 to 2011. The positive balance in this last interval is intriguing, and is clearly reflective of unusual dynamics at Margerie, but we note that our mass balance rate has large uncertainties for this glacier due to an important absence of data between 1300 and 2200 meters where a steep icefall prevents our aircraft from flying at suitable range.

Konamoxt and Melbern Glaciers were once tributaries, but now are both calving into glacial Lake Melbern. Our measurements on these related glaciers are asynchronous: Konamoxt was flown in 1996 and 2011 (Figure 73), and Melbern was flown in 2009 and 2011 (Figure 74). Data coverage on both glaciers is poor, omitting significant higher elevation areas. Over the longer interval 1996-2011, Konamoxt had a mass balance rate of -1.28 m/yr w.e., reflecting substantial thinning of up to 7 m/yr near its terminus (over 100 m of total thinning over that 15-interval), while Melbern had a rate of -0.8 m/yr w.e. over the two years of its flights.

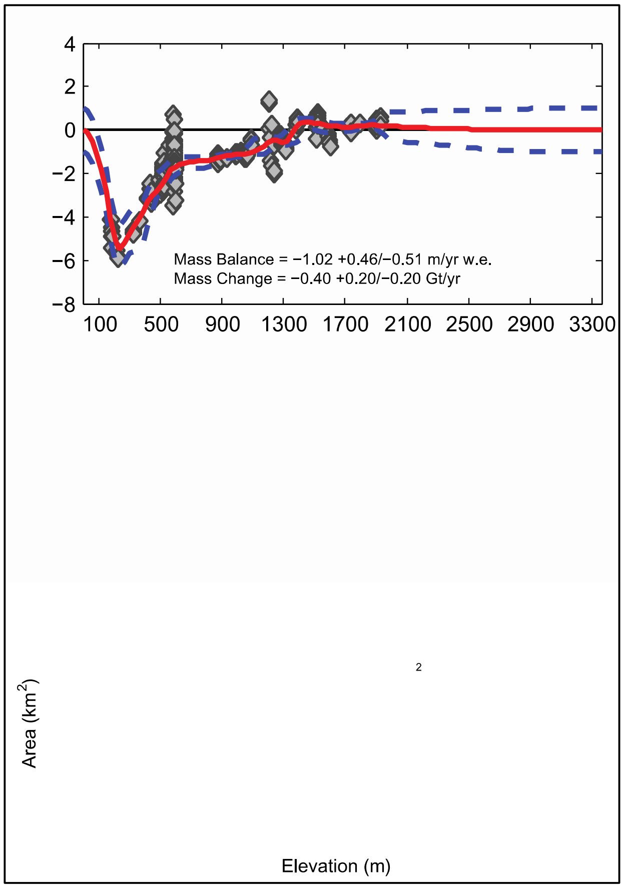

Figure 71. Elevation change and AAD for Grand Plateau Glacier.

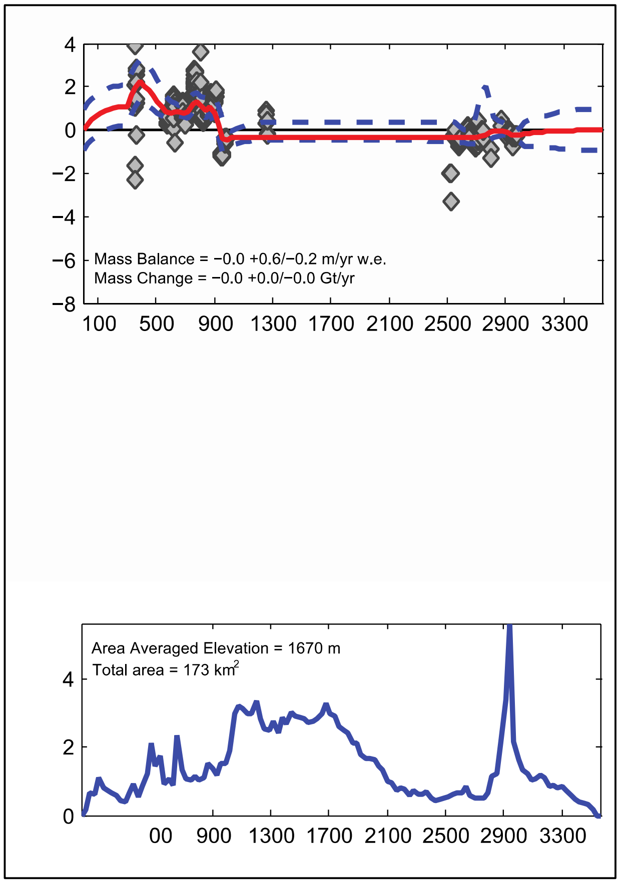

Figure 72. Elevation change and AAD for Margerie Glacier.

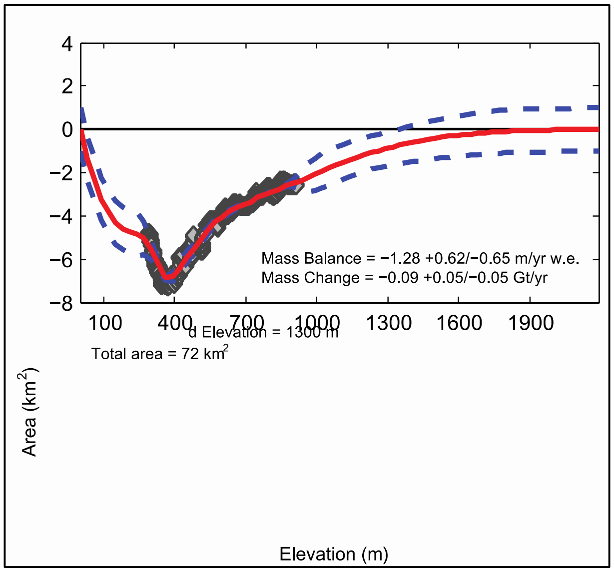

Figure 73. Elevation change and AAD for Konamoxt Glacier.

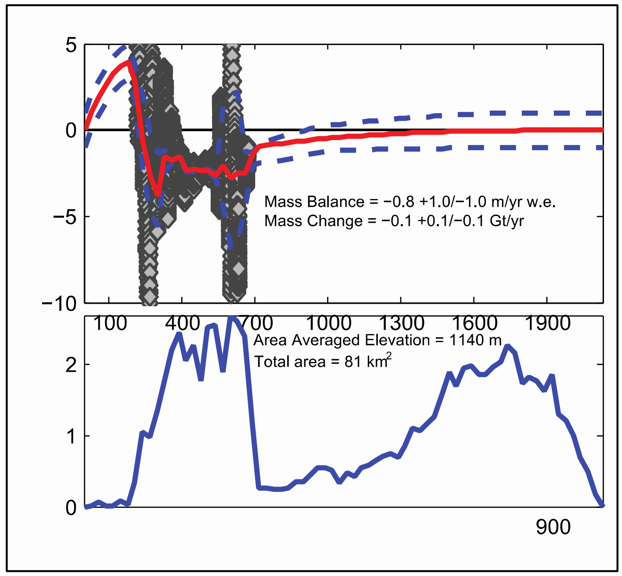

Figure 74. Elevation change and AAD for Melbern Glacier.

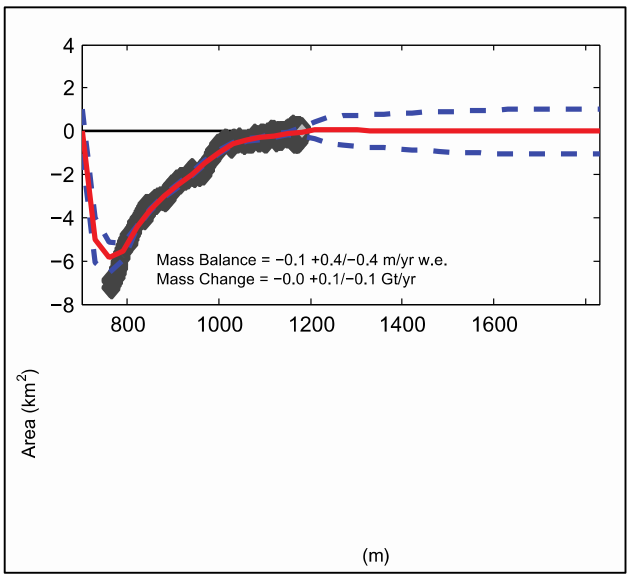

Figure 75. Elevation change and AAD for Tkope Glacier.

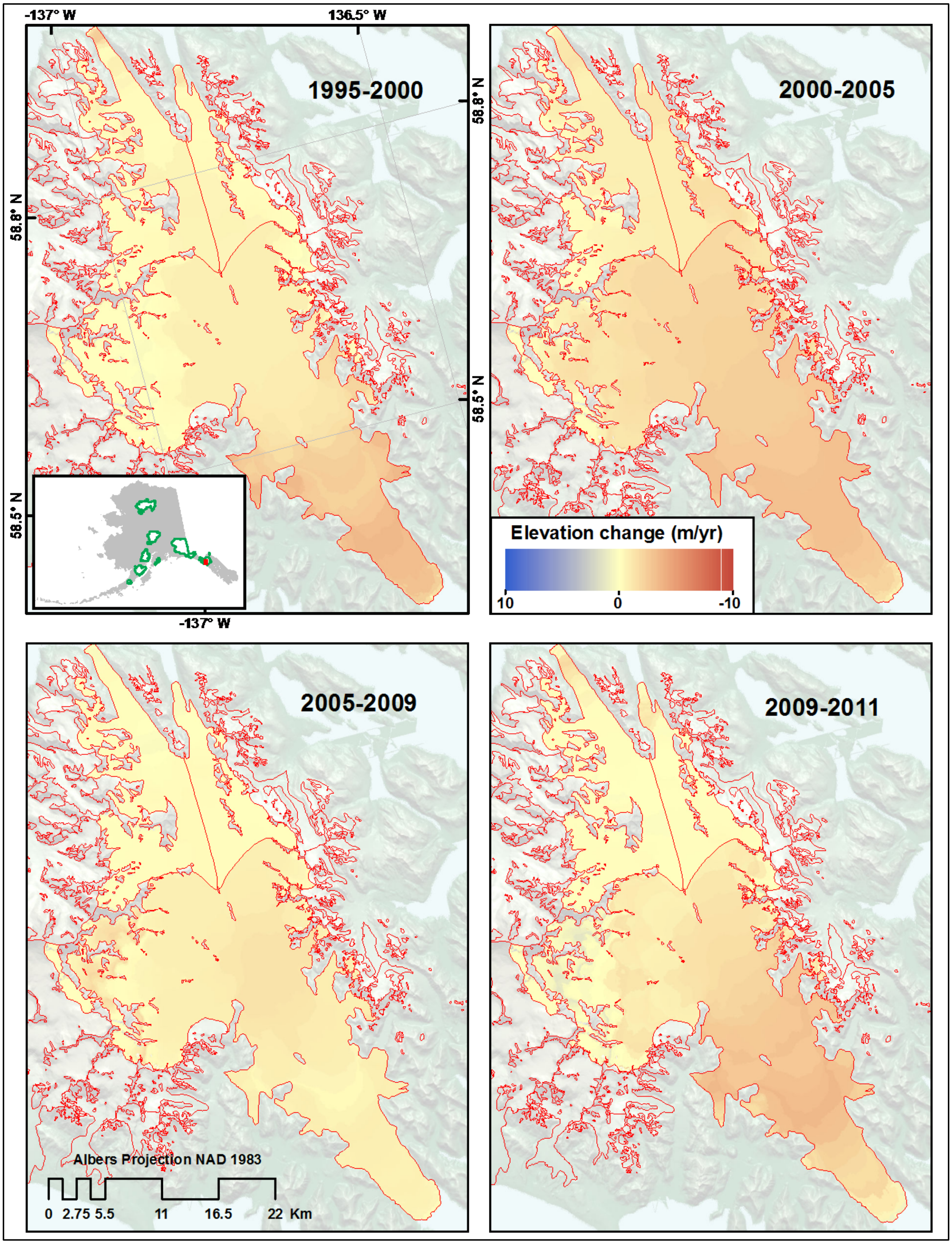

Figure 76. Annual rates of elevation change, by elevation, for Brady, Lamplugh, and Reid Glaciers in Glacier Bay NP&P. Values are averages over the indicated time intervals.

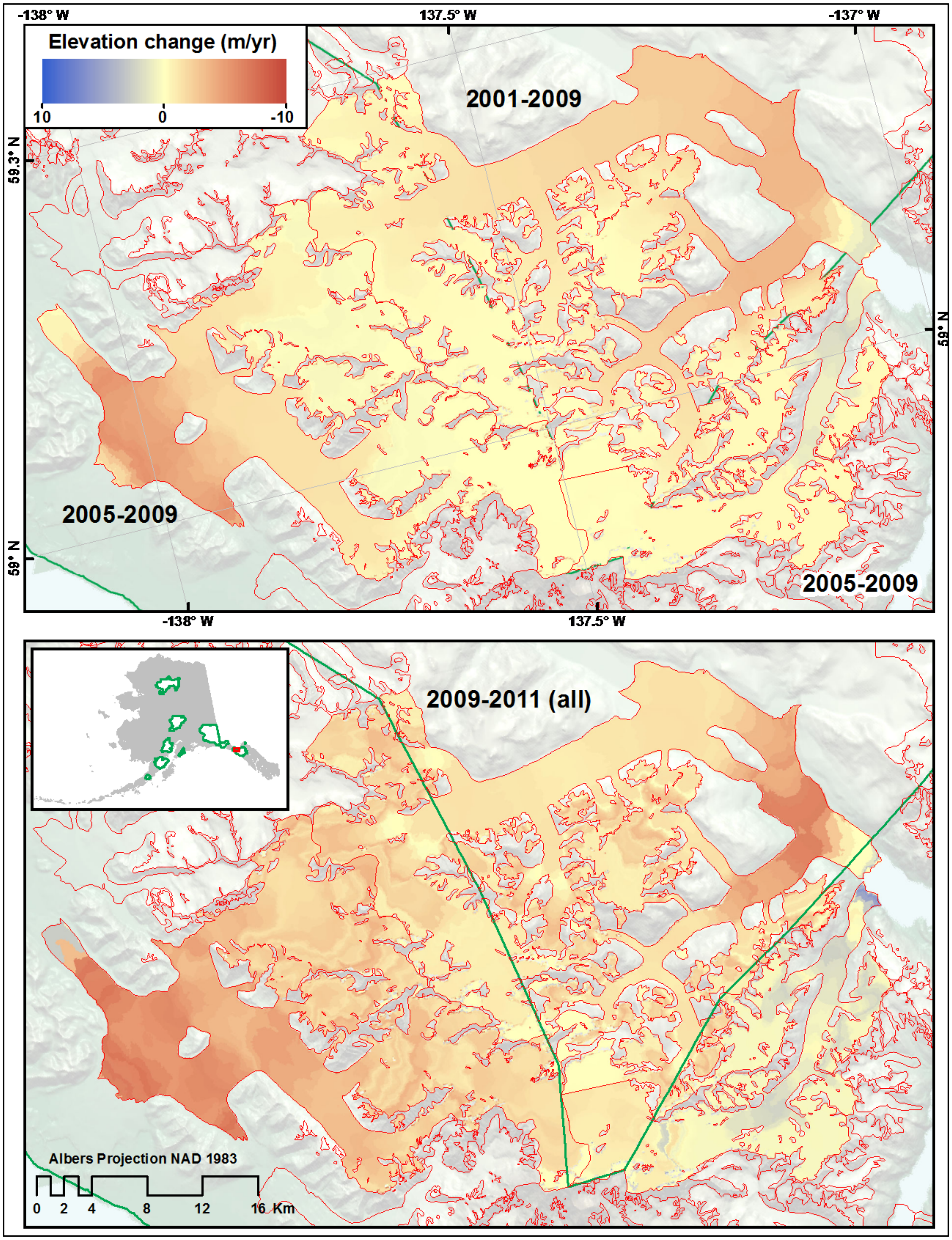

Figure 77. Annual rates of elevation change, by elevation, for Margerie, Grand Plateau, Konamoxt, Melbern and Grand Pacific Glaciers in Glacier Bay NP&P. Values are averages over the indicated time intervals.

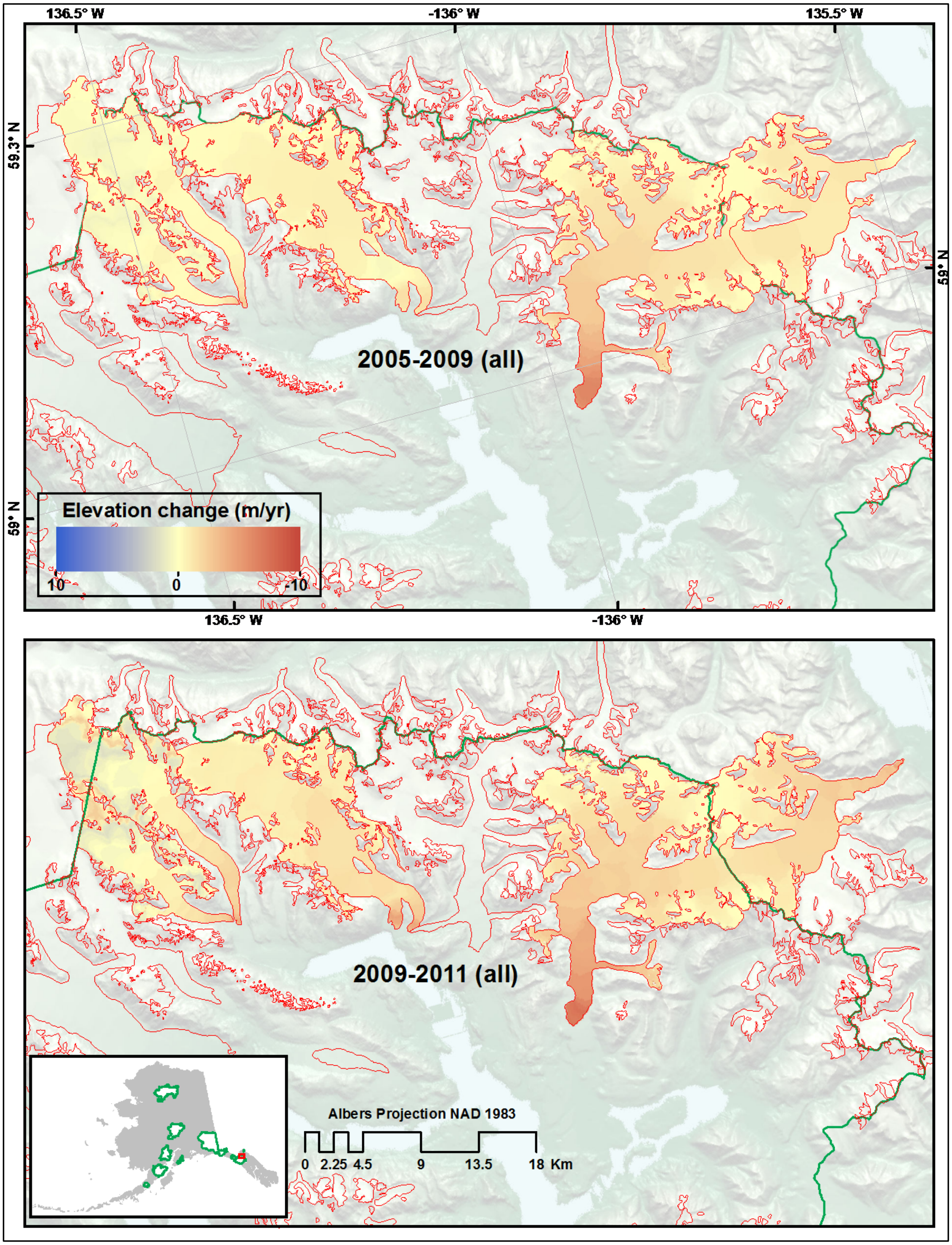

Figure 78. Annual rates of elevation change, by elevation, for Muir, Riggs, Carroll, Casement, and Davidson Glaciers in Glacier Bay NP&P. Values are averages over the indicated time intervals.

Kenai Fjords National Park

We measured elevation change on 12 glaciers in Kenai Fjords NP and present results for 35 discrete intervals of glacier change (Table 19). Glacier names, locations, and flight tracks are shown in Figure 80. Glacier-wide mass balance rates for all sampled glaciers are summarized in Figure 81, which shows that between 1995 and 2001 the park's sampled glaciers showed a mix of modest mass gain and predominantly loss, while from 2001 to 2007 all sampled glaciers lost mass—sometimes at fairly substantial (>1 m/yr w.e.) rates. Some glaciers' results are also shown in map view in Figure 94.

We note here that averaged over the entire period of record, all glaciers sampled in KEFJ lost mass. The mass gains by some glaciers in the earlier interval are in that respect anomalous, and are partly an artifact of the timing of the middle measurement interval (May 17-19, 2001) with respect to the earlier and later measurement intervals (late-May to early-June for other years). Measurement of a slightly earlier season snowpack would tend to yield relatively high surface elevations, translating to a positive mass balance bias in the early interval and a negative balance bias from 2001-2007. An additional influence on the early interval positive balances is the evidence for relatively high winter accumulation measured at nearby Wolverine Glacier in spring 2001 (van Beusekom 2010; Figure 79). In 2001, the winter snowpack on Wolverine contained, on average, over 1 m more water equivalent than the median of 47 years measurements. This would lead to greater than otherwise expected surface elevations in our measurements that year. It would also imply an anomalous density profile in places where we measured elevation gains.

In the descriptions that follow, we therefore minimize our emphasis on these 2001 results by focusing our descriptions of trends in individual glacier elevation changes on the overall 1994/1996 – 2007 interval. We do, nonetheless, present DZ plots of the early and late periods individually, and acknowledge that these results, though perhaps exaggerating positive balances in the early interval, may nonetheless reflect a real trend of neutral or even slightly positive balances in that period.

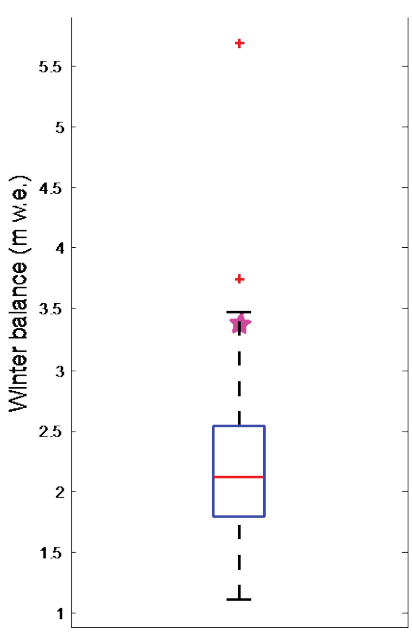

Figure 79. Boxplot showing distribution of winter accumulation measurements for years 1966-2012 at Wolverine Glacier. Median is red line, blue box is interquartile range. 2001 value (red star) was fourth largest winter accumulation in the record.

Table 25. Mass balance and mass change of glaciers in Kenai Fjords NP inferred from laser altimetry at discrete time intervals. 'MB+', 'MB-', 'MC+', and 'MC-' give positive and negative 95% confidence intervals for mass balance and mass change, respectively. Note that "Harris" Glacier is an informal name not shown on maps, but used in this report for consistency with altimetry data using that nomenclature.

Glacier	Type	Size (km^2)	Mean Elev (m)	Start date	End date	Mass Balance (m/yr)	MB+	MB-	Mass Change (gt/yr)	MC+	MC-
Aialik	(T)	70	1040	5/29/94	5/18/01	0.00	0.20	0.30	0.00	0.00	0.00
Aialik	(T)	70	1040	5/29/94	6/14/07	-0.41	0.28	0.25	-0.03	0.02	0.02
Bear	(LK)	143	830	5/28/94	5/19/01	-1.14	0.38	0.65	-0.16	0.09	0.09
Bear	(LK)	143	830	5/28/94	6/14/07	-1.62	0.42	0.33	-0.23	0.05	0.05
Bear	(LK)	143	830	5/19/01	6/14/07	-2.28	0.62	0.50	-0.33	0.07	0.07
Chernof	(L)	51	1110	5/20/96	5/18/01	0.00	0.30	0.30	0.00	0.00	0.00
Chernof	(L)	51	1110	5/20/96	6/14/07	-0.89	0.24	0.25	-0.05	0.01	0.01
Chernof	(L)	51	1110	5/18/01	6/14/07	-1.54	0.58	0.26	-0.08	0.01	0.01
Dinglestadt	(LK)	71	1050	5/20/96	5/18/01	0.10	0.30	0.30	0.00	0.00	0.00
Dinglestadt	(LK)	71	1050	5/20/96	6/14/07	-0.70	0.13	0.14	-0.05	0.01	0.01
Dinglestadt	(LK)	71	1050	5/18/01	6/14/07	-1.53	0.34	0.35	-0.11	0.02	0.02
Exit	(L)	29	1060	5/28/94	6/14/07	-0.68	0.24	0.25	-0.02	0.01	0.01
Exit	(L)	29	1060	5/14/99	5/18/01	1.12	0.46	0.38	0.03	0.01	0.01
Exit	(L)	29	1060	5/18/01	6/14/07	-1.21	0.27	0.27	-0.03	0.01	0.01
"Harris"	(L)	209	1200	5/29/96	5/17/01	0.60	0.80	0.80	0.10	0.20	0.20
"Harris"	(L)	209	1200	5/29/96	6/14/07	-0.20	0.40	0.70	0.00	0.20	0.20
"Harris"	(L)	209	1200	5/17/01	6/14/07	-0.95	0.60	0.63	-0.20	0.13	0.13
Holgate	(T)	78	1000	5/29/94	5/18/01	-0.20	0.40	0.40	0.00	0.00	0.00
Holgate	(T)	78	1000	5/29/94	6/14/07	-0.57	0.29	0.31	-0.04	0.02	0.02
Holgate	(T)	78	1000	5/18/01	6/14/07	-0.96	0.37	0.39	-0.08	0.03	0.03
Kachemak	(L)	21	1040	5/19/96	5/18/01	0.20	0.40	0.40	0.00	0.00	0.00
Kachemak	(L)	21	1040	5/19/96	6/14/07	-0.67	0.41	0.41	-0.01	0.01	0.01
Kachemak	(L)	21	1040	5/18/01	6/14/07	-1.40	0.48	0.50	-0.03	0.01	0.01
McCarty	(T)	113	1160	5/20/96	5/18/01	0.40	0.30	0.70	0.00	0.10	0.10
McCarty	(T)	113	1160	5/20/96	6/14/07	-0.50	0.60	0.40	-0.06	0.05	0.05
McCarty	(T)	113	1160	5/18/01	6/14/07	-1.25	0.53	1.01	-0.14	0.11	0.11
Northwestern	(T)	36	1010	5/19/96	5/17/01	0.70	0.50	1.20	0.00	0.00	0.00
Northwestern	(T)	36	1010	5/19/96	6/14/07	-0.30	0.40	0.40	0.00	0.00	0.00
Northwestern	(T)	36	1010	5/17/01	6/14/07	-1.20	1.40	1.50	0.00	0.10	0.10
Skilak	(LK)	118	1050	5/29/94	5/19/01	-0.32	0.13	0.19	-0.04	0.02	0.02
Skilak	(LK)	118	1050	5/29/94	6/14/07	-0.65	0.25	0.26	-0.08	0.03	0.03
Skilak	(LK)	118	1050	5/19/01	6/14/07	-1.19	0.24	0.26	-0.14	0.03	0.03
Tustumena	(LK)	384	1180	5/29/94	5/19/01	-0.46	0.18	0.11	-0.18	0.04	0.04
Tustumena	(LK)	384	1180	5/29/94	6/14/07	-0.86	0.06	0.07	-0.33	0.03	0.03
Tustumena	(LK)	384	1180	5/19/01	6/14/07	-1.34	0.29	0.30	-0.51	0.12	0.12

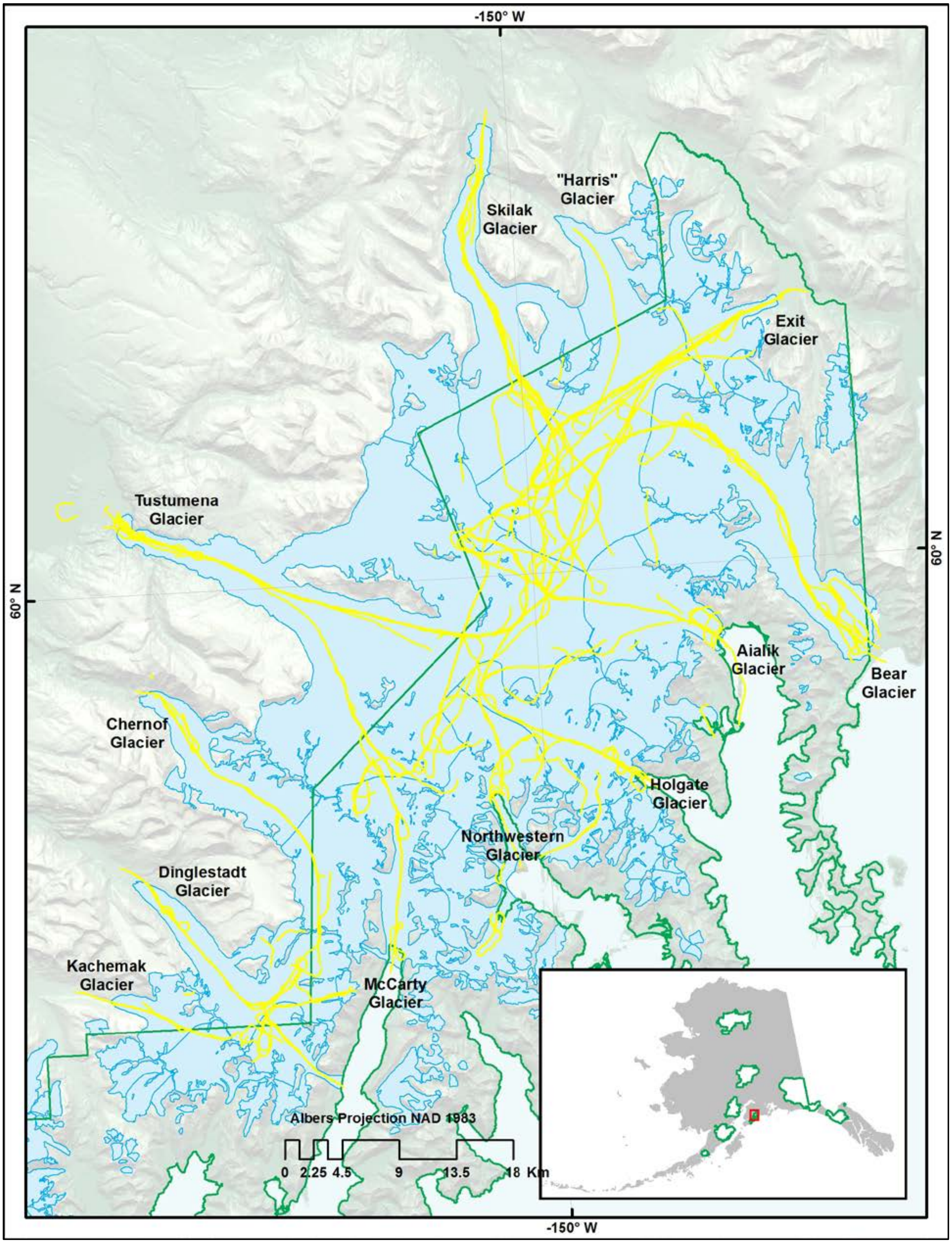

Figure 80. Locations of glaciers in Kenai Fjords with elevation change results reported in this paper. Laser altimetry tracks are shown in yellow. "Harris" Glacier is an informal name not shown on maps, but used in this report for consistency with altimetry data using that nomenclature.

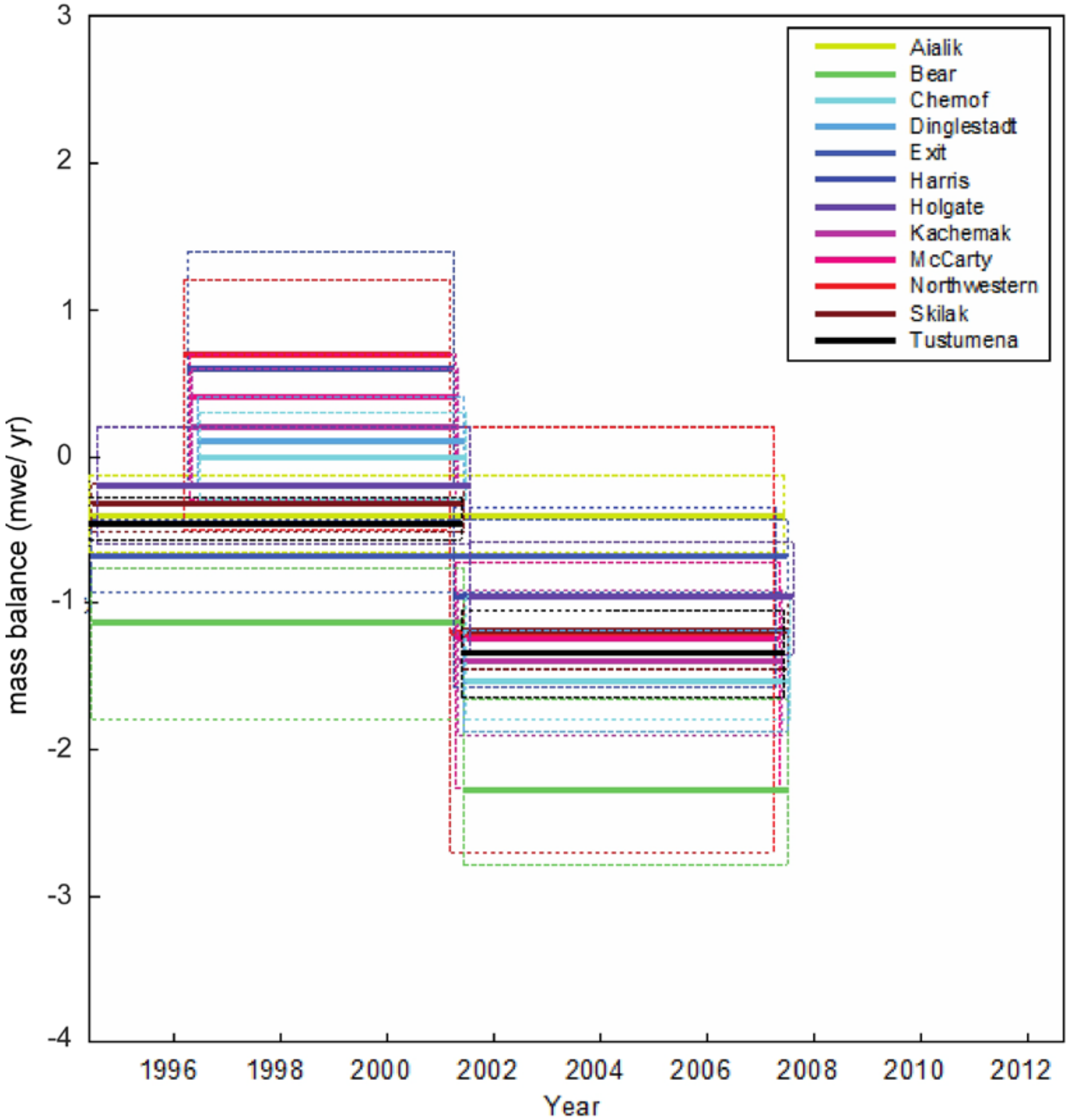

Figure 671. Mass balance of select glaciers in Kenai Fjords National Park. Thick solid lines are mass balances; upper and lower dashed lines reflect confidence intervals for each time period. For clarity, some lines have been shifted a few pixels left or right to minimize overlap. As discussed in the text, anomalies in the 2001 data may be responsible for the systematic shift towards more negative balances in the later interval.

Aialik Glacier was flown in 1994, 2001, and 2007 (Figure 82), and over the entire time period had a mass balance rate of -0.41 m/yr w.e. The thinning was greatest near the terminus, but even there was less than 2 m/yr, and it remained slightly negative up to the highest sampled elevations.

Bear Glacier (1994, 2001, and 2007), which is near Aialik but has a lake-calving rather than terrestrial terminus, exhibited a typical and deeply negative elevation change profile over the 1994-2007 interval, with thinning rates of nearly 6 m near the terminus. Bear's overall mass balance rate was -1.62 m/yr w.e. Chernof Glacier was flown in 1996, 2001, and 2007 and showed essentially the same pattern as Bear Glacier but with more moderated thinning rates. Maximum thinning near the terminus was 4 m/yr, and the overall rate was -0.89 m/yr w.e. Dinglestadt Glacier (Figure 85) was flown in 1996, 2001, and 2007 and had nearly identical results, over the longer interval, to Bear Glacier. Its mass balance was -1.53 m/yr w.e.

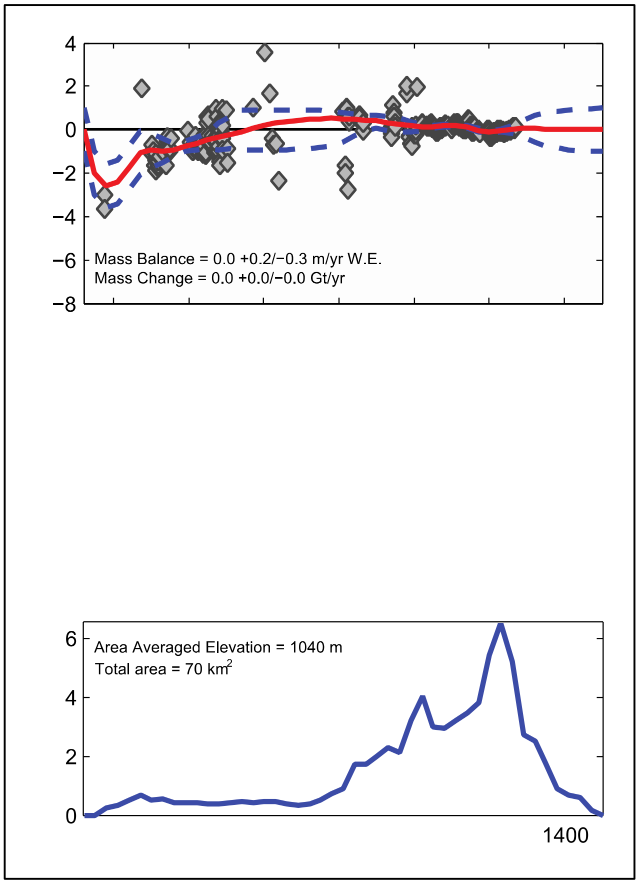

Figure 82. Elevation change and AAD for Aialik Glacier.

Exit Glacier was flown in 1994, 1999, 2001, and 2007 (Figure 86). Over the full period of record, Exit's mass balance rate was -0.68 m/yr w.e. Data coverage was sparse during that interval between 350 and 600 m, but little of the AAD resides in this elevation band so that the confidence intervals are still less than half the magnitude of the estimated shrinkage. The mass balance estimated for the 1999-2001 interval is the largest of any in KEFJ (1.12 m/yr w.e.), but we note that this is also the shortest interval (2 years) of any that relies on the high accumulation year 2001. Exit's estimated rate of annual change would therefore be the most sensitive of all KEFJ glaciers to a systematic shift like the one we discussed earlier, and we consider that value to be especially questionable.

Harris, Holgate, and Kachemak Glaciers all have sparse data coverage and modestly negative mass balances. (We note that "Harris Glacier" is an informal name not in common usage, but we retain the name here for consistency with laser altimetry results that adopt this informal name.) Harris Glacier was flown in 1996, 2001, and 2007 (Figure 87), but overlapping data for this glacier were very sparse. They do, however, cover the most important portions of the AAD. Based on those elevations alone, and with large confidence intervals, we estimate a mass balance rate of -0.2 m/yr w.e. Holgate Glacier was flown in 1994, 2001, and 2007 (Figure 88), and like Harris has a somewhat sparse data coverage. Unlike Harris, the missing data omit a significant portion of the AAD. Nonetheless, we estimate (with wide confidence intervals) a 1994-2007 mass balance rate of -0.57 m/yr w.e. Kachemak Glacier was flown in 1996, 2001, and 2007 (Figure 89). The long interval is missing data near the terminus and above 1050 m, but imply a negative mass balance of -0.67 m/yr w.e.

McCarty Glacier was flown in 1996, 2001, and 2007 (Figure 90), and over the long interval had an overall mass balance rate of -0.5 m/yr w.e. Its pattern of thinning was typical, with strong thinning of up to 7 m/yr at the terminus tapering to no change at the head. Northwestern Glacier was flown in 1996, 2001, and 2007 (Figure 91), and has data only over a narrow (but important) portion of the AAD. It is therefore difficult to say much about the pattern of thinning by elevation, and the confidence intervals are greater than the inferred mass balance rate of -0.3 m/yr w.e.

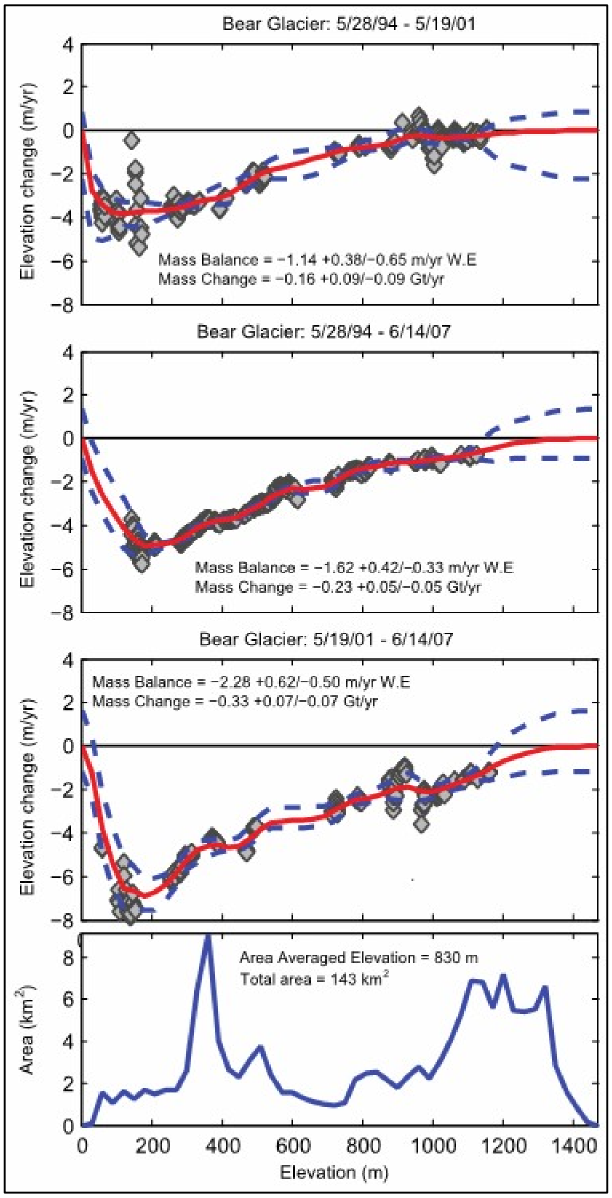

Figure 83. Elevation Change and AAD for Bear Glacier.

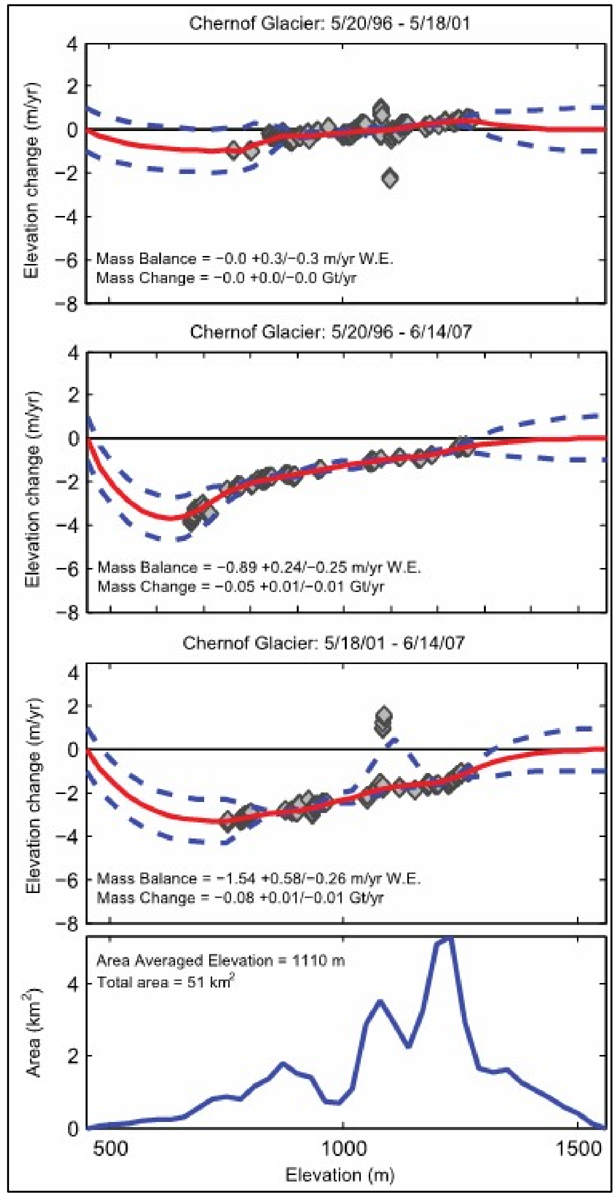

Figure 84. Elevation Change and AAD for Chernof Glacier.

Skilak Glacier was flown in 1994, 2001, and 2007 (Figure 92) and has generally good data coverage through most of its elevation range. Thinning was somewhat uniform at all elevations, in contrast to the more typical pattern of rapid thinning near the terminus and no change at the head. The mass balance was negative, at -0.32 m/yr w.e.

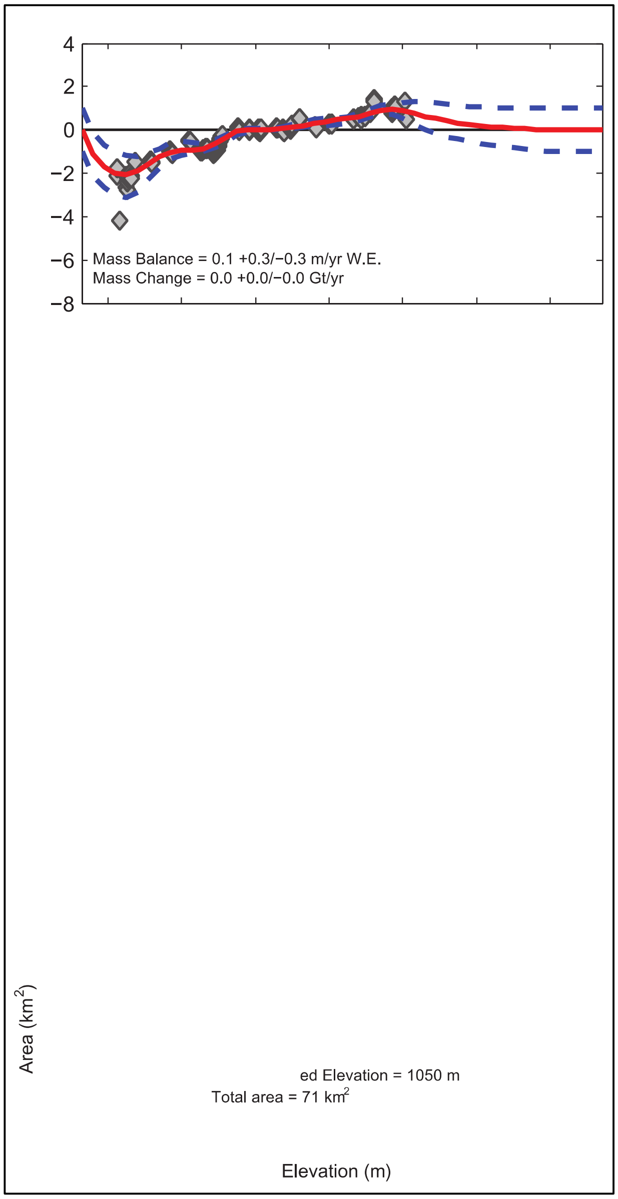

Figure 85. Elevation change and AAD for Dinglestadt Glacier.

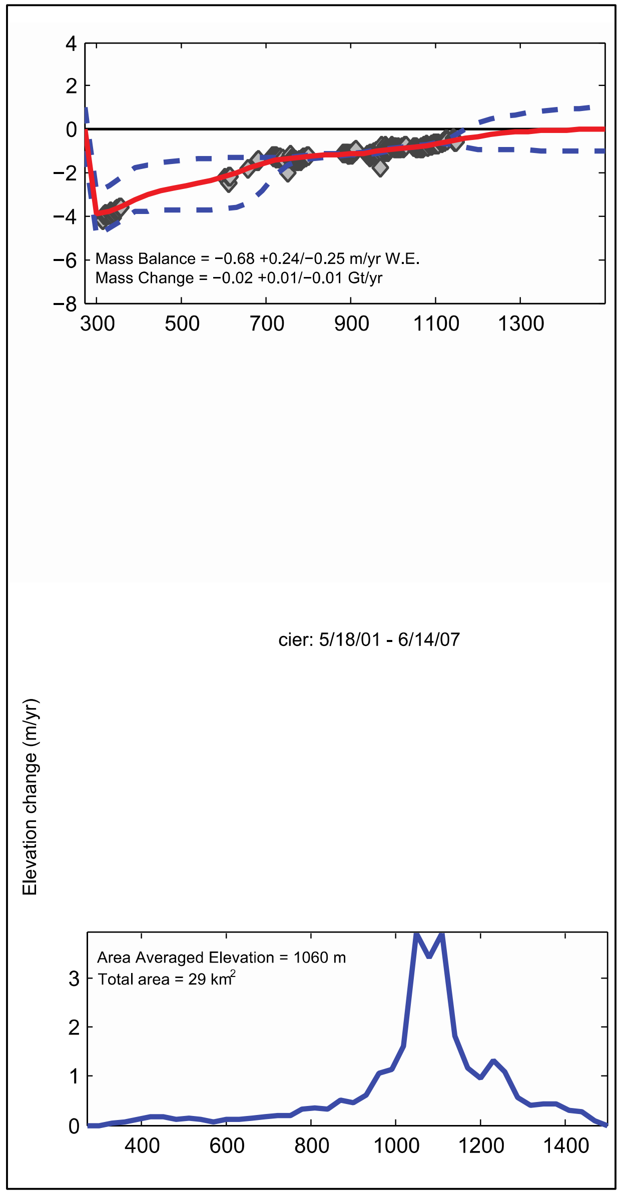

Figure 86. Elevation change and AAD for Exit Glacier.

Finally, Tustumena Glacier was flown in 1994, 2001, and 2007 (Figure 93) and showed a typical pattern of greatest thinning near the terminus at all time intervals. The long interval had excellent data coverage and a mass balance rate of -0.86 m/yr w.e. Given the large size of the glacier (384 km^2), this translates to the largest mass change of all the KEFJ glaciers: -0.33 Gt/yr.

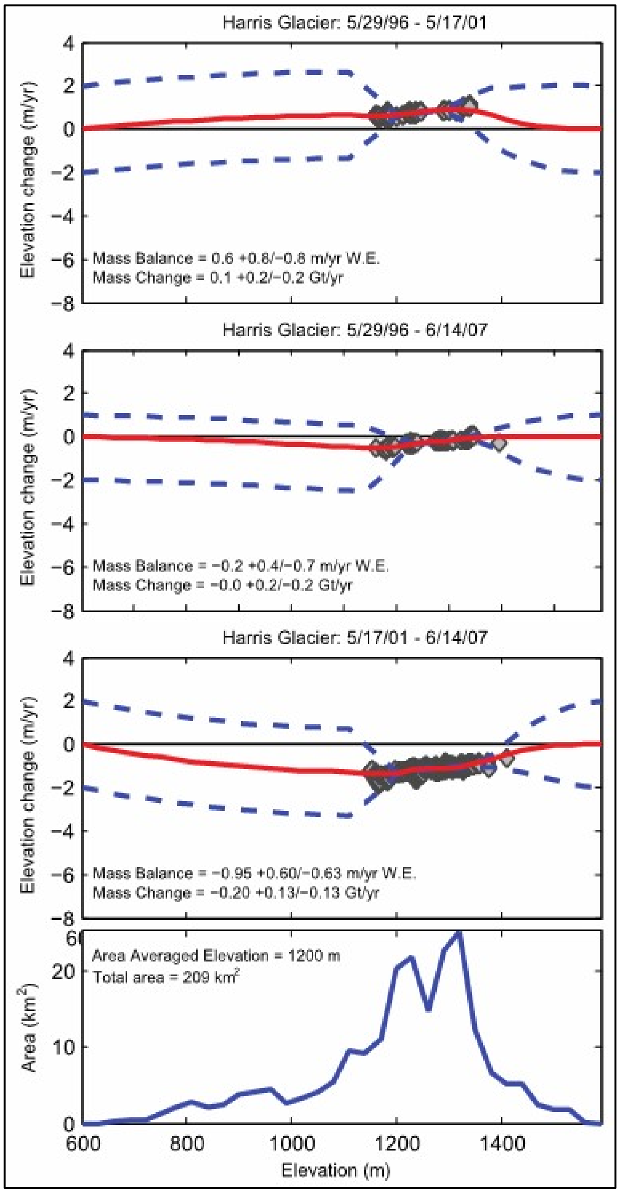

Figure 87. Elevation change and AAD for Harris Glacier.

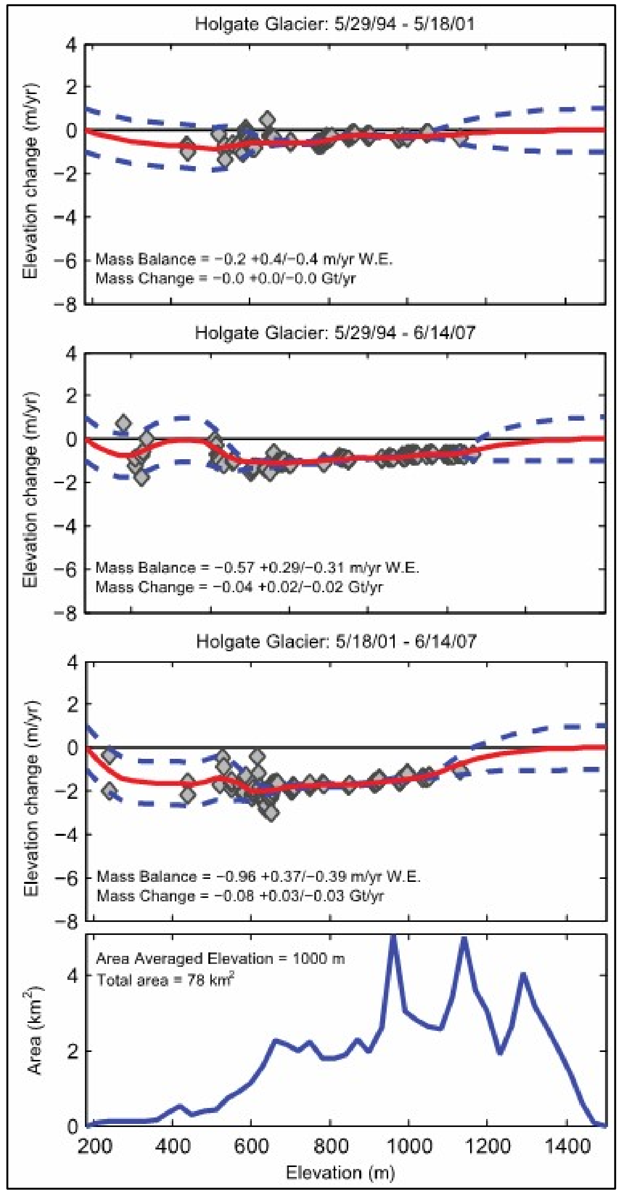

Figure 88. Elevation change and AAD for Holgate Glacier.

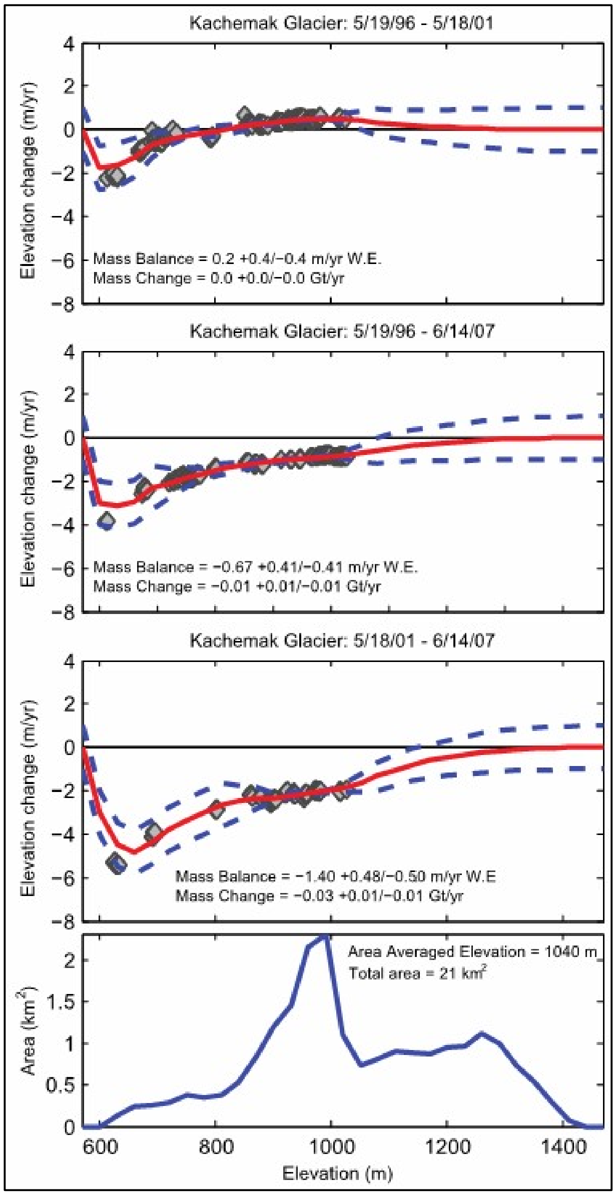

Figure 89. Elevation change and AAD for Kachemak Glacier.

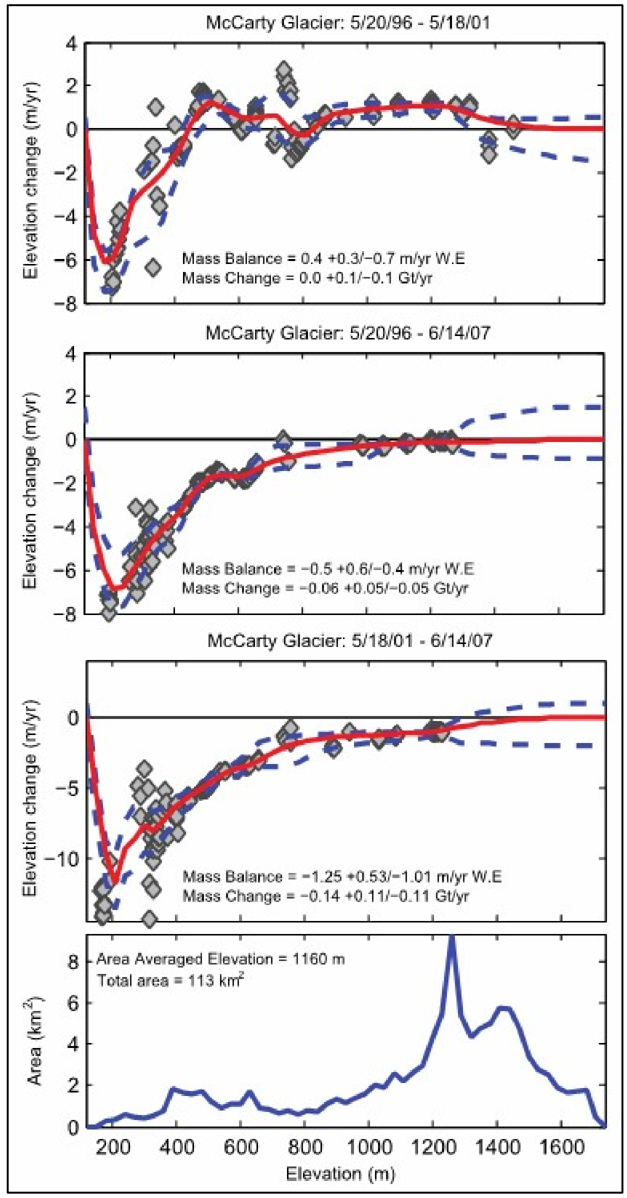

Figure 90. Elevation change and AAD for McCarty Glacier.

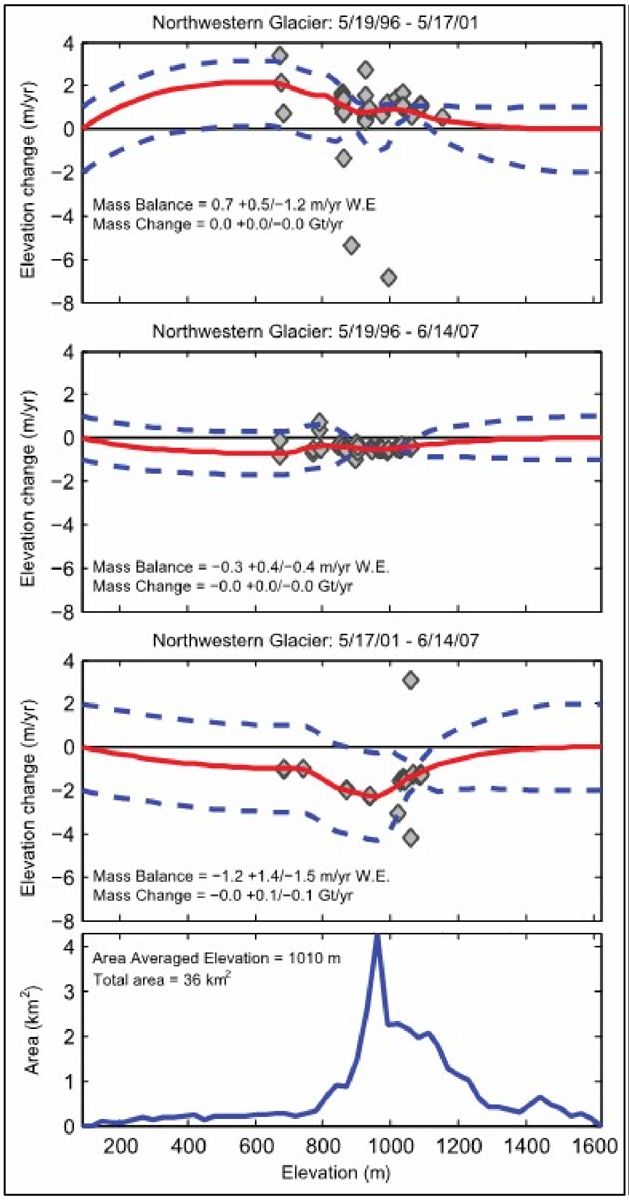

Figure 91. Elevation change and AAD for Northwestern Glacier.

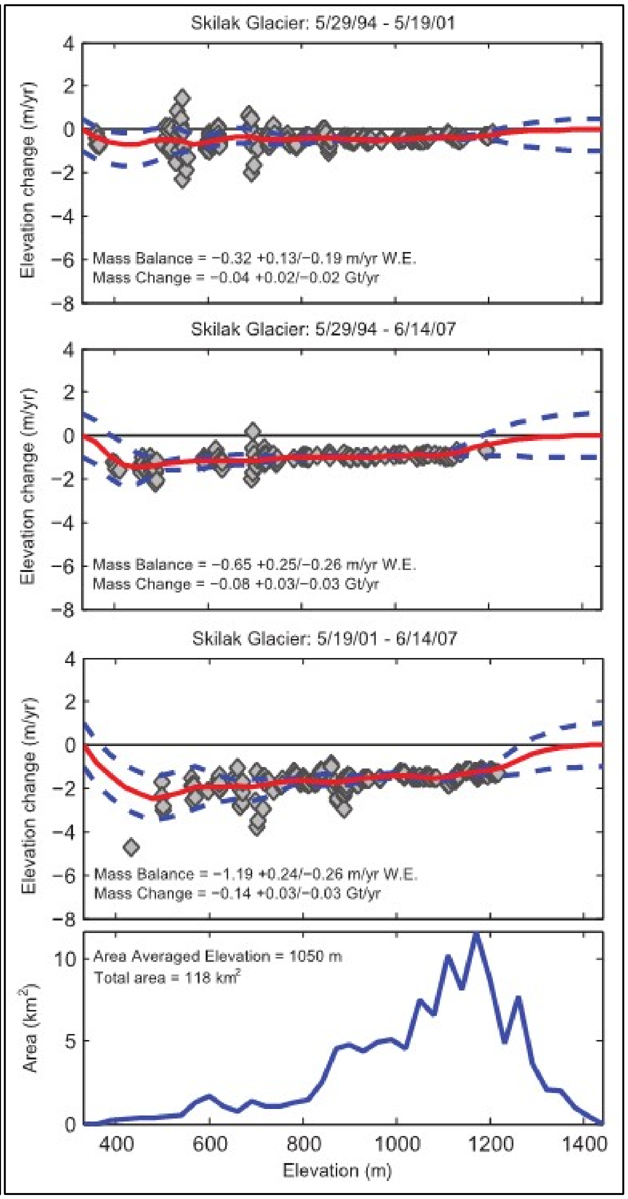

Figure 92. Elevation change and AAD for Skilak Glacier.

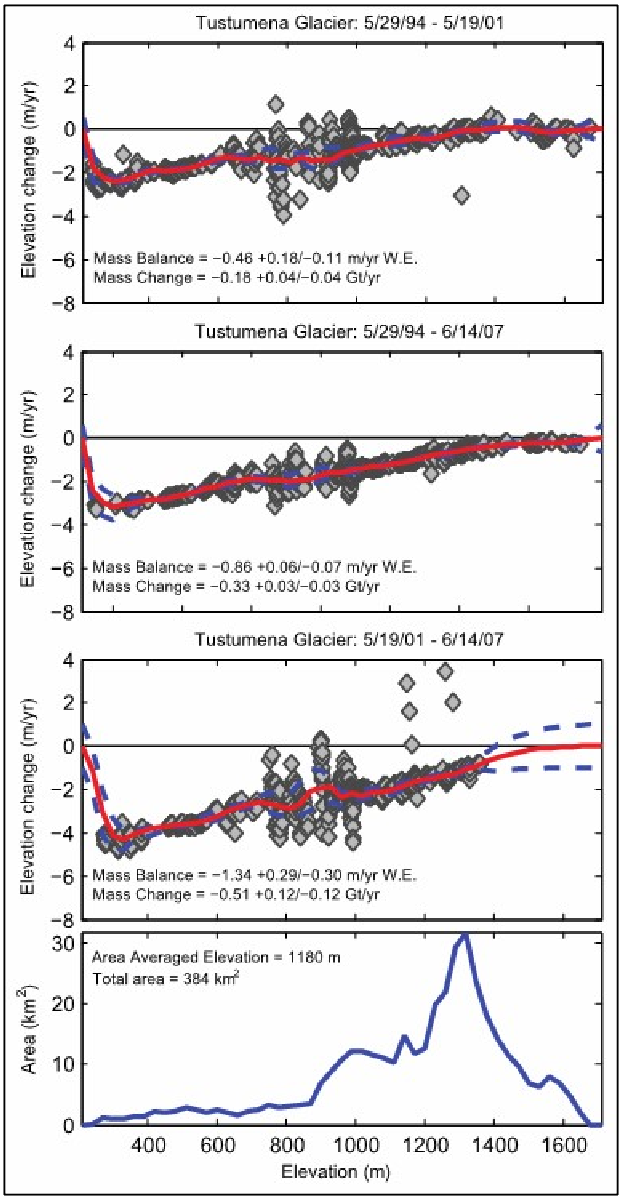

Figure 93. Elevation change and AAD for Tustumena Glacier.

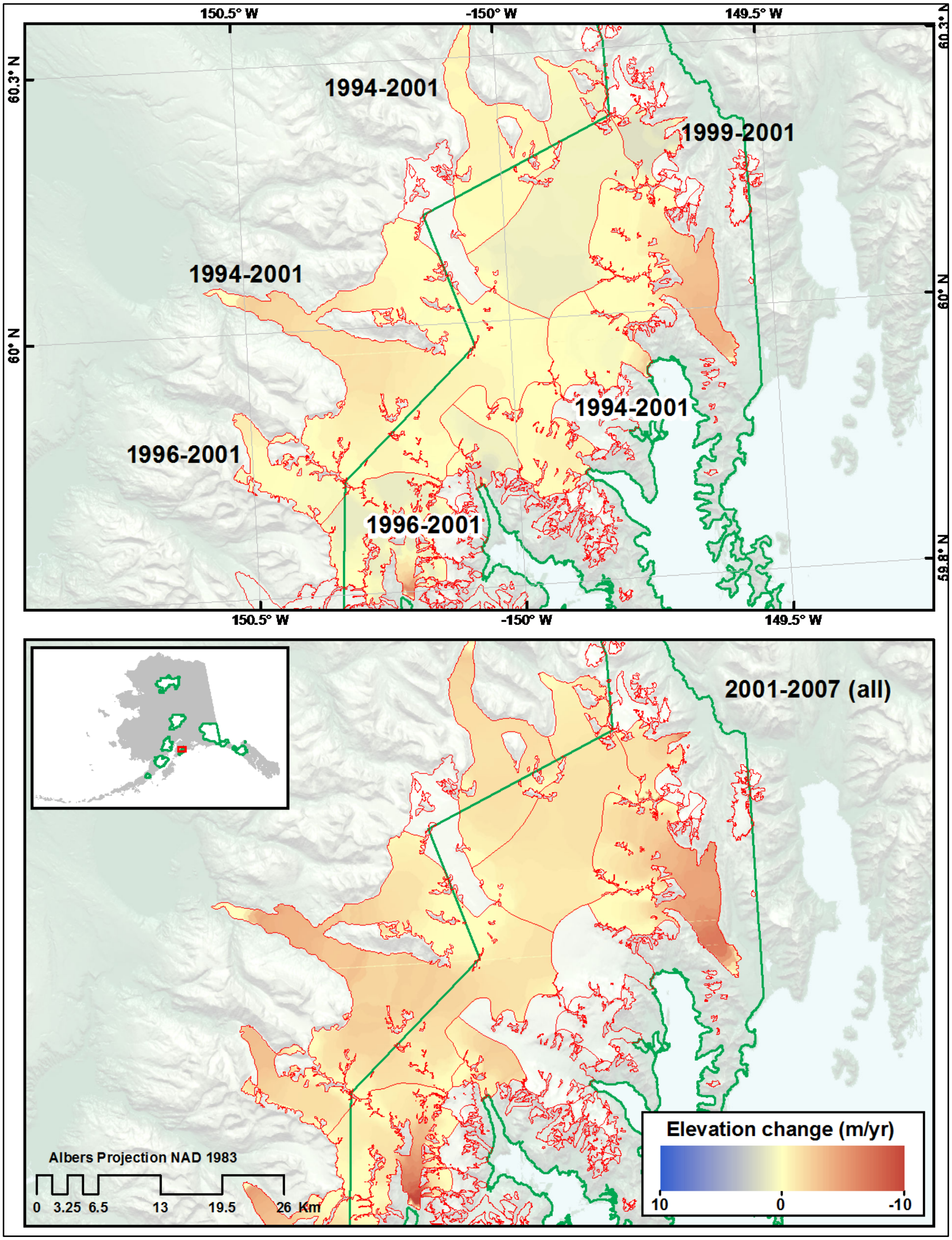

Figure 94. Annual rates of elevation change, by elevation, for glaciers in Kenai Fjords NP. Values are averages over the indicated time intervals.

Lake Clark National Park and Preserve

We measured elevation change on eight glaciers (including both branches of Double Glacier and Tlikakila Glacier) in Lake Clark NP&P and present results from 16 discrete intervals of glacier change (Table 20). Glacier names, locations, and flight tracks are shown in Figure 90. We note here that Tlikakila and Turquoise are informal names, albeit ones in common usage, for those two glaciers. Overall, glacier-wide mass balance rates were modestly positive for most glaciers sampled between 1996 and 2001 (Turquoise Glacier was the only exception, with a mass balance of -0.70 m/yr w.e.), but all measured glaciers had negative mass balance rates between 2001 and 2008 (Figure 96). The positive balances observed on some glaciers in the early interval may have been biased by anomalously high precipitation in the winter of 2001/2001, as described previously for the KEFJ glaciers. Unlike KEFJ, the LACL glaciers were sampled close to the same dates in 1996 and 2001, however, minimizing the relative impact of this potentially positive bias. Some of these the latter interval balances exceeded -1.0 m/yr w.e., including both forks of Tlikakila Glacier, Turquoise Glacier, and Tuxedni Glacier. We describe these trends by individual glacier below, and show some results in map view in Figure 104 and Figure 105.

Table 26. Mass balance and mass change of glaciers in Lake Clark NP&P inferred from laser altimetry at discrete time intervals. 'MB+', 'MB-', 'MC+', and 'MC-' give positive and negative 95% confidence intervals for mass balance and mass change, respectively.

Glacier	Type	Size (km^2)	Mean Elev (m)	Start date	End date	Mass Balance (m/yr)	MB+	MB-	Mass Change (gt/yr)	MC+	MC-
Double all	(L/LK)	202	1230	5/14/96	5/13/01	0.21	0.14	0.13	0.04	0.03	0.03
Double all	(L/LK)	202	1230	5/13/01	5/26/08	-0.83	0.39	0.30	-0.17	0.06	0.06
Double N	(LK)	135	1260	5/14/96	5/13/01	0.23	0.14	0.20	0.03	0.03	0.03
Double N	(LK)	135	1260	5/13/01	5/26/08	-0.95	0.25	0.18	-0.13	0.02	0.02
Double S	(L)	67	1150	5/14/96	5/13/01	0.30	0.40	0.10	0.02	0.01	0.01
Double S	(L)	67	1150	5/13/01	5/26/08	-0.74	0.49	0.41	-0.05	0.03	0.03
Shamrock	(LK)	123	1620	5/14/96	5/13/01	0.25	0.12	0.13	0.03	0.02	0.02
Shamrock	(LK)	123	1620	5/13/01	5/21/08	-0.51	0.19	0.13	-0.06	0.02	0.02
Tanaina	(L)	156	1520	5/14/96	5/13/01	0.20	0.20	0.10	0.03	0.01	0.01
Tanaina	(L)	156	1520	5/13/01	5/21/08	-0.63	0.27	0.13	-0.10	0.02	0.02
Tlikakila GF	(L)	107	1350	5/13/01	5/21/08	-1.05	0.18	0.25	-0.11	0.03	0.03
Tlikakila NF	(L)	31	1320	5/13/01	5/21/08	-1.40	0.32	0.48	-0.04	0.01	0.01
Turquoise	(L)	16	1630	5/16/96	5/13/01	-0.70	0.10	0.09	-0.01	0.00	0.00
Turquoise	(L)	16	1630	5/13/01	5/26/08	-1.16	0.28	0.22	-0.02	0.00	0.00
Tuxedni	(S)	92	870	5/13/96	5/13/01	0.54	0.45	0.37	0.05	0.03	0.03
Tuxedni	(S)	92	870	5/13/01	5/26/08	-1.02	0.45	0.47	-0.09	0.04	0.04

Both branches of Double Glacier were flown and analyzed separately in 1996, 2001, and 2008. DZ plots for the two branches are shown in Figure 92, and a combined analysis that reflects a meaningful whole-glacier mass balance rate is shown in Figure 93. Trends by elevation were similar for all treatments: very minor thickening in the uppermost elevations combined with modest thinning that reached a maximum near the terminus. In all cases, the values were more negative in the latter (2001-2008) interval, with the whole-glacier mass balance rate decreasing from 0.21 m/yr w.e. before 2008 to -0.83 m/yr w.e. after 2008.

Shamrock and Tanaina Glaciers were also flown in 1996, 2001, and 2008, and both exhibited trends (Figure 99 and Figure 100) similar to the Double Glacier. The general trend of more negative values at low elevations was maintained through the two time intervals, with modest thickening in the upper elevations between 1996 and 2001 and almost ubiquitously negative DZ values after 2001. Like at Double, the glacier-wide mass balances declined from modestly positive (0.25 and 0.20 m/yr w.e. for Shamrock and Tanaina respectively) to negative (-0.51 m and -0.63 w.e./yr respectively) between 2001 and 2008.

Turquoise Glacier was also flown in 1996, 2001, and 2008, and results from there mimic those of Shamrock and Tanaina except that the mass balances at Turquoise were consistently more negative. From 1996 to 2001, Turquoise lost mass at virtually all elevations and had a negative mass balance of -0.70 m/yr w.e., the lowest mass balance measured in LACL during that interval. From 2001 to 2008, the lower elevations, below 1700 m in particular, lost even more mass, and the mass balance was -1.16 m/yr w.e. Only the North Fork of Tlikakila Glacier was more negative in that interval.

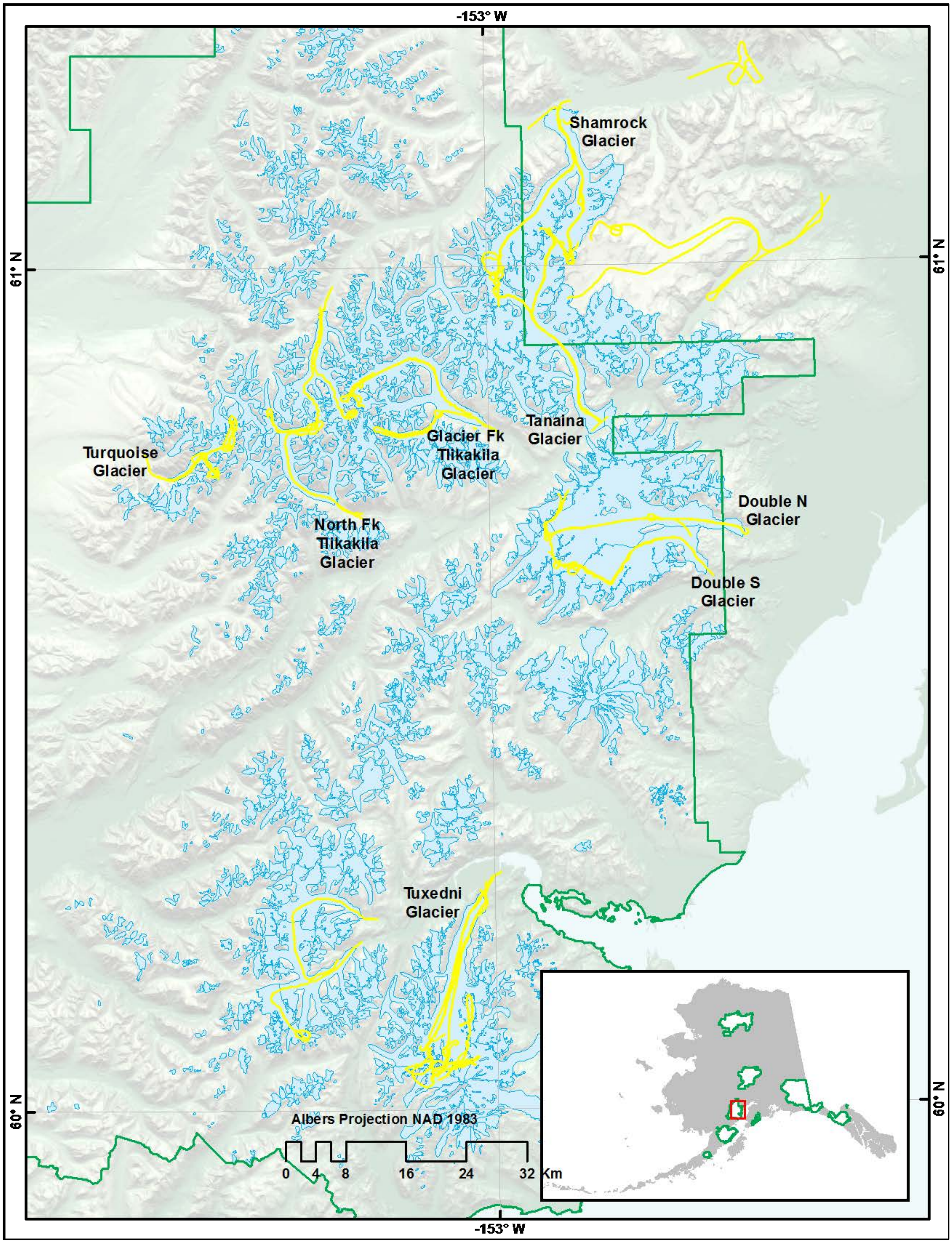

Figure 95. Locations of glaciers in Lake Clark with elevation change results reported in this paper. Laser altimetry tracks are shown in yellow.

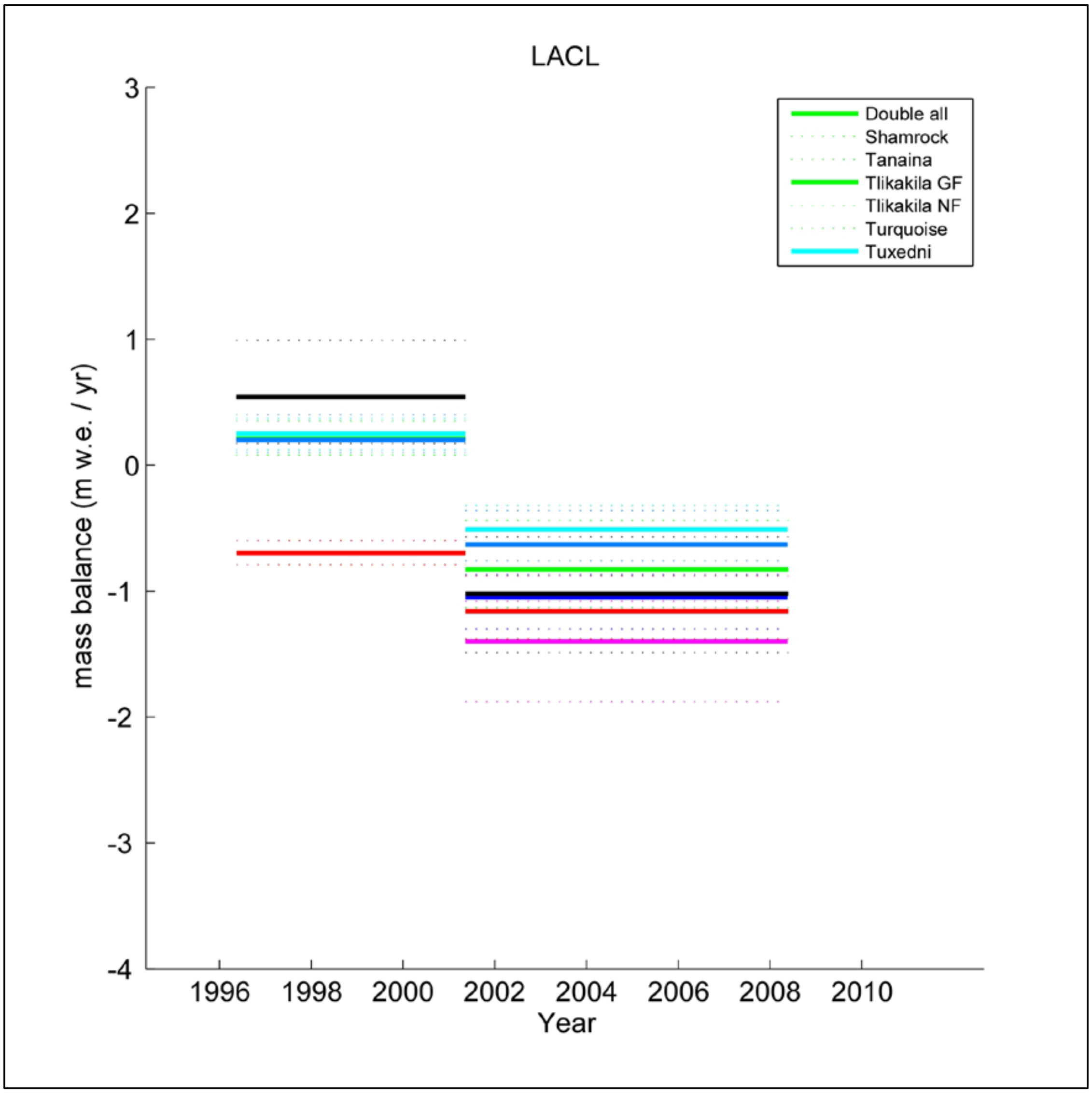

Figure 686. Mass balance of select glaciers in Lake Clark National Park & Preserve. Thick solid lines are mass balances; upper and lower dashed lines reflect confidence intervals for each time period. For clarity, some lines have been shifted a few pixels left or right to minimize overlap.

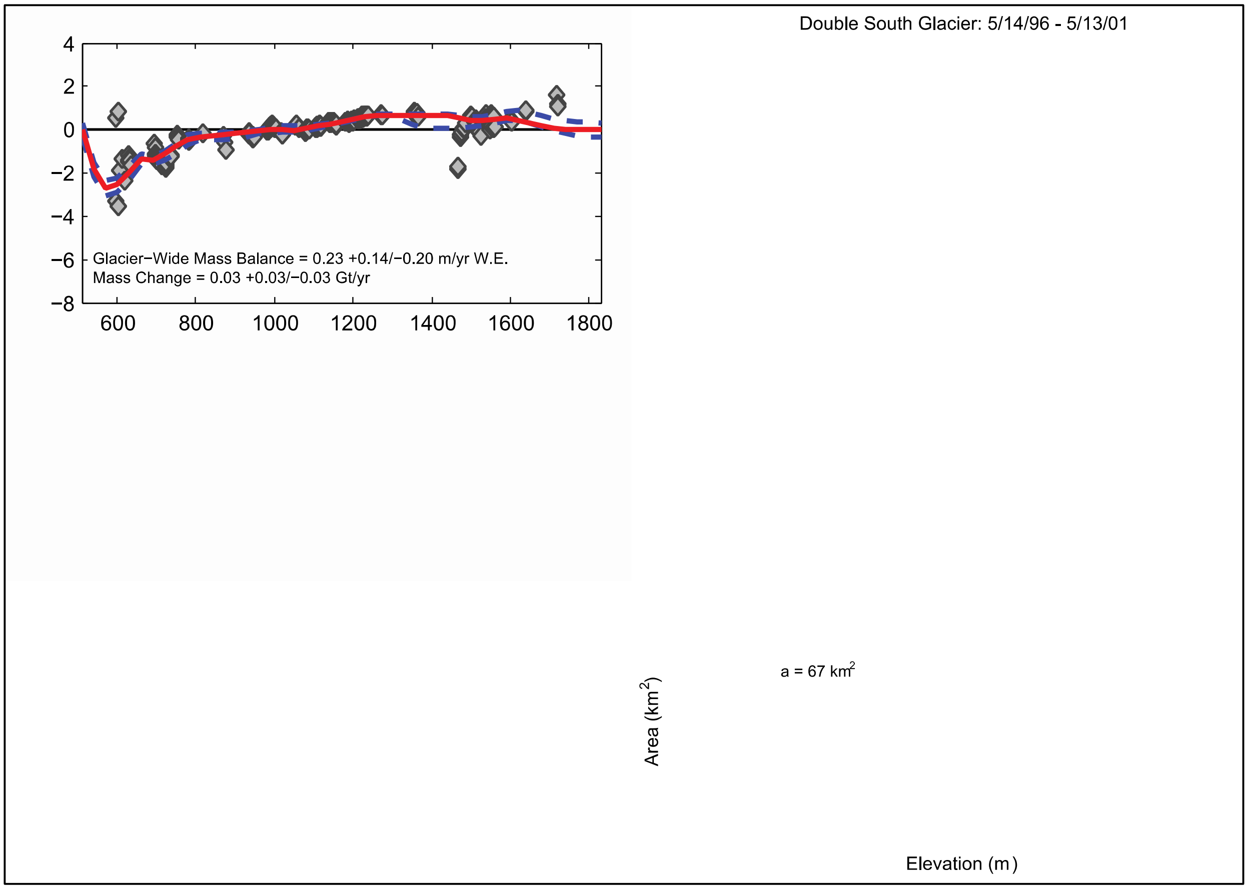

Figure 697. Elevation change and AAD for two individual forks of Double Glacier. Note that MB and MC are not in either case reflective of the entire accumulation and ablation areas.

Tuxedni Glacier (1996, 2001, 2008) has been identified as a surging glacier (Post, 1969), but a confirmed observation of surging behavior has never been recorded for this glacier. If it does indeed surge, the pattern of elevation change observed during our measurement intervals suggests that it was primarily in a quiescent phase with strong thinning at low elevations and some equivocal evidence for post-surge thickening at higher elevations. Between 1996 and 2001, the glacier exhibited severe elevation loss below ~600 m while showing strong elevation gains at higher elevations—and particularly around 700 m, close to the modal elevation for that glacier and thus contributing to the highest overall mass balance in LACL for this interval: 0.54 m/yr w.e. Like other glaciers in LACL, the 2001-2008 pattern of mass loss is similar to that of the preceding interval but with an overall trend towards more negative numbers. The strong thinning at lower elevations persisted, but the thickening at higher elevations was more modest, and in some areas was actually slightly negative, yielding a mass balance of -1.02 m/yr w.e.

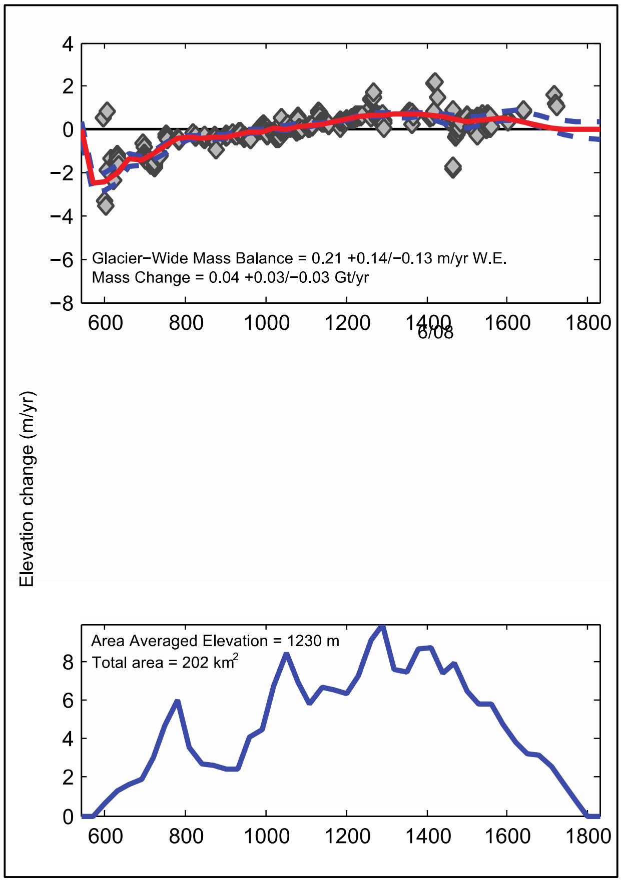

Figure 718. Elevation change and AAD for Double Glacier, reflecting both forks shown in Figure 92.

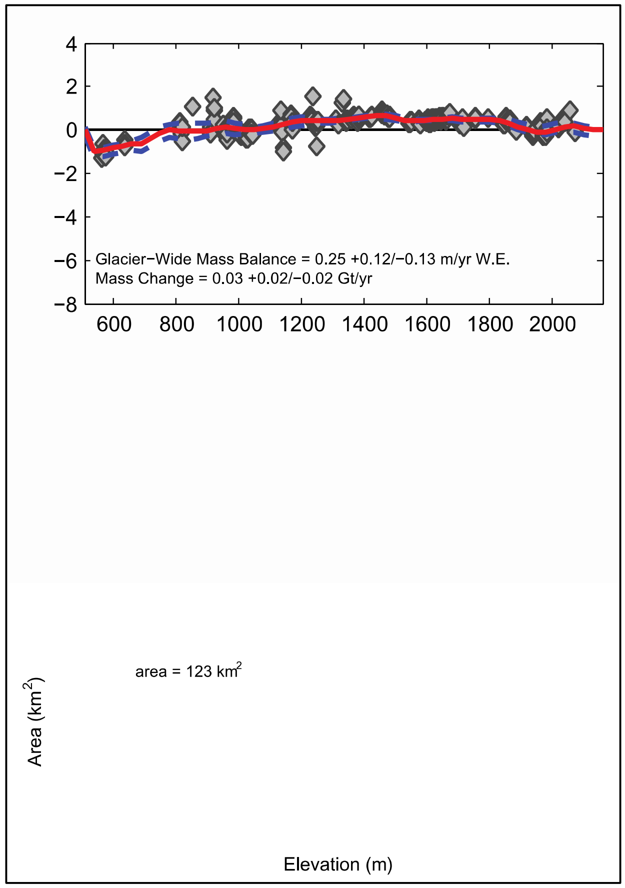

Figure 719. Elevation change and AAD for Shamrock Glacier.

The two “Forks” of the Tlikakila Glacier are in fact independent ice masses that were each independently surveyed in 2001 and 2008 (Figure 103). Both changed in ways similar to other nearby glaciers, such as Turquoise, Tanaina, and Shamrock, with negative mass balances (-1.05 and -1.40 m/yr w.e. on the Glacier Fork and North Fork respectively). The pattern of mass change with elevation was similar in both cases, with losses increasing steadily from high elevation to low, although we note that on both glaciers and the North Fork especially, data coverage is sparse at higher elevations. The only exception to the general pattern of change is an anomalous patch of apparently thickening ice around 950 m on the Glacier Fork. It is unclear whether this reflects an aberrant patch of advected topography or some other phenomenon, but the limited spatial extent of this anomaly minimizes its impact on the overall observed mass balance.

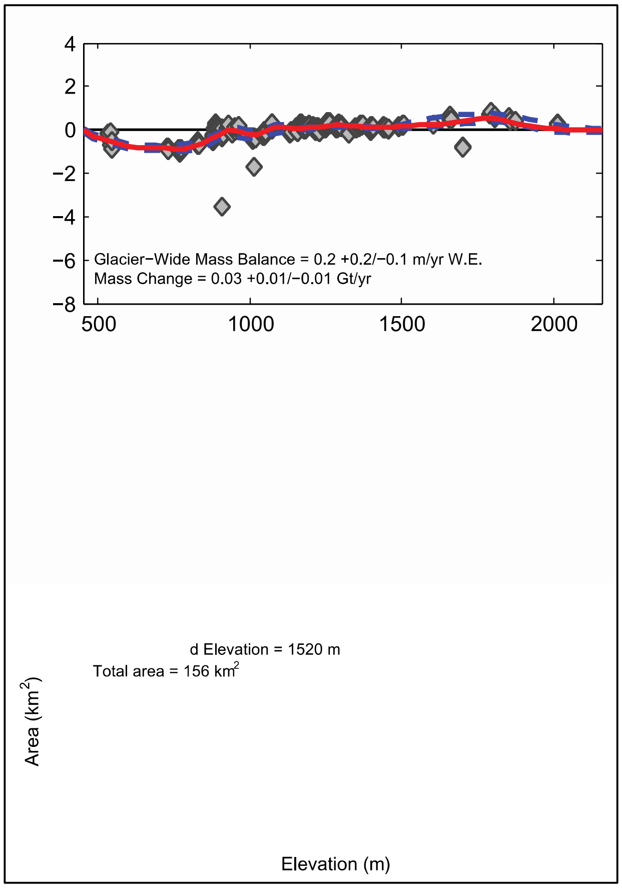

Figure 100. Elevation change and AAD for Tanaina Glacier.

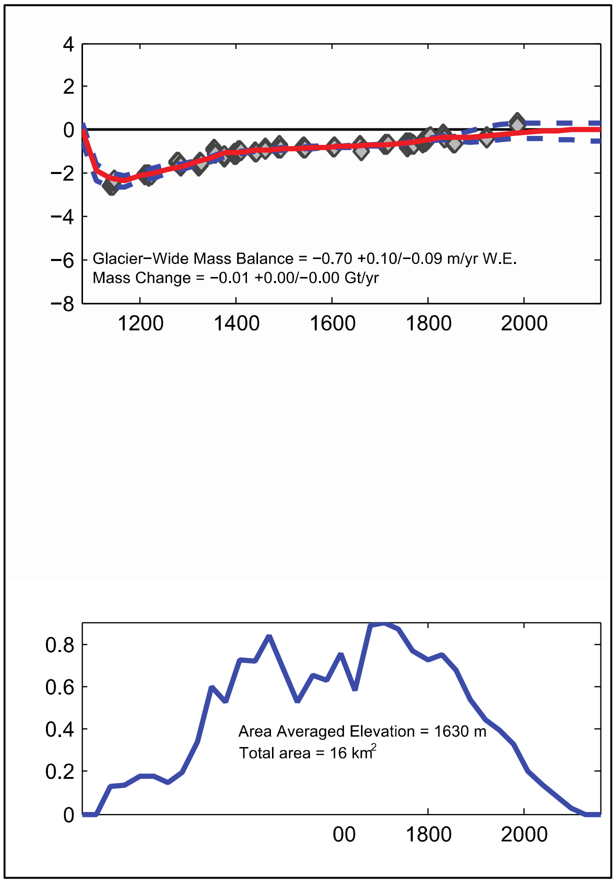

Figure 101. Elevation change and AAD for Turquoise Glacier.

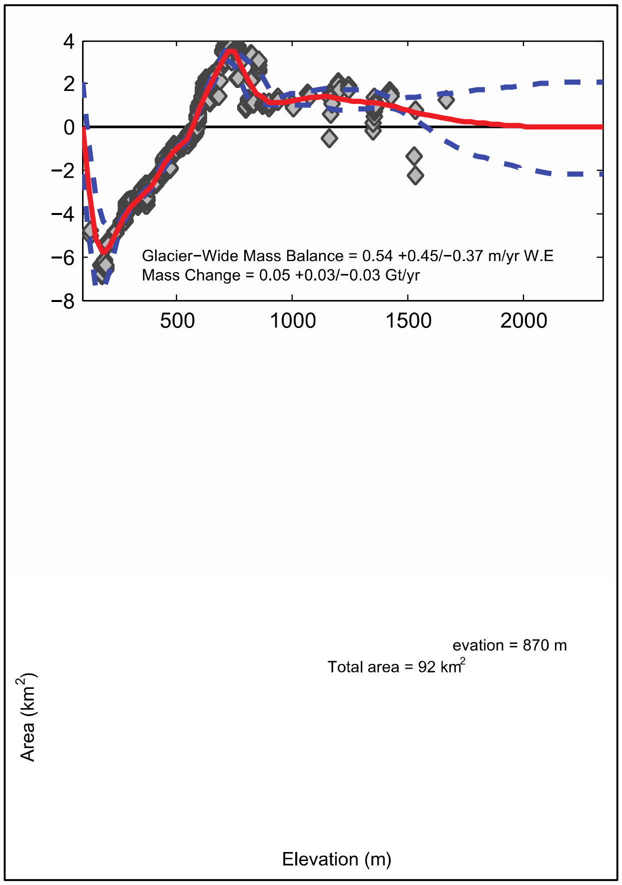

Figure 102. Elevation change and AAD for Tuxedni Glacier.

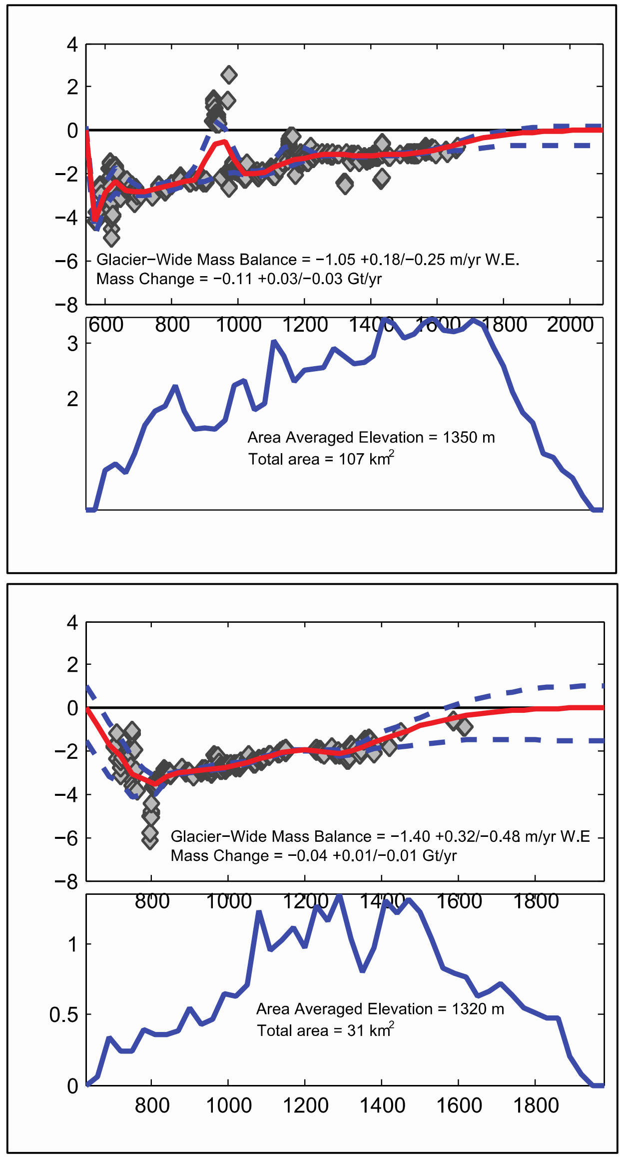

Figure 103. Elevation change and AAD for both forks of Tlikakila Glacier: Glacier Fork above and North Fork below.

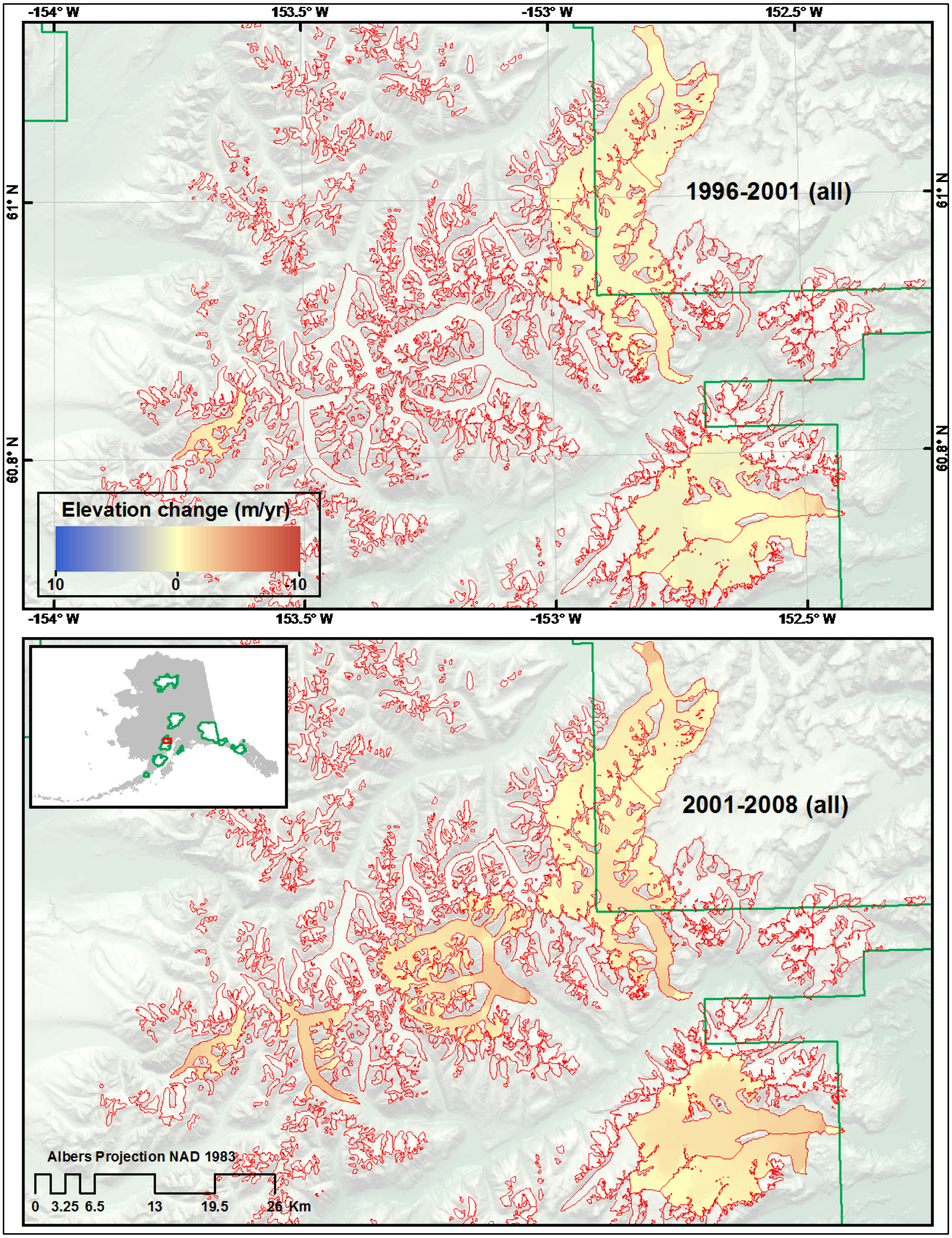

Figure 104. Annual rates of elevation change, by elevation, for glaciers in Lake Clark NP&P. Values are averages over the indicated time intervals.

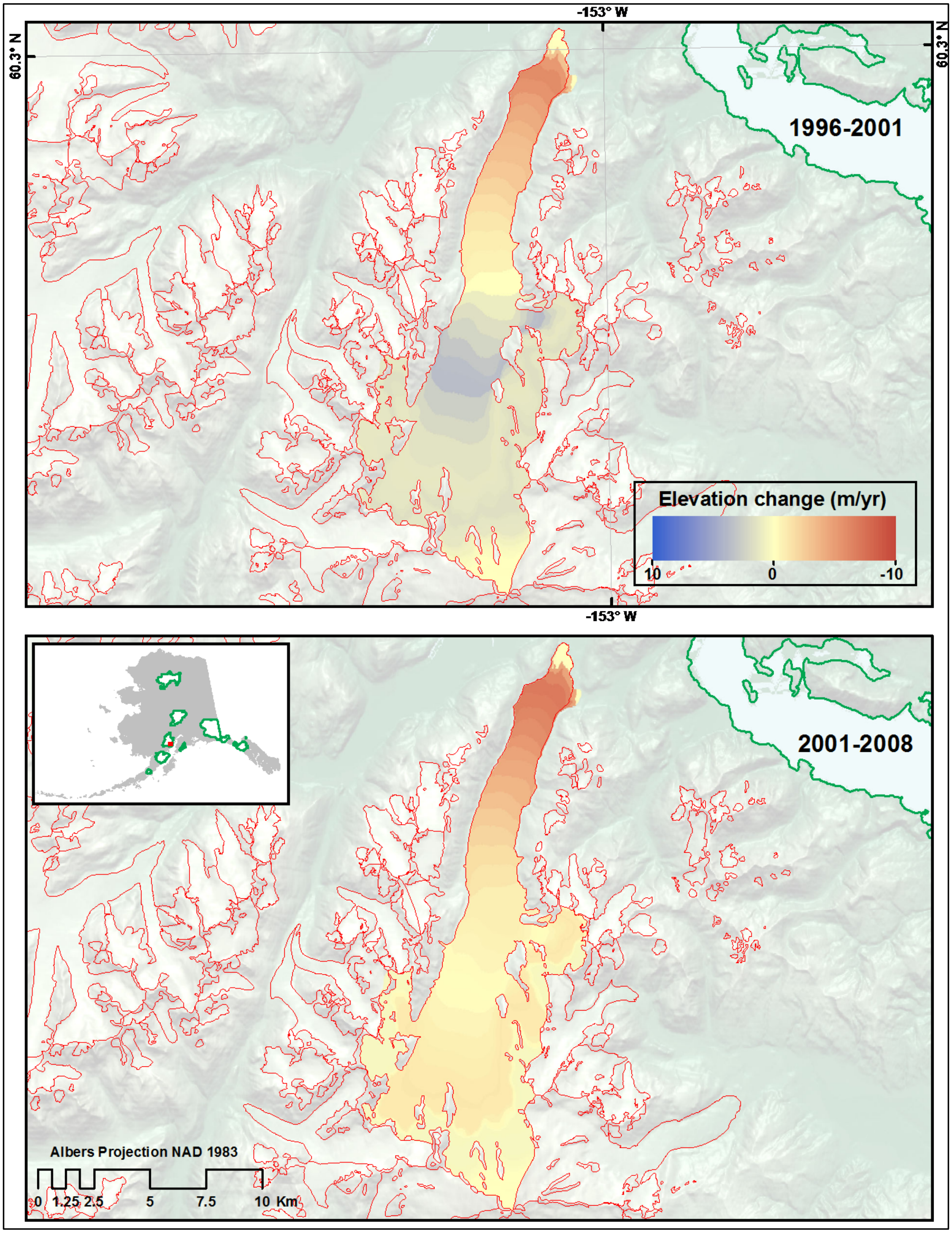

Figure 105. Annual rates of elevation change, by elevation, for Tuxedni Glacier in Lake Clark NP&P. Values are averages over the indicated time intervals.

Wrangell-St. Elias National Park and Preserve

We measured elevation change on 17 glaciers (including multiple contributing portions of the Bagley/Bering Icefield system and the Logan/Ogilvie/Walsh branches of Chitina Glacier) in Wrangell-St. Elias NP&P and present results from 56 discrete intervals of glacier change (Table 21). Glacier names, locations, and flight tracks are shown in Figure 106.

Overall, glacier-wide mass balance rates were quite variable throughout the park (Figure 107), an unsurprising result given the diversity of glaciers represented, from interior valley glaciers to calving tidewater glaciers to coastal piedmont glaciers. We note that this figure purposely omits the Bagley/Bering and Chitina systems, since (as discussed previously) their mass balance rates, when taken as individual components, are not appropriately comparable to the other full-glacier rates depicted in the figure. Below, we discuss trends on all measured glaciers, including components of those two systems mentioned above, and we show some results in map view in Figure 126 through Figure 129.

The Bagley/Bering Glacier system is large and complicated, and confusion over the nomenclature associated with ice in this area was summarized recently by Beedle et al. (2008). Like Beedle, we treat the Steller Glacier (including the Steller Lobe) separately, but our Bagley/Bering Glacier system is not strictly coincident with what Beedle calls the Surging Bering Glacier System. Ours, which we map for clarity at the top of Figure 112, includes (with approximate but inexact correlations to Beedle's terminology in italics) Bering Glacier (*Bering Lobe* and *Central Valley Reach*), Bagley West (*Waxell Glacier*), Bagley East (*Bagley Ice Valley* and *Quintino Sella Glacier*), Jefferies Glacier (not included by Beedle), and Tana Glacier (not included by Beedle).

Here, we present separate DZ plots for all these components except Tana Glacier. Bagley East Glacier was flown in 1995, 2000, 2003, 2007, 2010, and 2012 (Figure 108). Both Bagley West Glacier (Figure 105) and Jefferies Glacier (Figure 106) were flown in 2003, 2007, 2010, and 2012. These components drain in two directions, southwards via the Bering Glacier (flown in 1995, 2000, 2003, 2007, 2010, 2011, and 2012; Figure 109), and northwards via the Tana Glacier, for which we present no completed DZ maps. Here, we first discuss the trends of these individual components, ignoring the mass balance values. We then move on to discuss the complex problem of assessing mass balance for this system.

Elevation changes on Bagley East (Figure 108) and Bering Glacier (Figure 109) are complex, and must interpreted in the context of surges that occurred in 1993-95 and again in 2008-2011. A detailed analysis of surface velocities and elevation changes during these events was presented by Burgess et al. (2012), and we only summarize those results here. Perhaps the most conspicuous general feature of the DZ plots is the scale of the y-axis on the Bering Glacier: changes on the Bering are measured in tens of meters per year instead of m/yr, as is typical of most other glaciers in this dataset including Bagley East. This gives a sense of the magnitude of changes since 1995. On both Bagley and Bering, those changes are most typically thinning, but a zone of substantial thickening that started in Bagley East glacier around 1500 m between 1995-2000 and was centered on ~1200 m elevation between 2000 and 2003. This same thickening was seen on the Bering Glacier during that interval, then intensified and moved downvalley to about 800 m between 2003 and 2007, grew more intense around 400 m from 2007 to 2010, and culminated in an almost 100 m/yr thickening rate near the terminus between 2010 and 2011. The

Table 27. Mass balance and mass change of glaciers in Wrangell-St. Elias NP&P inferred from laser altimetry at discrete time intervals. 'MB+', 'MB-', 'MC+', and 'MC-' give positive and negative 95% confidence intervals for mass balance and mass change, respectively. Table continues on next page.

Glacier	**Type**	**Size (km^2)**	**Mean Elev (m)**	**Start date**	**End date**	**Mass Balance (m/yr)**	**MB+**	**MB-**	**Mass Change (gt/yr)**	**MC+**	**MC-**
Bagley E	(LK)	1940	2023	6/10/95	8/27/00	0.30	0.70	0.70	0.60	1.50	1.50
Bagley E	(LK)	1940	2023	8/27/00	8/22/03	0.60	0.70	0.70	1.20	1.40	1.40
Bagley E	(LK)	1940	2023	8/22/03	8/24/07	-1.32	0.21	0.25	-2.66	0.50	0.50
Bagley E	(LK)	1940	2023	8/24/07	8/21/10	-1.57	0.23	0.16	-3.18	0.32	0.32
Bagley E	(LK)	1940	2023	8/21/10	8/18/12	-2.05	0.20	0.21	-4.14	0.42	0.42
Bagley W	(LK)	300	1400	8/22/03	8/28/07	-0.94	0.24	0.23	-0.28	0.07	0.07
Bagley W	(LK)	300	1400	8/28/07	8/21/10	-1.27	0.18	0.18	-0.38	0.05	0.05
Bagley W	(LK)	300	1400	8/21/10	8/18/12	-1.68	0.14	0.32	-0.51	0.10	0.10
Barnard	(L)	376	2250	8/19/03	8/18/07	-0.56	0.39	0.40	-0.21	0.14	0.14
Barnard	(L)	376	2250	8/19/03	8/16/12	-0.52	0.30	0.27	-0.20	0.10	0.10
Barnard	(L)	376	2250	8/18/07	8/16/12	-0.48	0.47	0.39	-0.18	0.15	0.15
Bering	(LK)	620	1574	6/10/95	6/22/00	-3.59	1.22	1.12	-5.65	1.76	1.76
Bering	(LK)	620	1574	6/22/00	8/22/03	-3.29	1.10	1.07	-5.18	1.69	1.69
Bering	(LK)	620	1574	8/22/03	8/24/07	-0.80	0.90	0.80	-1.20	1.30	1.30
Bering	(LK)	620	1574	8/24/07	8/21/10	0.92	0.87	0.60	1.45	0.94	0.94
Bering	(LK)	620	1574	8/21/10	8/16/11	-8.56	1.87	3.00	-13.48	4.72	4.72
Bering	(LK)	620	1574	8/16/11	8/18/12	5.87	3.10	2.78	9.24	4.37	4.37
Guyot	(L)	223	1270	8/26/07	8/23/10	-0.60	0.80	1.00	-0.10	0.20	0.20
Guyot	(L)	223	1270	8/26/07	8/22/12	0.20	0.60	0.50	0.00	0.10	0.10
Guyot	(L)	223	1270	8/23/10	8/22/12	1.55	1.07	1.09	0.35	0.24	0.24
Hubbard	(T)	2511	1920	5/3/00	6/10/07	0.20	0.20	0.30	0.40	0.80	0.80
Hubbard	(T)	2511	1920	5/3/00	5/25/12	0.10	0.10	0.10	0.30	0.40	0.40
Hubbard	(T)	2511	1920	6/10/07	5/25/12	0.10	0.40	0.70	0.30	1.80	1.80
Jefferies	(L)	191	1600	8/22/03	8/19/07	-0.98	0.13	0.14	-0.19	0.03	0.03
Jefferies	(L)	191	1600	8/19/07	8/23/10	-1.10	0.18	0.13	-0.21	0.03	0.03
Jefferies	(L)	191	1600	8/23/10	8/18/12	-0.10	0.10	0.10	-0.03	0.02	0.02
Kennicott	(LK)	242	1880	6/17/00	6/3/07	-0.40	0.50	0.50	-0.10	0.10	0.10
Klutlan	(L)	626	1560	8/19/03	8/19/07	-0.30	0.50	0.50	-0.20	0.30	0.30
Klutlan	(L)	626	1560	8/19/03	8/16/12	-0.20	0.30	0.40	-0.10	0.30	0.30
Klutlan	(L)	626	1560	8/19/07	8/16/12	-0.36	0.23	0.22	-0.22	0.14	0.14
Logan	(L)	706	2420	8/19/03	8/19/07	-0.58	0.41	0.44	-0.41	0.31	0.31
Logan	(L)	706	2420	8/19/03	8/16/12	-0.39	0.35	0.32	-0.27	0.22	0.22
Logan	(L)	706	2420	8/19/07	8/16/12	-0.50	0.70	0.40	-0.37	0.28	0.28

Table 21 (continued). Mass balance and mass change of glaciers in Wrangell-St. Elias NP&P inferred from laser altimetry at discrete time intervals. 'MB+', 'MB-', 'MC+', and 'MC-' give positive and negative 95% confidence intervals for mass balance and mass change, respectively.

Glacier	Type	Size (km^2)	Mean Elev (m)	Start date	End date	Mass Balance (m/yr)	MB+	MB-	Mass Change (gt/yr)	MC+	MC-
Malaspina	(L/LK)	3274	1220	6/5/95	6/24/00	-1.00	0.59	0.58	-3.28	1.90	1.90
Malaspina	(L/LK)	3274	1220	8/27/00	8/25/03	-0.93	0.48	0.48	-3.05	1.57	1.57
Malaspina	(L/LK)	3274	1220	8/27/00	8/22/12	-0.88	0.23	0.19	-2.89	0.64	0.64
Malaspina	(L/LK)	3274	1220	8/25/03	8/26/07	-0.87	0.38	0.39	-2.86	1.28	1.28
Malaspina	(L/LK)	3274	1220	8/26/07	8/23/10	-1.46	0.86	0.78	-4.78	2.55	2.55
Malaspina	(L/LK)	3274	1220	8/23/10	8/22/12	0.20	0.50	0.40	0.70	1.50	1.50
Miles	(LK)	375	1060	9/2/04	8/19/09	-1.65	0.36	0.37	-0.62	0.14	0.14
Miles	(LK)	375	1060	9/2/04	8/30/12	-1.36	0.27	0.22	-0.51	0.08	0.08
Miles	(LK)	375	1060	8/19/09	8/30/12	-0.93	0.35	0.36	-0.35	0.13	0.13
Nabesna	(L)	1002	2270	6/21/00	6/3/07	-0.42	0.24	0.23	-0.42	0.23	0.23
Ogilvie	(L)	248	2240	8/24/03	8/19/07	-0.30	0.60	0.60	-0.10	0.20	0.20
Ogilvie	(L)	248	2240	8/24/03	8/16/12	-0.62	0.34	0.37	-0.15	0.09	0.09
Ogilvie	(L)	248	2240	8/19/07	8/16/12	-0.61	0.58	0.59	-0.15	0.15	0.15
Steller	(LK)	745	1110	8/22/03	8/28/07	-1.25	0.36	0.33	-0.93	0.25	0.25
Steller	(LK)	745	1110	8/22/03	8/18/12	-0.83	0.23	0.21	-0.62	0.16	0.16
Steller	(LK)	745	1110	8/28/07	8/21/10	-1.42	0.49	0.46	-1.06	0.35	0.35
Steller	(LK)	745	1110	8/21/10	8/18/12	0.76	0.51	0.50	0.57	0.37	0.37
Walsh	(L)	713	2410	8/19/03	8/19/07	-0.10	0.40	0.60	-0.10	0.40	0.40
Walsh	(L)	713	2410	8/19/03	8/16/12	-0.46	0.45	0.43	-0.33	0.30	0.30
Walsh	(L)	713	2410	8/19/07	8/16/12	-0.40	0.60	0.40	-0.30	0.30	0.30
Yahtse	(T)	772	1310	8/29/06	8/22/12	0.20	0.20	0.10	0.12	0.10	0.10
Yahtse	(T)	772	1310	8/26/07	8/23/10	-0.36	0.25	0.27	-0.28	0.21	0.21
Yahtse	(T)	772	1310	8/23/10	8/22/12	1.17	0.37	0.32	0.90	0.24	0.24

latter two intervals clearly reflect the most recent surge phase, but thickening in the earlier "quiescent phase" intervals is also likely dynamic, in that it reflects smaller scale ice accelerations in more upstream portions of the glacier.

Bagley West Glacier, though contributing to Bering Glacier's ice flow, is less clearly involved in the surging behavior described above (Figure 110). Thinning dominated the glacier over all intervals, with localized rates of ranging from 0 to 4 m/yr. At most intervals, the thinning was greatest at lower elevations, but during the 2010-2012 intervals (which includes the peak of the 2008-2011 surge) it is interesting to note that the maximum thinning was higher upglacier, centered on about 1500 m elevation at the approximate peak of the AAD.

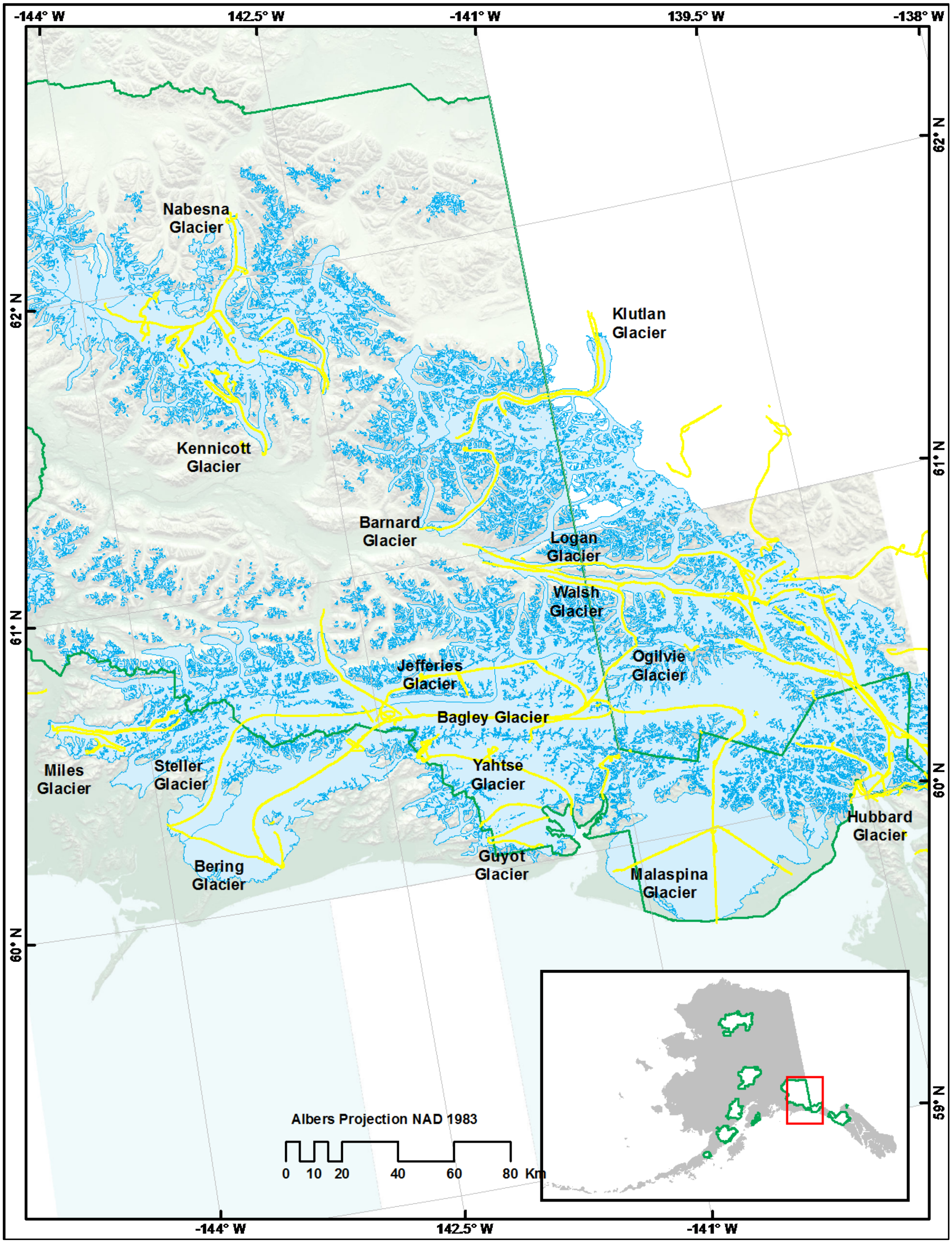

Figure106. Locations of glaciers in Wrangell-St. Elias with elevation change results reported in this paper. Laser altimetry tracks are shown in yellow.

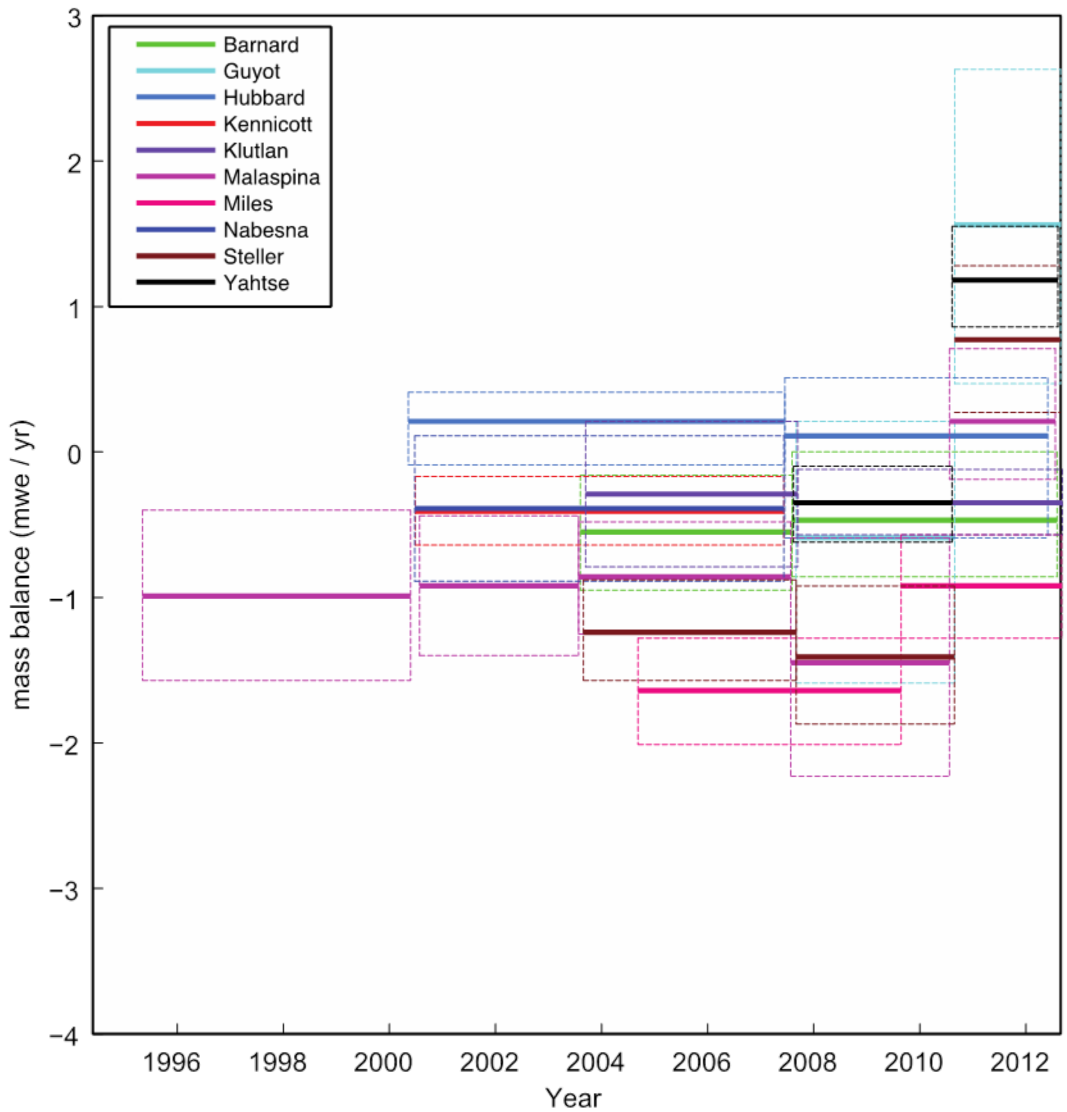

Figure 107. Mass balance of select glaciers in Wrangell-St. Elias National Park & Preserve. Thick solid lines are mass balances; upper and lower dashed lines reflect confidence intervals for each time period. For clarity, some lines have been shifted a few pixels left or right to minimize overlap.

Jefferies Glacier (Figure 111), which is contiguous with the Bagley East Glacier, contributes ice to the north flowing Tana Glacier. Dynamics on Jefferies are typical, and include thinning during all intervals that peaks at about 2 m/yr near the 1100 m terminus between 2003 and 2007.

Relating the elevation changes just described to glacier mass balance is a difficult problem. As noted above, the mass balance rates given in our individual DZ plots are clearly not correct, as they reflect area-averaged elevation changes for only discrete portions of the interconnected glacier system. Simply combining them, however, is also challenging. Beedle et al. (2008), who addressed the issue of volume/mass change on the Bering Glacier with different data, highlighted the challenges posed by use of differing nomenclatures, definitions, outlines, and hypsometries by various investigators. The surge behavior of the Bering further complicated this. Because of these challenges, distillation of our results to a single mass balance rate is beyond the scope of this work, but we provide a quantitative summary of the elevation change data presented above in Figure 112. The uppermost panel in that plot shows the outlines of the various system components in oblique aerial view, and the next panel down provides the area-altitude distributions for the system components: Bering and Bagley East combined, Bagley West, Tana, and Jefferies. The lowest three panels summarize elevation changes for these components, as functions of elevation, over three time intervals. The following trends stand out from these results: 1) the Bering/Bagley East segment is far and away the largest of the group; 2) Elevation changes on that system have been dominated by the dynamics of surging and are not clearly related to climate; 3) Bagley West and Jefferies Glaciers have each thinned a little; and 4) Tana Glacier has shown surprisingly large elevation gains (from 2003-2007) and losses (from 2007-2010).

Steller Glacier was flown in 2003, 2007, 2010, and 2012 (Figure 113). This 745 km^2 glacier, which flows west from a divide at the western edge of the Bagley Icefield and then merges with the lower Bering Glacier, had fairly negative mass balance in the first two intervals, ranging

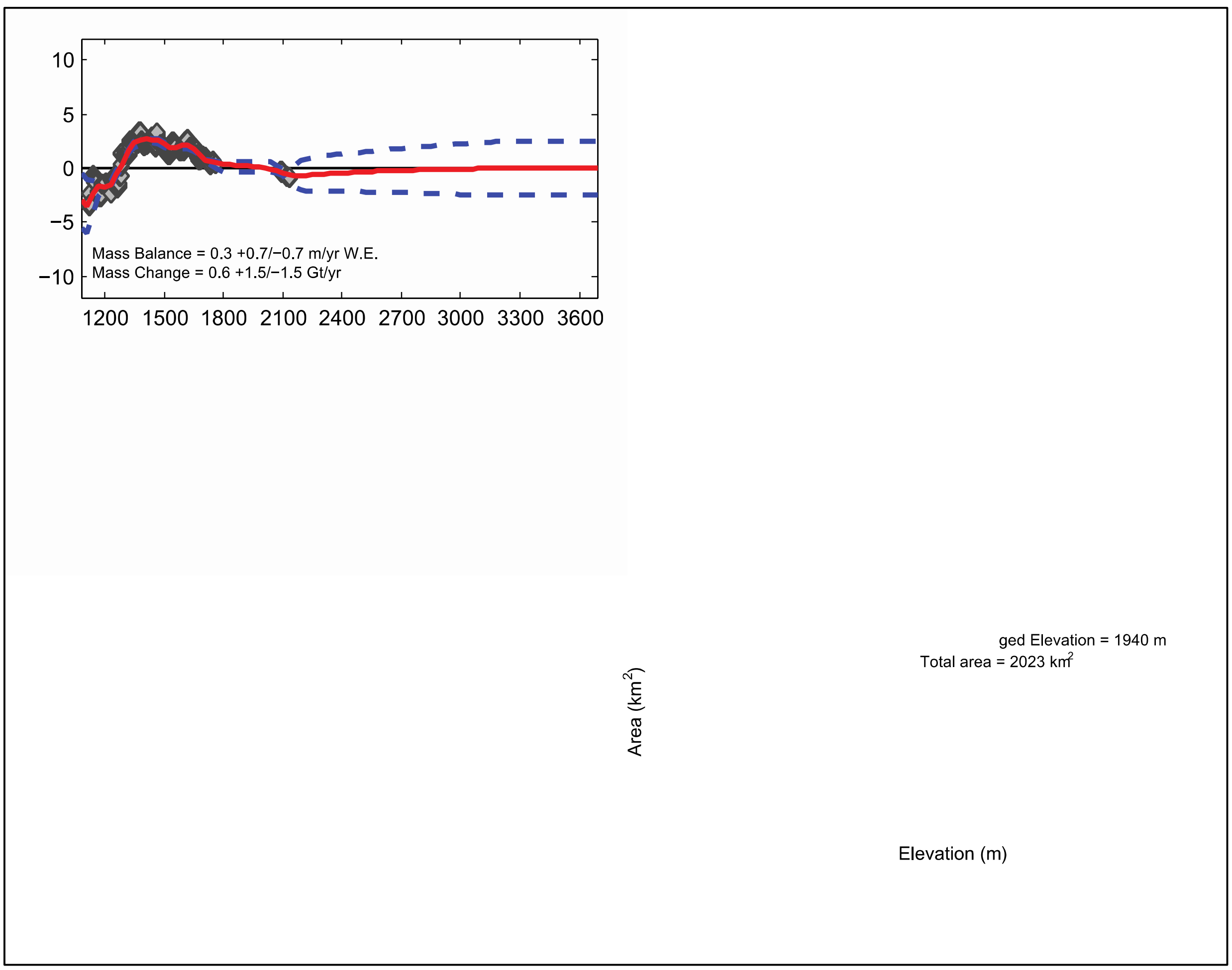

Figure 108. Elevation change and AAD for Bagley East Glacier. Bagley East is one tributary of the Bering Bagley Glacier system and its MB and MC alone do not reflect the full accumulation and ablation zones. See Figure 107 for context.

from -1.25 m/yr w.e. (2003-2007) to -1.42 m/yr w.e. (2007-2010). From 2010 to 2012, however, the mass balance was positive 0.76 m/yr w.e. and showed consistent thickening below 1400 m, with thickening rates of up to 4 m/yr near the broad terminus. Steller Glacier is not generally considered a surging glacier, and has in fact been distinguished from contiguous ice of the "surging Bering Glacier" by Beedle et al. (2008), but the timing of this terminus thickening is intriguingly correlated with the 2008-2012 surge of Bering Glacier (Burgess et al. 2012).

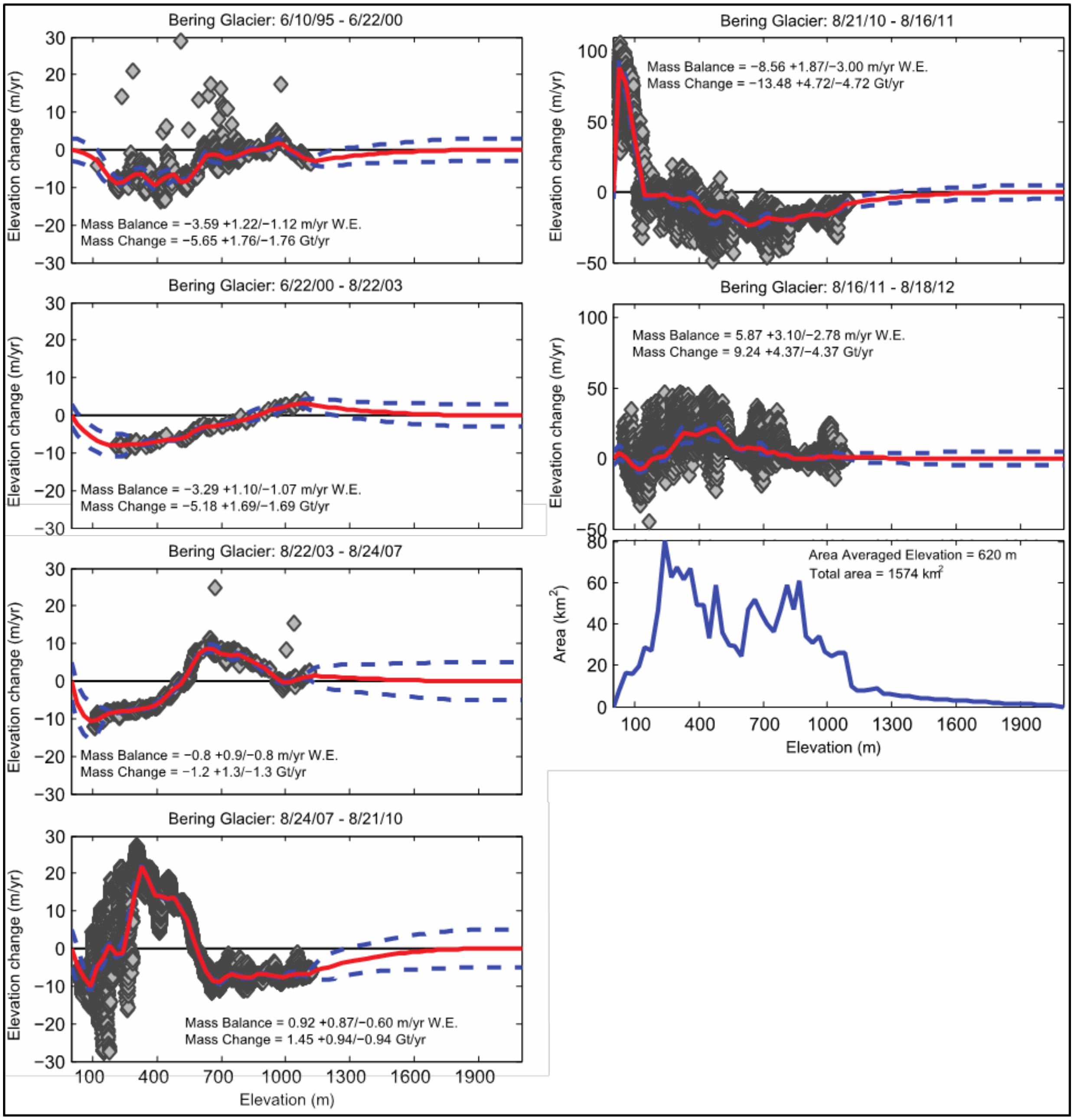

Figure 109. Elevation change and AAD for Bering Glacier. Bering is one part of the Bering Bagley Glacier system and its MB and MC alone do not reflect the full accumulation and ablation zones. See Figure 107 for context.

Lake-calving Miles Glacier was flown in 2004, 2009, and 2012 (Figure 114) and had more negative mass balance rates at both intervals than most other glaciers in WRST (-1.65 m/yr w.e. 2004-2009 and -0.93 m/yr w.e. 2009-2012). Thinning dominated the elevation change at all elevations, and reached 5 m/yr near the terminus in the earlier interval.

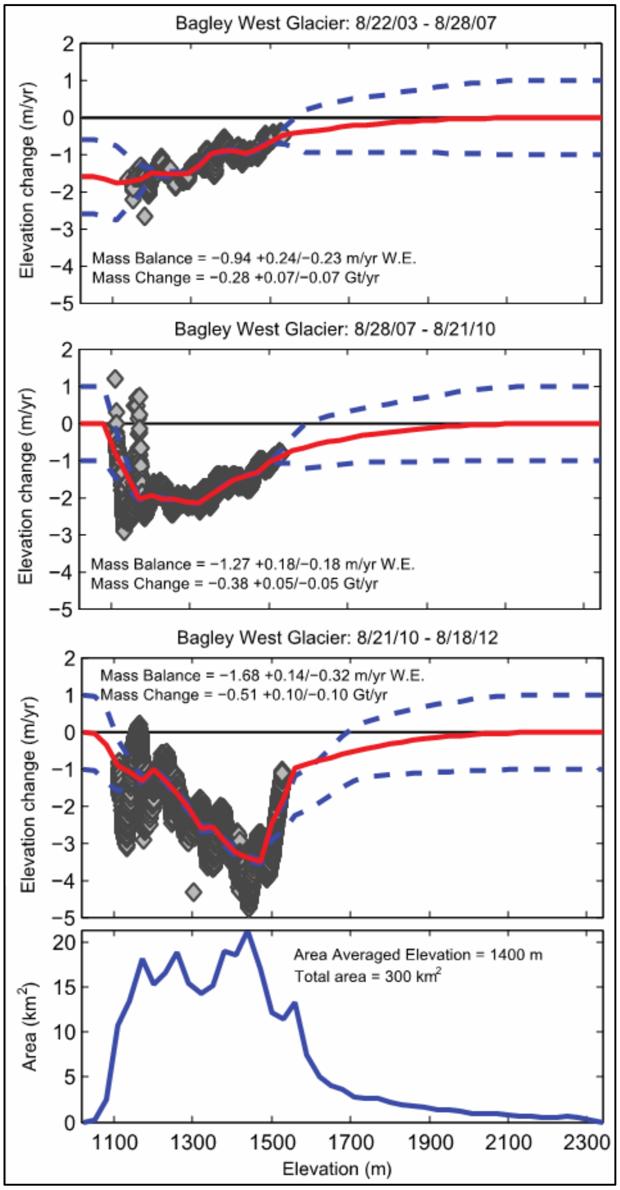

Figure 110. Elevation change and AAD for Bagley West Glacier. Bagley West is one tributary of the Bering Bagley Glacier system and its MB and MC alone do not reflect the full accumulation and ablation zones. See Figure 107 for context.

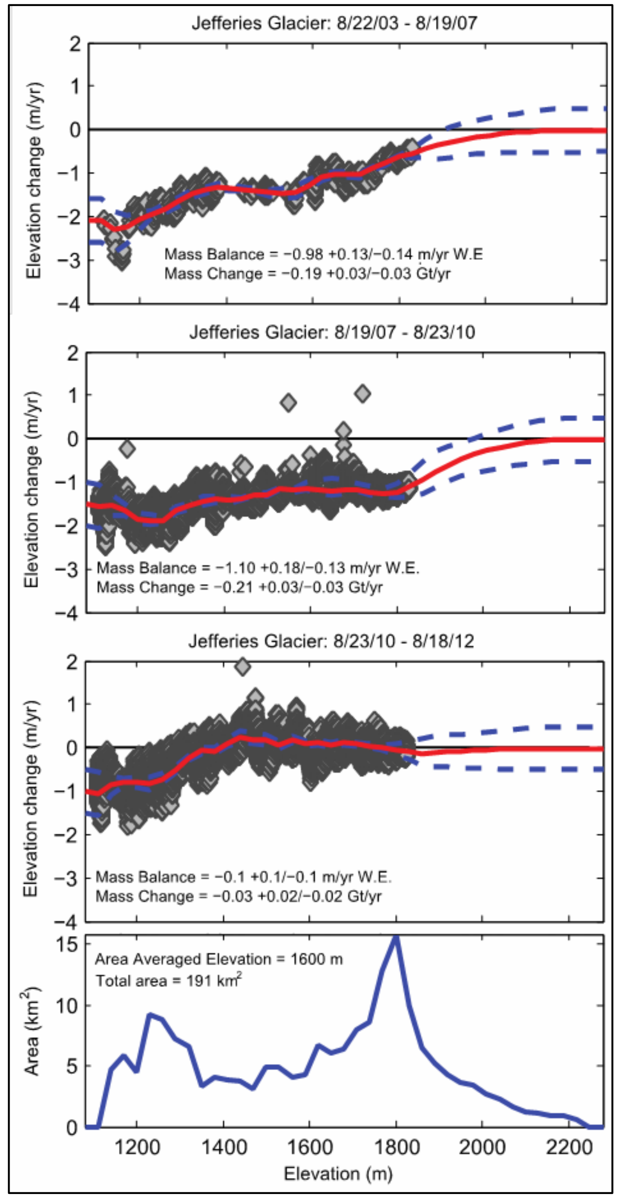

Figure 111. Elevation change and AAD for Jefferies Glacier. Jefferies is one tributary of the Bering Bagley Glacier system and its MB and MC alone do not reflect the full accumulation and ablation zones. See Figure 107 for context.

Both Barnard Glacier (Figure 115) was and Klutlan Glacier (Figure 116) were flown in 2003, 2007, and 2012. Both had negative mass balances with little change between intervals. From 2007 to 2012, Barnard was slightly more negative (-0.48 m/yr w.e.) than Klutlan (-0.36 m/yr w.e.). The pattern of thinning for Barnard Glacier was typical, with the greatest thinning near

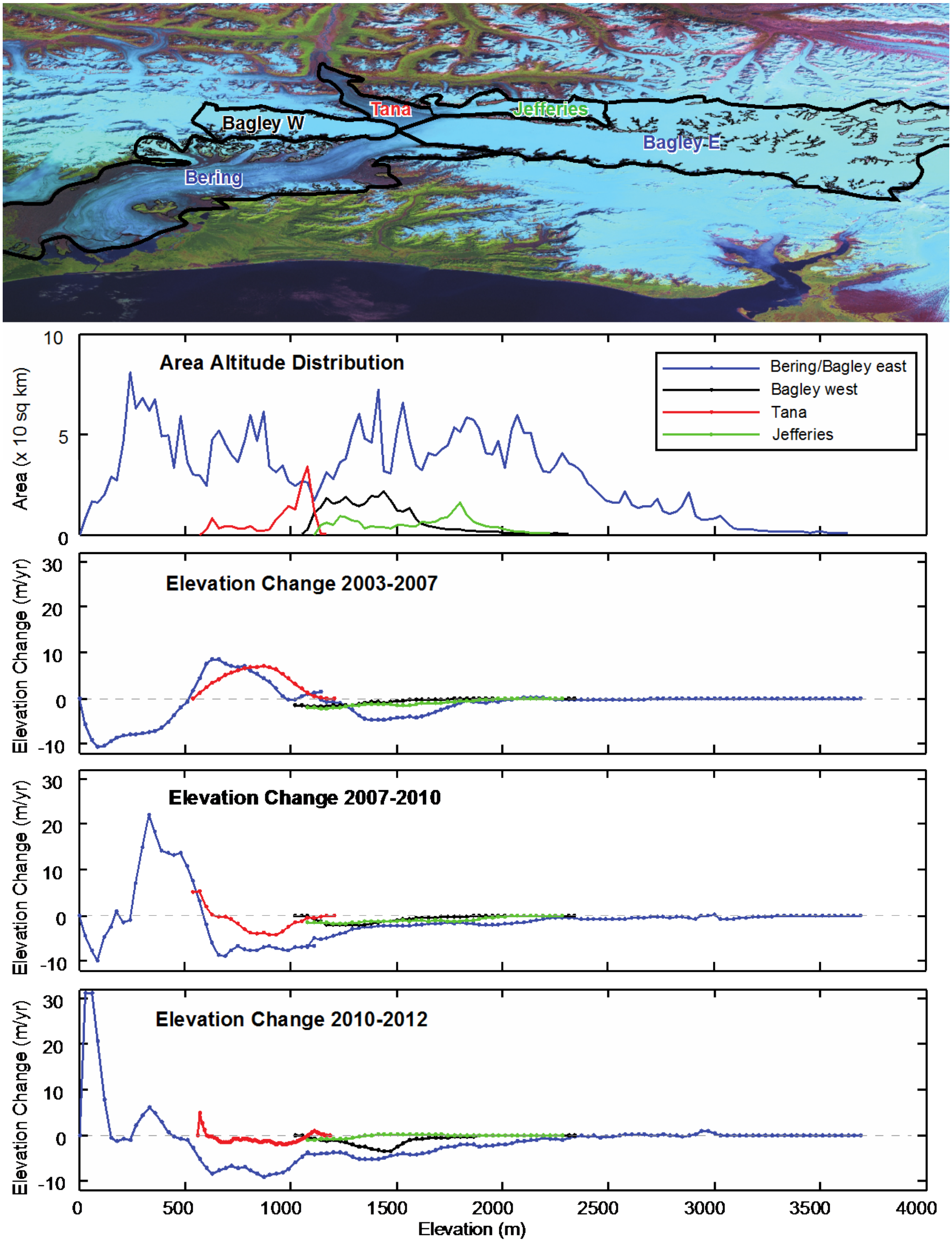

Figure 112. Area altitude distribution and elevation changes for the contributing tributaries of the Bering Bagley Glacier system, components of which are shown in the previous figures. The map at top shows approximate boundaries of the various tributaries in oblique aerial view from the south.

the terminus and tapering towards zero in upper elevations, but Klutlan had a distinctive pattern of slight thickening between 1800 and about 2800 m, and deep thinning (around 5 m/yr) near the terminus.

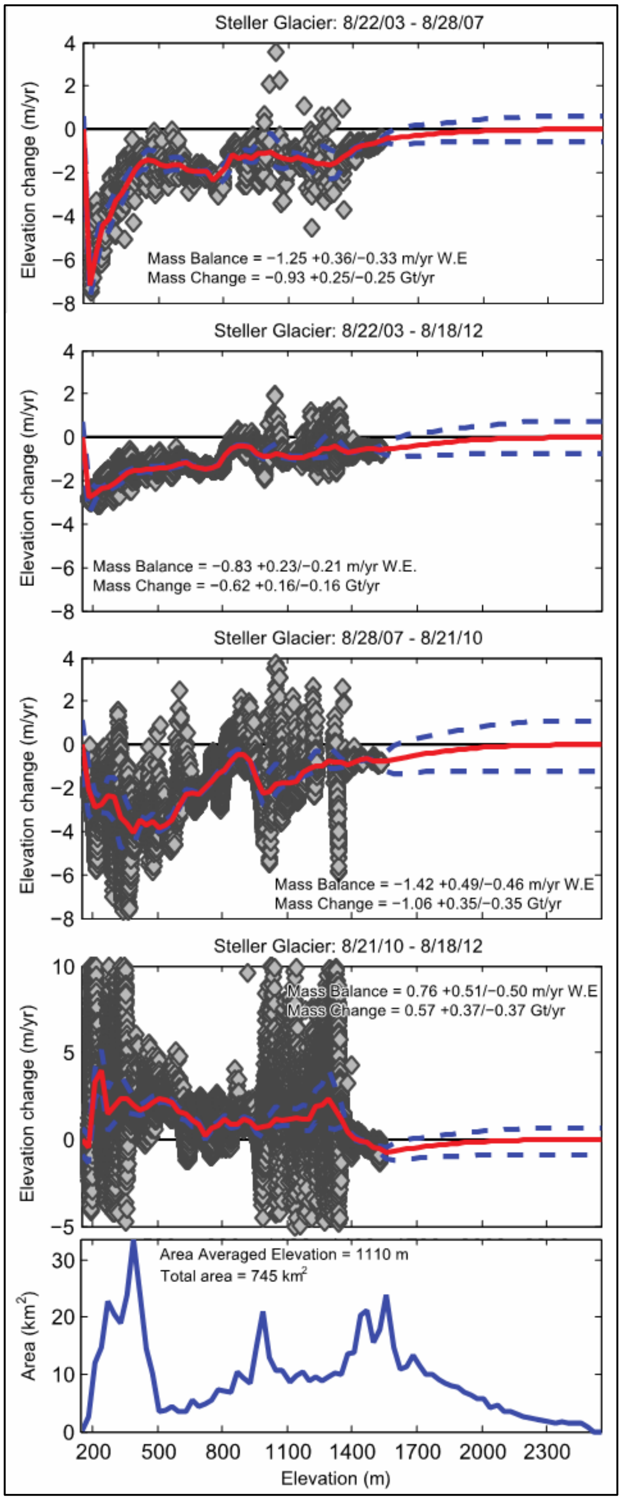

Figure 113. Elevation change and AAD for Steller Glacier.

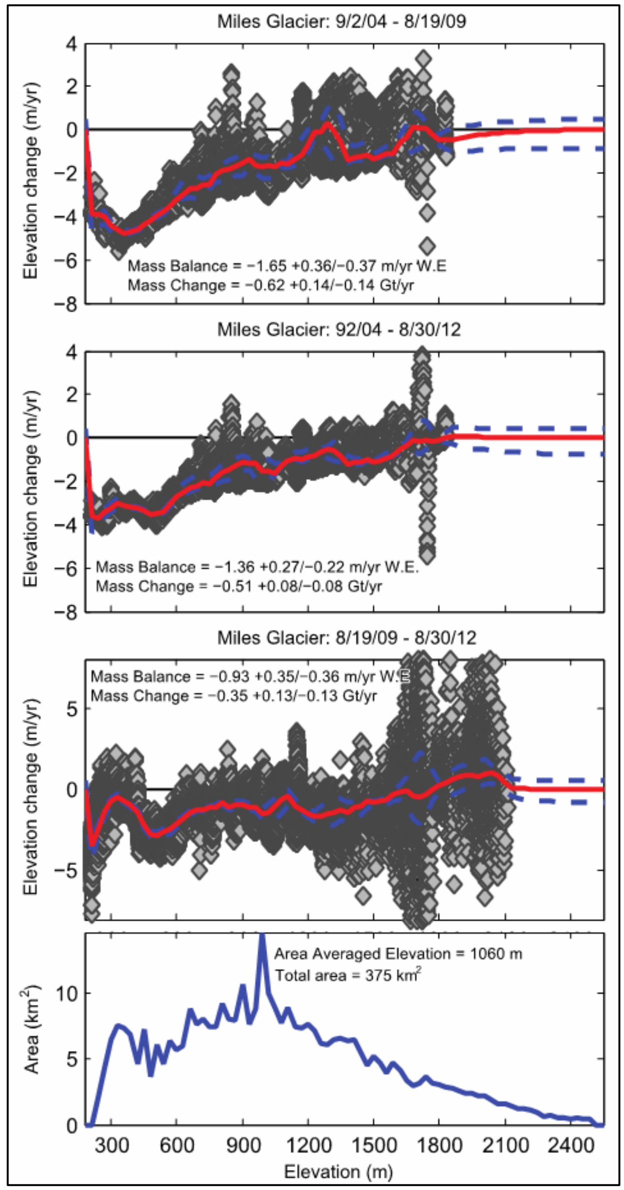

Figure 114. Elevation change and AAD for Miles Glacier.

Guyot Glacier, which shares Icy Bay with Yahtse Glacier, was flown in 2007, 2010, and 2012 (Figure 117). There is significant spread in the elevation change data from Guyot, and the glacier was not sampled above 1600 m, which leaves a non-trivial amount of the AAD unsampled. Nonetheless, the data suggest that the mass balance rate was negative from 2007-2010 (-0.6 m/yr w.e.) and positive from 2010-2012 (0.2 m/yr w.e.). The change to positive balance was accompanied by slight thickening (up to 5 m/yr) near the terminus. The absolute value of both estimates, however, is less than the confidence intervals, compromising our ability to make general statements about the trends of thinning or thickening.

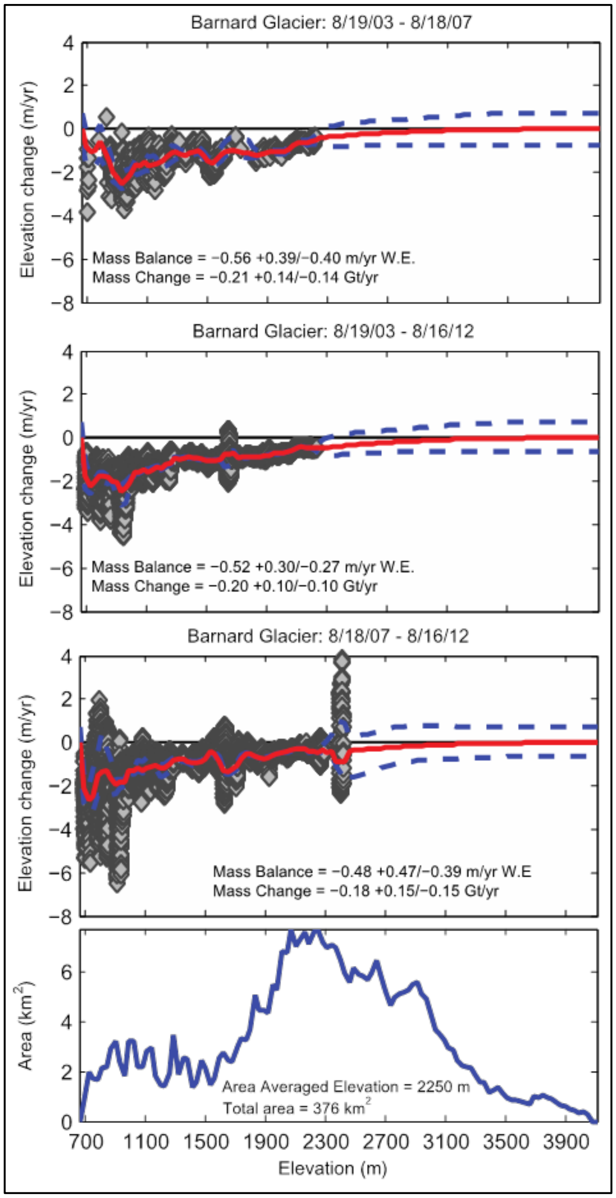

Figure 115. Elevation change and AAD for Barnard Glacier.

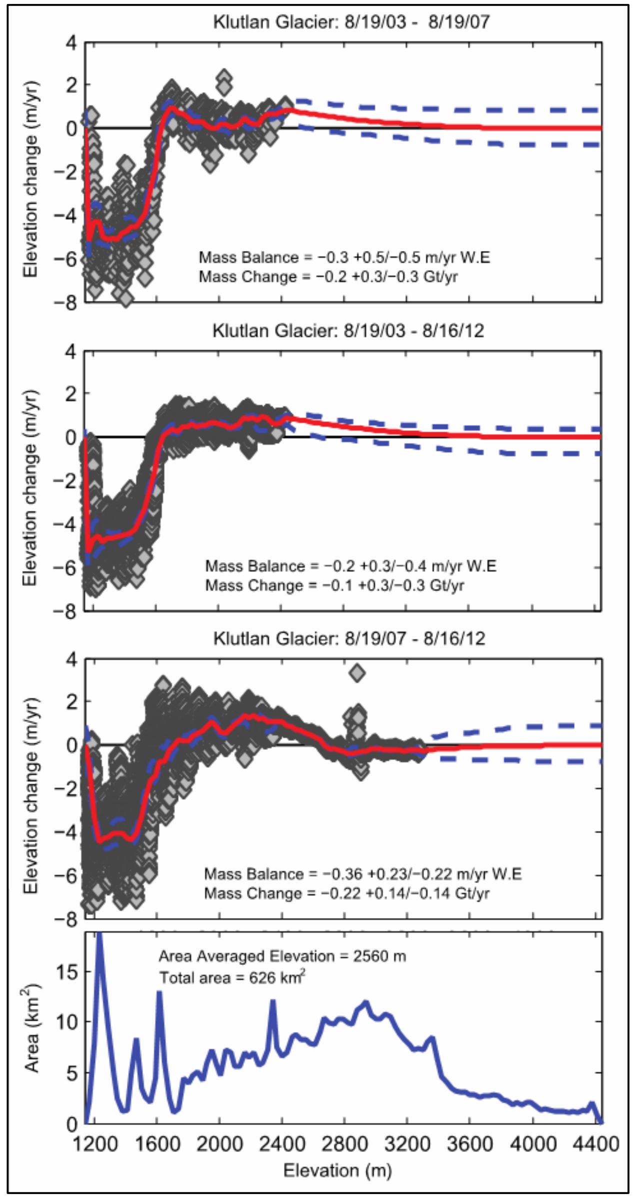

Figure 116. Elevation change and AAD for Klutlan Glacier.

Yahtse Glacier was flown in 2006, 2007, 2010, and 2012 (Figure 118), and the trends and data quality are relatively consistent throughout all measurement periods. Yahtse is well-known as an advancing tidewater glacier in Icy Bay, and indeed from 2006 to 2012, Yahtse consistently showed increases in surface elevation, especially near the terminus where thickening approached 15 m/yr, and positive mass balances. From 2006 to 2012 the mass balance was positive (0.2 m/yr w.e.) with mass balance increasing through the measured years to the highest value of 1.17 m/yr w.e. from 2010 to 2012.

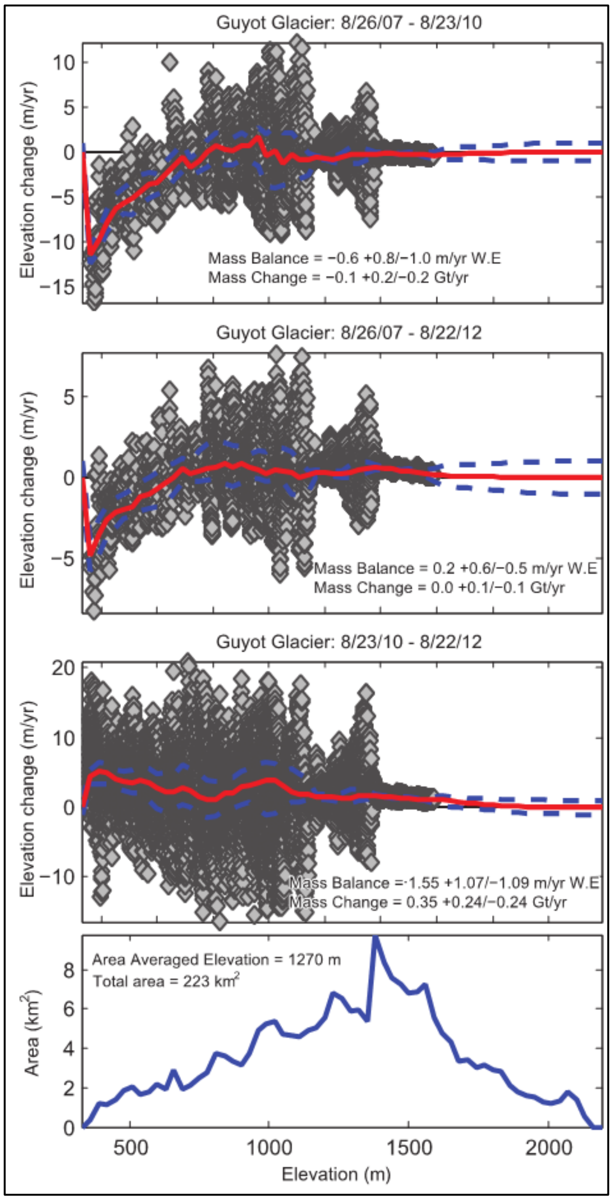

Figure 117. Elevation change and AAD for Guyot Glacier.

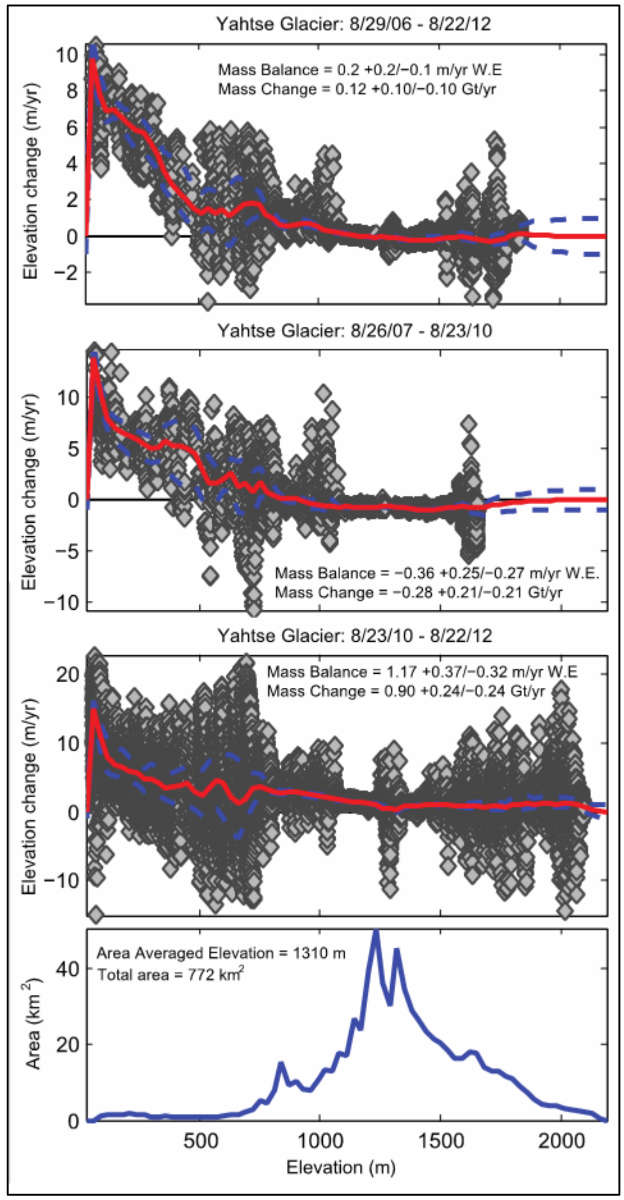

Figure 118. Elevation change and AAD for Yahtse Glacier.

Malaspina Glacier was flown in 1995, 2000, 2003, 2007, 2010, and 2012 (Figure 119). At all intervals, coverage is limited to <2100 m, well below the top of the AAD but incorporating the majority of the glacier's area since higher elevations include only a narrow zone on the steep

slopes of Mt. St. Elias. We note that the total area indicated in the AAD plot (3274 km^2) includes only the central portion of the Malaspina that is fed directly by the Seward Glacier throat, and excludes the east and west margins of the Malaspina Lobe that are fed by the Marvine and Agassiz Glaciers, respectively (Figure 127). The temporal pattern of mass balance on Malaspina started at -1.00 m/yr w.e. from 1995 to 2000, increased monotonically to -0.87 m/yr w.e. from 2003 to 2007, but then declined again 2007-2010 (-1.46 m/yr w.e.) and ended slightly positive in the final interval 2010-2012 (0.2 m/yr w.e.). During all but that last interval, the glacier thinned very slightly at upper elevations and thinned between 5 and 7 m/yr at the terminus. Between about 400 and 1000 m, however, the glacier's behavior was variable and included substantial thickening from 2000-2003 and 2007-2010. During the final—positive—interval, the ice thickened slightly over a broad range of elevations between 500 and 1600 m, but with large scatter and consequently high confidence intervals in the calculated mass balance.
Hubbard Glacier was flown in 2000, 2007, and 2012 (Figure 120). Hubbard is well known for its 20th century history of terminus advance and also for its sporadic ability to isolate Russell Fjord from the open ocean. Over the period of our measurements, the mass balance of Hubbard has been modestly positive, with rates of 0.2 m/yr w.e. from 2000 to 2007 and 0.1 m/yr w.e. from 2007 to 2012. Thickening was observed near the terminus and mid-elevations over both intervals, although we note that the data is quite scattered in the latter period and the uncertainties are therefore high.

Ogilvie Glacier (Figure 121), Logan Glacier (Figure 122), and Walsh Glacier (Figure 123) were all flown in 2003, 2007, and 2012. All three are tributaries of the large debris-covered Chitina Glacier, and as such their individual mass balances are not comparable to others in this document. They are therefore omitted from Figure 102, and we do not comment on them further except to note that there is a general pattern of thinning and mass loss. There are, however, some intriguing exceptions, perhaps related to surging that is known to impact all of these glaciers. Walsh Glacier surged in the early 1960s (Post, 1966), and thickening we observed around 2200 m may reflect a small surge event. Logan has also been reported as a surge-type glacier on the basis of looped moraines (Molnia 2008). It has not been formally reported as surging during the period of our measurements, but anecdotal observations of Logan Glacier in March 2013 suggested the possibility of a surge (Truffer, pers. comm.). Both Logan and Ogilvie glaciers showed thickening around 1600 m, the approximate elevation of their confluence, over both measured intervals (Figure 121 and Figure 122). Surface velocity data from Burgess et al. (2013) corroborates the evidence for a previously unreported surge in that area. Our data coverage of upper Logan Glacier is poor, but Ogilvie thinned substantially above 1600 m, suggesting a possible origin for the extra mass near the confluence.

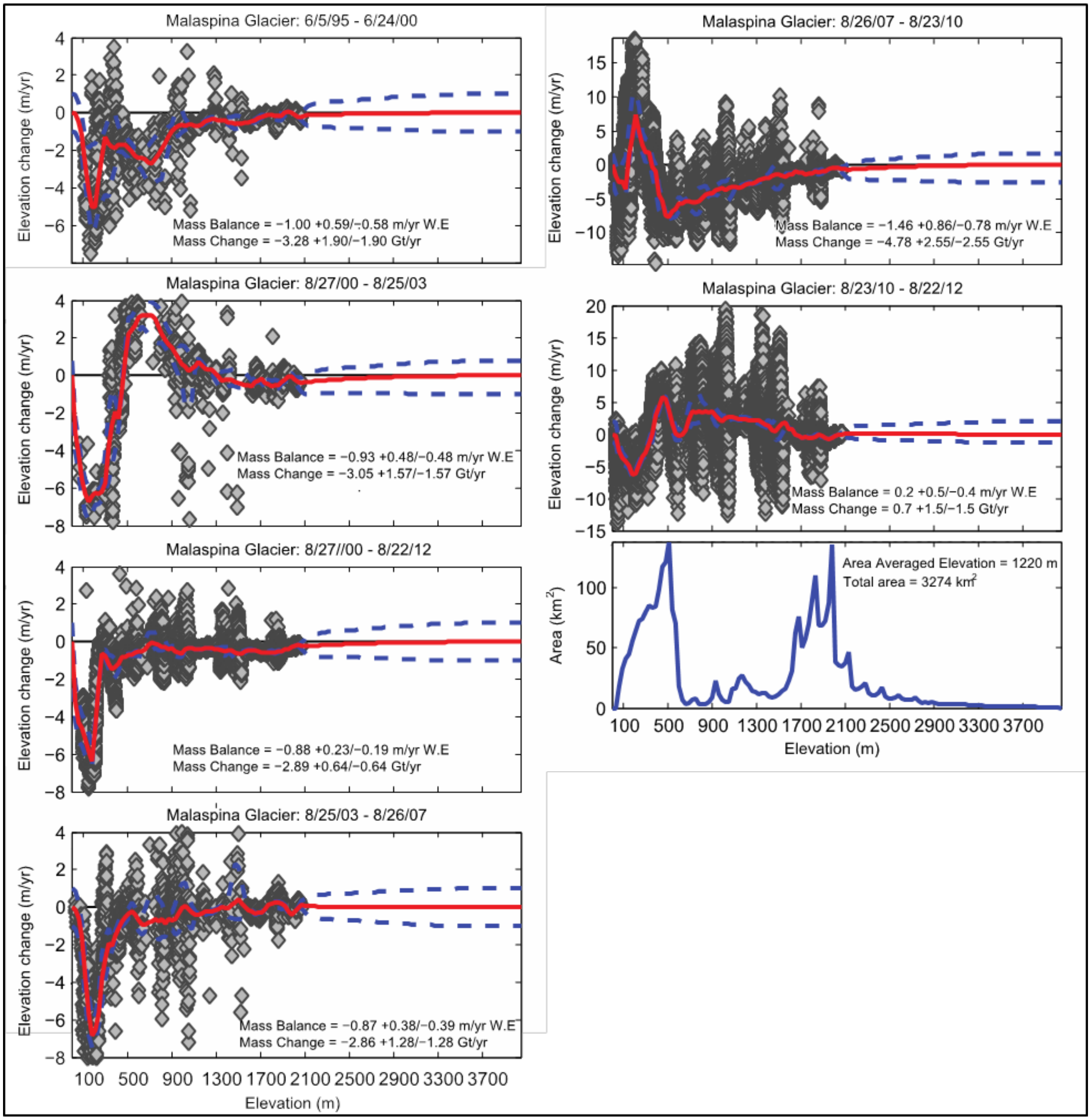

Figure 119. Elevation change and AAD for Malaspina Glacier.

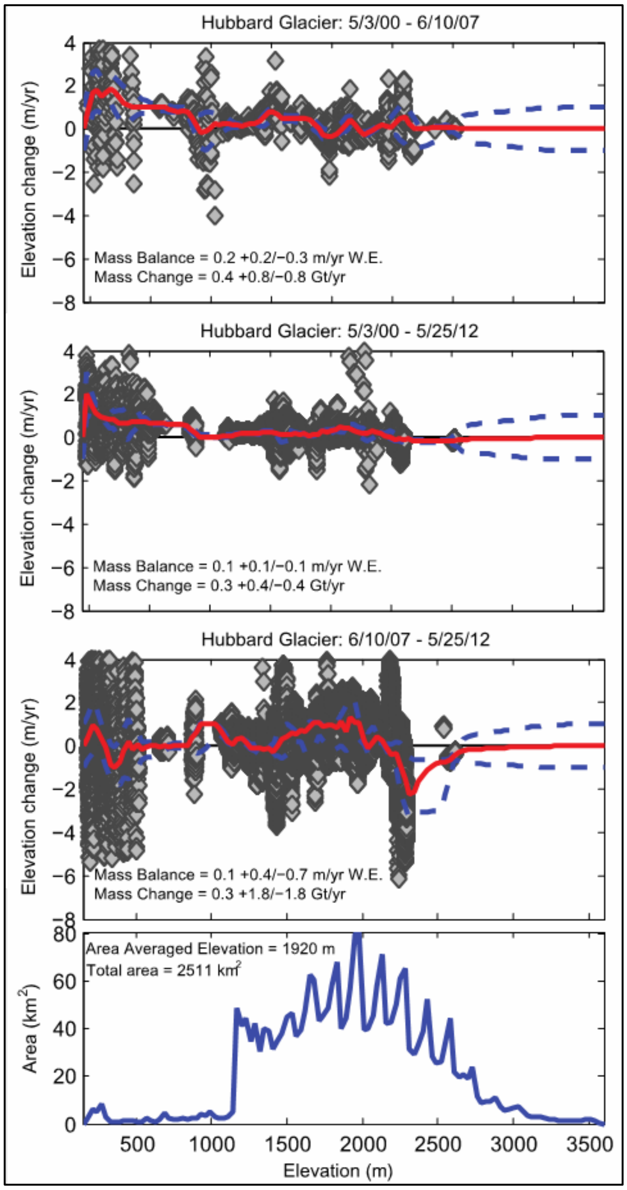

Figure 120. Elevation change and AAD for Hubbard Glacier.

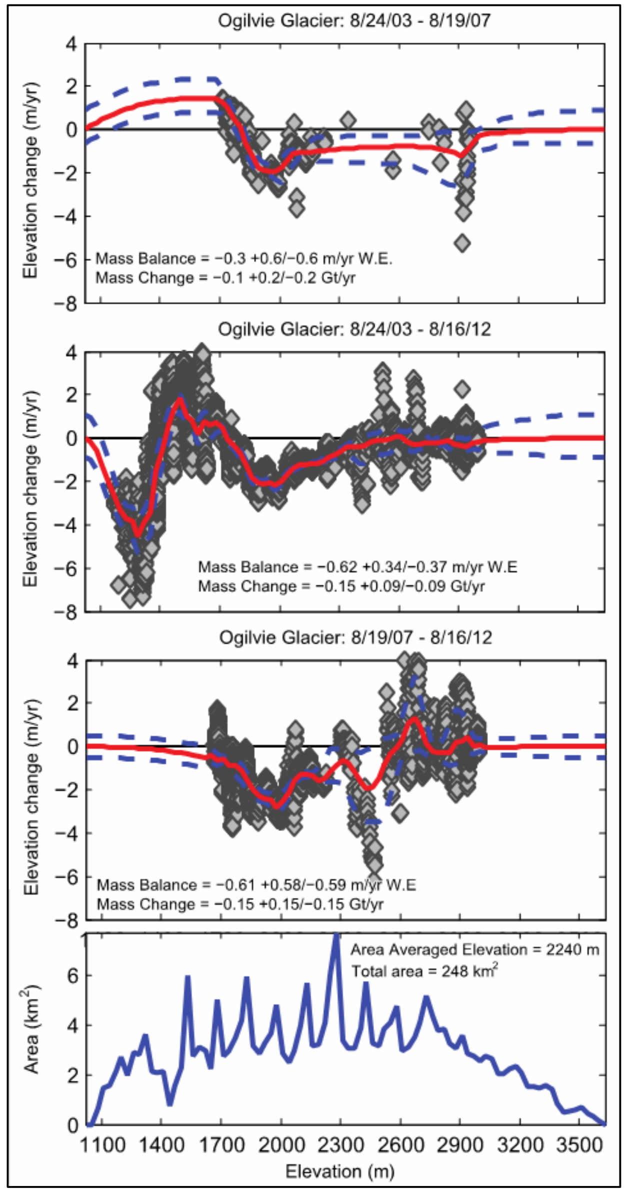

Figure 121. Elevation change and AAD for Ogilvie Glacier. Ogilvie is a tributary of Chitina Glacier, and its MB and MC do not reflect the full ablation or accumulation zones.

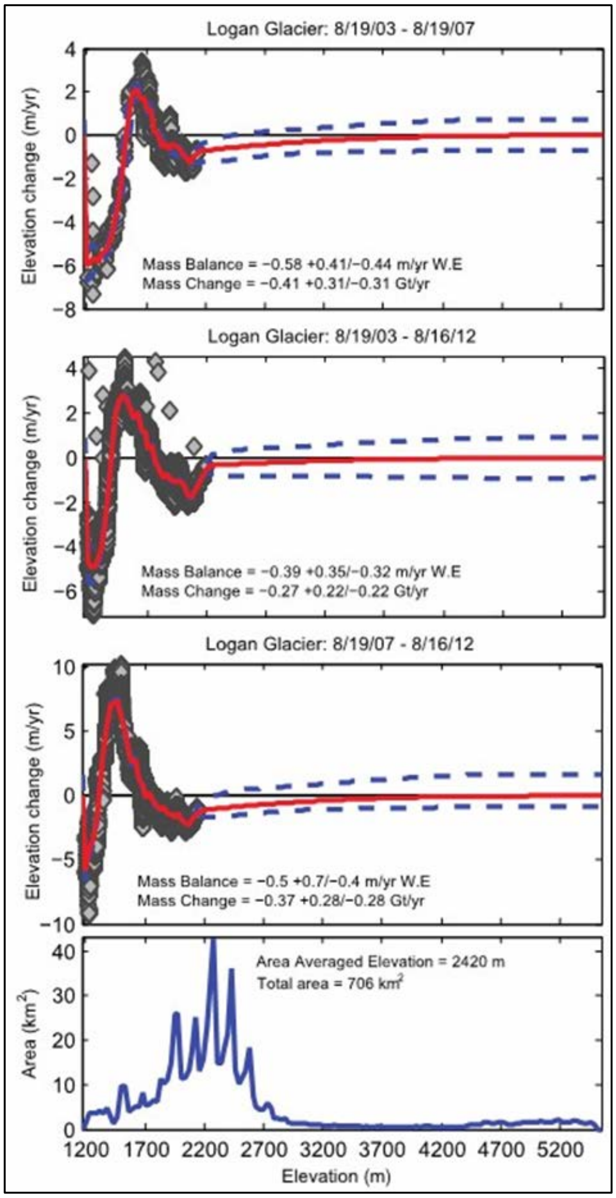

Figure 72. Elevation change and AAD for Logan Glacier. Logan is a tributary of Chitina Glacier, and its MB and MC do not reflect the full ablation or accumulation zones.

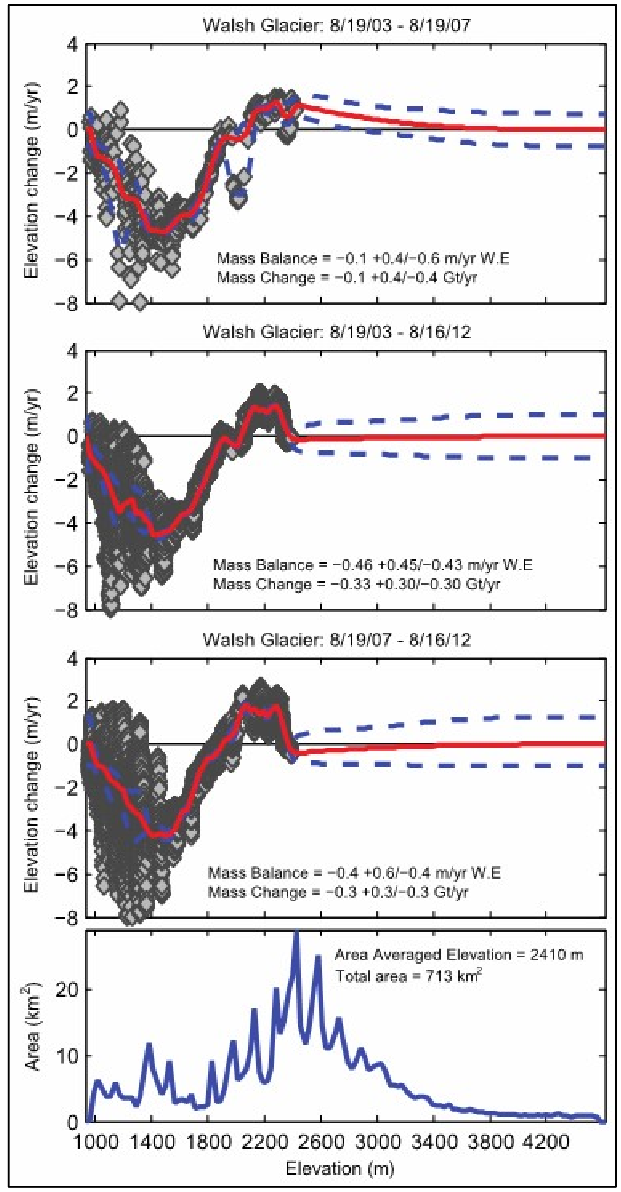

Figure 123. Elevation change and AAD for Walsh Glacier. Walsh is a tributary of Chitina Glacier, and its MB and MC do not reflect the full ablation or accumulation zones.

Kennicott Glacier was flown in 2000 and 2007 (Figure 124). For that single interval, we have good data coverage up to about 2500 m, but lack coverage on the upper portion of the large icefalls of the south face of Mt. Blackburn. We therefore have somewhat large confidence intervals (± 0.5 m/yr w.e.) on our estimate of -0.4 m/yr w.e. mass balance. Overall, the pattern of thinning is typical, with increasing rates of thinning—up to 2+ m/yr—near the terminus.

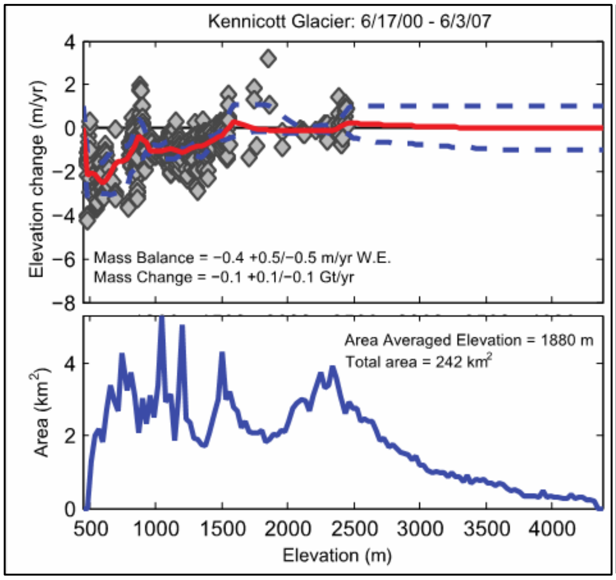

Figure 124. Elevation change and AAD for Kennicott Glacier.

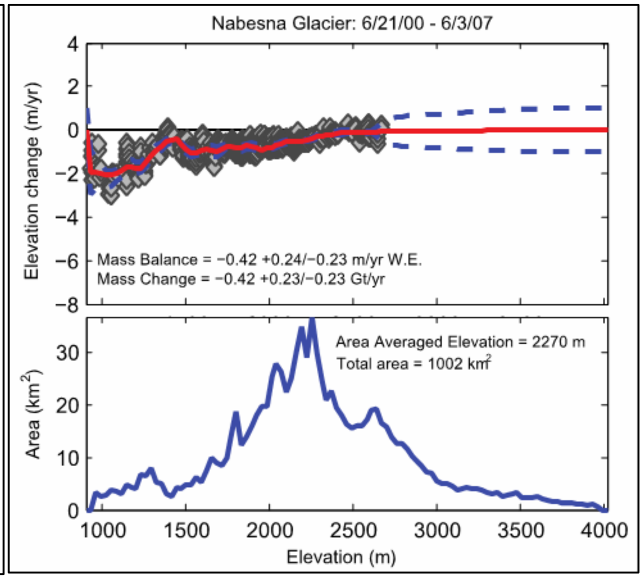

Figure 125. Elevation change and AAD for Nabesna Glacier.

On the other side of the Blackburn massif, Nabesna Glacier (2000, 2007) flows north and is the longest valley glacier in North America (Figure 125). Data coverage is slightly better for Nabesna than for Kennicott, but still omits the highest elevations. The pattern of thinning is also comparable to Kennicott, with rates up to 2+ m/yr near the terminus and an overall mass balance rate of -0.42 m/yr w.e.

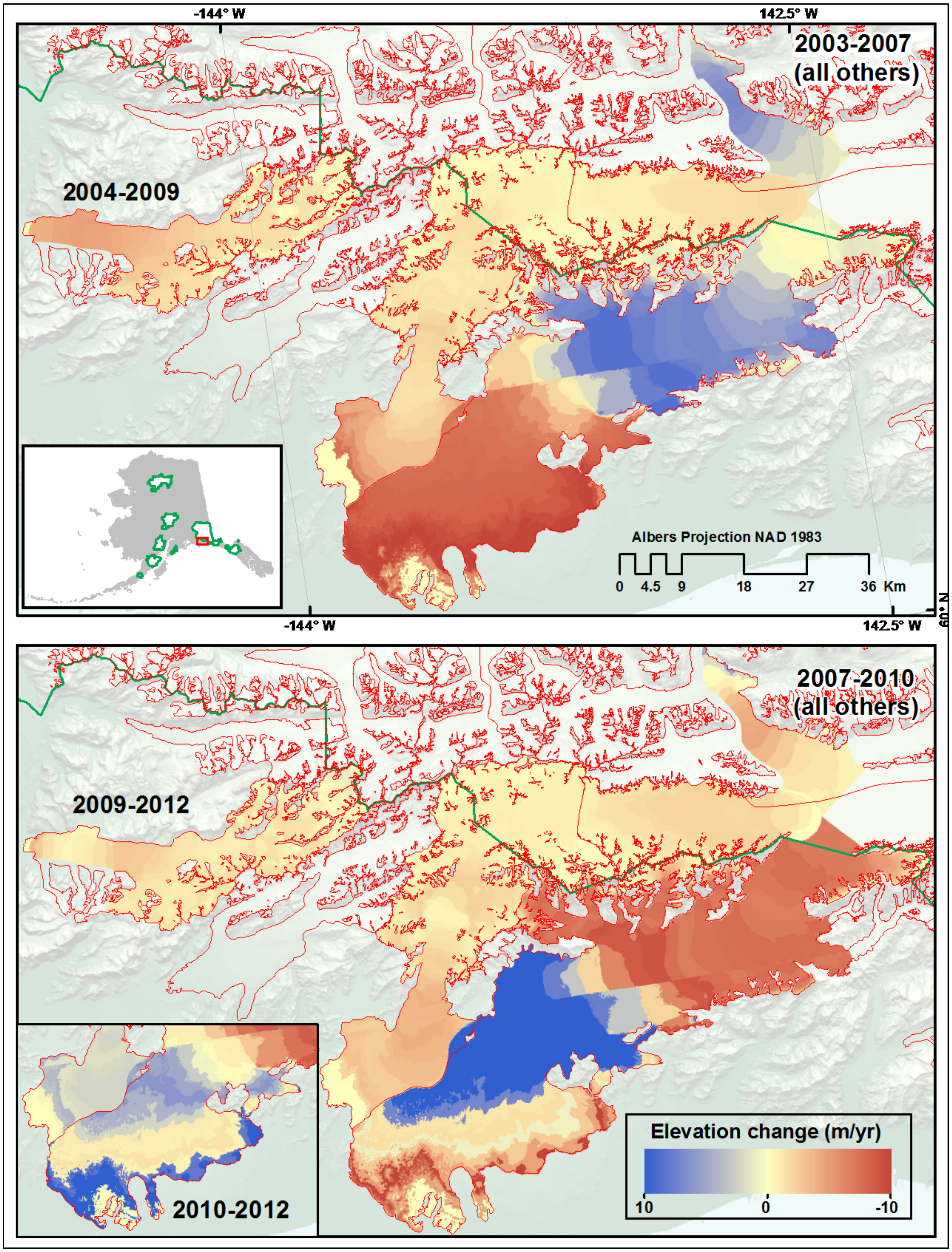

Figure 126. Annual rates of elevation change, by elevation, for Bering, Bagley West, Steller, and Tana Glaciers in Wrangell-St. Elias NP&P. Values are averages over the indicated time intervals.

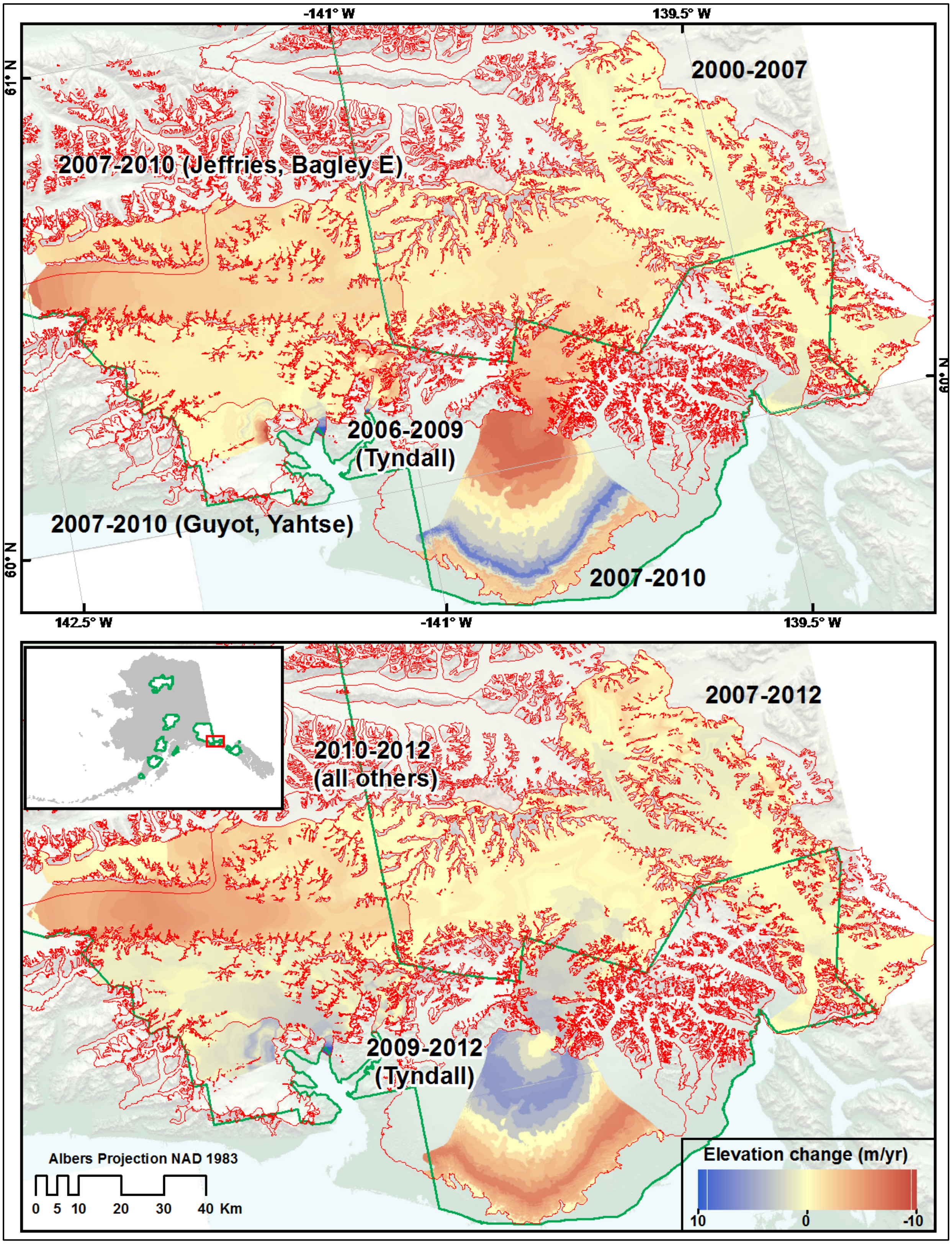

Figure 127. Annual rates of elevation change, by elevation, for Malaspina, Bagley East, Hubbard, and Icy Bay region Glaciers in Wrangell-St. Elias NP&P. Values are averages over the indicated time intervals.

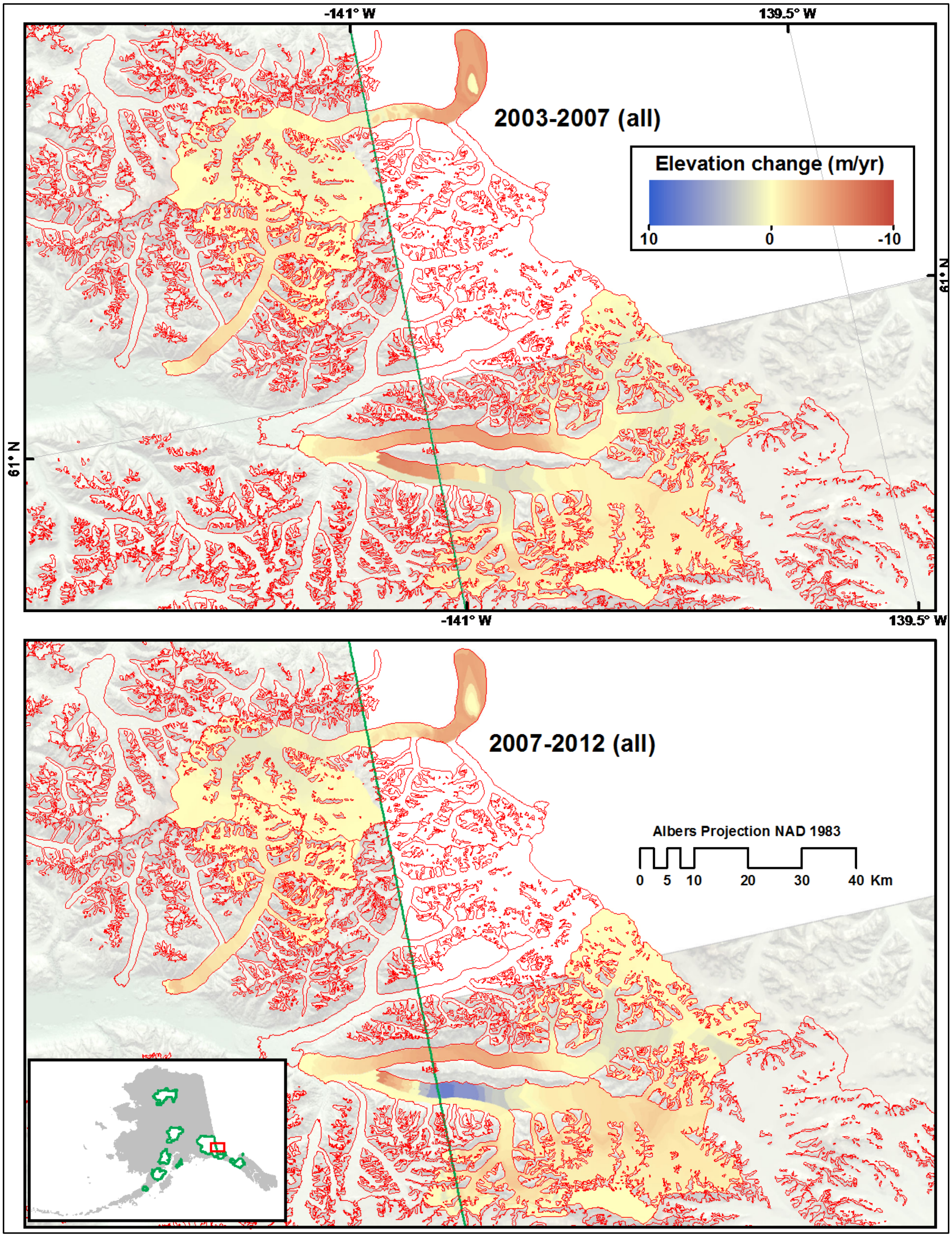

Figure 128. Annual rates of elevation change, by elevation, for Barnard, Klutlan, and Logan/Ogilvie/Walsh Glaciers in Wrangell-St. Elias NP&P. Values are averages over the indicated time intervals.

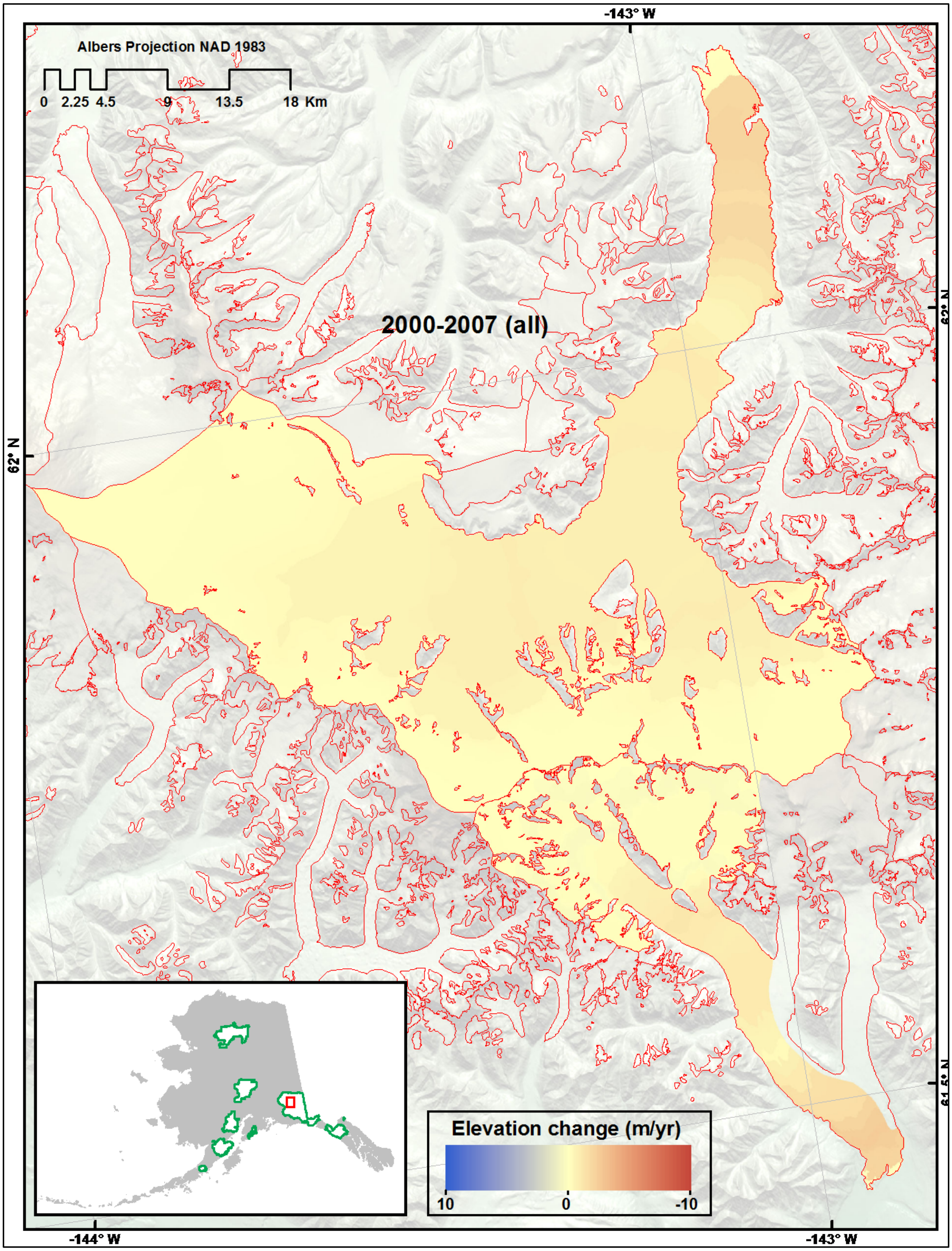

Figure 129. Annual rates of elevation change, by elevation, for Nabesna and Kennicott Glaciers in Wrangell-St. Elias NP&P. Values are averages over the indicated time intervals.

Discussion

This report, with the accompanying database, describes a half-century of change for the glaciers of Alaska's national parks. It builds on major earlier works by Field (1975) and Molnia (2008), and contributes to existing inventories such as GLIMS (Raup et al. 2013) and the RGI (Pfeffer et al. 2014). The sheer number of glaciers makes daunting the task of summarizing these changes. Each park, and indeed each glacier, is worthy of its own discussion. In the European Alps, or perhaps the rest of the United States, this level of attention is possible. At last count, however, Alaska's parks hold over 7500 glaciers. This in itself is a take home message. From a global perspective, Alaska's glaciers are still big, numerous, and active.

Alaska's glaciers are too numerous, in fact, to give them all the attention they deserve. For if there is a second, high priority take home message, it is that these many glaciers—taken as a whole—are in poor health. "Health" can be an ambiguous term, but we use it here in a plain and objective way: healthy glaciers are in equilibrium with their environment. Such glaciers have mass balances close to zero and do not, in response to typical interannual climatic variability, grow or shrink a great deal. This is clearly not the case for Alaska's park glaciers. The vast majority are shrinking in areal coverage, and where we have direct measurements of their surface elevations, they are deflating.

There are exceptions to this rule. Some glaciers, over some intervals, are growing. These make interesting stories, and good science. They often tell us a great deal about the other factors, besides climate, that govern a glacier's relationship to its environment. But the simple fact is that most glaciers are shrinking, and the sheer ubiquity of that trend makes the stories of these glaciers—the ones that are slowing going away—somehow less interesting. That should not be the case. Every glacier, to those who know it, is fascinating and unique. The diminishment of each one of those glaciers has important local impacts on the landscape, and collectively these changes have tremendous regional and local implications. Here we convey only the broadest perspectives on these changes, and point the reader towards the accompanying interpretive report to see some of the details, for a small set of "focus" glaciers, that we omit here.

Glacier Numbers

It seems there are many "new" glaciers in the Alaskan parks. Our inventory, strictly interpreted, outlined 968 more modern glaciers than map date, an increase of 15%. In comparison with the documented 8 percent reduction in total ice-covered area, this finding at first seems contradictory. Are new glaciers forming while most are shrinking?

In most cases, the answer is no. The increase in glacier numbers probably reflects three processes, only one of which reflects actual growth of new glacier ice. The first is a direct outcome of glacier shrinkage: large, multi-branch glaciers shrinking sufficiently that the branches are separating from the main trunk glacier, creating multiple small glaciers where before there was only one. This is very common, demonstrated by the fact that 81% of the 968 "new" glaciers partly or entirely overlap the locations of map date glaciers. In all the Alaskan parks, only 178 modern glaciers were mapped in locations where no ice at all was mapped by original USGS cartographers.

The size distribution of these few glaciers that seem truly “new” (Figure 130) suggests the second reason for an apparent increase in glacier numbers: that our use of high-resolution satellite imagery permitted the identification and mapping of very small glaciers that were present but missed (or ignored) by the original USGS cartographers. Most of these 178 glaciers are less than 0.15 km^2, and the vast majority are <0.5 km^2. These are precisely the glaciers that would be hard to map using older imagery. We interpret many of these glaciers as “newly discovered” rather than truly new.

Tiny is also, of course, the size you would expect for incipient glaciers forming in a climate with decreasing temperatures and/or increasing snow accumulation, the third possible explanation for our results. The altitude distribution of these new glaciers (not to mention the climate itself) argues, however, against that interpretation (Figure 131). These tiny glaciers are not concentrated at high elevations, where we might expect a few anomalous glaciers to form in favorable microclimates. Instead, they are apparently randomly distributed throughout a range of elevations. Their spatial distribution also seems random: the new glaciers are present in every park besides KLGO, further suggesting that our use of higher quality imagery, rather than climate, is responsible for the mapping of these brand new glaciers.

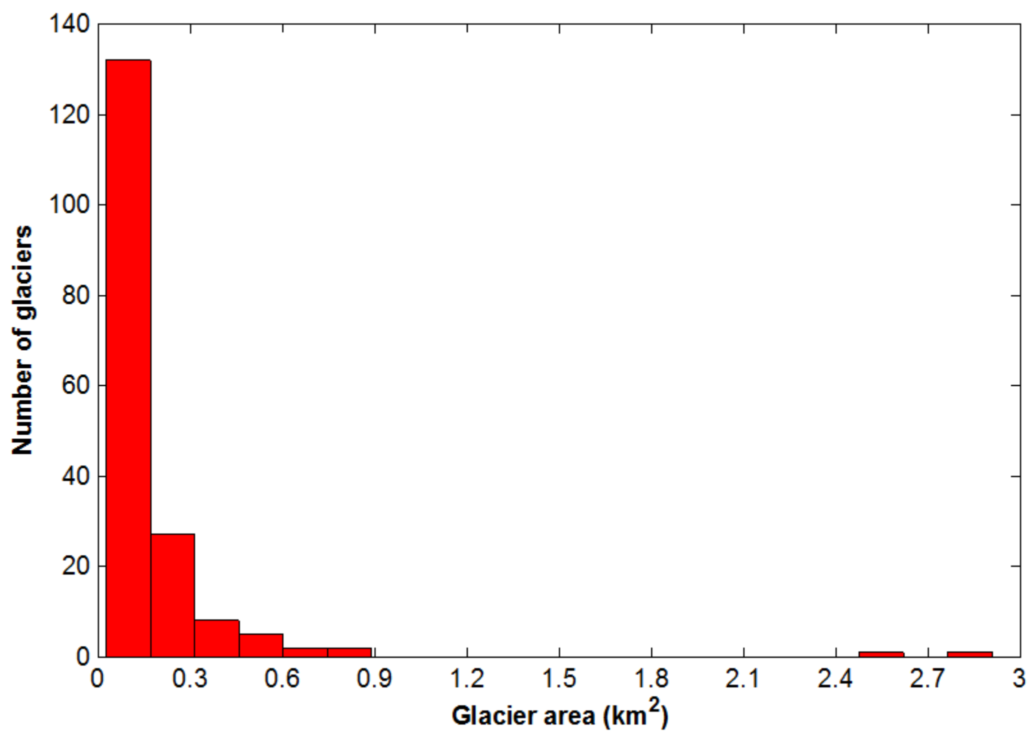

Figure 130. Histogram of glacier areas for Alaska park glaciers that were mapped in modern satellite imagery but that do not overlap at all with glaciers mapped on USGS topographic maps. These 178 glaciers are apparently “brand new.” See text for discussion.

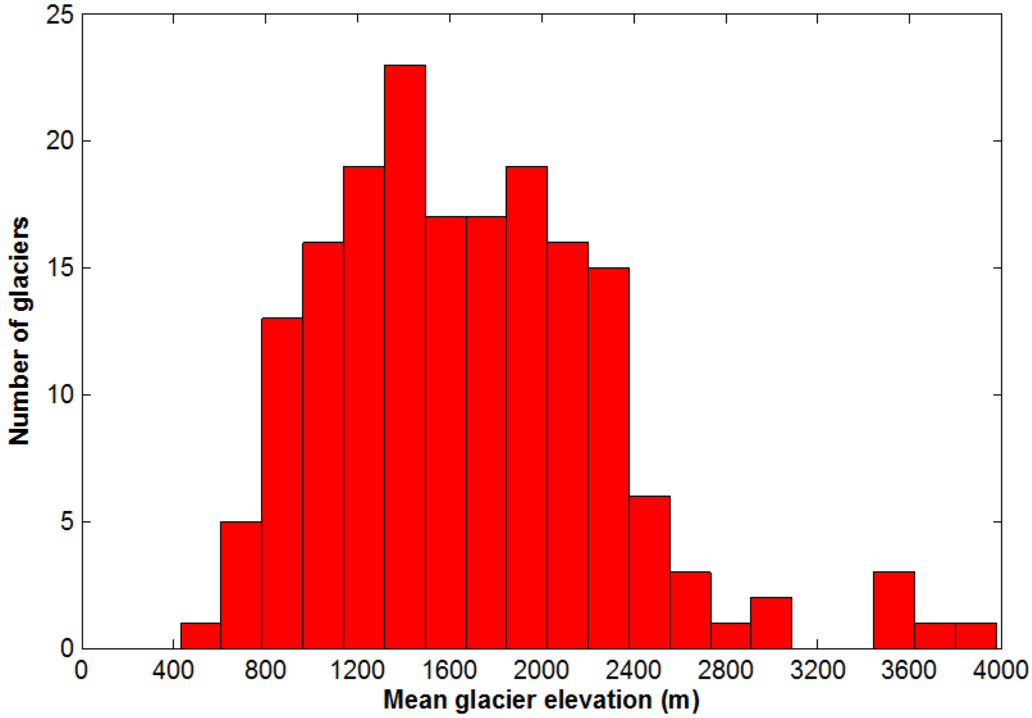

Figure 131. Histogram of mean elevations for the same group of apparently new (perhaps newly discovered) glaciers shown in Figure 125.

Glacier Area

Over the period of our inventory, approximately 50 years, the areal coverage of glaciers in (or partly in) the Alaskan national parks declined 8%, from 47,470 km^2 to 43,745 km^2. The trend of diminishing glacier area is fairly consistent among parks, in that it declined in eight of nine park units by anywhere from 5% (WRST) to 74% (KLGO, reflecting the retreat of one—out of only two—glaciers to outside the park boundary). Only ANIA showed an increase in glacier-covered area, a change that we argued above reflects our ability to better map small, debris-covered glaciers that we interpret as present, but unmapped, in the original topographic maps (e.g., Figure 13). In any case, that increase of 14% was, in absolute terms, trivial: 0.6 km^2. In comparison, we find that the park glaciers lost 3725 km^2 of area, a figure 18% larger than the size of Rhode Island.

This decline in glacier area is a conservative estimate—in other words, the errors in our analysis very likely underestimate the magnitude of the decline. We base this on two observations. First, as described above we believe that our satellite date outlines include many small glaciers that the original cartographers "missed." Second, the original cartographers also omitted the debris-covered portion of many map date glaciers (e.g. Muldrow and Arrigetch Glaciers). We are aware of no contradictory examples where the topographic maps systematically overestimate glacier sizes. Together, these items suggest a systematic bias in the map date glacier area. Our satellite date inventory, in contrast, has random errors but to our knowledge has no such bias. It is therefore likely the original map date outlines underestimate the true glacier area at that time, and thus falsely minimize the extent of subsequent glacier shrinkage.

The complete catalog of glacier outlines provides an opportunity to consider volume changes of the complete population using area-volume scaling (Bahr et al. 1997). As discussed previously, however, this empirical approach has potentially large unconstrained errors. We have therefore refrained from calculating volume change results using our volume results, but the intrepid reader can easily calculate for themselves that the area-based volumes declined 20% over the course of this inventory, a volume loss of about 4100 km^3 ice. Using the median map date and satellite dates of 1953 and 2009, this suggests that Alaskan park glaciers lost mass at an average rate of 66 Gt/yr. We have low confidence in this estimate, however, and it appears in comparison with several other estimates of volume change to be an overestimate of mass loss (Berthier et al. 2010; Arendt et al. 2010). We prefer a more robust assessment of changes in glacier volumes based on surface elevation data. We discuss the results of that analysis in the "Glacier Surface Elevations and Volume" section, below.

Glacier Geometry

The geometric results summarized in our results section are not likely unique to park glaciers, and reveal trends that are common to glaciers around Alaska: glaciers generally face north; large valley glaciers have lower overall slopes than small glaciers; and high elevation glaciers tend to be steeper than the population mean. Some parks stand out for particular features: Wrangell-St. Elias has many big, long, high elevation glaciers; Denali has the highest glaciers; tidewater glaciers are limited to Wrangell-St. Elias, Kenai Fjords, and Glacier Bay; Gates of the Arctic has almost exclusively small north-facing glaciers; and Katmai has the longest median glacier length, not because it has the biggest glaciers but because it lacks small ones.

The outlines provided with this project provide an opportunity to investigate trends in these and other geometric characteristics over time. Assessments of geometric changes, over time, in individual glaciers will likely be of great interest to NPS staff, researchers, and visitors, but with over 7000 glaciers this is beyond the scope of this report. In the interest of facilitating such subsequent investigations, some NPS staff have asked whether it is possible to give each glacier in our database a unique name, or code, that persists over time and facilitates tracking. The answer, after much discussion, is no. Like GLIMS, RGI, and other glacier inventory projects, we have concluded that the time-transgressive nature of individual glaciers—that is, their tendency to frequently divide through shrinkage or, less commonly, merge through growth—makes such a naming scheme impractical. However, we remind our audience that the best solution to this challenge is inherent to our presentation of the database in a spatially explicit format: it is very easy, using ArcMap or other spatial analysis software, to pull up the outline files from different time intervals and select the glaciers that overlap each other in space. These, despite their different names (GLIMS IDs), are the "same" glacier. Finally, we point also to the accompanying interpretive report that will be a product of this project, where we examine, in detail, the temporal evolution of the selected "focus glaciers."

Glacier Surface Elevations and Volume

Our elevation change results, in accordance with the general pattern of diminished glacier area described by the glacier outline results, describe a population of glaciers that is generally shrinking. We have calculated the glacier-wide mass balance rate for 158 distinct (but in some cases overlapping) time intervals on 59 separate glaciers. If we eliminate those glaciers that are subcomponents of larger linked glacier systems and hence have complicated mass balances (such as the Bering/Bagley system), we are left with 124 intervals. Of these, 97 intervals are negative.

The measurements range from -2.85 to 1.55 m/yr w.e., and the average mass balance in that population of intervals is -0.59 m/yr w.e.

The most obvious generalization about these results is the obvious predominance of negative balances. The population of measured glaciers that had negative mass balances includes land-terminating, tidewater, lake calving, and surging glaciers. So, too, does the population of glaciers with positive balances. Negative balances occurred at early intervals and late ones—so, too, did positive balances. One group of positive balances does stand out: several glaciers in KEFJ and LACL had positive or very slightly negative balances between 1997 and 2001 (Figure 81 and Figure 96). As noted previously, we attribute this particular result in part to the timing of the 2001 measurements, which occurred earlier than usual after a particularly snowy winter. But indeed, every glacier, at every interval, has a particular history that helps to make sense of its particular pattern of elevation changes.

The granular details of these results are of tremendous value when looking at individual glaciers in this way, but what do they tell us about volume loss in the parks as a whole? Several other papers that have investigated volume change for the Alaska region (Arendt et al. 2002; Arendt et al. 2006; Berthier and Toutin 2008; Larsen et al. 2007; Luthcke et al. 2008; Berthier et al. 2010; Radic and Hock 2010; Johnson et al. 2013), but none with a focus on NPS lands specifically.

Extrapolating our laser altimetry results to the park level is beyond the scope of this project, but happily such an analysis is nearly complete for the state of Alaska overall, and our colleague Evan Burgess has allowed us to subsample those results for the NPS park glaciers specifically. The approach of Burgess et al. (in prep) follows closely the methods recently employed for Glacier Bay by Johnson et al. (2013). Working with essentially the same elevation data presented here, Johnson et al. (2013) tested three different techniques for extrapolating altimetry data to the entire glacier population of the Glacier Bay region. He concluded that the best technique was a "normalized elevation (NE)" technique that converts surface elevations of each glacier in the region before calculating a mean dh/dt vs normalized elevation curve that can then be applied to each unsurveyed glacier. Burgess et al. (in prep) applies a very similar approach to the laser altimetry results presented in this report (and including some additional results from non-park glaciers), and we present a preview of those results subsampled for just the park glaciers.

Based upon the Burgess et al. (in prep) analysis of laser altimetry results mostly from southcentral Alaska between 1995 and 2013, we estimate that park glaciers are collectively losing approximately 36 Gt of ice per year (Table 22). The obvious and important corollary to this result is that these glaciers are annually releasing 36 Gt of water, mostly through Alaskan rivers, to the oceans. This translates to approximately one-tenth of a millimeter of sea level rise per year, with responsibility partitioned among the nine parks. The contribution of Wrangell-St. Elias is by far the most important, with 65% of the total (almost 24 Gt/yr), followed by Glacier Bay (12% of the total), Denali (9%), Lake Clark (6%), and Kenai Fjords (4%).

Table 28. Annual mass change (gigatons per year) and sea level rise equivalents (mm per year) for the glaciated Alaskan parks. Results extrapolated from altimetry data in this report by Burgess et al. (in prep).

Park	Mass Change (Gt/yr)	SLR (mm/yr)
ANIA	-0.006	0.000
DENA	-3.427	0.009
GAAR	-0.061	0.000
GLBA	-4.405	0.012
KATM	-0.918	0.003
KEFJ	-1.526	0.004
KLGO	-0.002	0.000
LACL	-2.051	0.006
WRST	-23.794	0.066
All NPS	-36.192	0.100

Climate Context

Glaciers in the Alaskan national parks persist because of our climate. Alaska is relatively wet and cold. To the extent that the climate has changed over time, and will change in the future, the glaciers themselves are also changing. Although it is critical to emphasize that many factors other than climate impact glacier extent and thickness, and that these factors are in some cases much more important than prevailing regional climate (as in the case of surging glaciers and some tidewater glaciers, to name two examples), it is nonetheless clear that there are some basic and obvious relationships between regional climate and glacier extent. All other things being equal, glaciers grow when mass inputs from snow accumulation exceed mass losses from ablation—melting and calving (Oerlemans et al. 1998). The opposite is also true.

It is therefore instructive to examine the record of Alaskan climatic change over the approximate period during which our inventory takes place, and then to look forward at projections of future change. We do so here, but emphasize that our approach is descriptive in nature, and that any conclusions drawn from this comparison should be considered tentative.

Past climate

To characterize climate over the last half of the 20th century, approximately concurrent with the timing of our inventory, we used a gridded climate product that interpolates monthly anomalies of 1961-2009 station data from 1971–2000 monthly climate normals over a 2 km x 2 km grid (personal communication from D.F. Hill and S.E. Calos, 2011). The climate normals were derived from the Parameter Regression on Independent Slopes Model (PRISM; Daly et al. 1997). A description of this climate product and its use in comparison to glacier mass balances is summarized in Arendt et al. (2013). We subsampled this statewide dataset over the nine national park units to obtain spatially averaged climate and precipitation data. These data estimate temperature and precipitation at the average elevation of each grid cell. Our sampling approach is similar to, but more simplistic than, that of Johnson et al. (2013), who describe this technique in more detail. Here, we present time-series of average temperature (annual and summer months only) and total precipitation (annual and winter months only) for each park. We defined the summer melt season as June, July, and August and the winter accumulation season (narrowly, mainly for consistency with the future climate predictions obtained from SNAP) as December (of the previous calendar year), January, and February.

Trends in temperature are shown in Figure 132 and show generally similar patterns in all park units with the possible exception of KLGO, which seems to lag the trends of the other parks and may simply reflect the presence of very few grid cells (and hence limited data) in that park unit. Taking temperature first, it appears that mean annual temperatures have been slightly more variable than summer temperatures alone. Both records suggest a general trend of coolest temperatures around 1970 and warmest temperatures from the early-1990s to the mid-2000s. Mean annual temperature decreased in most parks just before 2010, but this trend is very subtle in the summer-only record. The only Arctic park, GAAR, exhibits the largest swings.

Precipitation trends are shown in Figure 133, and show annual values in the top panel and seasonal (winter, in this case) trends below. Annual variability appears greater than seasonal variability, as it was with temperature, but in the case of precipitation this trend is only an artifact of the choice to sum, rather than average, monthly values. KLGO again appears to deviate the most from general parkwide trends, especially with a major decrease in precipitation after 2005, but there is more variability among parks than was evident for temperature trends. In general, Gulf of Alaska parks (GLBA, KEFJ) had less precipitation than usual in the late-1960s and early-1970s, and more than average around 1990 and in the late-2000s. GAAR shows the least interannual variability, as it did with temperature.

In summary, since the 1960s summers in every park but KLGO warmed overall by cumulative values of less than 1° C. Meanwhile, winters in every park but DENA, KLGO, and WRST got wetter. The only three parks that got drier in winter did so only very slightly.

The trends in temperature and precipitation noted above have been strongly influenced by regime fluctuations in the Pacific Decadal Oscillation, a long-lived pattern of sea surface temperature variability that influences North Pacific climate (Mantua and Hare 2002). A significant PDO “regime shift” to the positive, warmer phase occurred in 1977. It is inappropriate, therefore, to extrapolate the trends discussed above to earlier or later time periods. It is also overly simplistic to interpret these trends as evidence of global climate change. We make neither assumption here, and emphasize instead our intention to document empirically the actual climate variability during the period over which glacier changes reported in this document occurred.

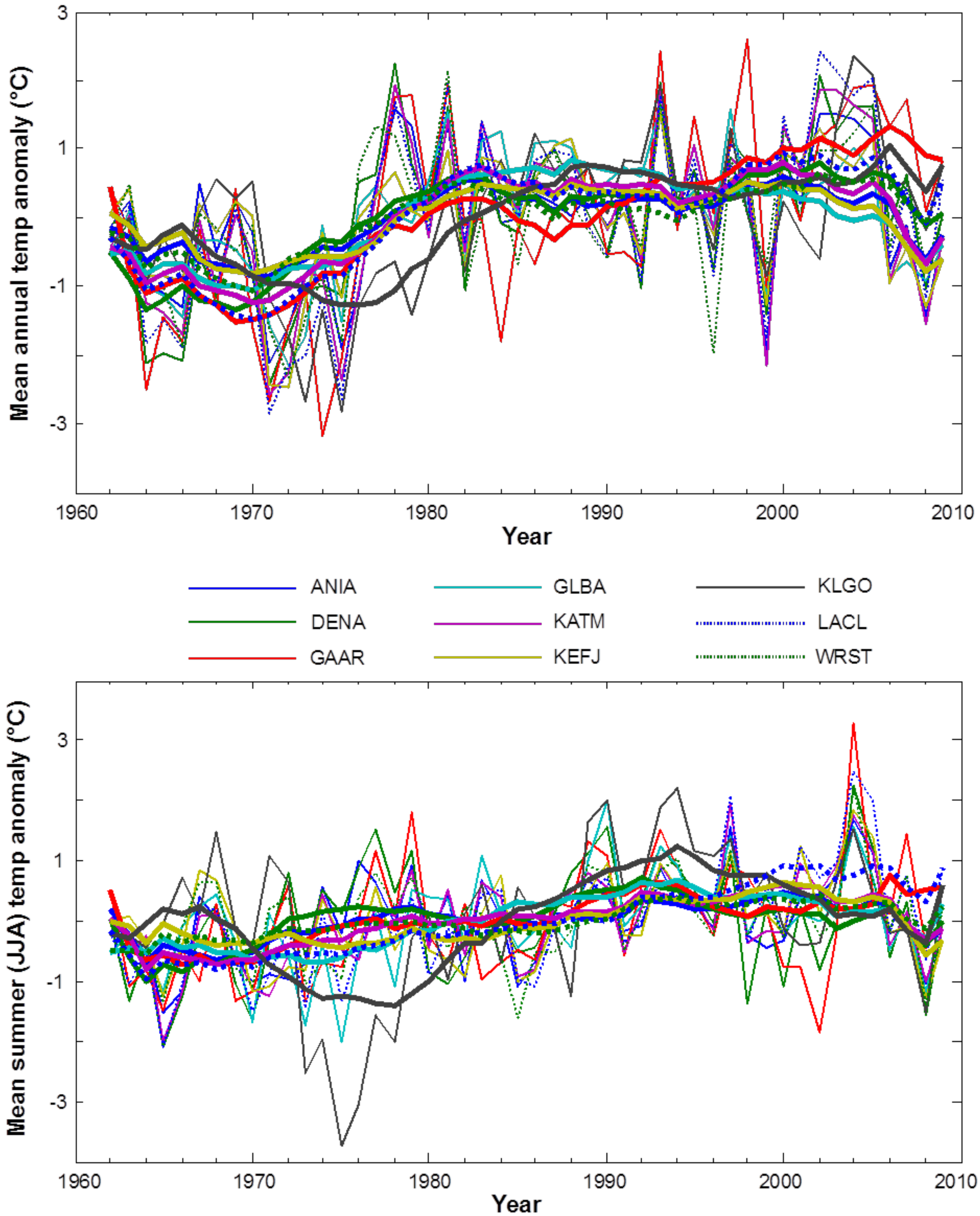

Figure 132. Temperature changes in each of the glaciated park units from 1962-2009, shown as anomalies from the mean value during the plotted interval. Upper panel shows mean annual temperatures and lower panel shows summer months ('JJA') only. Bold lines are ten year running means. All plotted values reflect climate conditions spatially averaged over a 2 km grid which was sampled within each of the NPS park boundaries.

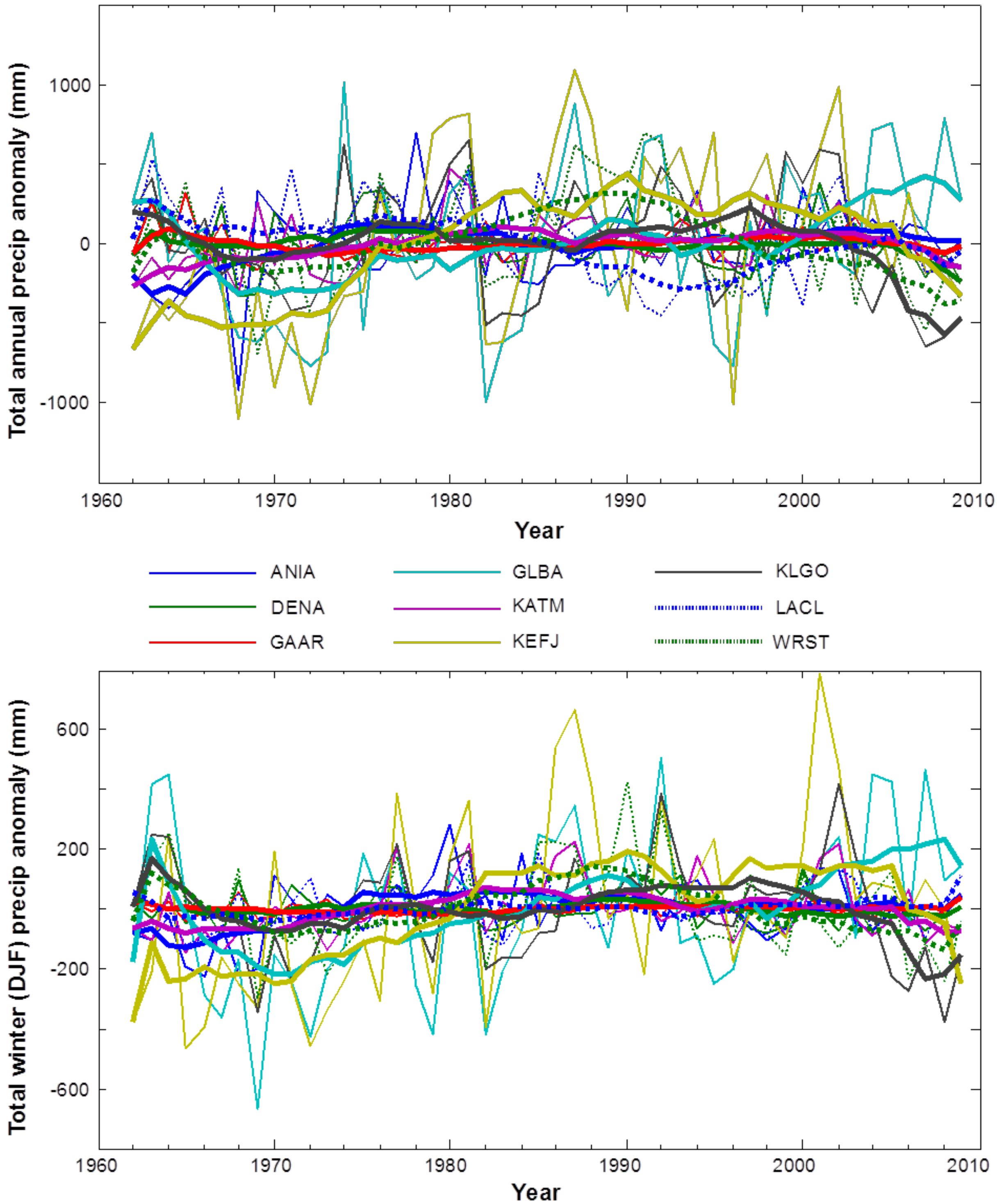

Figure 133. Precipitation changes in each of the glaciated park units from 1962-2009, shown as anomalies from the mean value during the plotted interval. Upper panel shows total annual precipitation and lower panel shows winter months ('DJF') only. Bold lines are ten year running means. All plotted values reflect climate conditions spatially averaged over a 2 km grid.

Future climate

For consideration of possible future climatic influences on the glaciers in this inventory, we draw upon data from the Scenarios Network for Alaska & Arctic Planning (SNAP), a regional institute of the University of Alaska Fairbanks (SNAP 2013). SNAP provides online access to downscaled global model outputs for Alaskan users, where downscaling refers to the process of taking Global Climate Model (GCM) outputs (typically on a global grid of 2.5°-sided pixels) and projecting them to a more detailed grid (in this case, a grid of 0.77 km-sided pixels) by taking into account land features such as slope, elevation, and proximity to coastlines. These data estimate temperature and precipitation at the average elevation of each grid cell.For this paper, we utilized SNAP results that reflect the averaged predictions of five GCMs judged best in their performance on Alaska's climate, and we present the average outputs of those five models for three distinct scenarios. Here, "scenarios" refers to three differing combinations of greenhouse gas emissions and other forcing agents that collectively impact global climate. The three scenarios represent a range of possible global developments that would differentially impact our future climate (IPCC SRES, 2000). The details of these scenarios, the GCMs used, and SNAP's downscaling approach are presented on the SNAP website (SNAP 2013).

SNAP provides a variety of data products, but we subsampled their outputs to visualize potential future changes in temperature and precipitation over a half-century timescale comparable to the above consideration of past climate. We compared predicted average air temperature and precipitation—on the basis of three different forcing scenarios— from the period 2060-69 to the period 2010-2019 (nominally "2065" and "2015" in the figures. The three particular scenarios examined were the A1B, A2, and B1 scenarios (IPCC SRES, 2000), summarized here:

- A1B: A more integrated world with rapid economic growth, global population of 9 billion by 2050 and then declining, and a quick spread of efficient technologies.
- A2: A more divided world with self-reliant nations, continuously increasing population, and regionally oriented economic development.
- B1: An ecologically friendly world with rapid economic growth, rapid population growth to 9 billion by 2050 but then declining, reductions in material usage and an emphasis on environmental stability.

Of these scenarios, A2 has the highest greenhouse gas emissions between now and 2050, and B1 has the least. Collectively, these three provide snapshots of three potential levels of impact our society might have on global climate over the coming decades.

We show predicted annual and summer temperature changes in Figure 134. Warming is predicted for all parks at all time intervals under all three scenarios, with the greatest warming seen under scenario A1B and the least under B1. As was the case in the past climate, warming trends are predicted to be greatest when measured on an annual basis (because the most warming is expected in winter), but if we focus on summer—when glaciers are most sensitive to temperature—we see a very consistent prediction of 1-2° warming for all parks under scenarios A1B and A2, and a slightly more modest prediction of 0-1° C warming under B1 (except for slightly higher warming under that scenario in parts of GLBA, WRST, and GAAR).

Comparable maps of predicted precipitation trends are shown in Figure 135. The dominant statewide prediction is an increase of total precipitation by 0-25 cm. Over the winter months of

DJF, this trend is uniform under all scenarios, with small differences in the degree of enhanced (25-50 cm) wetting in the coastal mountains. Differences among scenarios are greater for annual precipitation, with more significant increases in precipitation in the coastal mountains and, for scenarios A2 and A1B, in the Alaska Range as well. In scenario B1 only, annual precipitation in ANIA is predicted to diminish slightly.

In summary, the generalized trend of warmer summers and (less consistently) wetter winters that prevailed over the last 50 years in most Alaskan parks is expected to continue in the next 50. This prediction is based on the averaged results of five global climate models and remains true over a range of emissions scenarios. Even the most conservative scenario suggests that the trend will in fact accelerate, with greater than 1° C of warming and consistently wetter winters in all parks.

Translating these trends to a quantitative prediction of glacier change is outside the scope of this project, and at minimum would require consideration of greater spatial and temporal detail, of the change in frequency of rain vs. snow at different seasons, of individual glacier dynamics, and of each glacier's particular seasonal sensitivity characteristic (SSC, Oerlemans and Reichert 2000). The SSC, a measure of the glacier's mass balance sensitivity to changes in precipitation and temperature throughout the year, would be particularly important since the trend towards wetter winters will, to varying degrees, tend to counteract the tendency towards more summer melt. In general, however, the SSC is much greater for temperature than for precipitation (Leclercq and Oerlemans 2013), and it is thus reasonable to suggest that the predicted intensification of recent climatic trends will on most glaciers lead to a comparable intensification of recent glacier trends: negative mass balances, diminished ice cover, and reduced ice volume.

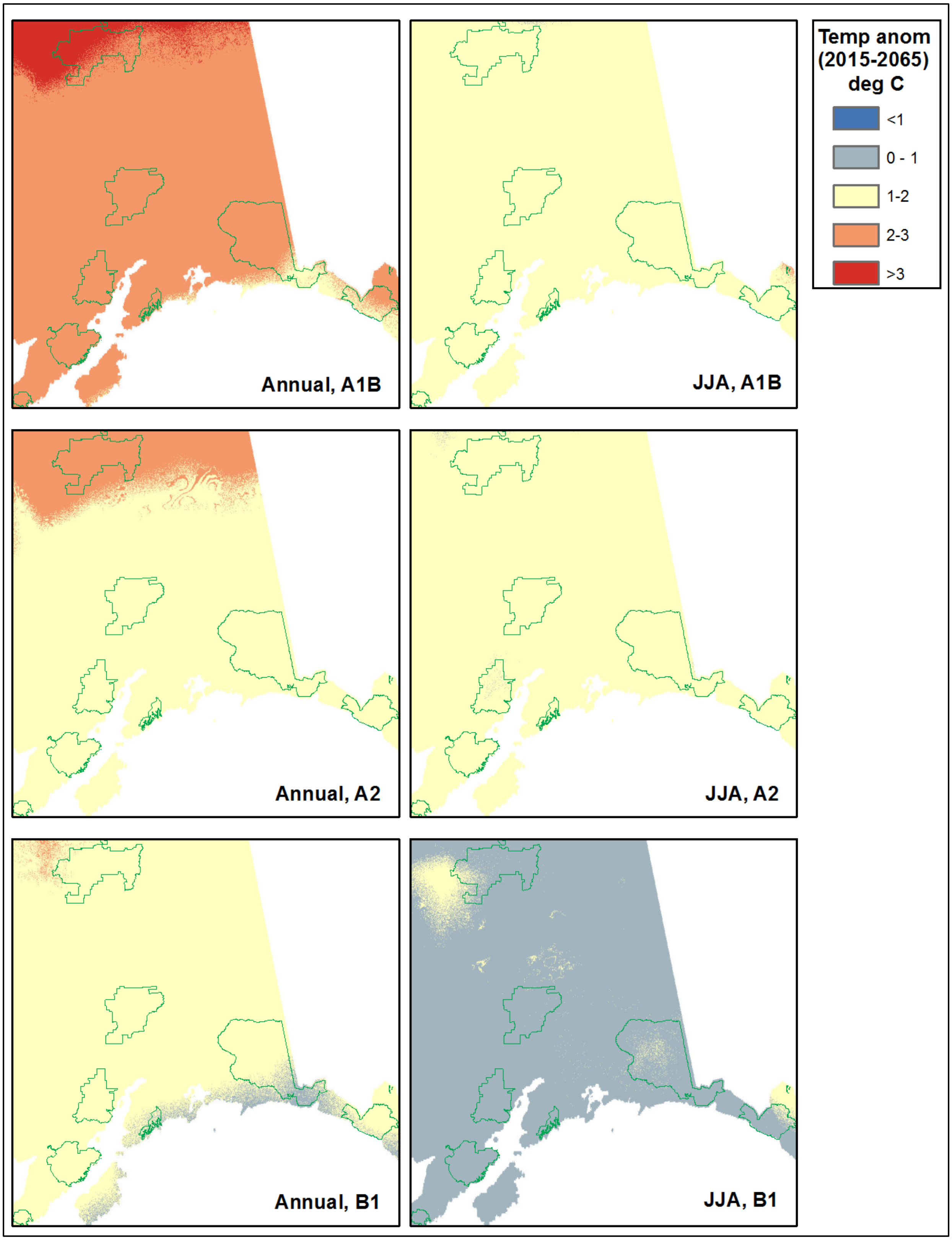

Figure 134. Temperature anomalies predicted for three different emissions scenarios. Anomalies compare predicted average temperatures from 2060-2069 to 2010-2019. Annual averages at left, summer months only on right ('JJA').

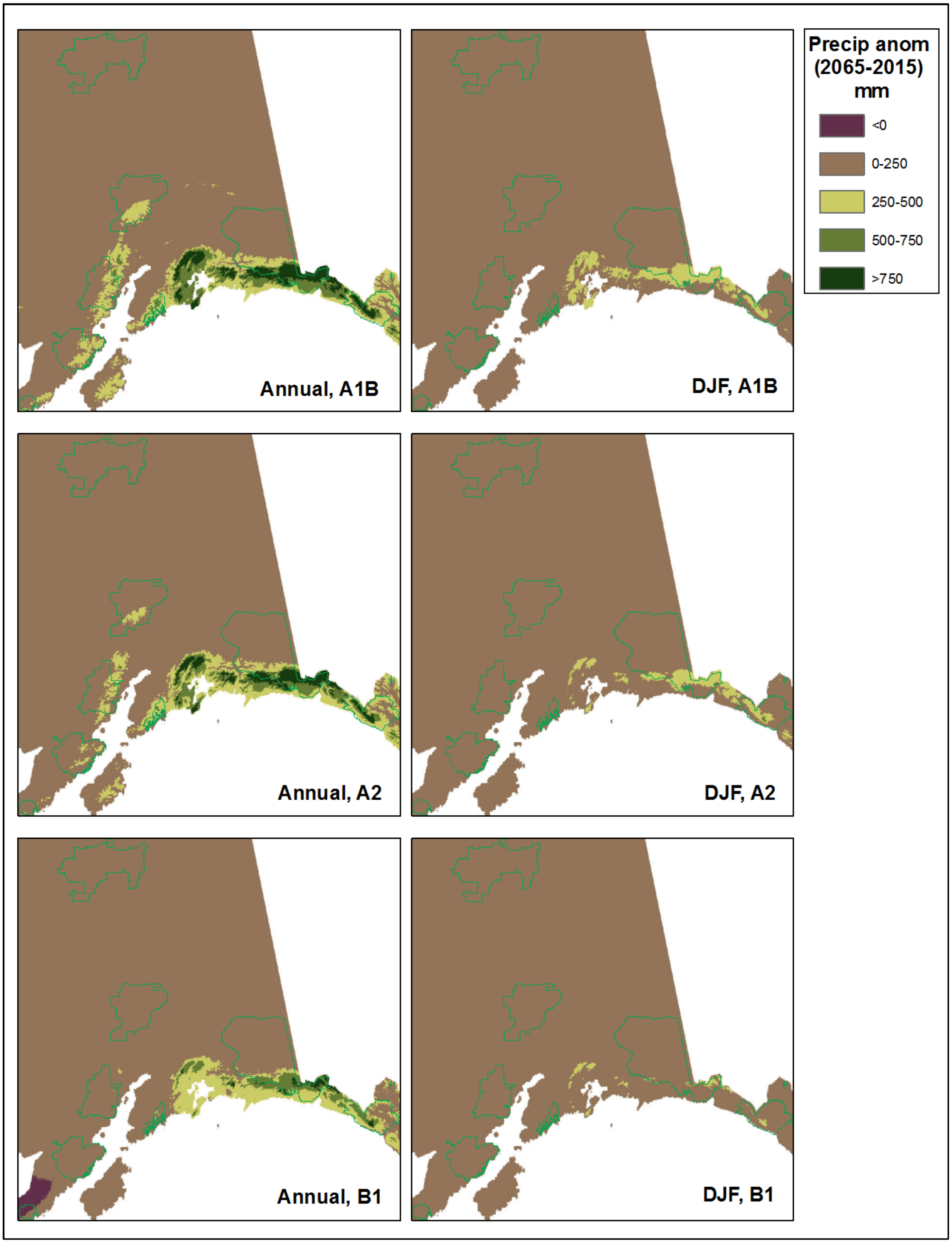

Figure 135. Precipitation anomalies predicted for three different emissions scenarios. Anomalies compare predicted average precipitation from 2060-2069 to 2010-2019. Annual averages at left, winter months only on right ('DJF').

Conclusions

With respect to climate change, glaciers have been called "the canary in the coal mine." The implication—that by watching the glaciers we can more easily infer the more subtle changes occurring in our climate system—depends on somebody actually watching the canary. In the present case, that means a regular, systematic, and comprehensive program of glacier monitoring. Prior to the work we describe here, however, many of Alaska's glaciers had not been remapped since the US Geological Survey made its original topographic maps in the 1950s and 1960s—maps that modern backcountry travelers still use, but have learned to view with some skepticism when navigating through glaciated terrain. The outdated glacier boundaries and surface elevations from old maps have challenged scientists, too: lacking even the most basic information on the current extent of glaciers, Alaskan geologists and ecologists had no basis for inferring trends over time or the relationship of these trends to climatic changes. With this project, NPS has taken a major step towards accomplishing the goal of regularly monitoring the vast glacier-covered area of the Alaskan national parks.

There is one obvious reason why all the glaciers in Alaska's parks had not been remapped since the mid-20th century. There are a lot of them. Our new inventory includes 7561 distinct modern glaciers that are contained wholly or at least partly within the boundaries of nine Alaskan National Park units. Those glaciers cover about 43,745 km^2 of land. The present work has contributed substantially to the broader goal of completing a comprehensive inventory of all glaciers in Alaska and neighboring Canada, and we now know that the parks constitute approximately half of the region's total ice coverage.

Comparing our modern inventory to the USGS maps of the 1950s, the most important result is evidence for an 8% loss of glacier cover over the intervening half-century. Interpretation of trends in glacier numbers is complicated by changes in mapping techniques, but the overall loss of glacier cover is robust, corroborated by scores of other independent works, and broadly consistent across parks, regions, elevations, and glacier types. In all, Alaska's parks have lost 3725 km^2 of glacier ice, an area bigger than the state of Rhode Island.

Over the last two decades, we measured surface elevation change on 59 of the park glaciers and found that most of them, as would be expected during a period of areal shrinkage, have thinned and lost mass at area-averaged rates of 0 to 1.5 meters water equivalent per year. We infer this mass loss to be generally typical of other, unmeasured glaciers.

At the broad, statewide scale, there is a clear scientific consensus that warming temperatures are the primary factor driving this loss of glacier ice. But every glacier is different, and behind this generalization are many complications. The interpretive product that accompanies this technical report highlights these complications for a subset of "focus glaciers" throughout the Alaskan park system. The overall trend, however, is clear and unambiguous. Alaska's glaciers are significantly diminished relative to the middle of the last century, and present trends suggest that the next inventory, whenever it occurs, will document an even more extensive retreat of the glaciers and icefields that dominate the landscapes of Alaskan national parks, attract visitors from around the world, and constitute an invaluable part of our national natural heritage.

Literature Cited

Aðalgeirsdottir, G, Echelmeyer KA, and Harrison WD. 1998. Elevation and volume changes on the Harding Icefield, Alaska. *Journal of Glaciology*, 44(148): 570–582.

Arendt AA, Echelmeyer KA, Harrison WD, Lingle CS, Valentine VB. 2002. Rapid wastage of Alaska glaciers and their contribution to rising sea level. *Science* 297: 382–386.

Arendt A, Echelmeyer KA, W Harrison, C Lingle, S Zirnheld, V Valentine, B Ritchie, and M Druckenmiller. 2006. Updated Estimates of Glacier Volume Changes in the Western Chugach Mountains, Alaska, and a Comparison of Regional Extrapolation Methods. *Journal of Geophysical Research: Earth Surface.* 111: F3.

Arendt A, Bolch T, Cogley JG, Gardner, J-O Hagen, R Hock, G Kaser, WT Pfeffer, G Moholdt, F Paul, V Radić, L Andreassen, S Bajracharya, N Barrand, M Beedle, E Berthier, R Bhambri, A Bliss, I. Brown, D. Burgess, E. Burgess, F. Cawkwell, T. Chinn T, Copland L, Davies B, De Angelis H, Dolgova E, Filbert K, Forester RR, Fountain A, Frey H, Giffen B, Glasser N, Gurney S, Hagg W, Hall D, Haritashya UK, Hartmann G, Helm C, Herreid S, Howat I, Kapustin G, Khromova T, Kienholz C, Köonig M, Kohler J, Kriegel D, Kutuzov S, Lavrentiev I, Le Bris R, Lund J, Manley W, Mayer C, Miles E, Li X, Menounos B, Mercer A, Mölg N, Mool P, Nosenko G, Negrete A, Nuth C, Pettersson R, Racoviteanu A, Ranzi R, Rastner P, Rau F, Raup B, Rich J, Rott H, Schneider C, Seliverstov Y, Sharp M, Sigurðsson O, Stokes C, Wheate R, Winsvold S, Wolken G, Wyatt F, Zheltyhina N. 2013, Randolph Glacier Inventory – A Dataset of Global Glacier Outlines: Version 3.2. Global Land Ice Measurements from Space, Boulder Colorado, USA. Digital Media.

Bader H, 1954. Sorge's Law of densification of snow on high polar glaciers. *Journal of Glaciology* 2: 319–323.

Bahr DB, Meier MF, Peckham SD. 1997. The physical basis of glacier volume-area scaling. *Journal of Geophysical Research*. 102: 20355–20.

Beedle MJ, Dyurgerov M, Tangborn W, Khalsa SJS, Helm C, Raup B, Armstrong R, Barry RG. 2008. Improving estimation of glacier volume change: a GLIMS case study of Bering Glacier System, Alaska. *The Cryosphere.* 2: 33–51.

Berthier E, Schiefer E, Clarke GKC, Menounos B, and Rémy F. 2010. Contribution of Alaskan Glaciers to Sea-level Rise Derived from Satellite Imagery." *Nature Geoscience* 3(2): 92–95. doi:10.1038/ngeo737.

Berthier E, Toutin T. 2008. SPOT5-HRS digital elevation models and the monitoring of glacier elevation changes in North-West Canada and South-East Alaska. *Remote Sensing of Environment.* 112: 2443–2454.

Burgess EW, Forster RR, Larsen CF, Braun M. 2012. Surge dynamics on Bering Glacier, Alaska, in 2008-2011. *The Cryosphere* 6: 1251–1262.

Burgess EW, Larsen CF, Arendt AA, O'Neel S, Johnson AJ, McNabb RW, Zirnheld SL, and

Keinholz C. in prep. The impact of tidewater dynamics on glacier mass loss in Alaska.

Burgess EW, Larsen CF, and Forster RR. 2013. Summer melt regulates winter glacier flow speeds throughout Alaska. *Geophysical Research Letters*. 40: 6160-6164.

Cogley, JG, Hock R, Rasmussen LA, Arendt AA, Bauder A, Braithwaite RJ, Jansson P, Kaser G, Moller M, Nicholson L, and Zemp M. 2011. Glossary of Glacier Mass Balance and Related Terms. IHP-VII Technical Documents in Hydrology No. 86. Paris: UNESCO-IHP.

Daly C, Taylor GH, and Gibson WP. 1997. The PRISM Approach to Mapping Precipitation and Temperature." *Proceedings, 10th Conference on Applied Climatology, American Meteorology Society*. 10-12.

Echelmeyer K, Harrison W, Larsen C, Sapiano J, Mitchell J, DeMallie J, Rabus B, Adalgeirsdottir G, Sombardier L. 1996. Airborne surface profiling of glaciers: A case-study in Alaska. *Journal of Glaciology*. 42: 538–547.

Field WO. 1975. Mountain glaciers of the Northern Hemisphere, Vols 1&2 and Atlas. Hanover NH: U.S. Army Cold Regions Research and Engineering Laboratory.

Fountain AG (submitter). 2005. GLIMS Glacier Database. Boulder, CO. National Snow and Ice Data Center. http://dx.doi.org/10.7265/N5V98602.

Giffen BA, Hall DK, and Chien JYL. In press. Glaciers of Kenai Fjords National Park and Katmai National Park and Preserve, Kargel JS, Bishop MP, Kääb A, Raup BH, and Leonard G (eds.) *Global Land Ice Measurements from Space: Satellite Multispectral Imaging of Glaciers*. Praxis-Springer.

Hall DK, Bayr KJ, Schöner W, Bindschadler RA, and Chien JYL. 2003. Consideration of the errors inherent in mapping historical glacier positions in Austria from the ground and space (1893-2001). *Remote Sensing of Environment*. 86: 566-577.

Huss M. 2013. Density Assumptions for Converting Geodetic Glacier Volume Change to Mass Change. *The Cryosphere.* 7(3): 877–887. doi:10.5194/tc-7-877-2013.

IPCC SRES. 2000. Special report on emissions scenarios: a special report of Working Group III of the Intergovernmental Panel on Climate Change. Nakicenovic N and Swart R (eds.). Cambridge University Press, Cambridge UK.

IPCC. 2013. Climate Change 2013: The Physical Science Basis. Contribution of Working Group I to the Fifth Assessment Report of the Intergovernmental Panel on Climate Change. T.F. Stocker et al. (eds.). Cambridge University Press, Cambridge UK.

Johnson AJ, Larsen CF, Murphy N, Arendt AA, and Zirnheld SL. 2013. Mass balance in the Glacier Bay area of Alaska, USA, and British Columbia, Canada, 1995–2011, using airborne laser altimetry. *Journal of Glaciology*. 59: 632–648.

Kienholz C, Hock R, and Arendt AA. 2013a. A new semi-automatic approach for dividing glacier complexes into individual glaciers. *Journal of Glaciology* 59(217): 925-937.

Kienholz, C., Rich JL, Arendt AA, and Hock R. 2013b. A new method for deriving glacier centerlines applied to glaciers in Alaska and northwestern Canada. *The Cryosphere Discussion.* 7: 5189-5229.

Larsen CF, Motyka RJ, Arendt AA, Echelmeyer KA, and Geissler PE. 2007. Glacier changes in southeast Alaska and northwest British Columbia and contribution to sea level rise. *Journal of Geophysical Research.* 112: doi.1029/2006JF000586.

Luthcke SB, Arendt AA, Rowlands DD, McCarthy JJ, and Larsen CF. 2008. Recent glacier mass changes in the Gulf of Alaska region from GRACE mascon solutions. *Journal of Glaciology*. 54: 767–777.

Leclercq PW and Oerlemans J. 2011. Global and hemispheric temperature reconstruction from glacier length fluctuations. *Climate Dynamics.* 38: 1065–1079.

Mantua J and Hare SR. 2002. The Pacific Decadal Oscillation. *Journal of Oceanography*. 58: 35-44.

Molnia BF, 2008. Glaciers of North America - Glaciers of Alaska. United States Government Printing Office, Washington, DC.

Oerlemans J, Anderson B, Hubbard A, Huybrechts P, Johannesson T, Knap WH, Schmeits M, Stroeven AP, van de Wal RSW, and Zuo Z. 1998. Modeling the response of glaciers to climate warming. *Climate Dynamics*. 14(4): 267-274.

Oerlemans J and Reichert B. 2000. Relating glacier mass balance to meteorological data by using a seasonal sensitivity characteristic. *Journal of Glaciology* 46: 1–6.

Paul F, Barry RG, Cogley JG, Frey H, Haeberli W, Ohmura A, Ommanney CSL, Raup B, Rivera A, and Zemp M. 2009. Recommendations for the compilation of glacier inventory data from digital sources. *Annals of Glaciology* 50(53): 119-126.

Paul F, Barrand NE, Baumann S, Berthier E, Bolch T, Casey K, Frey H, Joshi SP, Konovalov V, Le Bris R, Mölg N, Nosenko G, Pope A, Racoviteanu A, Rastner P, Raup B, Scharrer K, Steffen S, Winsvold S. 2013. On the Accuracy of Glacier Outlines Derived from Remote-sensing Data." *Annals of Glaciology.* 54(63): 171–182. doi:10.3189/2013AoG63A296.

Pfeffer WT, Arendt AA, Bliss A, Bolch T, Cogley JG, Gardner S, Hagen J, Hock R, Kaser G, Kienholz C, Miles ES, Moholdt G, Mölg N, Paul F, Radić V, Rastner P, Raup BH, Rich J, Sharp MJ, and the Randolph Consortium. 2014. The Randolph Glacier Inventory: a globally complete inventory of glaciers. Journal of Glaciology. 60(221): 537-552.

Post A. 1960. The exceptional advances of the Muldrow, Black Rapids, and Susitna glaciers. *Journal of Geophysical Research*. 65(11): 3703-3712.

Post A. 1966. The recent surge of Walsh glacier, Yukon and Alaska. *Journal of Glaciology* 6(45): 375-381.

Post A. 1969. Distribution of surging glaciers in western North America. *Journal of Glaciology* 8(53): 229–240.

Radić V and Hock R. 2010. Regional and global volumes of glaciers derived from statistical upscaling of glacier inventory data. *Journal of Geophysical Research: Earth Surface*. 115.

Raup B, Arendt AA, Armstrong R, Barrett A, Jodha Khalsa S, and Racoviteanu A. 2013. GLIMS and the RGI: relationships present and future. *EGU General Assembly Conference Abstracts*. 15: 11831.

SNAP (Scenarios Network for Alaska and Arctic Planning, University of Alaska). 2013. Data. Retrieved 1 September 2013 from http://www.snap.uaf.edu/data.php.

Svoboda F and Paul F. 2010. A New Glacier Inventory on Southern Baffin Island, Canada, from ASTER Data: I. Applied Methods, Challenges and Solutions." *Annals of Glaciology*. 50(53): 11–21.

Young J. 2013. Temperature Index Modeling of the Kahiltna Glacier: Comparison to Multiple Field and Geodetic Mass Balance Datasets. Masters Thesis. University of Alaska. Print. 83 pp.

Van Beusekom AE, O'Neel SR, March RS, Sass LC, and Cox LH. 2010. Re-analysis of Alaskan benchmark glacier mass-balance data using the index method. USGS Sci. Invest. Rep 5247.

The Department of the Interior protects and manages the nation's natural resources and cultural heritage; provides scientific and other information about those resources; and honors its special responsibilities to American Indians, Alaska Natives, and affiliated Island Communities.

NPS 953/127194, November 2014

National Park Service
U.S. Department of the Interior

Natural Resource Stewardship and Science
1201 Oakridge Drive, Suite 150
Fort Collins, CO 80525

www.nature.nps.gov